ALKALINE MAGMATISM, its sources and plumes

Щелочной магматизм, его источники и плюмы

IRKUTSK
NAPOLI
2007

Russian Academy of Sciences
Siberrian Branch
Vinogradov Institute of Geochemistry
Dipartimento di Scienze Della Terra
Università di Perugia, Italy
Russian Foundation of Basic Research

Alkaline magmatism, its sources and plumes

(Щелочной магматизм, его источники и плюмы**)**

PROCEEDING
of VI International Workshop
« Alkaline magmatism, its sources and plumes »

Edited by Dr. N.V. Vladykin

IRKUTSK

NAPOLI

2007

UDK 552.33+552.32

Alkaline magmatism, its cources and plume

Proceedings of the VII International Conference. Naples. Italy. Publishing House of the Institute of Geography SB RAS, 2007, 192 p., ISBN 978-594797-128-6. Vol.1.

This book offers invited papers of the international workshop organized in Irkutsk and Naples. Alkaline rocks represent unique formations on the Earth. They are associated with large Nb, Ta, Zr, Y, TR, Cu and P deposits, gemstones of charoite, Cr-diopside, dianite. In Australia diamonds are recovered in lamproites. The complicated processes of their formation provoked scientific disputes still going on. The newly developed analytical methods and techniques provided abundant information on the composition of alkaline rocks. The data on geochemistry of isotopes confirm the evidence on the mantle --ources of the substance of alkaline rocks. Features of mineral parageneses and origin of mantle rocks can help in interpreting the deep-seated geodynamics of the Earth.

These papers view the features of alkaline, carbonatite and kimberlite magmatism. They also disclose the influence of the fluid on the thermal regime of mantle plumes. They discuss thermodynamic analysis of magnetite+titanite+ clinopyroxene equilibria in apatite-bearing intrusion of the Khibina alkaline complex, geochemistry of the dyke alkaline complex of the Kola Peninsula. They show geologic and petrologic characteristics of alkaline rocks of Italy. As to the kimberlites are concerned the papers consider variations of picroilmenite composition from many kimberlite pipes of Siberia; discuss the behavior of some minerals-indicators in kimberlites, mantle xenoliths from Nyurba pipe. The melted inclusions in olivines demonstrate mineral called rhönite and some papers give thermodynamic parameters of renite formation.

The articles give grounds for distinguishing formation types of lamproites and give types of their mantle sources. ASM diagrams are suggested to be used for genetic analysis of magmatic rock series.

The book might present interest to specialists involved in petrological and geochemical investigations as well as those studying deep alkaline and kimberlite magmatism, students and teaching staff of universities.

Published following the decision of the Scientific Council
of Vinogradov Institute of Geochemistry SB RAS

Chief Editor: Prof. N.V. Vladykin

Reviewers: *Prof. O.M. Glazunov*
and Prof. V.S. Antipin

Original-maket: *S.S. Tsypukova, T.S. Torbeeva*

Consultant: *Dr. Perepelov A.B.*

Institute of Geography SB RAS
664033, Irkutsk, Ulanbatorskaya str. 1

Published in Glazkovskaya printing House
Irkutsk, Gogol str., 53.
Order № 2792. Edition 100 copies.

ISBN 5-94797-095-3

TABLE OF CONTENTS

FOREWORD

The fact is well accepted that alkaline rocks represent unique formations on the Earth. They have been long attractive for research because large Nb, Ta, Zr, Y, TR, Cu and P deposits, gemstones of charoite, Cr-diopside, dianite are associated with them. For instance, in Australia diamonds are recovered in lamproites. The complicated processes of their formation provoked scientific disputes still going on. The newly developed analytical methods and techniques provided abundant information on the composition of alkaline rocks. The data on geochemistry of isotopes confirm the evidence on the mantle sources of the substance of alkaline rocks. The new concepts of plume tectonics are applied by scientists when studying alkaline rocks as the deep-seated geodynamics of the Earth is interpreted based on these data.

These problems were discussed at the international workshops held in 2001 at the Institute of Geochemistry in Irkutsk; in 2002 at the Far-East Geological Institute, Vladivostok; in 2003 at the Institute of Tectonics and Geophysics in Khabarovsk, in 2004 at Geological Institute in Ulan-Ude, in 2005 at the Institute of Volcanology and Seismology in Petropavlovsk-Kamchatski and 2006 at TsNIGRI of the Stock Company “ALROSA” (Mirnyi).

This book offers invited papers of the international workshop organized in Irkutsk and Naples under the title “Alkaline magmatism, its sources and plumes”.

These papers view the features of alkaline, carbonatite and kimberlite magmatism. They also disclose the influence of the fluid on the thermal regime of mantle plumes. They discuss thermodynamic analysis of magnetite+titanite+ clinopyroxene equilibria in apatite-bearing intrusion of the Khibina alkaline complex, geochemistry of the dyke alkaline complex of the Kola Peninsula. They show geologic and petrologic characteristics of alkaline rocks of Italy.

As to the kimberlites are concerned the papers consider variations of picroilmenite composition from many kimberlite pipes of Siberia; discuss the behavior of some minerals-indicators in kimberlites, mantle xenoliths from Nyurba pipe. The melted inclusions in olivines demonstrate mineral called rhönite and some papers give thermodynamic parameters of renite formation.

The articles give grounds for distinguishing formation types of lamproites and give types of their mantle sources. ASM diagrams are suggested to be used for genetic analysis of magmatic rock series.

The book might present interest to specialists involved in petrological and geochemical investigations as well as those studying deep alkaline and kimberlite magmatism.

Chairman of Organizing Committee,
Chief Editor Dr. N.V. Vladykin

UDK 550,42+552

Thermodynamic analysis of magnetite + titanite + clinopyroxene equilibria in apatite-bearing intrusion of the Khibina alkaline complex

Ryabchikov I.D.[1], Kogarko L.N. [2]

[1]*Institute for Geology of Ore Deposits, Russian Academy of Sciences, Moscow, Russia.*
[2]*Vernadsky Institute of Geochemistry, Russian Academy of Sciences, Moscow, Russia.*

ABSTRACT

Most titanomagnetite in the Khibina alkaline igneous complex, sampled through 500 m of a vertical cross-section, is represented by Ti-rich varieties. The ulvöspinel component is most commonly around 55 mol %, rarely reaching up to 80 mol %.

We calculated an f_{O2}-T diagram for magnetite + ilmenite + titanite + clinopyroxene + nepheline + alkali feldspar and magnetite + titanite + clinopyroxene + nepheline + alkali feldspar phase assemblages at a hedenbergite activity of 0.2. The diagram shows that magnetites with 55 mol % of ulvöspinel crystallized at oxygen fugacities just slightly below the quartz-fayalite-magnetite buffer. More Ti-rich varieties crystallized at higher temperatures and slightly lower □QMF values, whereas more Ti-poor magnetites crystallized at or below about 650°C.

Under the redox conditions estimated for the apatite-bearing intrusion of the Khibina complex (close to the QFM buffer), substantial quantities of methane may only form during cooling below 400°C in equilibrium with magma. However, even at higher orthomagmatic temperatures and redox conditions corresponding to ΔQMF=0, the hydrogen content in the early magmatic stage is not negligible. This hydrogen present in the gas phase at magmatic temperatures may migrate to colder parts of a solidifying magma chamber and trigger Fischer-Tropsch-type reactions there. We propose therefore, that methane in peralkaline systems may form in three distinct stages: orthomagmatic and late-magmatic in equilibrium with a melt and – due to Fischer-Tropsch-type reactions – post-magmatic in equilibrium with a local mineral assemblage.

Keywords: Oxygen fugacity; Khibina complex; Fe-Ti oxides; Titanite; Alkaline magmas; hydrocarbons

INTRODUCTION

Oxygen fugacity is an important parameter controlling the evolution of magmatic systems. It may determine the crystallizing mineral assemblage and thereby govern the path of fractional crystallization. The most striking example of this effect is strong iron enrichment without increase in silica content during the crystallization of tholeiitic basalts at relatively low oxygen fugacities (Fenner trend) and the fast growth of the silica content due to the early crystallization of magnetite (Bowen trend of calk-alkaline magmatic series) under oxidizing

conditions [29, 35]. In peralkaline systems, higher redox conditions may favour the crystallization of acmite-rich clinopyroxene, whereas at lower *f*O2 alkaline amphiboles may appear.

Oxygen fugacity may also control the partitioning of trace elements between melt and solid phases, particularly for elements with variable valency under the conditions of magmatic processes. Such elements include for example Eu, V and Cr. Recently, the behaviour of V in komatiites and other magmatic series was shown to be an efficient indicator of redox conditions [7-9].

Oxygen fugacity also controls the speciation of volatile components and their impact on magma genesis and differentiation. It has been suggested by some investigators, that reduced C-H-O volatiles initiated partial melting of mantle rocks after their ascent from greater depths and after their oxidation [13]. In alkaline magmatic systems, oxygen fugacity determines the presence of hydrocarbons and hydrogen which are commonly found in peralkaline, especially agpaitic rocks [3, 15, 18, 20, 23, 26, 27, 32-34, 40].

Several approaches have been used to estimate oxygen fugacities in magmatic systems. Some of them are based on equilibrium constants for the reactions between components of solid solutions including both ferrous and ferric iron. Pioneering work by Buddington and Lindsley [6] presented experimental data for equilibria of Ti-bearing magnetites with ilmenites, allowing simultaneous estimates of temperature and oxygen fugacity from compositions of coexisting Fe-Ti oxides. Later, this method was extended to spinels and ilmenites of more complex compositions by elaborated thermodynamic models of these phases in a multicomponent system [39]. This method has been successfully applied to fresh volcanic rocks, but is not useful for plutonic mineral assemblages due to the fast reequilibration of Fe-Ti oxides during slow cooling. For plutonic assemblages, it has been suggested to use equilibria of magnetites and ilmenites with ferromagnesian silicates [10, 11].

Wones [44] discussed the significance of the titanite-magnetite-quartz assemblage. He calculated the equilibrium T and f_{O2} conditions of titanite-involving reactions for pure phases in the system $CaO\text{-}FeO\text{-}Fe_2O_3\text{-}TiO_2\text{-}SiO_2$ at 1 bar. Later, these reactions were studied experimentally [46]. These experimental data were used to refine thermochemical data for titanite, which permitted the complete T-f_{O2} diagrams for this system to be constructed [47]. The experimental data were also used to estimate f_{O2} and T for mineral equilibria in some magmatic rocks [48]. Numerous estimates of oxygen fugacities for mantle peridotites and mantle-derived basaltic magmas were performed on the basis of redox reactions between components of magnetite-bearing spinels, olivines and orthopyroxenes [1, 2, 28, 38, 45].

Many authors have addressed the problem of oxygen fugacities in alkaline rocks. On the basis of stability relations between alkaline pyroxenes, amphiboles and aenigmatite it has been suggested that typical values for the Lovozero peralkaline massif are close to the quartz-fayalite-magnetite buffer [18]. Data on

spinels from OIBs, which include many alkaline basalts, nephelinites and melilitites, show relatively high oxygen fugacities, from the QFM buffer to 2 log units above this level [1]. Volcanics from Trindade, including late peralkaline differentiates [36], also show relatively high oxygen fugacities. Extremely high oxygen fugacities were found for high-Mg effusives and dyke rocks (meimechites and alkali picrites) from the Russian Maimecha-Kotuy province of alkaline rocks and carbonatites [37, 42]. Even higher oxygen fugacities were estimated for the Gronnedal-Ika Carbonatite-Syenite Complex, South Greenland [14].

Low oxygen fugacities, possibly reaching the field of Fe-Ni alloy stability, were reported for the peralkaline Ilimaussaq massif in South Greenland [23, 24]. It has also been suggested that f_{O2} rose during the evolution of the Ilimaussaq magmatic system, during the late stages exceeding the QFM buffer [23, 24]. Thus, alkaline rocks may form under extremely variable redox conditions.

GEOLOGICAL BACKGROUND, PETROGRAPHY AND SAMPLING STRATEGY

The Khibina magmatic complex in Russia's Kola Peninsula is one of the largest known alkaline intrusions. It has a concentric, zonal structure with well-developed primary igneous layering. There are eight zones in the complex – distinct rings and conical structures formed by successive phases of intrusion. The oldest rocks tend to occur towards the margins with successively younger intrusions encountered towards the center. Phase 1 comprises nepheline and alkali syenites and nepheline syenite-porphyries. Phase 2 consists of massive khibinites (see Table 1 for explanation of rock names), Phase 3 of trachytoid khibinites, Phase 4 of rischorrites (potassium-rich nepheline syenites). Phase 5 is composed of ijolites, melteigites and urtites and includes a stratified complex of rocks containing the well-known apatite ore deposits. Phase 6 consists of medium-grained nepheline syenites, phase 7 of foyaites, and phase 8 of carbonatites. Phase 5 of the Khibina Complex is of special interest because of the rich apatite ore it contains. The Phase 5 intrusion is shaped like a conical sheet which outcrops as a discontinuous ring with a diameter of 26-29 km and a length of ~ 75 km.

The Phase 5 intrusion has been separated into 3 subphases [49]: pre-ore (I), ore (II) and post-ore (III). Subphase I consists of ijolites interlayered with subordinate amounts of melteigite, urtite, juvite and malignite. Their total thickness is less than 700 m. Subphase II consists of massive feldspathic urtite, ijolite-urtite and apatite ore with a total thickness of 200 to 700 m. Subphase III is from 10 to 1400 m thick and includes leucocratic and melanocratic ijolites and malignites. The principal phosphate ore deposits are found in Subphase II where the apatite-rich rocks are found in the hanging wall of an ijolite-urtite intrusion. Common accessory minerals in the rocks of this phase are magnetite, titanite and apatite. It has been suggested that apatite crystallized from silicate magma and accumulated in the upper part of the magma chamber due to crystal sorting in the convecting melt [18, 19]. The upper parts of the apatite-rich bodies contain titanite-

apatite ores (~18% titanite) with elevated Fe-Ti oxide content (>4% magnetite). The main rock types of Phase 5 and their mineral composition are presented in Table 1.

Table 1.

Representativ mineral composition from the rocks of the Khibina massiv.

№	1	2	3	4	5	6	7	8	9
mineral	Mt	Mt	Mt	Mt	Mt	Mt	Mt	Mt	Ilm
SiO2	0.42	0.28	0.36	0.33	0.33	0.38	0.67	0.33	0.24
TiO2	2.85	17.76	19.67	10.34	24.19	18.17	28.91	13.99	53.26
Al2O3	0.09	0.10	0.01	0.08	0.05	0.11	0.03	0	0
Cr2O3	0.07	0.05	0.08	0.04	0.05	0.05	0.04	0.07	0.03
V2O3	0.40	0.33	0.65	0.26	0.33	0.31	0.22	0.39	0
Fe2O3	61.99	33.35	28.83	48.12	20.82	32.83	10.55	40.12	na
FeO	33.93	44.70	46.84	39.72	50.28	45.8	56.13	42.55	43.18
MnO	0.29	2.02	2.43	1.17	2.92	2.12	2.10	1.48	3.99
MgO	0	0.55	0.01	0.15	0.26	0.28	0.08	0.08	0.21
CaO							0.01	0	0
SrO							na	na	na
NiO							0.02	0.01	0.01
ZnO	0.07	0.13	0.23	0.07	0.20	0.17	0.05	0.01	0.01
Na2O							na	na	na
F							na	na	na
total	100.13	99.26	99.12	100.30	99.41	100.23	98.81	99.03	100.93

№	10	11	12	13	14	15	16	17	18
mineral	Ilm	Ttn	Ttn	Ttn	Ttn	Cpx	Cpx	Cpx	Cpx
SiO2	0.24	30.00	29.74	29.88	31.57	52.33	52.09	51.58	51.18
TiO2	52.87	37.68	37.54	38.76	36.31	3.70	2.46	0.78	1.15
Al2O3	0	0.37	0.21	0.22	0.79	0.54	0.45	0.44	1.07
Cr2O3	0.05	0	0.02	0	0	0.01	0	0.04	0
V2O3	0	na	na						
Fe2O3	na	na	na	na	na	21.9	25.47	14.37	6.70
FeO	41.25	1.42	1.14	0.91	1.28	4.85	2.90	7.82	7.21
MnO	6.08	0.07	0.07	0.08	0.06	0.78	0.45	0.52	0.57
MgO	0.13	0	0.02	0	0.01	0.75	1.09	4.67	9.29
CaO	0.02	26.94	26.38	26.83	25.19	3.33	2.76	13.23	20.24
SrO	na	0.35	0.59	0.47	0.44	na	na	na	na
NiO	0.01	na	na	na	na	0	0	0.02	0.01
ZnO	0.10	na	na						
K2O				0.08	0.06	0.01	0	0	0
Na2O	na	0.28	0.40	0.48	1.37	11.78	12.00	6.20	2.58
F	na	0.56	0.64	0.43	0.61	na	na	na	na
total	100.73	97.42	96.47	97.87	97.42	99.98	99.67	99.68	99.99

Magnetite and titanite are accessory minerals, present in almost all rock types of the Khibina pluton with the exception of rare lujavrites. Clinopyroxene is the most widespread coloured mineral. Both titanite and clinopyroxene are mainly

represented by euhedral grains. Magnetite in many cases also forms euhedral crystals, but may be present as subhedral grains squeezed in between silicate minerals. All three minerals are undoubtedly solid phases crystallized from the magma, and there are no reaction relations among them. They tend to occur in close spatial association in the rocks of the apatite-bearing complex [22]. Aggregates of all three minerals are often composed of grains with curvilinear boundaries (Fig. 1), suggesting that these minerals formed simultaneously during a specific magmatic stage. Magnetite is always more common (up to 11 vol. %) in titanite-rich cumulates in the upper part of this complex. All these observations indicate that magnetite, titanite and clinopyroxene belong to an equilibrium mineral assemblage.

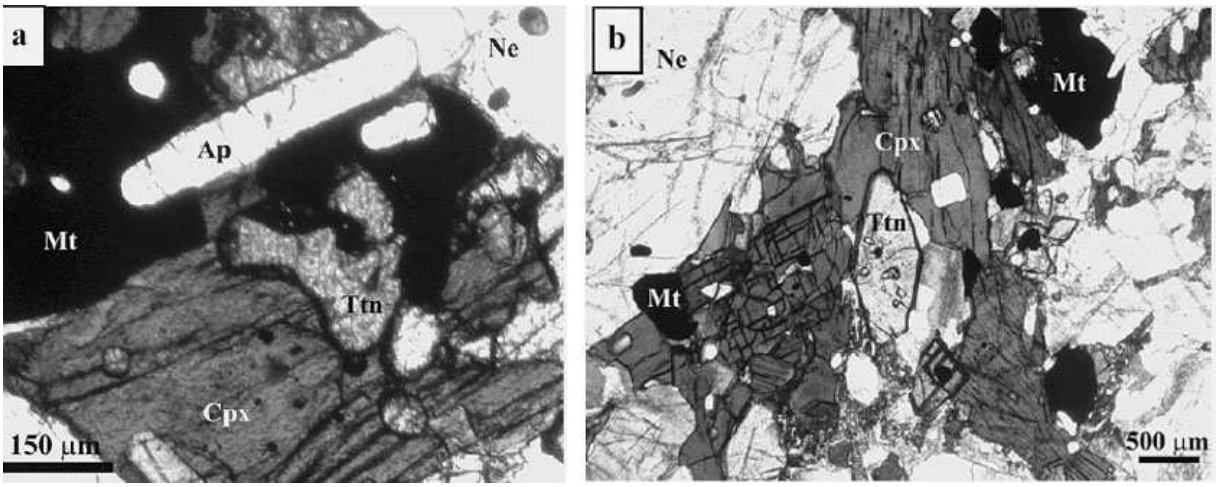

Fig. 1. **Clinopyroxene (Cpx), titanite (Ttn), magnetite (Mt) and apatite (Ap) surrounded by nepheline (Ne) in ijolites from the apatite-bearing intrusion of the Khibina complex.**

a) Aggregate of clinopyroxene, titanite and magnetite with curvilinear equilibrium boundaries;b) Euhedral titanite surrounded by clinopyroxene with magnetite grains near the margins of clinopyroxene.

In this study, we analyzed magnetites, titanites and clinopyroxenes from a vertical cross-section of the Phase 5 ijolite-melteigite-urtite intrusion using a core from the Koashva apatite deposit Borehole No 1312, from the southern part of the Khibina massif. The core covered depths from 450-750 meters and intersected rock series underlying the apatite-rich lode. The core contains juvites and feldspathic juvites in the upper part of the section and ijolites and melteigites in the lower part. Based on data from this core, we calculated the equilibria of magnetite with other minerals to estimate upper and lower limits for oxygen fugacity during their formation.

ANALYTICAL METHODS

Minerals from the investigated rocks were analyzed on a JEOL RL-8900 electron microprobe at the Max Planck Institut für Chemie, Abteilung Geochemie, Mainz, Germany, at 20 kV accelerating voltage, 20 nA sample current, and 2 □m

beam diameter. Counting times were 30-s for all elements on peak and 16-s on the background. Natural and synthetic minerals were used as calibration standards. Fe-Ti oxides showing no signs of exsolution under the electron microprobe might have had tiny exsolution features only visible with the TEM. However, nanoscale exsolution features would not have affected our measurements, because the 2 □m electron beam would have integrated their effects.

MINERAL COMPOSITIONS

Table 1 reports representative analyses of Fe-Ti oxides, titanite and clinopyroxene from the Borehole No 1312 core. The magnetites show a slight increase in V_2O_5 content towards the lower part of the magmatic body and no other significant compositional trends. The mode of TiO_2 content in the samples is 18-19 wt %. Similar compositions (17-19 wt.% TiO_2) are typical for magnetites from other parts of the Khibina pluton including apatite ores and titanite-apatite segregations [22].

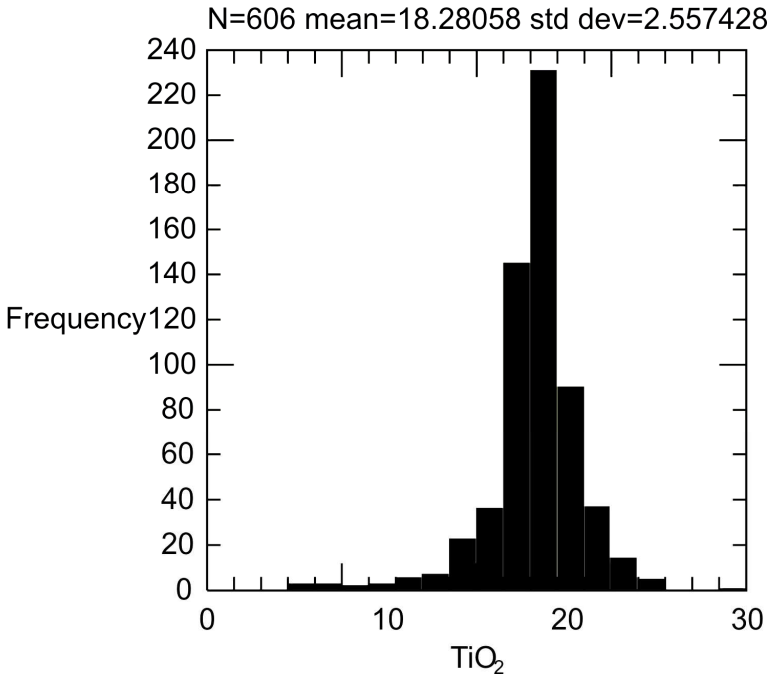

Fig. 2. **Histogram of TiO_2 contents in magnetites from Khibina massif, Borehole 1312.**

Most analyzed magnetite grains are homogeneous. Rarely we found ilmenite intergrowths with a texture similar to oxyexsolution textures. Titanomagnetite and ilmenite occasionally formed larger discrete grains. A number of analyzed grains exhibit higher TiO_2 contents (20-25 wt %), and one grain has 29 wt % TiO_2 which corresponds to 85 mol.% ulvöspinel. MgO contents in magnetites vary between 0.01 and 0.56 wt %, and MnO concentrations are relatively high, up to 3 wt % in Ti-rich varieties. As shown in Fig. 2, the analyzed samples average about 55 mol. % ulvöspinel.

Clinopyroxenes in the investigated rocks exhibit a wide range of compositions from diopside-rich (80 mol% of diopside) to acmite-rich varieties (80 mol% of acmite component). The hedenbergite content remains rather constant and is close to 20 mol% (the average of 196 analyses is 19 mol%), and only in late acmite-rich varieties, the hedenbergite content drops significantly.

Titanites are characterized by relatively constant composition. In addition to Ca, Ti and Si they contain 0.3 – 0.8 wt% Na_2O (average 0.48 %), 0.1 – 0.8 % Al_2O_3 (average 0.32%), 1 – 2 % FeO (average 1.25 %), 0.1 – 0.7 % SrO (average 0.41 %), and 0.4 – 1 % F (average 0.57 %). They may also contain 0.5 – 1 % Nb_2O_5+Ta_2O_5, about 0.5 % REE, 0.2 – 0.4 % ZrO_2, and possibly some H_2O [22]. We have, however, not analyzed titanites for these elements.

THERMODYNAMIC CALCULATIONS

We estimated f_{O2} values for the Khibina rocks based on data for the magnetite + ilmenite + titanite + hedenbergite + SiO_2 phase assemblage [46, 47], corresponding to the reaction:

$$3\ CaTiSiO_5 + 2\ Fe_3O_4 + 3\ SiO_2 = 3\ CaFeSi_2O_6 + 3FeTiO_3 + O_2 \quad (1).$$

These results were obtained for a_{SiO2}=1 and an activity of hedenbergite very close to 1. We recalculated the reaction with lower silica and hedenbergite activities defined by the nepheline + alkali feldspar phase assemblage and compositions of clinopyroxenes present in the Khibina rocks. For this task, we calculated a_{SiO2} values from the equilibrium constant of the reaction:

$$NaAlSiO_4 + 2\ SiO_2 = NaAlSi_3O_8 \quad (2)$$

Nepheline and albite activities were estimated from the compositions of nepheline and K-feldspar solid solutions present in Khibina melteigites [22] Published excess thermodynamic properties of framework silicates were used [31], Gibbs free energies for substances participating in this reaction are from Shapkin and Sidorov [41].

Most clinopyroxenes from the apatite-bearing Khibina intrusion have hedenbergite mole fractions around 0.2 [22], (Borutsky, 1988; see also Fig. 3). In clinopyroxene solid solutions with substitution of Ca^{2+} by Na^{1+} and Fe^{2+} or Mg^{2+} by Al^{3+}, activity coefficients are ~ 1 [30, 43]. As a first approximation, we therefore assumed that mixing properties of our $CaMgSi_2O_6$ – $CaFeSi_2O_6$ – $NaFeSi_2O_6$ pyroxenes are close to ideal, and for all our calculations accepted a_{Hed} = 0.2. We contend that this approximation is a serious source of uncertainty for the estimation of f_{O2} values. For example, an activity coefficient of 1.5 for hedenbergite in clinopyroxene solid solution would shift oxygen fugacity for phase assemblages with clinopyroxene and titanite towards lower values by half a log unit.

Compositions of titanites in the investigated rocks are relatively constant, and on the average they correspond to the following formula:

$$Ca_{0.948}Na_{0.031}Mn_{0.002}Sr_{0.008}Fe_{0.035}Ti_{0.944}Al_{0.013}Si_{0.996}O_4(O_{0.940}F_{0.060}).$$

Assuming that the thermodynamics of this phase may be approximated by the ideal multisite mixing model, the estimated activity of $CaTiSiO_4O$ is 0.85. Substitution of this value into the equilibrium constant of reaction (1) shows that oxygen fugacity would be lowered by 0.2 log units by comparison with pure end-member titanite. In fact, due to the ordering of the cation and anion distribution in various structural positions, the activity of the titanite component in the solid solution would be closer to 1.

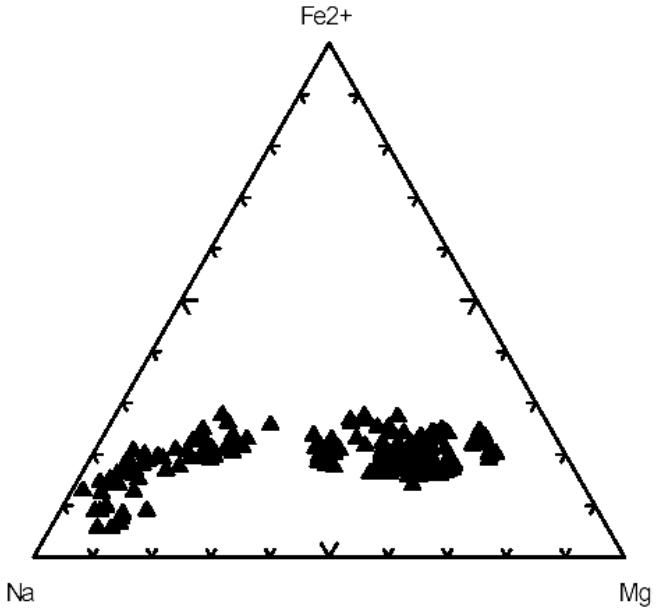

Fig. 3. **Triangular diagram for mole fractions of Na, Fe^{2+} and Mg in clinopyroxenes from the rocks in Borehole 1312.**

□QFM values for various temperatures ($\Delta QFM = \log_{10}(f_{O2}(rock)/f_{O2}(QFM)$, where QFM is the quartz – fayalite – magnetite oxygen buffer) were taken from the diagram for 1 bar of [47]. Using these values, activities and mole fractions of the Fe_2TiO_4 and Fe_3O_4 components were calculated by the solution of two simultaneous equations based on the equilibrium constants of the reactions:

$$2\ Fe_3O_4 + 6\ FeTiO_3 = 6\ Fe_2TiO_4 + O_2 \quad (3)$$

$$6\ Fe_2O_3 = 4\ Fe_3O_4 + O_2 \quad (4)$$

for which a_{usp} and a_{mt} were calculated from the mixing and thermodynamic properties of the endmembers of magnetite and ilmenite solid solutions [12, 39]. These values of a_{usp} and a_{mt} together with □QFM from [47] were used to calculate for a given temperature the equilibrium constant of the reaction:

$$CaFeSi_2O_6 + 3\ FeTiO_3 = CaTiSiO_5 + 2\ Fe_2TiO_4 + SiO_2 \quad (5)$$

Subsequently, this equilibrium constant was used to obtain □QFM, and the compositions and activities of components in both Fe-Ti oxides at $a_{Hed}<1$ and $a_{SiO2}<1$. For this, we used the constraint that the value of this equilibrium constant must be the same if $a_{Hed}=1$; $a_{SiO2}=1$ or $a_{Hed}<1$; $a_{SiO2}<1$. This permits to find a relation between ilmenite and ulvöspinel activities for these two cases, which may

be expressed as $a_{usp}^2/a_{ilm}^3 = a_{usp(0)}^2/a_{ilm(0)}^3 \cdot (a_{hed}/a_{SiO2})$, where $a_{usp(0)}$ and $a_{ilm(0)}$ are the previously estimated values of ulvöspinel and ilmenite activities at $a_{Hed}=1$ and $a_{SiO2}=1$. Using this new value of a_{usp}^2/a_{ilm}^3 we solved the simultaneous equations based on the equilibrium constants of reactions (3) and (4) and obtained the compositions of magnetite and ilmenite solid solutions and □QFM for a magnetite + ilmenite + titanite + clinopyroxene + nepheline + alkali feldspar phase assemblage at $a_{Hed}<1$ and $a_{SiO2}<1$.

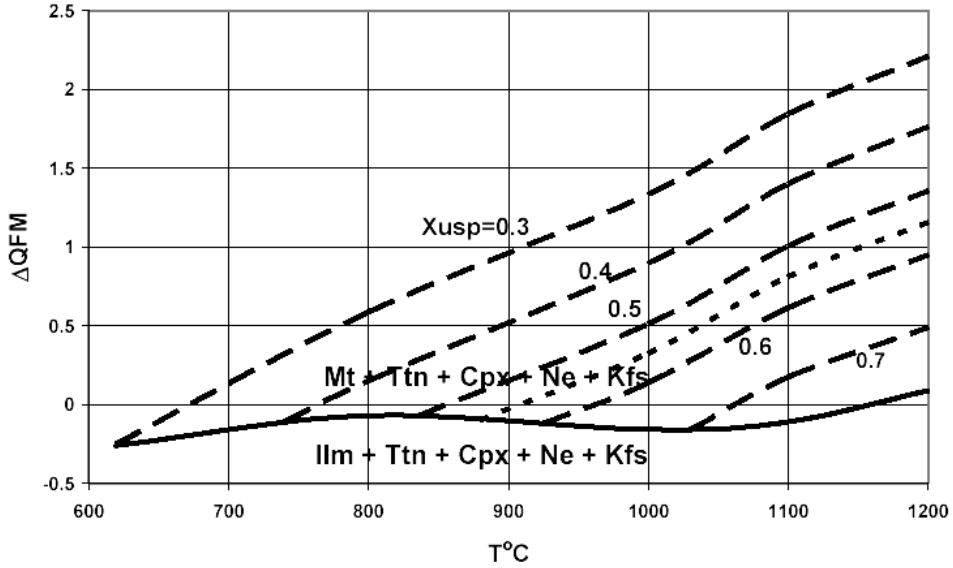

Fig. 4. **T - □QFM diagram for equilibria of Fe–Ti oxides.**

With titanite, clinopyroxene, nepheline and K-feldspar at P=1 bar, activity of hedenbergite equal to 0.2 and a_{SiO2} buffered by nepheline and K-feldspar with compositions typical of Khibina rocks. The solid line is the univariant reaction for the equilibrium of Ttn+Cpx+Ne+Kfs with both magnetite and ilmenite solid solutions. Dashed lines are isopleths for equilibria among Mt+Ttn+ Cpx+Ne+Kfs with fixed Xusp values for magnetites.

These values of □QFM for the magnetite + ilmenite + titanite + clinopyroxene + nepheline + alkali feldspar phase assemblage are shown by a solid line in Fig 4. At higher oxygen fugacities, magnetite may be present, but ilmenite is unstable in equilibrium with titanite + clinopyroxene + nepheline + alkali feldspar. At lower oxygen fugacities, there is a magnetite-free field with ilmenite. Thus, when titanite and clinopyroxene are present, the calculated lower limit for magnetite solid solution stability lies at much higher f_{O2} than when clinopyroxene and titanite are absent. In the absence of titanite and clinopyroxene, the lower limit for magnetite solid solution stability is much lower and is defined by the following reactions:

$$3\ CaSiO_3 + 3\ Fe_2TiO_4 + O_2 = 3\ CaTiSiO_5 + 2\ Fe_3O_4 \qquad (6)$$

$$3\ Fe_2SiO_4 + O_2 = 2\ Fe_3O_4 + 3\ SiO_2 \qquad (7)$$

In the ilmenite-free field above Fig. 4's magnetite+ilmenite univariant line, oxygen fugacity is fixed for each temperature and magnetite composition. To find f_{O2} for various temperatures and magnetite compositions, we recalculated the

previously estimated □QFM values for the magnetite + ilmenite + titanite + clinopyroxene + nepheline + alkali feldspar phase assemblage to the new composition of magnetite based on the equation for the equilibrium constant of the reaction:

$$2\ CaTiSiO_5 + 2Fe_3O_4 + 2\ SiO_2 = 2\ CaFeSi_2O_6 + 2\ Fe_2TiO_4 + O_2 \qquad (8)$$

using the following formula:

$$\square QFM = \square QFM(i) + 2\cdot\log_{10}(a_{usp}(i)/a_{mt}(i)/a_{usp}\cdot a_{mt})$$

where □QFM(i), $a_{usp}(i)$ and $a_{mt}(i)$ are values for a phase assemblage with ilmenite and magnetite and □QFM, a_{usp} and a_{mt} represent an ilmenite-free assemblage for a given magnetite composition. Calculated isopleths of magnetite composition are shown as dashed lines in Fig. 4. As in the case of reaction (5), we have not calculated □G of reaction (8) from tabulated thermodynamic data, but only used the fact that the equilibrium constant of this reaction must be the same for a phase assemblage with both ilmenite and magnetite (for which □QFM has already been estimated) and for ilmenite-free phase assemblages at the same temperature.

This diagram has been calculated at a pressure of 1 bar, whereas the mineral assemblages in the rocks of the Khibina pluton equilibrated at higher pressures. However, since the oxygen fugacities of Fig. 4 are expressed relative to the QFM buffer, pressure does not affect it significantly because f_{O2} values for the QFM buffer and for the other redox reactions with ferric and ferrous iron are displaced with increasing pressure in the same direction and approximately to the same extent. Therefore, increase in pressure by 0.1 GPa would shift the calculated □QFM values by not more than 0.1 log unit.

Magnetite containing 55 mol% ulvöspinel is the most common composition for the borehole 1312 core sample. For this composition, Fig. 4 shows that magnetite should crystallize at temperatures above 880°C and oxygen fugacities close to the QFM buffer (□QFM = – 0.1 at 880°C and □QFM = + 0.3 at 1100°C).

The observed variations in magnetite composition imply that crystallization took place at a range of temperatures and oxygen fugacities. According to Fig. 4, more Ti-rich magnetites with about 25 % TiO_2 (70 mol% ulvöspinel, Table 3, analysis 5) would have crystallized above 1030°C and □QFM close to – 0.2. The intergrowth of discrete magnetite (40 mol% ulvöspinel) and ilmenite grains (Table 3, analyses 8 and 9) would correspond to 740°C and □QFM = – 0.1. Magnetite grains with oxyexsolution textures (Table 3, analyses 1 and 10) crystallized at even lower temperatures.

The most likely temperature range of magnetite crystallization may be accessed from the fact that gravitational sorting in the convecting magma of the Khibina pluton resulted in the accumulation of magnetite together with apatite and titanite in the upper part of the intrusion. This implies that magnetite crystallized simultaneously with apatite. An investigation of melt inclusions in nephelines and apatites from the Khibina intrusion yielded magmatic temperatures of 850-950°C [18] which is consistent with the current estimate of >880°C for the most common magnetite composition in the borehole No. 1312 core.

Based on our calculations, we estimate oxygen fugacities in this temperature range (850 – 950°C) close to the QFM buffer. A similar conclusion was reached for the peralkaline rocks of the Lovozero massif – adjacent to the Khibina massif – based on the relative stabilities of aegirine, arfvedsonite and aenigmatite [18]. However, a much lower range of oxygen fugacities has been proposed for the Ilímaussaq massif and neighbouring dykes [23-25]. According to these authors, QFM decreased during fractionation in the augite syenite of the Ilímaussaq massif from about –1 to below – 4, but increased in the peralkaline stage to values above QFM.

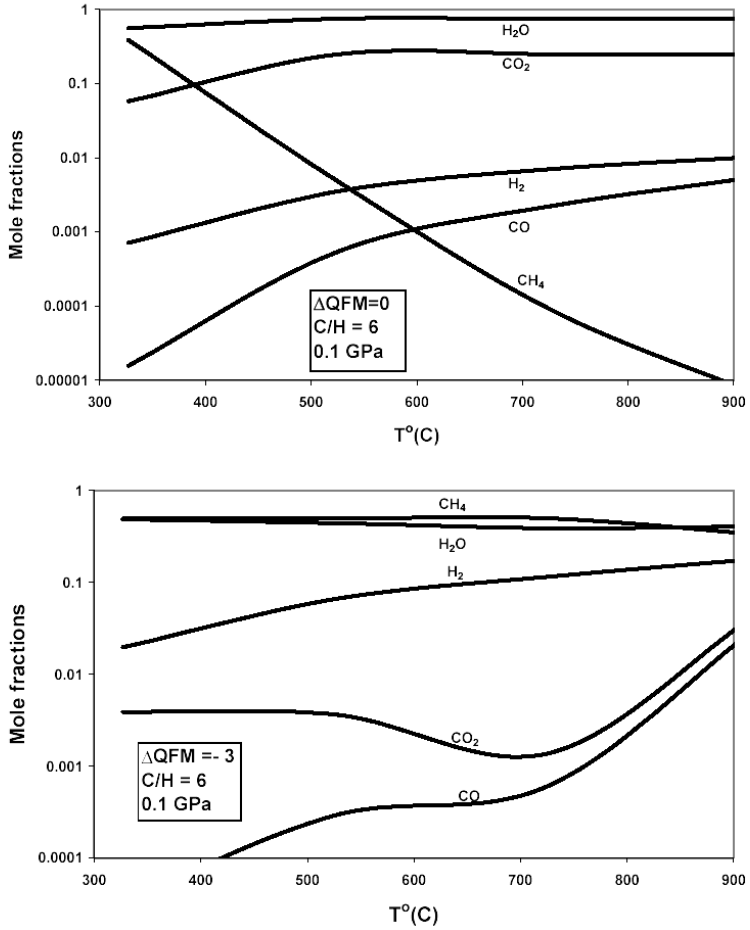

Fig. 5. **Composition of the C−H−O gas as a function of temperature at ΔQMF of 0 and -3. P=0.1 GPa. H/C=6.**

Wide variations of oxygen fugacity in alkaline rocks, with very reducing conditions in local areas, raise the question of whether hydrocarbon-bearing fluids – present in microinclusions in minerals of peralkaline rocks – may have formed in the magmatic stage, or whether they could only be produced by non-equilibrium synthesis at low temperatures [3, 20, 34, 40]. We calculated the composition of gas in the C-H-O system at ΔQFM equal to 0 and –3 by simultaneously solving several equations for the equilibrium constants of the following reactions which were calculated from the standard thermodynamic properties of components by [41] and fugacities of gases from [4]:

$CH_4 + 2O_2 = CO_2 + 2H_2O$ (9)

$CO + 0.5\ O_2 = CO_2$ (10)

$H_2 + 0.5\ O_2 = H_2O$ (11)

We used the additional constraints $\sum X_i=1$ and $(4X_{CH4}+2X_{H2O}+2X_{H2})/(X_{CH4}+X_{CO2}+X_{CO}) = 6$. We assumed H/C = 6 for all calculations, because many fluid inclusions in alkaline rocks contain substantial amounts of hydrogen in addition to methane [20, 34] and our unpublished data).

The results of these calculations are shown in Fig. 5. Even at ΔQFM = 0, the hydrogen content at early magmatic temperatures approaches 1 mol%. Methane is low at 900°C but becomes one of the major species in gas below 400°C [20]. At ΔQFM = -3, the methane content in the gas is comparable to that of water at both high and low temperatures. The hydrogen content is high at high temperatures (X_{H2} > 0.1 at 900°C), but falls during cooling. However, even below 400°C the hydrogen content remains >1 mol% at ΔQFM = -3.

These results indicate that under the very reducing conditions found in some alkaline magmatic systems [23], hydrocarbons may be present even at the early magmatic stage through equilibration of the gas phase with the magma. Under more oxidizing conditions – close to QFM buffer as is the case for Khibina magma – methane may form in substantial quantities during cooling below 400°C in the equilibrium gas phase.

Migration of hydrogen formed at high magmatic temperatures to the cooler parts of the magmatic system facilitated by fast diffusion of H_2 may cause the production of hydrocarbons at lower temperatures by Fischer-Tropsch synthesis. The supply of hydrogen is important for this type of reaction, advocated by some authors for the production of abiogenic hydrocarbons [17, 34, 40]. It has been suggested that hydrogen is produced by dehydration of amphibole in alkaline magmatic systems [34]. However, this explanation does not seem satisfactory. Hydrogen may appear during amphibole dehydration in substantial quantities only if oxygen fugacity is sufficiently low, which has not been demonstrated for reactions with amphibole in alkaline rocks. There is no convincing evidence of widespread amphibole dehydration in Khibina or Lovozero, partly because amphiboles present in these rocks are fluor-amphiboles with low water contents. In our opinion, migration of hydrogen from hot to cold parts of a magmatic system, triggering Fischer-Tropsch synthesis, is a more plausible mechanism.

CONCLUSIONS

1. Most magnetite in the Khibina alkaline igneous complex, sampled through a vertical cross-section of 500 m, is represented by Ti-rich varieties with typical ulvöspinel contents of about 55 mol %. In rare cases, ulvöspinel reaches 80 mol %.

2. The calculated f_{O2}-T diagram (Fig. 4) shows that magnetites with 55 mol % of ulvöspinel component in equilibrium assemblages with clinopyroxene

and titanite crystallize above 900°C at oxygen fugacities just below the quartz-fayalite-magnetite buffer. More Ti-rich varieties crystallize at higher temperatures and lower □QMF, while more Ti-poor magnetites crystallize at or below 650°C.

3. Under the redox conditions estimated for the apatite-bearing intrusion of the Khibina complex – close to the QFM buffer – methane may form in substantial quantities during cooling below 400°C in the equilibrium gas phase. However, even at ΔQMF=0, the hydrogen content at orthomagmatic temperatures is not negligible.

4. Under very reducing conditions found in some alkaline magmatic systems (Markl et al., 2001), hydrocarbons may be present even at high, orthomagmatic temperatures as a result of equilibration of the gas phase with magma.

5. Hydrogen present in a gas phase at magmatic temperatures may migrate to colder parts of a solidifying magma chamber and trigger Fischer-Tropsch type synthesis there.

ACKNOWLEDGEMENTS

This work has been financially supported by the Russian Foundation for Basic Research. The authors are grateful to Gregor Markl and Brennan Klose for constructive criticism, useful suggestions and considerable linguistic improvement.

REFERENCES

1. **Ballhaus C.** Redox states of lithospheric and asthenospheric upper mantle // Contrib. Mineral. Petrol., 1993, v. 114, p. 341-348.
2. **Ballhaus C., Berry R.F., Green, D.H.** Oxygen fugacity controls in the Earth's upper mantle // Nature, 1990, v. 348, p. 437-440.
3. **Beeskow B., Treloar P.J., Rankin A.H., Vennemann T.W., Spangenberg, J.** A reassessment of models for hydrocarbon generation in the Khibiny nepheline syenite complex, Kola Peninsula, Russia // Lithos, 2006, (This issue).
4. **Belonoshko A., Saxena S.K.** Equations of state of fluids at high temperature and pressure (water carbon dioxide, methane, oxygen, and hydrogen) // In: S.K. Saxena (Editor), Thermodynamic Data: Systematics and Estimation (Adv Phys Geochem). Springer-Verlag, New York, 1992, v.10, p. 79-97.
5. Borutsky B.E., Rock-forming minerals of highly alkaline complexes (in Russian) // Nauka Publishers, Moscow, 1988, 215 p.
6. **Buddington A.F., Lindsley D.H.** Iron-titanium oxide minerals and synthetic equivalents // Journ. Petrology, 1964, v. 5, p. 310-357.
7. **Canil D.** Vanadium partitioning and the oxidation state of Archean komatiite magmas // Nature, 1997, v. 389, p. 842-845.
8. **Canil D.** Vanadium partitioning between orthopyroxene spinel and silicate melt and the redox states of mantle source regions for primary magmas // Geochim. Cosmochim. Acta, 1999, p. 557-572.
9. **Canil D.** Vanadium in peridotites, mantle redox and tectonic environments: Archean to present // Earth Plan. Scien. Let., 2002, v. 195, p. 75-90.

10. **Frost B.R., Lindsley D.H.** Occurence of iron-titanium oxides in igneous rocks, in: Oxide minerals: petrologic and magnetic significance // In: D.H. Lindsley (Editor), Mineral. Soc. Am., Washington D.C., 1991, p. 433-467.
11. **Frost B.R., Lindsley D.H., Andersen, D.J.** Fe-Ti oxide - silicate equilibria: assemblages with fayalitic olivine // Am. Mineral., 1988, v. 73, p. 727-740.
12. **Ghiorso M.S., Sack R.O.** Thermochemistry of the oxide minerals // In: D.H. Lindsley (Editor), Rev. in Mineral. Miner. Soc. of Am., Washington D.C., 1991, p. 221-264.
13. **Green D.H., Falloon T.J., Taylor W.R.** Mantle-derived magmas - roles of variable source peridotite and variable C-O-H fluid compositions // In: B.O. Mysen (Editor), Soc. Spec. Pub., 1987, p. 139-154.
14. **Halama R., Vennemann T., Siebel W., Markl G.** The Gronnedal-Ika Carbonatite-Syenite Complex, South Greenland: Carbonatite Formation by Liquid Immiscibility // J. Petrology, 2005, v. 46, № 1, p. 191-217.
15. **Ikorsky S.V., Shugurova N.A.** New data on the composition of gases in minerals of the alkaline rocks of the Khibina Massif (in Russian) // Geokhimiya, 1974, v. 6, p. 953-947.
16. **Kamenev E.A.** Structures of ore fields of the Khibina apatite-nepheline deposits (in Russian). Prospecting and geological-industrial evaluation of the Khibina type apatite deposits (methodical basis). Nedra, Leningrad, 1987, p. 188.
17. **Kelley D.S.** Methane-rich fluids in the oceanic crust // J. Geophys. Res., 1996, v. 101 (B2), p. 2943– 2962.
18. **Kogarko L.N.** Problems of the genesis of agpaitic magmas (in Russian) // Nauka Publishers, Moscow, 1977, 294 p.
19. **Kogarko L.N., Khapaev V.V.** The modelling of the formation of apatite deposits of the Khibina massif (Kola Peninsula) // In: I. Parsons (Editor), Origins of igneous layering. Reidel Publishing Company, Dordrecht, 1987, p. 589-611.
20. **Kogarko L.N., Kosztolanyi C., Ryabchikov I.D.** Geochemistry of the reduced fluid of alkaline magmas (in Russian) // Geokhimiya, 1986, p. 1688-1695.
21. **Kostyleva-Labuntsova E.E. et al.** Mineralogy of the Khibina massif (magmatism and postmagmatic formations) (in Russian) // Nauka Publishers, Moscow, 1978a, 1, 228 p.
22. **Kostyleva-Labuntsova E.E. et al.** Mineralogy of the Khibina massif (minerals) (in Russian) // Nauka Publishers, Moscow, 1978b, 2, 586 p.
23. **Markl G., Marks M., Schwinn G., Sommer H.** Phase equilibrium constraints on intensive crystallization parameters of the Ilimaussaq Complex, South Greenland // Jour. Petr., 2001, v. 42, p. 2231-2258.
24. **Marks M., Markl G.** Fractionation and assimilation processes in the alkaline augite syenite unit of the Ilimaussaq Intrusion, South Greenland, as deduced from phase equilibria // Jour. Petrol., 2001, v. 42, p. 1947-1969.
25. **Marks M., Markl G.** Ilimaussaq 'en miniature': closed system fractionation in an agpaitic dyke rock from the Gardar Province, South Greenland (contribution to the mineralogy of Ilimaussaq no. 117) // Mineral. Mag., 2003, v. 67, p. 893-920.
26. **Nivin V.A.** Gas concentrations in minerals with reference to the problem of the genesis of hydrocarbon gases in rocks of the Khibiny and Lovozero massifs // Geochem. Int., 2002, v. 40, p. 883–898.
27. **Nivin V.A., Treloar P.J., Konopleva N.G., Ikorsky S.V.** A review of the occurrence, form and origin of C-bearing species in the Khibiny Alkaline Igneous Complex, Kola Peninsula, NW Russia // Lithos, 2005, v. 85, p. 93-112.
28. **O'Neill H.S.C., Wall V.J.** The olivine-spinel oxygen geobarometer, the nickel precipitation curve and the oxygen fugacity of the upper mantle // J. Petrol., 1987, v. 28, p. 1169-1192.
29. **Osborn E.F.** Role of oxygen pressure in the crystallization and di□erentiation of basaltic magma // Am. J. Sci., 1959, v. 257, p. 609-647.

30. **Perchuk A.L., Aranovich L.Y.** Thermodynamics of the jadeite diopside hedenbergite solid-solution model // Geokhimiya, 1991, № 4, p. 539-547.
31. **Perchuk L.L., Podlesskii K.K., Aranovich L.Y.** Themodynamics of some framework silicates and their equilibria: application to geothermobarometry // In: L.L. Perchuk (Editor), Progress in metamorphic and magmatic petrology. Cambridge University Press, Cambridge, 1991, p. 131-164.
32. **Petersilie I.A.** Hydrocarbon gases and bitumens of the intrusive massifs of the central part of Kola Peninsula (in Russian) // Doklady AN SSSR, 1958, v. 122, № 6, p. 1086-1089.
33. **Petersilie I.A., Sørensen H.** Hydrocarbon gases and bituminous substances in rocks from the Ilimaussaq alkaline intrusion, South Greenland // Lithos, 1970, v. 3, p. 59-76.
34. **Potter J., Rankin A.H., Treloar P.J.** Abiogenic Fischer–Tropsch synthesis of hydrocarbons in alkaline igneous rocks; fluid inclusion, textural and isotopic evidence from the Lovozero complex, N.W. Russia // Lithos, 2004, v. 75, p. 311-330.
35. **Presnall D.C.** The join forsterite-diopside-iron oxide and its bearing on the crystallization of basaltic and ultramafic magmas // Am. J. Sci., 1966, v. 264, p. 753-809.
36. **Ryabchikov I.D., Kogarko L.N.** Redox equilibria in alkaline lavas from Trindade Island, Brasil // International Geol. Rev., 1994, v. 36, p. 173-183.
37. **Ryabchikov I.D. et al.** Thermodynamic Parameters of Generation of Meymechites and Alkaline Picrites in the Maimecha–Kotui Province: Evidence from Melt Inclusions // Geoch. Inter., 2002, v. 40, № 11, p 1031-1041.
38. **Ryabchikov I.D., Ukhanov A.V., Ishii T.** Redox equilibria in upper mantle ultrabasites in the Yakutia kimberlite province // Geoch. Int., 1986, v. 23, p. 38-50.
39. **Sack R.O., Ghiorso M.S.** An internally consistent model for the thermodynamic properties of Fe-Mg-titanomagnetite-aluminate spinels // Contrib. Mineral. Petrol., 1991, v. 106, p. 474-505.
40. **Salvi S., Williams-Jones A.** Alteration, HFSE mineralisation, and hydrocarbon formation in peralkaline igneous systems: Insights from the Strange Lake Pluton, Canada // Lithos, 2006, (this issue).
41. **Shapkin A.I., Sidorov Y.I.** Thermodynamic models in cosmochemistry and planetology // Geoch. Inter., 2003, v. 41, suppl. 1: S1-S144.
42. **Sobolev A.V., Kamenetskaya V.S., Kononkova N.N.** New data on petrology of Siberian meimechites // Geoch. Inter., 1991, v. 8, p. 1084-1095.
43. **Vinograd V.L.** Thermodynamics of mixing and ordering in the diopside-jadeite system: I. A CVM model // Mineral. Mag., 2002, v. 66, № 4, p. 513-536.
44. **Wones D.R.** Significance of the assemblage titanite + magnetite + quartz in granitic rocks // Am. Miner., 1989, v. 74, p. 744-749.
45. **Wood B.J., Bryndzya L.T., Johnson K.E.** Mantle oxidation state and its relationship to tectonic environment and fluid speciation // Science, 1990, v. 248, p. 337-345.
46. **Xirouchakis D., Lindsley D.H.** Equilibria among titanite, hedenbergite, fayalite, quartz, ilmenite, and magnetite: Experiments and internally consistent thermodynamic data for titanite // Am. Miner., 1998, v. 83, № 7-8, p. 712-725.
47. **Xirouchakis D., Lindsley D.H., Andersen D.J.** Assemblages with titanite ($CaTiOSiO_4$), Ca-Mg-Fe olivine and pyroxenes, Fe-Mg-Ti oxides, and quartz: Part I. Theory // Am. Miner., 2001a, v. 86, p. 247-253.
48. **Xirouchakis D., Lindsley D.H., Frost B.R.** Assemblages with titanite ($CaTiOSiO_4$), Ca-Mg-Fe olivine and pyroxenes, Fe-Mg-Ti oxides, and quartz: Part II. Application // Am. Miner., 2001b, v. 86, p. 254-264.
49. **Zak S.L. et al.** The Khibina alkaline massif (in Russian) // Nedra, Leningrad, 1972, 175 p.

UDK 552.321

Formation types of lamproite complex – systematics and chemistry.

Vladykin N.V.

. Vinogradov Institute of Geochemistry, Siberian Branch, Russian Academy of Sciences

ABSTRACT

Lamproites of Russia and the whole world have been thoroughly studied for the last 25 years. The samples, collected in abundance do not fit into one group of rocks due to various chemical and mineral compositions of lamproites. Analyzing all available data the author suggests distinguishing 4 formation types of lamproite complexes. The article gives a critical review of lamproite classification and offers a rational option. The article discusses lamproites of two large areas of lamproite magmatism occurrence in Siberia – Aldan and Anabar Region, discovered by the author when studying alkaline rocks in these regions. We discuss mineral and chemical compositions of lamproites, their petrochemical and geochemical features and chemical composition of composing minerals. An intrusive type of lamproites has been revealed. Using the geochemistry of Nd and Sr isotopes we give an analysis of their mantle sources. We also discuss problems of diamond-bearing potential of lamproites.

INTRODUCTION

When it was discovered that Australian lamproites are potential for diamonds, the scientists started comprehensive investigations, which have been performing in different provinces of the world for at least the last 25 years. Thanks to those investigations the “lamproite problem” expanded, however it has not been solved. A great number of samples collected do not fit into one group of rocks or formation due to various chemical and mineral compositions of lamproites. When lamproites were discovered among kimberlites (Finland, China, Anabar Region) it becomes evident, that lamproites can have a different origin and can be related to different formations of rocks. The published monographs [1, 2, 3] give the detailed description of many provinces of lamproite volcanism (in particular Australian), discuss mineralogical and geochemical features and genesis of magma. However, the criteria towards the lamproite prospecting as well as the criteria in regard to diamond-bearing potential are still lack. There is no clear classification of lamproites that is in particular true for Russian literature sources. Scientists studying kimberlites but not studying lamproites when making reference to different literature sources, "consider" pyropes present in lamproites as the diagnostic features; however lamproites are usually free of pyropes [2]. When scientists discuss diamond-bearing potential of lamproites they mainly take into account features of only Australian lamproites, in particular those typical of leucite

(diamond-free) lamproites. These features include high concentrations of titanium, niobium, zirconium which are accumulated as a result of drastic differentiation of high-alkali agpaitic leucite lamproites. These features are less common to primary diamond-bearing poorly-differentiated olivine lamproites.

NOMENCLATURE AND CLASSIFICATION OF LAMPROITES

Lamproites were first described by Gross in 1897 for Leucite-Hills (USA), and in 1906 for Spain. Australian lamproites were studied in 1940-ies by Wade and Prider. The first classification of lamproites was proposed by Niggli in 1923. Thus, lamproites of all three provinces but not only Australian one can be considered as proper lamproites. In each of these provinces lamproites have the local names (about 20), that is very inconvenient for the classification. Within the last 20 years in different areas of the world the scope of rocks, considered as lamproites has considerably expanded, several lamproite classifications have appeared [1, 2, 3]. Classification of lamproites becomes more complicated because of variations in chemical composition of lamproites, for example: with respect to MgO - from 30 to 5 %; SiO_2 - from 40 to 65 %; K_2O from 3 to 13 % that is connected with specific mineral composition of lamproites. Lamproites demonstrate six characteristic rock-forming minerals. Contrast chemical composition of minerals (Table 1) and their varying quantitative ratios in the rock lead to sharp changes in chemistry of lamproites. It also results in a unique drastic differentiation of lamproites even at the stage of crystallization of volcanics - from olivine to leucite varieties [11, 15]. Elements of classification should correspond to standard for all other rocks. The nomenclature and classification of rocks (intrusive and volcanic) available at present includes two main elements: 1) chemical composition, 2) mineral composition. For example: if in terms of chemical and mineral compositions the considered rocks correspond to granites irrespective of their genesis, they are considered to be granites. And a further explanation is followed, they could be magmatic, metasomatic, etc. The same is to be true for lamproites. If by the chemical and mineral compositions a volcanic or an intrusive rock corresponds to lamproite, irrespective of its genesis, it has to be regarded as lamproites [17]. Another problem whether it could be diamond-bearing? When we have to resolve this problem we have to compare it with diamond-bearing lamproites, i.e. with early olivine, but not with leucite (diamond-free) lamproites. There are also disputes, whether intrusive analogs of volcanic lamproites are available? Undoubtedly, they have to exist, because if the magma didn't erupt, it could give rise to intrusive analogs. Such rocks are available [10, 14, 15, 17]; however, it is difficult to distinguish them from alkaline rocks of another origin. To distinguish between them we have to apply the geochemical factor. What rocks can be regarded as lamproites?

Lamproites represent volcanic, subvolcanic and intrusive rocks consisting of different ratios of main six rock-forming minerals (which demonstrate a relatively stable chemical composition): olivine, clinopyroxene ,

mica, leucite, K-alkaline amphibole and K-feld spar (sanidine). Occurrence of at least three out of these minerals is required. Depending on ratios of minerals the chemical composition of the rock significantly varies: SiO_2 - 40-65 %, Al_2O_3 - 5-12 %, MgO--30-5 %, K_2O - 3-12 %, MgO> CaO, K_2O>> Na_2O [17].

Lamproites, as opposed to other rocks, represent high-potash and high-magnesium rocks of the leucite series. At different variations of mineral ratios lamproites can be similar to rocks of different series: kimberlites, picrites, alkaline melasyenites (minettes), foidites, alkaline basaltoids, and thus it is necessary to find the distinguishing border between rocks of these series and lamproites.

The first, very important diagnostic mineral feature of lamproites includes a complete **absence of sodium leucophases: plagioclase and nepheline**. If the potash alkaline rock demonstrates plagioclase it is evidence that this rock doesn't belong to the lamproite series.

Table 1

Element concentrations in minerals of lamproite.

mineral	SiO	MgO	CaO	K2O	Al2O3
olivine	41	50	-	-	-
diopside	55	18	26	-	-
mica	35-40	24	-	10	8-10
K-richterite	50	18	10	5	-
leucite	58	-	-	20	22
feld spar	64	-	-	16	20

The second diagnostic feature is the composition of rock-forming minerals: olivine - 86-94 % of forsterite minal, clinopyroxene – diopside- salite series, mica - Fe-phlogopite-Ti-phlogopite – tetraferriphologopite, amphibole – series of K-richterite - K-arfvedsonite, leucite contains usually FeO - 1-4 % and surplus of SiO_2, potash feld spar - sanidine, pure potash, and contains 0,5-4 % of FeO. In respect of accessory minerals the characteristic include: chromite, Cr-magnetite, perovskite, titanate – priderite, jeppeite, armalcolite; Zr-Ti-silicates - wadeite, K-batisite, davainite. However, the majority of them occur in differentiated agpaitic, leucite lamproites, while the diamond-bearing olivine lamproites usually demonstrate: chromite, Cr-magnetite, perovskite, in cases perovskite, sphene, apatite and, infrequently, zircon. By the mineral association early olivine lamproites are insignificantly different from massive (non-brecciated) magmatic kimberlites. Most likely the main difference from massive kimberlites is potential ability of the primary magma for differentiation. Massive crystallized kimberlites represent extreme differentiates of kimberlitic magma; the magmatic process is accomplished. The magma differentiation starts with olivine lamproites (it is the earliest product), and later differentiates originate further (leucite and sanidine varieties of lamproites). Such difference can be connected with various primary composition of magma, which results from the degree of partial melting of the

mantle substratum. In order to distinguish similar kimberlites and lamproites one has to study melted inclusion. Such inclusions are usually lack in kimberlites (that is due to various reasons), while inclusions in lamproites contain melts of later differentiates.

High-baric **minerals, such as pyrope and picroilmenite are not characteristic of lamproites; this is a feature distinguishing them from lamproites** [2, 17]. Xenoliths of mantle rocks are rare in lamproites. It does not mean, that when the primary lamproite magma formed it was free of xenoliths, pyrope and picroilmenite. As the primary lamproite magma is high-alkaline and has a high reactivity, deep-seated xenoliths and megacrysts are simply dissolved in it that can result in high titanium concentration in late differentiates of lamproites.

Geochemical diagnostic features include: high concentrations of Cr - 500-3000 ppm, Ni - 300-2000 ppm (Cr> Ni), increased contents of Zr, Nb, Ti and cerium TR. Depending on the degree of lamproite differentiation (early - olivine, late - leucite) rare element concentrations are also varying. Early lamproites show high Cr and Ni concentrations, which decrease in later differentiates, while Zr, Nb, Ti, TR contents sharply increase in late lamproites. At relatively high Ba and Sr concentrations early lamproites frequently contain more Ba than Sr, while in late lamproites Sr content significantly increases, as opposed to early ones.

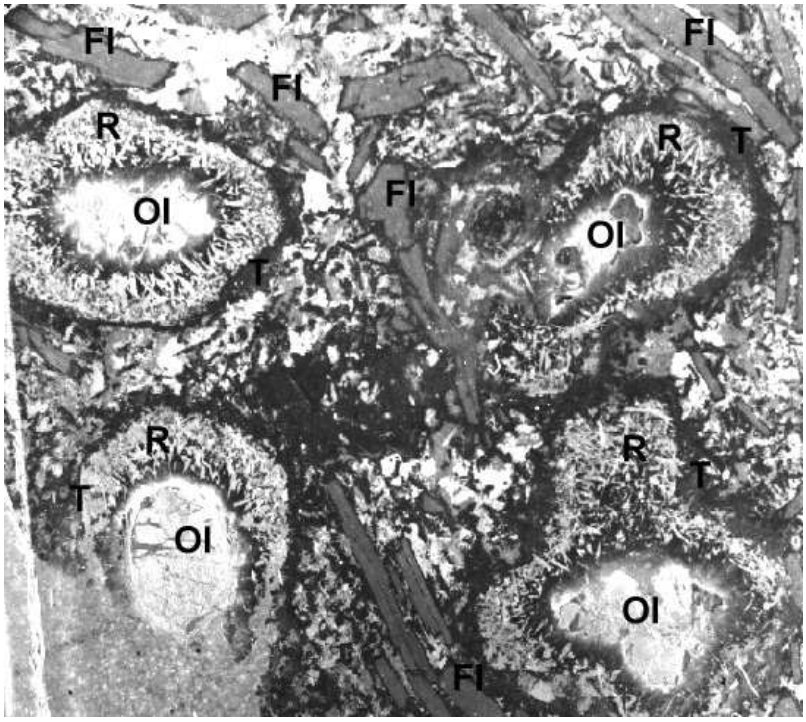

Fig. 1. **Magmatic dissolution (peritectic reaction) of olivine in lamproites. Ol-olivine, R –К-richterite, T-tetraferriphlogopite, Fl-phenocrysts of phlogopite.**

The high titanium content is a feature of differentiation, and a sign that a rock is free of diamonds. Central parts of mica phenocrysts contain 2-3 % of TiO_2 and 0,5% Cr, while the external margin, which crystallized together with matrix

contains 5-8 % TiO_2 and 0.001 Cr, correspondingly. Similar zoning is observed not only in lamproites, but also in alkaline basalts and alkaline rocks. By the way, the most titanic mica (12-13 % TiO_2) was discovered by us, as xenocryst, in alkaline basalts, in Mongolia.

The most rational is the classification proposed by the Australian geologists [1] who divided lamproites into olivine and leucite end members with a complete series of intermediate varieties. It is necessary to add sanidine (feld spar) varieties, which succeed leucite. Depending on prevalence of a certain mineral in lamproite phenocrysts, several varieties of lamproites are distinguished, for example: phlogopite-pyroxene-leucite or phlogopite-K-richterite-sanidine. Mitchell [2] suggested a more modified classification, taking into account mica in the matrix. The rock containing phlogopite phenocrysts, is called following this classification [2] as phlogopite lamproite, and if the rock contains phlogopite both in the matrix and as poikilocrystals it is called madupite lamproite. So, there is a problem how to call a rock if it contains mica both in phenocrysts and matrix? It should be noted, that early olivine lamproites containing over 20 % of olivine, do not contain leucite. It is crystallized later from a more differentiated and silicate magma residue. Olivine becomes unstable; it reacts and is dissolved in more silicate leucite magma (Fig. 1) This process of olivine «corrosion» is visible in dykes of the Murun lamproites [11, 14, 15]. It is characteristic of intrusive lamproites. We observed similar structures in lamproites of the Central Aldan and Leucite-Hills. In some cases, for example in sanidine lamproites of Spain, olivine hadn't been dissolved and was preserved in glassy varieties of lamproites. In lamproites of the Anabar Region, Urals Mountains and India olivine and leucite are often completely replaced by carbonate [13].

FORMATION TYPES OF LAMPROITE COMPLEXES

There are several options of geologic relations of lamproites with other rocks.

1. Lamproites form separate volcanoes and diatremes, which are not genetically associated with other rocks. They include lamproites of Australia, Spain and the USA. They are of Tertiary and Quaternary age and it is probable that their differentiates are not outcropped by the erosion.
2. Lamproites form separate bodies (sills, dykes and diatremes) and are frequently genetically related to kimberlites and picrites. This type includes lamproites of Anabar Region, Finland, China, India. Their age is similar to that of kimberlites.
3. Lamproites form separate bodies (sills and dykes) and even volcanic flows among other K-alkaline rocks. Lamproites are spatially and genetically related to these rocks, are of the same age and form a common petrochemical trend of compositions. This type involves lamproites of different massifs of alkaline rocks of the Aldan shield.
4. Lamproites form different bodies (dykes) among other dykes of rocks, demonstrating a higher Na content. Their age is similar. They include lamproites of

Altai, Paraguay [4], Montana (USA). The lamproites of the Urals and Karelia can be regarded as belonging to this type.

These 4 genetic types of lamproites can be united into the following formation complexes: 1) “pure” (proper) lamproites, 2) picrite (kimberlite) - alnoite - lamproite, 3) massifs of K-alkaline rocks, 4) dyke belts. The above formations can comprise other important rocks of the association.

Depending on dynamics of intrusion and crystallization lamproites can be divided into volcanic (flows of lava and diatremes), subvolcanic (sills and dykes) and intrusive (separate bodies, dykes, stocks, and phases of intrusion in massifs).

Inside the formation of "pure" (proper) lamproites we distinguish petrogenetic varieties (olivine-bearing) and olivine-free. The first variety includes lamproites of Australia and Spain. The second one comprises lamproites of Leucite Hills (USA). The Australian lamproites contain an early phase of olivine (absolutely without leucite) lamproites, while the leucite differentiates can contain scarce olivine. Lamproites of Spain do not show proper olivine varieties, and olivine is found almost in all varieties. Lamproites of Leucite-Hills most likely belong to another genetic group. They do not contain olivine. Their early varieties (madupites) consist of phenocrysts of pyroxene and mica and glassy (crystallized) matrix. By the chemical composition these rocks correspond to micaceous pyroxenites and are their volcanic analogs. By all parameters they are similar to biotite pyroxenites of K-alkaline-lamproite complexes of the Aldan shield [10, 14, 15]. It is most likely that these two varieties of lamproites were formed at partial melting of different mantle rocks: magma of Leucite Hills from the pyroxenite mantle, and the rest ones - from olivine-containing ultrabasic rocks of the mantle.

LAMPROITES OF SIBERIA

There are several lamproite magmatism occurrences of various genesis in Siberia. The most studied among them include: 1) lamproites of the Aldan shield associated with K-alkaline magmatism [10, 11, 14, 15]; 2) lamproites of the Eastern Anabar Region and Tomtor massif [12, 13, 16, 18], belonging to kimberlite-picrite-lamproite-carbonate association (formation); 3) veined and diatreme lamproites of Taimyr, lamproites of Sayan mountains [7] and lamproites of Altai, related to dyke complex of alkaline rocks. In the Asian region of Russia we have lamproite occurrences in Kamchatka, which are derivatives of basaltic magmatism, Urals Mountains lamproites, some bodies in the Okhotsk Region in Sete-Davan area and diatreme in the Koksharovskyi massif, Primorski Krai [18].

LAMPROITES OF THE ALDAN SHIELD

Lamproites of the Aldan shield are regarded as belonging to massifs of K-alkaline rocks. 14 lamproite occurrences [10, 11] have been found on the Aldan shield by now. They compose sills, necks, eruptive breccias, as well as dykes, stocks and layers in massifs of layered K-alkaline complexes. In the Western Aldan

lamproites are found on the Murun, Khani massifs, and dyke of Molbo River. In the Central Aldan lamproites have been studied in Yakokut, Ryabinovyi, Inagli, Yllymakh, Tommot, Yukhta massifs, separate diatremes of the Khatastyr field and Kaila pipe. In East Aldan they are available in Bilibin and Konder massifs. Lamproitic dykes Khani have the Archean age, determined from zircon as 2600-2700 Ma. These are the most ancient lamproites of the world. Other Aldan lamproites are Mesozoic (J and C). The rocks of the lamproite series form eruptive breccias with crystallized cement (Kaila and Khatastyr) and volcanic and intrusive bodies. By mineral composition scientists distinguish the following varieties: olivine, leucite and sanidine lamproites and intermediate varieties.

The lamproites of the Murun massif are well studied. 5 varieties of lamproites are found here.

The first variety of lamproites – [olivine (Ol) + pyroxene (Py) + mica (Bt) + sanidine (KFsp)] forms sill, being 20 m thick, in the western endocontact of the Small Murun massif. The sill was penetrated by a borehole 111 at the depth of 180 m. Lamproite contains phenocrysts of olivine (Fo 92) - 20 %, diopside - 20 %, Cr-phlogopite (0,5 % Cr) - 10 % and the matrix consisting of pyroxene, tetraferriphlogopite and sanidine (10 %). Sanidine replaced leucite; however leucite isometric rounded shapes are still preserved. Primary leucite is found in melt inclusions [4, 5] in pyroxene. Olivine phenocrysts crystallized at deeper horizons, and when intruding and with the pressure decrease they became unstable and reacted with the alkaline magma. Thin sections (fig. 1) show such a zoning: olivine – K-richterite - tetraferriphlogopite. Frequently olivine preserves only the shape of crystals filled with tetraferriphlogopite aggregate. This process is very characteristic of lamproites, in particular, sub-effusive and intrusive. Accessory minerals include: wadeite, apatite, chromite, Cr-magnetite.

The second variety of lamproites – olivine-phlogopite -pseudoleucite - [Ol + Py + Bt + Lp + KFsp)] composes an intrusive body, being 100 m thick in the stratified complex of biotite pyroxenites in the north-east of the massif. These rocks are penetrated by borehole 3 at the depth of 50-150 m. Lamproites are medium-grained, crystallized. They consist of crystals of olivine (10 %), diopside (30 %), micas (10 %), pseudoleucite (40 %), which are cemented by the sanidine matrix. Accessory minerals include: Cr-magnetite, wadeite, apatite, sulfides.

The third variety of lamproites - K-richterite-phlogopite-diopside-pseudoleucite [K-Richt+Bt+Py+Lp] involves dykes being from 10 sm to 2 m thick, which cut lamproites-2. These dykes demonstrate zones of quenching and crystallized central part. They consist of phenocrysts of mica (5 %), K-richterite (10 %), pseudoleucite (5 %), replaced olivine (5 %), and fine-grained matrix (75 %). The matrix contains pseudoleucite, K-richterite, diopside, mica. Accessory minerals include: apatite, K-vatisite, priderite (?), sulfides. In cases the central parts of these dykes contain pegmatoid sites consisting of mica (5 %), K-richterite – arfvedsonite (20 %), aegirite-diopside (10 %), K-batisite (20 %), sanidine (45 %) which are similar to pegmatoids of Walgidee-Hills in Australia.

The fourth variety of lamproites - K-richterite-sanidine [K-Richt+Bt+Py+KFsp (L)] composes a number of sills in the south-east of the massif among rocks of the charoite complex. The thickness of sills varies from 20 sm to 2 m. Lamproites comprise phenocrysts of K-richterite (10-20 %), mica (20 %,), diopside (5-10 %) and sanidine matrix with fine grains of mica and pyroxene. The matrix contained earlier leucite and was replaced sanidine. At present leucite is found in inclusions in pyroxene. Olivine phenocrysts, replaced by tetraferriphlogopite, is scarce. These sills are similar to dykes of olivine minettes from Highwood Montana (USA).

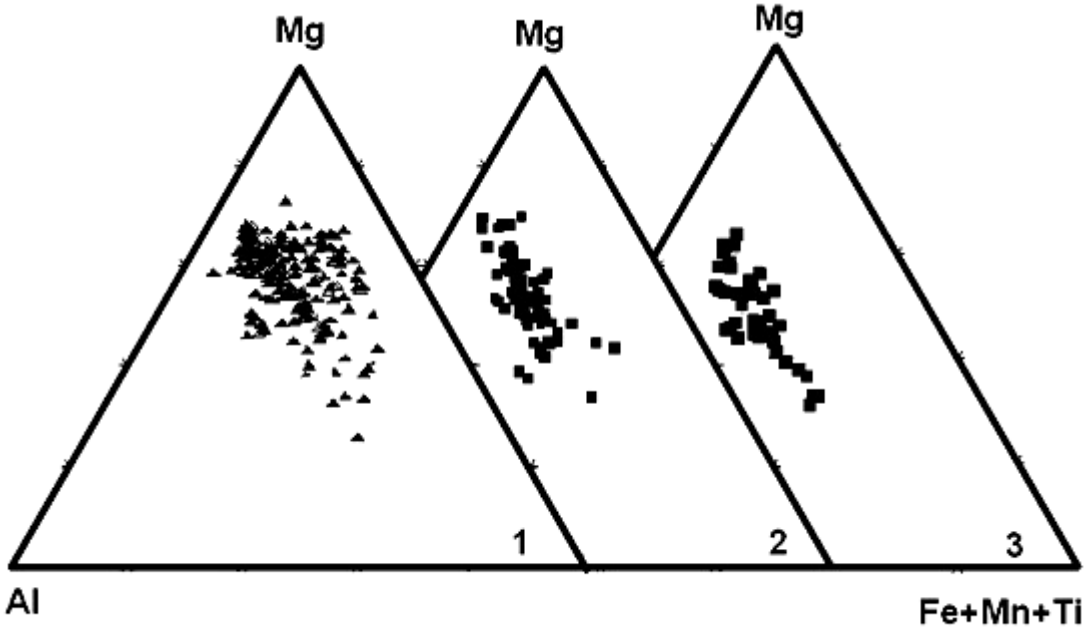

Fig. 2. **Composition of mica from lamproites of the world (1), Aldan (2) and Anabar Region (3).**

The fifth variety of lamproites - K-richterite-phlogopite-leucite: [K-rich+Bt+L]. Lamproites compose banded lava flows in the effusive field of the massif among tuff-lavas and lava-breccias of leucite phonolites. Lamproites contain phenocrysts of K-richterite, phlogopite, apatite, leucite (pseudoleucite) and fine-grained matrix consisting of the same minerals. Accessory minerals comprise Cr-magnetite, priderite, wadeite, apatite.

Lamproites of Molbo River occur in the Murun volcanic-plutonic complex. They are different from Murun lamproites in more chilled (fine-grained) matrix.

The composition of minerals of Murun lamproites is not different from that of other lamproites of the World. By the chemical composition olivines are similar to forsterite (Fo 86-94 = 40 %), pyroxenes - diopsides, amphiboles - K-richterites, mica of phlogopite-annitite series with low Al contents, leucites and sanidines are completely potash, being lack in Al which is compensated by Fe. Fig. 2 represents composition of mica from the Aldan and Anabar Region lamproites as well as

lamproites of the World. They belong to one and the same isomorphic series and form a rather compact field on the diagram. Early olivine lamproites demonstrate more magnesium mica, while in leucite ones it is more ferriferous.

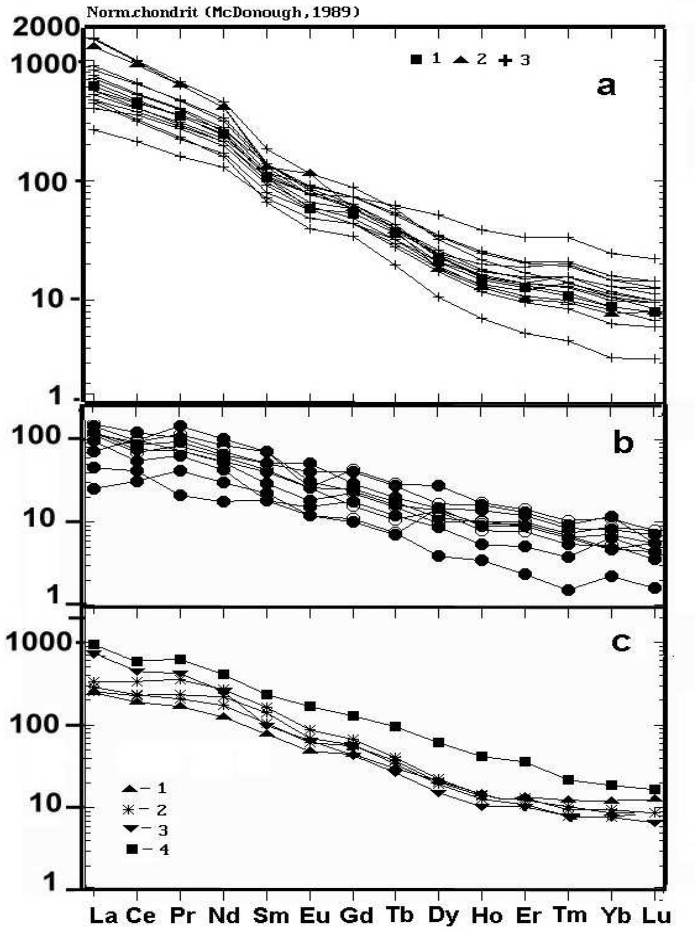

Fig. 3. **TR spectra in lamproites of Aldan (b), Anabar Region (a) and Australia (a): 1-Argail, 2-Ellendale- 11-olivine lamproites, 3-crosses – Anabar b-Aldan, c-other sites: 1.-Taimyr, 2-Altai, 3-Ural Mountains, 4-Primorsky Krai**

Plots of ternary correlations of petrogenic elements (Fig. 3) demonstrate a common trend of compositions of the Aldan lamproites. It coincides with a trend of these elements for lamproites of the Anabar Region, except for titanium, which is lower in the Aldan lamproiteas (regional difference).

LAMPROITES OF THE EAST ANABAR REGION

The Anabar diamond-bearing province is located in the eastern and southeastern part of the Anabar shield and extends as an arc-like zone 50 km wide and 300 km long. The province contains kimberlite and kimberlite-like rocks (picrites, alnoites and meimechites). In the rivers of the province there are over 300 diamond placers, their outcrops have not been found as the majority of kimberlitic rocks do not contain diamonds. Studies of the drill cores obtained from some magnetic anomalies of the Anabar province and within the Tomtor massif which is

regarded to be a large massif of alkaline rocks, indicated the discovery of lamproite rocks in the east part of the province [12, 13, 16]. Detailed analytical, geochemical and mineralogical investigations confirmed that these rocks belong to lamproite group. These lamproites are regarded as belonging to kimberlite-picrite-lamproite-carbonatite formation complex of rocks.

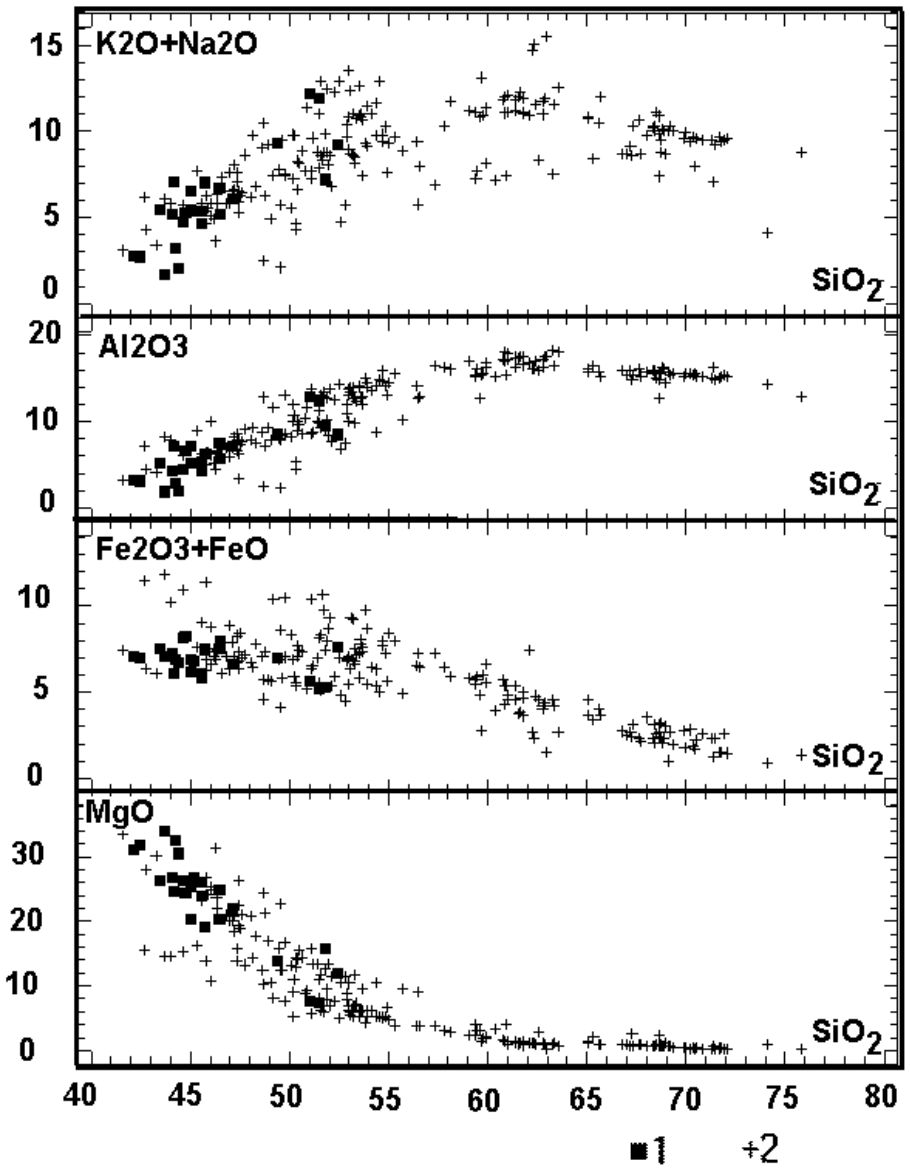

Fig. 4. **Pair correlation of petrogenic elements in rocks of the Bilibin massif: 1-Lamproites, 2-other alkaline rocks of the massif.**

We studied the core from all available boreholes in the settlements Ebelyakh and Amakin. Lamproite rocks and their intrusive analogs are found in the core from boreholes of the Tomtor massif and anomalies of the Eastern Anabar Region which penetrated the fields of picrite-kimberlite magmatism occurrences. The Tomtor massif in addition to lamproite rocks contains abundant altered rocks of the

picrite series. They are found in the core of the majority of boreholes (mainly at the top). Rocks the picrite group makes up a large horizontal body (sill or volcanic flow), occurring over a vast area of the massif and being genetically connected with alkaline rocks of the Tomtor massif; the potassium rocks are very significant here. Therefore, abundant lamproites discovered in the Tomtor massif are not surprising. Here they form sills, dykes and, less often, pipes (borehole 14, 71). Lamproites break early silicate alkaline rocks of the massif and are cut by carbonatite veins. The association between lamproites and syenite has not been observed. Early lamproites of the Tomtor massif are replaced by later carbonatites. It is known, that minerals of lamproites are not stable, and their intrusive varieties demonstrate replacement of early olivine phenocrysts by K-richterite and tetraferriphlogopite, and replacement of leucite by sanidine, in cases even to a complete disappearance of early minerals [19, 11]. In the Tomtor lamproites, owing to a high reactivity of later carbonatite magma -fluid, the olivine and leucite are completely replaced by carbonates and only shapes of former crystals are preserved. If the dissolution and replacement of olivine and leucite in the Aldan lamproites is an internal reaction taking place during the crystallization and differentiation of lamproites, the replacement of these minerals in the Tomtor massif is superimposed and consequently in addition to replaced olivine they contain unreplaced grains [20]. Another feature of lamproites of this province is a considerably lower content of pyroxene, as compared with other lamproites of the World. Ca-garnet is sometimes formed in them instead of pyroxene. The same feature is characteristic of kimberlite magmatism of the Siberian platform. By the mineral composition olivine and leucite lamproite varieties are distinguished in the Tomtor massif. [20].

Olivine lamproites are fine-grained (up to microgranular) rocks of green color. They consist of rounded and frequently faceted crystals of early olivine and mica phenocrysts with the size as 2-5 mm and trachyte-like fine-grained matrix. The matrix contains extended grains of mica and, less often, pyroxene (often altered), which give the trachyte-like texture, resulting from flow texture around early phenocrysts. In addition to mica and pyroxene the matrix contains altered olivine, infrequent amphibole, in cases garnet of andradite- schlorlomite series, apatite and, abundant spinellide (titanomagnetite, perovskite) and sulfides. Abundant mica, evenly distributed in the rocks is a characteristic feature of lamproites. Olivines are sometimes serpentinized and, more frequent, carbonatized even to a complete replacement by the carbonatite. Pyroxene is disintegrated up to the clay aggregate, while mica is chloritized. The analyses of carbonate dissolved in the hydrochloric acid indicate that its composition is more often calcitic, but it can be ankeritic and sideritic, that corresponds to the composition of carbonates of later carbonatite dykes.

Leucite lamproites are found only in the boreholes 0865 and 0855. They form horizontal bodies (sills) being up to 10 m thick. They are fine-grained (up to microgranular) very viscous rocks of dark gray color. They contain fine (1-2m)

white isolations of rounded (seldom with crystallographic faceting) leucite, completely replaced by carbonate. The matrix consists of fine-grained aggregates of mica, amphibole, infrequent altered pyroxene, apatite, calcite and ore minerals – including magnetite, perovskite, sulfides. Sometimes these rocks contain altered olivine.

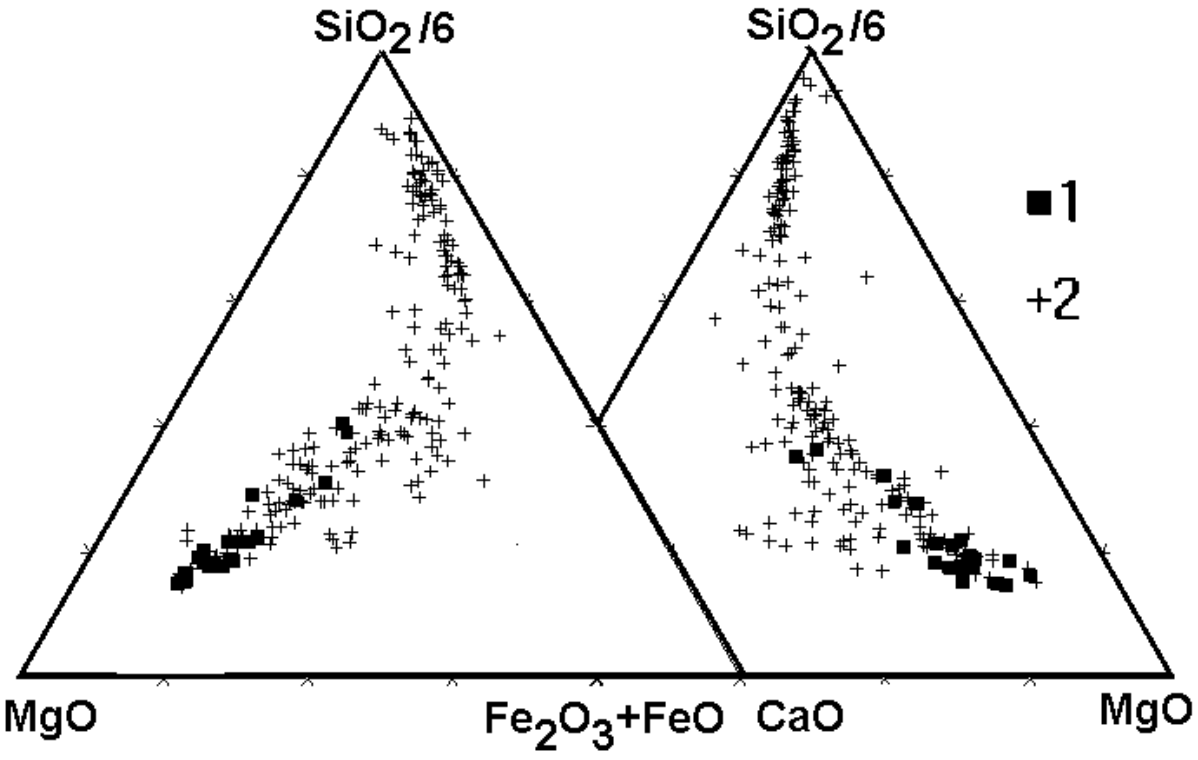

Fig. 5. **Ternary correlations of petrogenic elements in rocks of the Bilibin massif: 1-Lamproites, 2-other alkaline rocks of the massif.**

Diatreme breccias of lamproites (borehole 71) comprises early xenocrysts of olivine and mica, being up to 2 sm in size and strongly calcitized matrix. The carbonate rocks are predominant among xenoliths of the host rocks. By the texture and structure lamproite rocks of the Eastern Anabar Region are different from lamproites of the Tomtor massif. By these parameters they are similar to picrites and alnoites with which, they possibly, form a continuous series. Recently, among kimberlites of many provinces (for example in Finland, China, Prairie-Creek in the USA, etc.), the rocks related to kimberlites and contain abundant mica (over 20 %), are regarded as lamproites. A lot of reports devoted to kimberlites and associated lamproites were presented at the 7th International Kimberlite Conference in Cape Town. The Anabar anomalies contain only olivine lamproites. These are gray-green rocks of porphyritic texture, massive, with aphyric, infrequently glassy matrix. Phenocrysts include rounded isolations of early olivine (often fresh or

Table 2.

Chemical composition of the lamproites from Siberia (weight %).

	1	2	3	4	5	6	7	8	9	10	11	12
SiO_2	48,83	47,61	47,68	48,24	42,87	38,13	31,94	34,92	45,98	38,14	48,71	49,11
TiO_2	0,87	1,25	1,02	1,12	1,11	2,97	4,68	1,17	0,96	2,18	0,55	1,02
Al_2O_3	10,30	8,80	8,90	9,70	8,40	9,30	8,40	2,17	8,42	12,49	9,50	10,58
Fe_2O_3	2,46	2,83	2,94	4,23	3,04	3,76	11,27	2,08	5,70	2,40	4,21	8,17
FeO	5,45	3,31	4,92	3,58	4,02	7,51	7,96	6,80	3,50	10,96	4,13	4,04
MnO	0,15	0,11	0,13	0,14	0,13	0,16	0,30	0,11	0,15	0,25	0,14	0,21
MgO	6,80	11,60	15,40	11,70	11,60	11,80	12,70	27,95	13,51	18,20	13,27	4,99
CaO	8,40	4,30	4,80	6,10	6,10	8,80	9,80	6,72	7,43	0,42	6,47	3,96
BaO	0,50	0,30	0,50	0,90	0,20	0,40	0,20	0,12	0,26	0,26	0,46	0,37
SrO	0,18	0,14	0,09	0,10	0,03	0,12	0,13	0,10	0,30	0,13	0,16	0,17
K_2O	6,61	7,16	5,86	7,03	6,20	6,49	2,32	0,92	7,89	10,05	8,20	9,62
Na_2O	1,34	0,78	0,89	1,07	1,22	1,05	0,86	0,20	1,60	0,12	1,02	2,94
P_2O_5	1,14	1,25	1,22	1,48	1,02	2,24	2,01	0,45	1,96	0,07	0,98	1,31
H_2O	2,26	3,52	3,49	4,01	3,41	1,41	3,84	13,36	1,29	2,79	1,33	1,71
CO_2	4,03	6,36	1,54	0,46	10,04	5,36	3,02	3.00	0,79	0,50	0,10	1,00
F	0,19	0,55	0,32	0,38	0,38	0,45	0,20	0,1	0,90	1,00	0,12	0,80
S	0,43	0,03	0,04	0,10	0,05	0,02	0,06	0,20	0,20	0,30	0,30	0,20
Total	99,71	99,96	99,88	100,3	99,87	99,97	99,74	100,2	100,4	99,84	99,58	99,82

	13	14	15	16	17	18	19	20	21	22	23	24
SiO_2	46,46	48,60	47,02	4,27	46,48	42,29	38,89	36,89	30,86	26,33	30,49	32,42
TiO_2	0,33	0,66	0,62	0,81	1,23	0,69	2,04	3,61	7,04	2,63	3,66	4,74
Al_2O_3	7,49	9,95	8,04	8,50	8,52	5,57	5,48	3,07	7,53	4,30	4,58	2,88
Fe_2O_3	2,45	4,22	4,85	12,03	8,26	5,85	12,40	5,47	6,39	5,78	8,15	10,37
FeO	5,10	4,10	3,94	н/об.	3,00	4,30	6,11	7,27	8,35	4,76	3,68	3,68
MnO	0,14	0,15	0,12	0,17	0,11	0,15	0,33	0,13	0,23	0,25	0,21	0,20
MgO	20,43	12,11	15,65	10,86	7,86	27,66	12,91	16,17	8,65	20,58	22,08	24,01
CaO	8,01	8,44	7,13	12,23	4,55	6,16	15,06	11,19	11,12	11,32	10,69	7,13
BaO	0,08	0,30	0,20	0,24	1,25	0,32	0,30	0,14	0,22	0,27	0,21	0,23
SrO	0,13	0,17	0,17	0,08	0,58	0,03	0,40	0,06	0,13	0,10	0,09	0,05
K_2O	6,05	6,40	4,20	4,82	7,62	3,97	3,56	2,14	4,80	4,32	3,45	6,03
Na_2O	0,70	1,77	1,03	0,43	1,41	0,30	0,54	0,30	2,73	0,61	0,02	0,25
P_2O_5	1,17	0,69	0,68	0,78	1,80	0,09	1,15	0,54	1,30	0,58	0,77	0,17
H_2O	0,90	2,36	4,40	1,23	5,70	1,82	0,40	2,92	1,63	3,60	6,64	4,36
CO_2	0,05	0,06	1,50	0,50	1,00	0.30	0,10	8,33	7,75	13,50	4,92	3,20
F	0,30	0,15	0,05	0,29	0,05	0,30	0.50	0,28	0,46	0,85	0,41	0,36
S	0.15	0,20	0,10	0,30	0,15	0,10	0,05	1,87	0,31	0,80	н/о	0,11
Total	99,79	99,65	99,70	100,4	99,57	99,75	99,97	100,4	99,50	100,6	100,05	100,19

Note: 1- Taimyr (sample of Romanov A.P.); 2-5- Altai (sample of Obolenskyi A.A.); 6 – Urals Mountains (sample of Pushkareva E.V.); 7 – Koksharovskyi massif (sample Scheki S.A.); 8 – Ingashi, Sayan mountains; 9-12- Murun; 13 – Bilibin massif; 14 – Ryabinovyi massif; 15- Kaila pipe; 16- Yakokut; 17- dyke of Molobo River; 18 – Khani; 19 – Konder; 20-22 – Tomtor (20-bore-hole 101, 21-bore-hole 0865, 22-bore-hole 14/81); Easten Prianabar'e: 23-anomaly -36/63, 24-anomaly 97/63. Data of chemical and quantometr analysis, analytics: Matveeva L.N., Finkelshtein A.L. Institute of geochemistry SB RAS 1995-2002 гг.

replaced by serpentine) and mica laths. Mica sometimes forms a skeleton of the connected crystals, interstitials of which is filled with aphyric matrix. Olivine phenocrysts amount to 10 %, and mica makes up 20-30 % and more. Aphyric

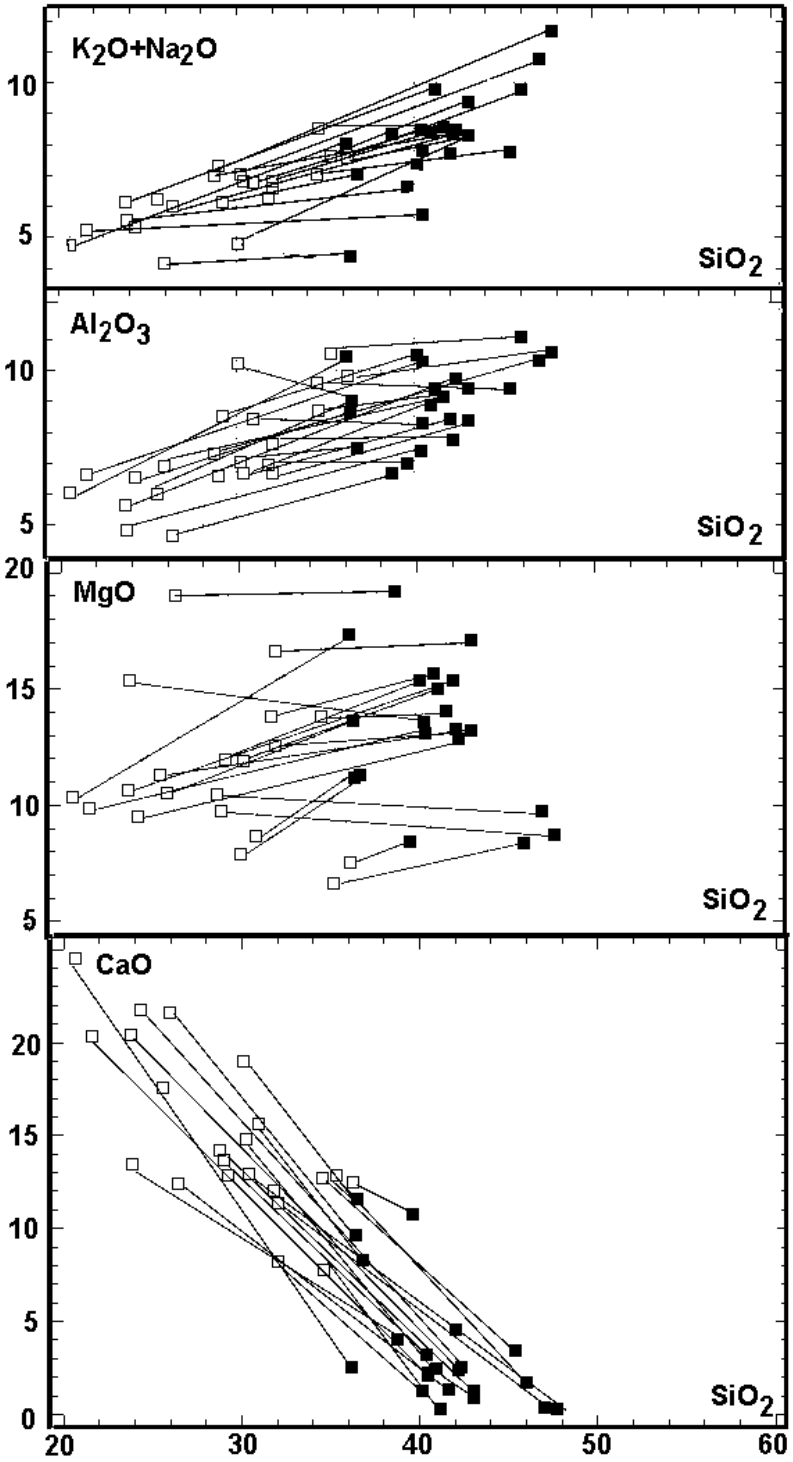

Fig. 6. **Pair correlation of rock-forming elements in lamproites of the Tomtor massif. Unfilled squares – primary analyses. Filled squares – samples after treatment by hydrochloric acid.**

matrix contains fine mica, altered olivine, less often pyroxene and amphibole, as well as apatite, carbonate, in cases garnet. Spinellide are abundant: titanomagnetite, and possible chromite, perovskite and sulfides. With respect to genesis these lamproites are less differentiated, as opposed to the Tomtor lamproites; instead of the superimposed carbonate they contain proper carbonate, which hadn't separated from the silicate magma. A special lamproite variety is the dyke in the anomaly 97/63. It represents a fine-grained rock consisting of fine olivine phenocrysts (20 %) which are surrounded by the aggregate of grown grains of light green amphibole and brown tertraferriphlogopite and ore mineral.

Petrochemical features of the Anabar lamproites.

By the chemical composition the studied rocks belong to lamproites. They demonstrate high concentration of MgO (8-28 %), K_2O (2-8 %), TiO_2 (3-7 %) and low concentration of Al_2O_3 (3-10 %), Na_2O (0.1-1 %). The lamproites show increased concentrations of CaO (3-15 %) and lower contents of SiO_2 (28-35 %) which are related to the late carbonate formation (up to 20 % of $CaCO_3$). Like xenogenic quartz (to 95%) in sandy diamond-bearing lamproite tuffs of Australia the superimposed carbonate in the Anabar Region lamproites results in changes of the chemical composition of rocks. Carbonates of calcium, magnesium and iron significantly influences the concentration of such light element as silicon, the concentration of which in the rock is sharply decreased. We made a chemical experiment for 20 samples. Lamproites with significant concentration of carbonates were treated by 10 % HCl during 3-5 minutes. Then the primary and treated samples were analyzed. The muriatic solution was analyzed as well. As the analyses show, the carbonates containing Ba, Sr and, possibly, apatite were dissolved in the solution. Insignificant amount of potassium is dissolved in the samples with disintegrated mica. In the treated samples concentrations of SiO_2 and to lesser extent of Mg, Ti, K [20] drastically increases, fig. 6. Their chemical composition completely corresponds to that of lamproites. The chemical composition of the Anabar lamproites is given in Table 3.

For normal picrites and kimberlites the concentration of K_2O as 0.5 % are regarded as limiting. The alkaline micaceous picrites and kimberlites can contain up to 3 % of K_2O. The lack of mellilite in these rocks means that they are not alnoites. The partial reconstruction of primary composition of rocks by chemical dissolution of the carbonate component gives rise to composition similar to lamproites. Lamproites of certain region has own specific features. The Anabar Region lamproites are not exception, and they have their own regional specific features. In addition to the abundant carbonates of different genesis, low SiO_2 values result from the increased concentrations of heavy minerals – spinelids with magnetite, perovskite and sulfides (considering a weight method to determine the abundance of elements). Ca-garnet is in cases crystallized instead of pyroxene. It becomes the main Ca concentrator in lamproites. It is possible that garnet formed

when pyroxene was replaced. Figure fig. 7 gives the pair correlations of rock-forming elements in lamproites of the World (a), Anabar Region (b) and Aldan (c).

Table 3.

Contains of rare elements in lamproites from Siberia, (p.p.m).

	1	**2**	**3**	**5**	**6**	**7**	**8**	**9**	**10**	**11**	**12**	**13**
Cr	205	1370	1301	1164	890	890	1800	2000	170	420	178	1200
Ni	79	472	394	157	157	157	580	1000	76	370	100	820
Co	26	33	48	40	41	59	84	110	26	57	37	84
V	177	275	201	229	204	309	290	110	260	120	390	50
Sc	20,3	15,6	18,1	14,3	17,1	14,4	3,4	17,0	14,0	30,0	22,0	46,0
Cu	96	91	82	78	26	193	33	47	80	24	220	15
Pb	50,5	66,9	112,5	72,8	6,7	4,7	1,9	2,0	52,0	13,0	7,5	2,6
Sn	н/о	н/о	н/о	н/о	н/о	н/о	2,0	8,0	0,8	3	5,7	0,7
Zn	н/о	н/о	н/о	н/о	н/о	н/о	54	80	110	65	320	46
Zr	240	418	254	244	153	191	15	60	185	120	490	45
Nb	10,4	15,2	7,1	7,3	65,5	81,6	16,2	1,0	20,0	5,0	50,0	4,0
TR	287	502	359	373	649	936	150	60	95	148	222	181,0
Y	23,8	23,3	23,0	18,5	15,6	54,5	10	7,2	10,0	14,0	67,0	12,0
Li	21	34	115	39	224	71	20	92	37	30	90	5
Rb	218	334	295	265	97	63	150	120	210	150	280	280
Cs	15,8	24,3	47,5	27,7	4,2	20,1	2,0	1,0	1,0	2,0	2,0	5,0
B	н/о	н/о	н/о	н/о	н/о	н/о	1,12	40,0	2,0	2,2	11,0	12,0
Be	н/о	н/о	н/о	н/о	н/о	н/о	40,0	18,0	5,4	2,2	30,0	1,2

	14	**15**	**16**	**17**	**18**	**19**	**20**	**21**	**22**	**23**	**24**
Cr	856	1200	580	94	320	69	1200	150	900	790	910
Ni	435	580	170	100	1300	94	2000	94	880	1100	1400
Co	86	48	56	24	160	55	250	100	46	65	60
V	219	160	220	320	100	670	400	440	200	230	170
Sc	33,0	32,0	45,0	18,0	8,0	44,0	15,0	16,0	8,9	15,0	11,0
Cu	122	83	84	380	18	320	76	52	15	120	23
Pb	30,0	14,0	6,0	140,0	1,0	2,0	6,7	8,0	15,0	2,2	20,0
Sn	1,6	2,8	2,0	10,0	1,0	3,6	3,4	4,5	2,6	3,4	2,6
Zn	60	73	130	140	97	180	150	96	97	82	100
Zr	150	140	125	230	87	120	109	568	248	360	859
Nb	5,0	6,0	3,0	1,0	1,0	5,0	30	40	100	50	1100
TR	131	126	126	184	52	171	857	517	842	552	1660
Y	15,0	12,0	15,0	18,0	2,0	25,0	20	2,9	10	15	28,0
Li	20	76	11	20	4	44	20	18	100	30	40
Rb	164	120	160	250	100	60	350	296	300	200	170
Cs	3,0	3,0	6,0	5,0	1,0	1,0	1,0	2,4	3,0	1,5	2,3
B	18,0	33,0	19,0	21,0	5,0	3,7	12,0	9,1	23,0	18,0	43,0
Be	5,5	5,5	1,8	9,0	1,0	1,4	1,8	8,9	2,7	2,8	15,0

Note: №№ analysis in table 1. Data of ACP-MS, analytic Mitrofanova A.Yu., and emissions spectral analysis, analytics: Smirnova E.V., Kuznetsova A.I., Institute of geochemistry SB RAS, 1995-2001г.

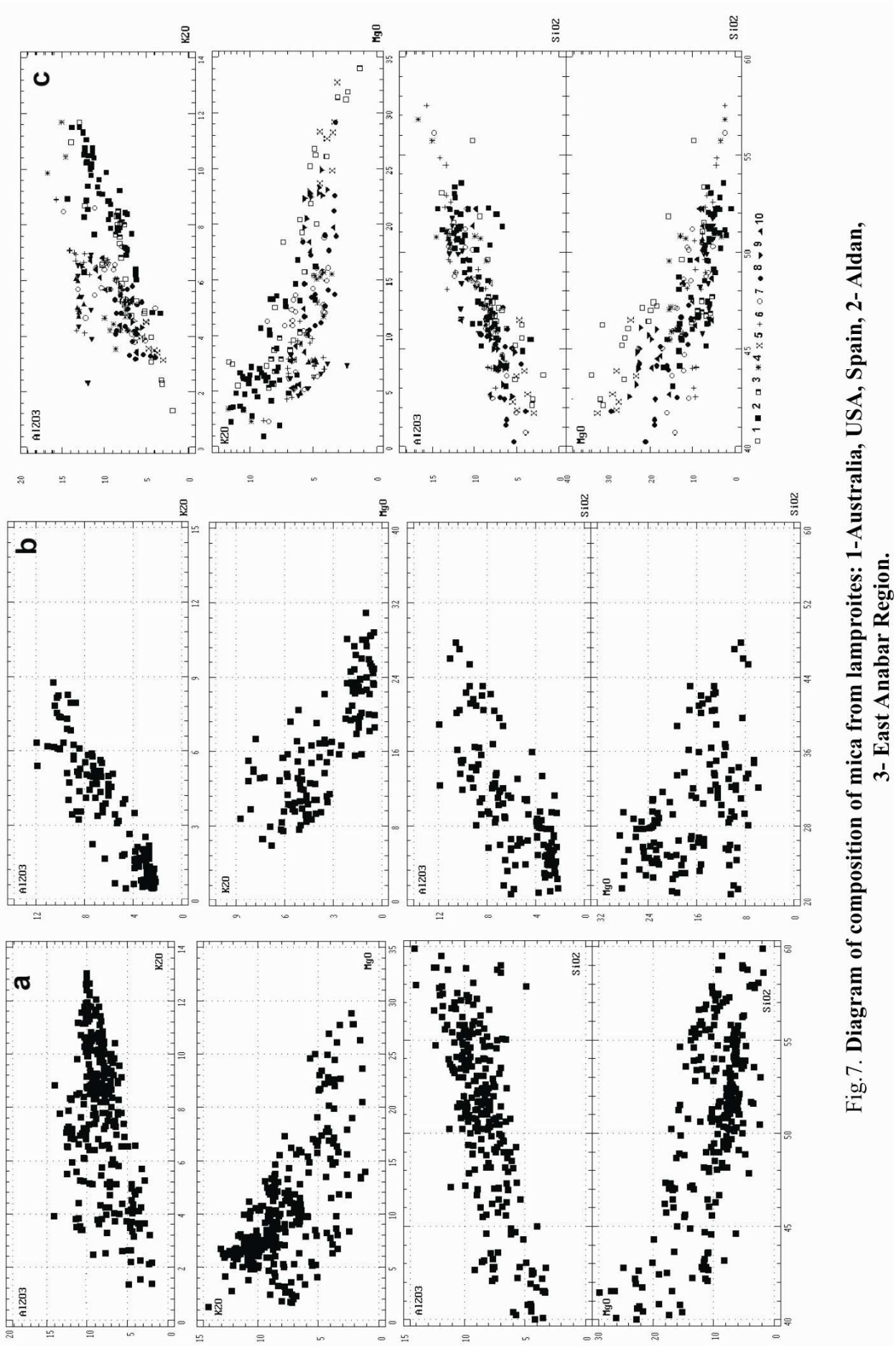

Fig.7. **Diagram of composition of mica from lamproites: 1-Australia, USA, Spain, 2- Aldan, 3- East Anabar Region.**

Figure 8 demonstrates triple correlations of rock-forming elements in lamproites of Aldan (c), in lamproites (b) and silicate rocks of the Tomtor massif (a) and lamproites of other regions (d). It is evident that trends of differentiation on all diagrams are similar. Composition trends of lamproites from the Tomtor massif lie within composition trends of all silicate rocks of the massif that suggests their genetic similarity. During the differentiation from early to late rocks concentrations of SiO_2, Al_2O_3, K_2O increase while MgO content decreases. Analyzing differentiation trends of lamproites one can arrive at the conclusion that the Anabar lamproites are less differentiated (Mg-Si ratio is shifted towards Mg angle of the diagram) as opposed to the Anabar Region lamproites. It increases diamond-bearing potential of the Anabar Region lamproites. In addition, the Anabar olivine lamproites demonstrate significantly higher titanium content than the Aldan ones. In our opinion, the increased titanium content suggests a greater differentiation of the mantle source of these rocks. However, some authors consider titanium content to be the indicator of diamond-bearing potential.

Mineralogical features of the Anabar Region lamproites.

Mica. Mica is one of typomorphic minerals of lamproites. In the studied rocks it has a magmatic origin and defines the trachyte-like texture. Scientists distinguish early mica-phenocrysts and mica in the matrix. We studied, mostly, mica-phenocrysts from volcanic and diatreme formations and medium-fine-grained mica from intrusive lamproites. By the chemical composition (Fig. 2) mica of the Anabar Region lamproites belongs to phlogopite-annite series that is characteristic of lamproites. Mica of tertraferriphlogopite composition is rare in porphyry lamproite as the olivine carbonate formation is not observed. Such mica is common to differentiated lamproites. Mica of the Anabar Region lamproites demonstrates low concentration of Al_2O_3, however, it is sufficient for a complete filling of tetrahedral positions. TiO_2 content in mica of lamproites is an indicator of differentiation, it sharply increases from olivine lamproites (2-3 % TiO_2) to leucite lamproites (5-8 % TiO_2). The highest TiO_2 content in mica of the Anabar region lamproites (5-7 %) is found in apoleucite lamproites that confirms our ideas concerning their belonging to leucite varieties, despite a complete replacement of leucite by carbonate. The studied lamproite mica demonstrates low contents of fluorine and lithophile elements - Li, Rb, Cs, and high contents of Ba and sierophile elements - Cr, Ni, Cu, Mo. The microprobe investigations of mica from leucite lamproites (borehole 0865) revealed mica (possibly xenogenic) with abnormal content of TiO_2 (14 %), as compared with xenocrysts of the mantle mica from alkaline basalt volcano Shavaryn-Tsaram in Mongolia, investigated by us earlier [8]. The chemical composition of mica and concentration of rare elements in them confirm our viewpoint that studied rocks of the Anabar Region are lamproites.

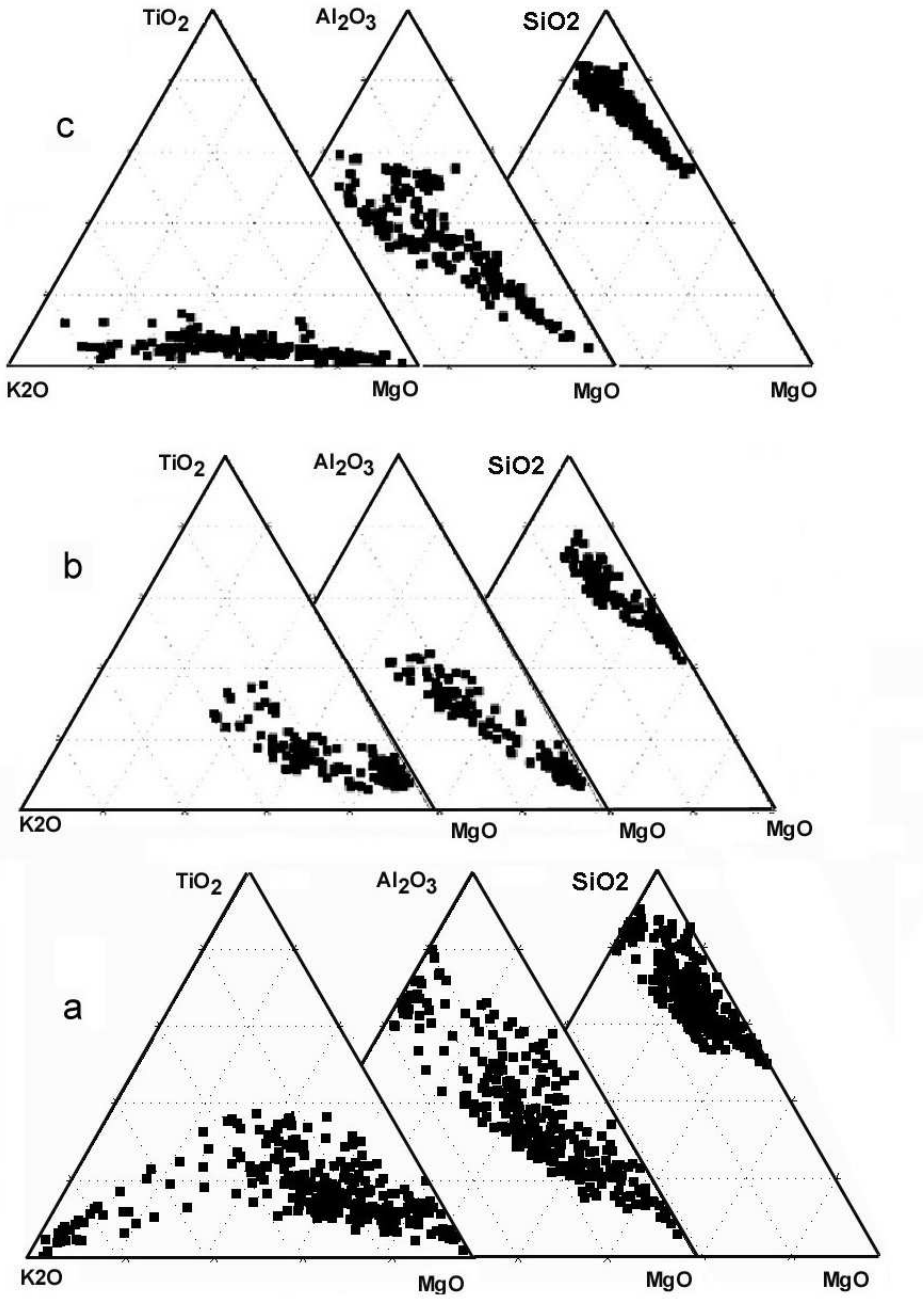

Fig. 8. **Diagram of ternary correlations of petrogenic elements.**

a – in silicate rocks and b – lamproites of Tomtor massif; c - in lamproites of Aldan.

Olivine. By composition olivines correspond to Fe-containing forsterites that is characteristic of lamproites. However, iron concentration in the Anabar lamproites are slightly overestimated, in comparison with typical ones. The increased admixture concentrations of CaO in olivine suggest higher temperatures of crystallization. Olivines in the studied lamproites are typical minerals of early phenocrysts and are rarely found, as the minerals of matrix. In lamproites, subjected to carbonate formation, olivine is completely replaced by carbonate, and only shape of former crystals is preserved.

Table 4

Contains of TR-elements in lamproites from Siberia, in (p.p.m.)

	1	**2**	**3**	**5**	**6**	**7**	**9**	**10**	**11**	**12**	**13**
La	59	79	68	60	175	221	11	23	29	39	35
Ce	116	206	145	140	278	357	26	34	53	67	59
Pr	16	34	20	22	40	60	2	6	9	10	14
Nd	59	127	82	103	120	193	8,2	20	31	36	48
Sm	11,9	25,0	15,9	21,6	15,0	36,1	2,8	2,8	7,9	12,0	11,0
Eu	2,83	5,13	3,58	4,08	3,84	9,77	0,70	0,90	3,00	3,50	1,80
Gd	9,25	14,01	11,60	11,87	9,05	26,93	2,10	3,70	6,10	23,00	5,00
Tb	1,13	1,49	1,38	1,28	1,01	3,56	0,26	0,45	0,74	2,80	0,61
Dy	5,45	5,71	5,29	5,02	3,87	15,74	3,80	2,20	3,80	12,00	3,60
Ho	0,84	0,83	0,80	0,74	0,59	2,38	0,52	0,31	0,81	2,00	0,55
Er	2,26	2,21	2,10	1,82	1,71	5,95	1,50	0,86	2,00	5,10	1,60
Tm	0,32	0,25	0,27	0,21	0,21	0,57	0,17	0,10	0,22	0,57	0,18
Yb	2,07	1,64	1,49	1,34	1,33	3,19	0,80	1,10	1,40	8,00	0,82
Lu	0,32	0,22	0,22	0,22	0,17	0,42	0,14	0,11	0,18	0,80	0,11
Total	287	502	359	373	649	936	60	95	148	222	181

	14	**15**	**16**	**17**	**18**	**19**	**20**	**21**	**22**	**23**	**24**
La	17	29	27	37	6	27	215	113	200	135	410
Ce	60	47	43	74	19	57	400	230	390	250	800
Pr	7	7	8	10	4	11	44	27	45	28	70
Nd	26	25	29	34	14	40	145	100	155	100	270
Sm	6,3	4,5	6,7	7,9	3,5	11,0	20,0	16,0	21,0	15,0	50,0
Eu	1,50	1,05	1,50	2,40	0,70	1,50	4,40	4,50	5,00	3,50	11,00
Gd	5,30	4,70	3,30	8,50	2,30	8,90	13,00	12,00	13,00	10,00	27,00
Tb	0,65	0,57	0,40	1,04	0,28	1,09	1,50	1,50	1,60	1,20	3,30
Dy	2,90	2,50	3,50	4,30	1,00	7,00	6,30	6,60	6,00	4,90	12,00
Ho	0,58	0,60	0,45	0,92	0,20	1,00	1,14	1,03	0,89	0,75	1,40
Er	1,70	1,50	1,30	2,20	0,40	2,40	3,10	2,50	2,30	1,80	3,20
Tm	0,19	0,17	0,14	0,24	0,04	0,27	0,52	0,41	0,33	0,26	0,28
Yb	1,50	1,20	0,91	2,00	0,38	1,90	2,50	2,20	1,70	1,40	1,50
Lu	0,20	1,40	0,09	0,14	0,04	0,20	0,36	0,28	0,24	0,17	0,18
Total	131	126	126	184	52	171	857	517	842	552	1660

Note: №№ analysis in table 1. Data of analysis ACP-MS and quantity emissions spectral analusis, Institute of gochemistry SB RAS.

Pyroxene. Pyroxenes in the Anabar Region lamproites are unstable, therefore they are scarce. They are sometimes replaced by garnet. Unaltered pyroxene is similar by composition to diopside with low concentration of iron that is characteristic of lamproites.

Spinellide. Characteristic minerals of the studied lamproites include magnetite and titanomagnetite. Unusual spinel is found in cases; by the composition it is similar to Ti-variety demonstrating significant contents of all main components - Cr, Fe, Mg, Al. Similar spinel was described by N.V. Sobolev in unusual

kimberlites. In addition to the above minerals lamproites contain abundant perovskite, apatite and sulfides. With respect to rock-forming and accessory minerals and chemical composition the studied rocks of the Anabar Region belong to lamproites. They do not contain plagioclase and nepheline which are uncommon to lamproites, they are free of alnoite minerals and picrites (melilite, monticellite). Some varieties contain garnet, which we relate to surplus of Ca and CO_2 in the magma. A similar garnet is abundant in kimberlites and lamproites of the Archangelsk province.

Geochemical features of the Anabar Region lamproites.

The geochemistry of lamproites is not well studied; however the first geochemical data confirm the appropriateness of rock diagnostics. Rare elements of lamproites are presented in Table 3, and TR spectra are given in Table 4. An imposed carbonate formation slightly affects trends of rare element compositions, but does not render an essential influence on the basic behavior during the crystallization. Concentrations of Ba, Sr, Cr, Ni in the studied lamproites lie within the limits of concentrations, characteristic of them. Greater variations of rare element concentrations in lamproites result from a wide range of their compositions, from olivine to leucite varieties. Changes of Ba/Sr and Cr/Ni ratios indicate significant magmatic differentiation during their origin. Concentrations of other rare elements are within the limits of content variations in lamproites. We will discuss in detail spectra of rare-earth elements, which are sensitive indicators of petrologic processes of differentiation. As the diagram (Fig. 4) shows, TR spectra of the Anabar Region lamproites, chondrite-normalized, completely coincide with spectra of diamond-bearing olivine lamproites of Australia, both by the spectrum inclination, and TR-element ratios that is rather rare for the lamproite group of rocks. The lack of Eu fractionation suggests a low differentiation from the origin of the melt to its crystallization that is a positive feature for diamond-bearing potential. Besides, it suggests the lamproite trend of rock composition, instead of the basaltoid one. In the basaltoids the isolated plagioclase selectively concentrates Eu that leads to its fractionation and thus gives rise to Eu minimum.

Figures 3, 4, 5 give individual analyses of the chemical composition and concentrations of rare elements in lamproites of other sites in Siberia and adjacent areas (Taimur, Altai, Sayan Mountains, Urals Mountains, Primorski Krai). As regard to all considered parameters they do not differ from lamproites of Aldan and Anabar Region. As Figure 8 shows, points of their compositions lie in fields of the Aldan and Anabar region lamproites. Spectra TR of these lamproites (Fig. 3) are similar to those of the Aldan and Anabar Region lamproites. All the above suggests that these rocks belong to lamproites.

Geochemistry of isotopes, genesis, and diamond-bearing POTENTIAL of lamproites

We studied the geochemistry of Sr, Nd, Pb isotopes in lamproites of Siberia [14, 19]. The olivine lamproites of the Kondera, Murun and Bilibin massifs demonstrate Sr^{87}/Sr^{86}=0.7045, while for other Aldan lamproites Sr87/Sr86 ratio

ranges within the limits from 0.706 to 0.709. In terms of ratio Pb as well as Nd and Sr isotopes [11, 14], lamproites from the Murun massif form a field between fields of Leucite-Hills and Smoky Butte, the USA. On the diagram of Sr and Nd isotopes ratio (Fig.9) lamproites from the Murun massif form the field close to the field of the North American lamproites. The source of their melting is the enriched EM-1 mantle. By geochemistry of rare elements the Aldan lamproites are similar to lamproites of the North America. Isotope characteristics indicate a deep-seated mantle origin of sources for lamproitic and K-alkaline Aldan magmas [11]. The age of the primary mantle substratum, which was used for melting magma of the Murun massif, is estimated as 3200 Ma using Pb isotopes.

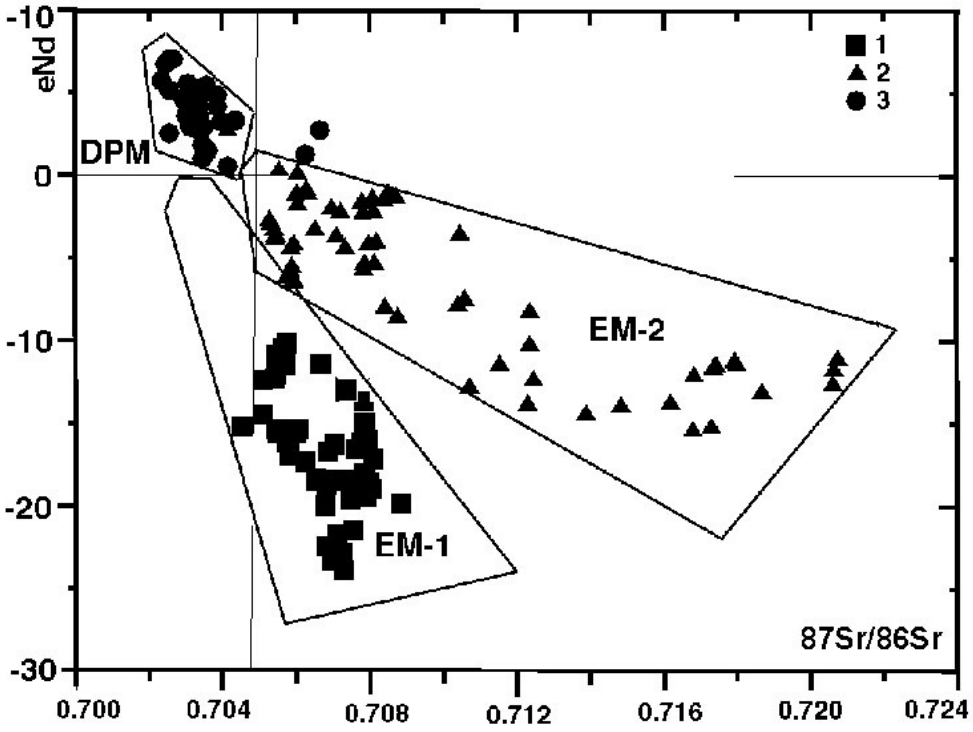

Fig. 9. **Diagram of ratios of epsilon Nd and 87Sr/86Sr in lamproites and carbonatites.**

Circles- carbanatites of the framing of the Siberian Platform, Squares – lamproites of Aldan, Russia and USA, Triangles-carbonatites and lamproites of folded areas.

In terms of the geodynamic aspect lamproites of Aldan and North America, located on the border between the shield and the platform show the enriched mantle source EM-1. Lamproites of Australia and Spain (Fig.9) are located on the periphery of craton in zones of completed folding. The enriched mantle source EM-2 is characteristic of them.

Diamond-bearing potential of lamproites is due to many factors. The majority of researchers suggest mostly xenogenic pattern of the most of diamonds, both in kimberlites, and in lamproites. There are two aspects of this problem.

The first aspect concerns the depth of magma origin that should be located in the area of diamond stability; and the second concerns the preservation of diamonds during the transportation and crystallization of magma. Taking into account isotope and geochemical characteristics of lamproites, they are regarded as deep mantle rocks, and the first condition is most likely observed. As to the second condition is concerned a fast magma transportation is required for preserving diamonds. Such fast magma transportation is the case in diatreme structures. A particular fast cooling is found in sandy tuff where quartz grains served as a good cooler, therefore similar lamproite tuffs are very rich in diamonds. It can be exemplified by the Argail lamproites. Diamond-bearing sandy tuffs, consisting of quartz sand (95 %) and lamproite substance (5 %) contain more diamonds (in one order of magnitude), than massive lamproites, consisting of 100 % of the lamproite substance. Diamonds in intrusive lamproites, most likely, burned down during a relatively slow magma crystallization.

CONCLUSIONS

1. The rocks which in terms of chemical and mineral composition and geochemical specific features correspond to lamproite group are lamproites.
2. The volcanic rocks (lamproites) have intrusive analogs which are also lamproites.
3. Lamproites can be of various origin and can be genetically related to different series of alkaline rocks and associations. We suggest to distinguish 4 genetic types of lamproites and to unite them in the following formation complexes: 1) “pure” (proper) lamproites, 2) picrite (kimberlite) - alnoite - lamproite, 3) massifs of K-alkaline rocks, 4) dyke belts.
4. After changes in chemical conditions of crystallization and owing to the imposed processes indicative minerals of lamproites (olivine and leucite) become unstable and are replaced by other minerals (micas, carbonates, potash feld spar). However, chemical and geochemical specific features of rocks are often preserved, though they are not so evident. Owing to high potassium content and leucite trend of crystallization, plagioclases and nepheline (even in cases when Na is higher, than K [3]) are not crystallized, as this is a forbidden association in lamproites. The primary chemical composition can be reconstructed either under chemical dissolution of carbonates or when studying melt inclusions which preserved metastable olivine and leucite.
5. Using the geochemistry of Nd and Sr isotopes it is shown, that lamproite complexes, occurring in rift zones between the shield and the platform, have a source enriched by EM-1 mantle, and lamproites located in folded areas on the peripheral part of platforms originated from enriched mantle source EM-2.
6. The main parameters of diamond-bearing potential of lamproites include the depth of sources for their magmas (deeper than the level of diamond stability in the mantle) and its preservation (incombustibility) before the magma cooled down. The most appropriate in this respect are early olivine lamproites and

their tuffs (especially those, containing abundant quartz sand) from diatreme structures.

The studies were supported by RFBR (grants 06-05-64416, 06-05-81016).

REFERENCES

1. **Jagues A.L., Lewis J.D., Smith C.B.** The kimberlites and lamproites of Western Australia // Geol. Surv. W. Australia. Bull., 1986, v. 132, p. 1-268.
2. Lamproites (ed. by Bogatikov O.A.). Nauka, 1991, pp. 1-302.
3. **Mitchell R.H., Bergman S.C.** Petrology of lamproites // New York, Plenum Publishing ‘corporation, 1991, p. 1-447.
4. **Panina L.I., Motorina I.V. Alkaline high-calcium sulfate-carbonate melted inclusions in montichellite-olivine rocks of the Small Murun massif** // Petrology, 1999, v. 7, № 6, p. 653-669.
5. **Panina L.I., Vladykin N.V. Lamproites of the Murun massif and their genesis** // Geology and Geophysics, 1994, v. 35, № 12, p. 100-113.
6. **Presser J.L.B, Vladykin N.V.** Consideraciones sorbe los lamproitos del campoYbytyruzu, Dpto. Del Guaira, Paragyay Orental // Jornadas Cientificas sobre la Geologia del Paraguay UNA-FaCEN- DPTO. Geologia/MOPC- Dir.Rec.Min. (24-6/11/1999). Ciudad Universitaria-Paraguay, 1999, № 6. p. 28-36.
7. **Sekerin A.P., Menshagin Yu. V., Laschenov V.A., Sayan province of high-potassium alkaline rocks and lamproites** // DAN, 1995, v. 342, № 1, p. 82-86.
8. **Vladykin N.V., Kovalenko V.I.** Isomorphism in mantle mica // Crystallochemistry of minerals. Proceedings of the 13th MMA Congress, 1986, Bulgaria, Sophia, p. 317-326.
9. **Vladykin N.V**. Bilibin massif –layered high-differentiated complex of K-ultrabasic-alkaline rocks // DAN, 1996, v. 349, № 6, p.972-975.
10. **Vladykin N.V.** Geochemistry and genesis of lamproites of the Aldan shield // Geology and Geophysics. 6 Inter. Kimber. Conf., Russia, Novosibirsk, 1997, v. 38, № 1, p. 130-145.
11. **Vladykin N.V.** Petrology and ore potential of K-alkaline rocks of the Mongol-Okhotsk magmatic area. Thesis as scientific report, 1997, p.1-80.
12. **Vladykin N.V., Lelyukh M.I., Tolstov A.V.** Lamproites of the Anabar region, Northern riming of the Siberian platform // 7 Kimber. Conf., Cape-Town, 1998, p. 946-948.
13. **Vladykin N.V., Lelyukh M.I** . Lamproite rocks of the eastern Anabar region // Deep-seated magmatism, magmatic sources and the problem of plumes. Vladivostok, Dalnauka, 2002, p.80-94.
14. **Vladykin N. V.** Malyi Murun Volcano-Plutonic Complex: An Example of Differentiated Mantle Magmas of Lamproitic Type // Geochemistry International, 2000, v. 38, suppl. 1, p. 573-583.
15. **Vladykin N.V.** The Aldan Province of K-alkaline rocks and carbonatites: problems of magmatism, genesis and deep sources // Alkaline magmatism and the problems of mantle sources, Irkutsk, 2001, p. 16 - 40.
16. **Vladykin N.V., Lelyukh M.I., Tolstov A.V., Serov V.P.** Petrology of kimberlite-lamproite-carbonatite rock association, East Prianabar’e (Russia) // Extended Abstracts of the 8 Inter. Kimber. Conf., 2003, FLA_0357.
17. **Vladykin N.V., Lelyukh M.I. Lamproites of Siberia – chemistry and systematics** // Problems of forecasting, prospecting and studies of deposits in the 21 century (Proceedings of the Conference), 2003, c. 365-370.
18. **Vladykin N.V.** Lamproites of the Siberian platform.//Alkaline complexes of the Central Siberia, Krasnoyarsk, 2003, p. 24-42.

19. **Vladykin N.V., Morikiyo T., Miyazaki T.** Sr and Nd isotopes geochemistry of alkaline and carbonatite complexes of Siberia and Mongolia and some geodynamic consequences // Problems of sources of deep magmatism and plumes. (Proceeding of the 5 Inter. Conf. Petropavlovsk- Kamchatsky), Irkutsk, 2005, v. 1, p. 19-37.
20. **Vladykin N.V., Torbeeva T.S.** Lamproites of the Tomtor massif // Geology and Geophysics, 2005, v. 46, № 10, p. 1038-1049.

UDK 550.42

Petrogenesis of alkali silicate, carbonatitic and kimberlitic magmas of the Kola Alkaline Carbonatite Province

Downes H[1], Mahotkin I L[2], Beard A D[1], Hegner E[3]

[1]*School of Earth Sciences, Birkbeck, University of London, Malet Street, London, UK*
h.downes@ucl.ac.uk
[2]*De Beers Moscow, Russia*
[3] *Institute of Mineralogy, Petrology and Geochemistry, University of Munich, Teresienstrasse 41/III, 80333, Munich, Germany*

ABSTRACT

Dyke rocks of the Devonian Kola Alkaline Carbonatite Province (KACP) range from kimberlites, through alkaline ultramafic silicate rocks, to carbonatites. We have studied dyke swarms in the south of the Kola Peninsula, near Kandalaksha, as well as kimberlite and melilitite pipes in Terskii Bereg. Dykes represent magmatic liquids, whereas plutonic alkaline silicate and carbonatite rocks in the KACP may be cumulates. The CaO/Al_2O_3 ratios for silicate dyke rocks are much higher than in Ocean Island Basalts (OIB), indicating a very small degree of melting of a carbonated mantle at depth. MgO-SiO_2 relationships suggest the presence of a spectrum of carbonate and silicate primary magmas.

The similarities of REE and isotopic compositions for ultramafic alkaline silicate rocks and carbonatite dykes indicate a strong relationship between the magma types. Their initial Sr and Nd isotope ratios fall in the Depleted Mantle field, suggesting a plume origin. Carbonate magmas were probably generated in the same region of the mantle by the same melting processes that formed the silicate magmas. Experimental results on the melting of carbonated mantle at 6GPa have shown that kimberlites and carbonatites can be formed from the same source during the same melting event. Pb isotopes show minor heterogeneity but generally cluster around an OIB mantle reservoir (interpreted as an asthenospheric mantle plume), except for one carbonatite that has high $^{207}Pb/^{204}Pb$ and $^{206}Pb/^{204}Pb$ ratios that require an ancient (ca. 1.75 Ga) enrichment in the lithospheric mantle source. Kimberlites and melilitites were formed at greater depths, as indicated by their HREE-depletion, and require phlogopite in their source.

Primary magmas in the KACP originated by a single process, triggered by the arrival of a mantle plume. A spectrum of magmas from carbonatite to damkjernite to melilitite to kimberlite was derived from melting of carbonated garnet peridotite. The plume provided heat that initiated the magmatism and caused melting of the carbonated garnet peridotite mantle, forming sodic magmas and carbonatites. Pockets of metasomatised lithospheric mantle also melted to form potassic magmas. Depth of melting and degree of melting are probably the major factors controlling the precise composition of the melts formed.

INTRODUCTION

The Kola Alkaline Carbonatite Province (KACP) contains numerous dykes and pipes of various ultramafic alkaline rocks, kimberlites and carbonatites [7, 12,

13, 24]. We present geochemical data for a representative suite of dykes and pipes, and discuss the significance of dyke and pipe magmatism in the region. We have chosen to study dyke and pipe rocks as these clearly represent magmatic liquids and have not experienced cumulate processes. Most of the silicate rocks in our data set have MgO contents > 6 wt%, and so are primitive liquid compositions.

Table 1.

Primitive magma compositions from Kola Alkaline Carbonatite Province (KACP)

	Kimberlite	Damkjernite	olivine-phlogopite melilitite	ultramafic lamprophyre	Melilitite	olivine-melilite melanephelinite	monticellite kimberlite	Carbonatite
	1	**2**	**3**	**4**	**5**	**6**	**7**	**8**
SiO_2	35.13	25.24	24.43	35.19	35.10	39.26	28.48	4.56
TiO_2	0.97	1.65	2.0	1.73	1.97	2.73	1.76	0.07
Al_2O_3	4.48	5.30	5.52	9.01	10.41	8.95	3.04	0.40
Fe_2O_3*	6.83	10.22	13.72	11.93	13.04	11.69	12.48	2.57
MnO	0.19	0.20	0.29	0.24	0.21	0.21	0.24	0.18
MgO	23.99	10.34	12.93	11.42	12.23	9.89	25.33	1.91
CaO	19.97	24.32	19.92	15.96	18.80	16.06	16.78	48.38
Na_2O	0.32	0.98	0.72	2.11	4.18	3.22	0.31	0.01
K_2O	2.75	1.46	2.26	1.66	1.42	1.49	0.77	0.13
P_2O_5	0.65	1.17	0.69	0.61	0.21	0.36	0.22	0.07
LOI	13.78	17.73	14.95	9.78	2.02	5.34	10.27	39.45
Total	99.06	98.61	97.44	99.64	99.59	100.89	99.68	97.82
K_2O/Na_2O	8.6	1.5	3.1	0.8	0.3	0.5	2.5	13.00
CaO/Al_2O_3	4.5	4.6	3.6	1.8	1.8	1.8	5.5	121
Rb	95	40	74	57	37	38	25.4	2.5
Sr	859	1869	1326	1174	1767	2660	972	3498
Ba	1571	951	1191	1351	405	2100	268	476
Sc	15	30	19	23	13	21	20	24.7
V	38	272	340	244	158		143	87
Cr	1316	196	211	497	300	223	1228	39.4
Ni	1180	106	247	313	272	137	1003	23.6
Y	16.4	19.7	24.5	24	16.7	22	9.7	26.6
Nb	237	159	189	157	124	120	106	8.5
Zr	123	353	328	251	131	252	90	87
Th	16.3	12.3	17.4	10	13.4	8.4	12.9	22.4
La	201	184.5	160.5	119.1	107.1	104	77.1	169.8
Ce	246	349.5	311.4	244.4	223.2	175	153.9	318.2
Pr		36.9	33.8	25.6				34.11
Nd	89	115.2	109.3	87.8	69.4	55	52.1	108
Sm	10.96	14.57	14.1	12.13	9.59	9.5	6.68	13.9
Eu	2.91	4.04	3.81	3.15	2.56	2.7	1.62	3.94
Gd	6.77	9.84	9.68	8.29	6.58		4.09	9.91
Dy	3.49	5.54	6.01	5.80	3.64		2.56	6.6
Ho		0.91	1.05	0.97				1.16
Er	1.15	1.67	2.25	2.09	1.28		0.96	2.46
Yb	1.04	1.2	1.89	1.87	1.04	1.7	0.74	1.71
Lu	0.16	0.16	0.28	0.31	0.15	0.14	0.10	0.22

Note: 1, 5: Beard et al. (1998), Terskii coast; 2, 3, 8: Downes and Mahotkin, unpub. data, Kandalaksha dyke swarm; 4: Beard et al. (1996), Kandalaksha Gulf; 6: Ivanikov et al (1998), Turiy peninsula; 7: Beard et al. (2007) Niva river, near Kandalaksha. * Total Fe as Fe_2O_3.

Two major Devonian dyke swarms are exposed on the south coast of the Kola peninsula. One swarm is located in the north-west part of the Kandalaksha Gulf and the other occurs on the Turiy Mys. Together they comprise more than 1000 bodies. From field relations, supported by sparse age determinations, dyke emplacement appears to have occurred in two stages in Early and Late Devonian times. The Early Devonian magmatism comprises alnoite, aillikite, damkjernite

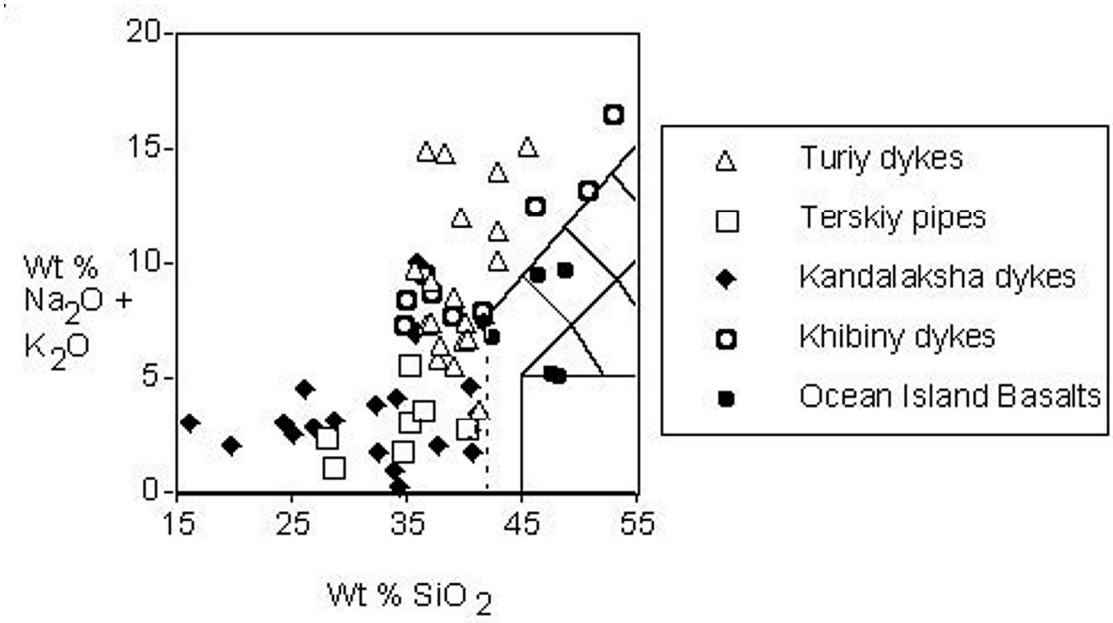

Fig. 1. **Total alkalis vs SiO_2 diagram for dyke rocks in KACP**

and carbonatite dykes, together with monticellite kimberlites and ultramafic lamprophyres [18]. The Late Devonian magmatism, particularly developed in the Turiy Mys, consists of dykes and pipes of kimberlites, alkaline and melilite picrites, melilites, nephelinites and carbonatites [9]. Some of the dykes and pipes contain crustal and mantle xenoliths that yield insights into the nature of the lithosphere beneath the region [3, 7]. We compare our results withy previously investigated carbonatite and ultramafic lamprophyre dykes from Kandalaksha [1], kimberlite pipes and dykes in Terskiy Bereg and Niva [2, 10], the melilitite-carbonatite-nephelinite dyke series of Turiy Mys [9] and dykes cutting the Khibiny massif [19].

GEOCHEMISTRY

Table 1 presents geochemical data for a selection of dyke and pipe rocks of the south Kola coast, assumed to represent true magmatic liquids. The values for LOI (Loss on Ignition) are high due to the presence of carbonate, phlogopite and, in the case of the kimberlites, serpentine. On the Total Alkalis vs Silica diagram (Fig. 1) the dykes and pipes fall outside the field of common magma types and

mostly have lower SiO_2 contents than common silica-undersaturated magmas such as basanites and nephelinites. They also generally have low total-alkali contents (<5 wt%). Only some evolved (< 7 wt% MgO) melilitites and melanephelinites, particularly those from Turiy Mys and the Khibiny massif, have higher total alkali

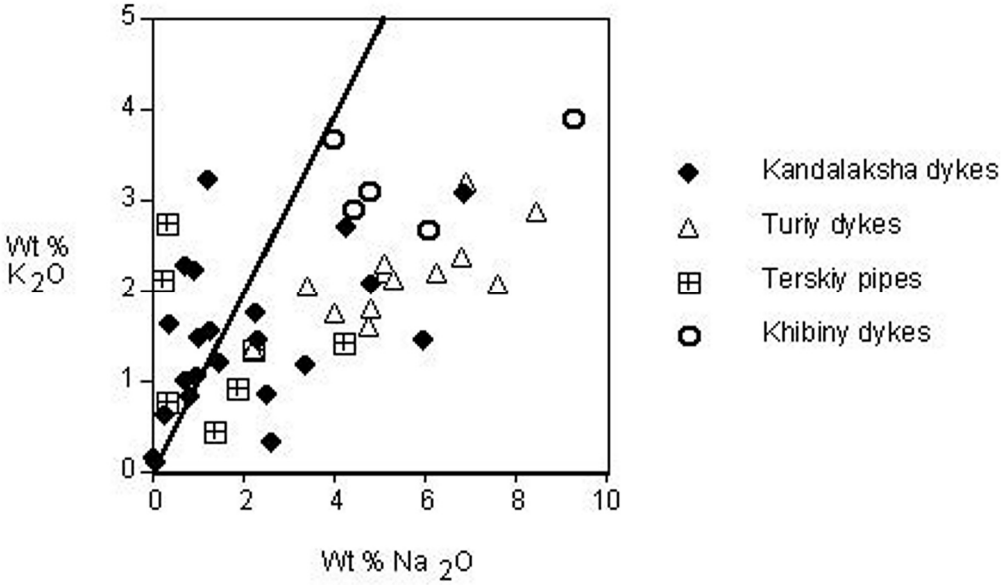

Fig. 2. **K_2O vs Na_2O diagram for dyke rocks in KACP**

contents. Within the dykes and pipes, sodic types are more abundant than the potassic varieties (Fig. 2), with the potassic rocks tending to be melilitites and damkjernites. Dykes from Turiy Mys and Khibiny massif tend to be only sodic varieties.

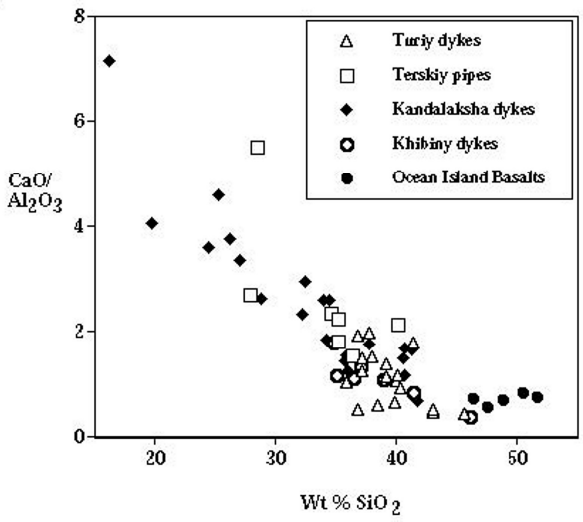

Fig. 3. **CaO/Al_2O_3 vs SiO_2 for dyke rocks in KACP**

Among the dyke rocks, CaO/Al_2O_3 ratios range from 1 to >5, with the higher values greatly exceeding those of ocean-island basaltic magmas (Fig. 3). Those from Kandalaksha and Terskii Bereg tend to be more extreme in composition than

those from Turiy Mys. The MgO-SiO_2 diagram (Fig. 4) shows that the dyke rocks display a wide variety of compositions. Some are highly magnesian (>12 wt % MgO) and have moderate SiO_2 contents (30-40 wt%). Carbonatite dykes are low in both MgO and SiO_2; damkjernites plot as intermediate between carbonatites and Mg-rich alkaline silicate magmas and form a positive trend between MgO and SiO_2. Some evolved magmas form a fractionation trend to high SiO_2 and low MgO (phonolites), mimicking the trend of the nepheline syenite plutonic complexes.

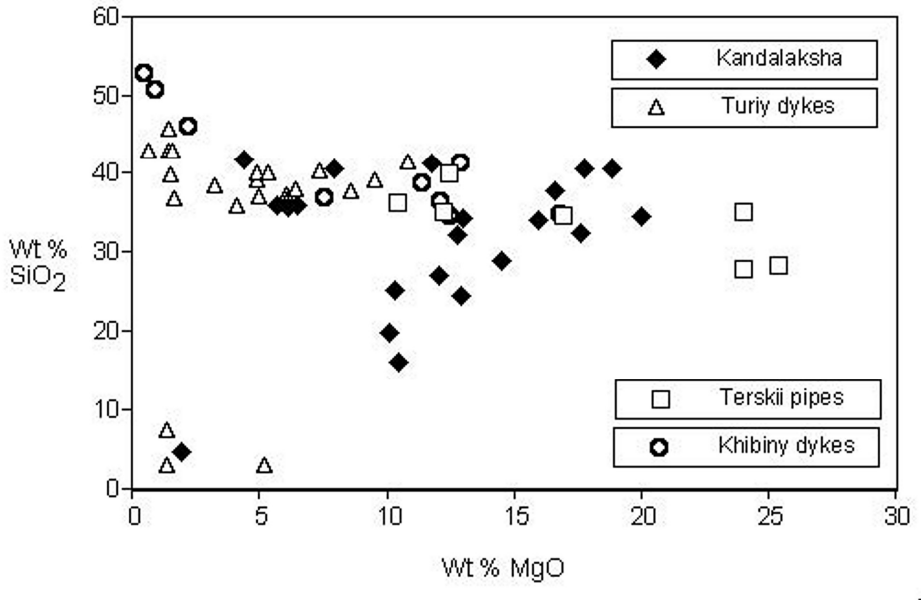

Fig. 4. **MgO vs SiO_2 for dyke rocks in KACP**

Figure 5 shows chondrite-normalised REE abundances of selected primitive dykes and pipes from the KACP. They show strong LREE enrichment with La/Yb between 70 and 200. The LREE abundances are much higher than those of OIB. Significantly, carbonatites have extremely similar REE patterns to those of the silicate magmas. Kimberlites and melilitites have lower HREE abundances than the other magma types (Fig. 5). Mantle-normalised incompatible trace element diagrams for dyke compositions from Kola (Fig. 6) show that they are enriched in strongly incompatible elements relative to ocean island basalts, especially Nb, Th and the LREE. Kimberlites and melilitites show a trough at Zr, which may be related to the specific mineralogy of their mantle source. Both potassic and sodic magmas show very similar trace element patterns. In contrast, a Kandalaksha carbonatite dyke shows distinct troughs at Rb and Nb, although in all other trace elements it is identical to melilitites and/or kimberlites, including the trough at Zr (Fig. 6).

A mantle origin for the parental melts within the Kola province is strongly supported by Sr and Nd radiogenic isotope studies [1, 2, 14, 15, 16]. Figure 7 shows the age-corrected Sr-Nd results for all analysed pipe and dyke rocks from the KACP. Initial $^{87}Sr/^{86}Sr$ ratios at 380 Ma for carbonatites show variations from

0.7030 to 0.7041. Most silicate dyke types plot within the Depleted mantle field with low $^{87}Sr/^{86}Sr$ and high εNd_i values; carbonatites tend to plot in a similar field or with even more depleted values. In contrast, potassic samples tend to show either higher $^{87}Sr/^{86}Sr_i$ ratios or lower εNd_i. In detail, these variations in isotope compositions have previously been explained by mixing of melts from two, three

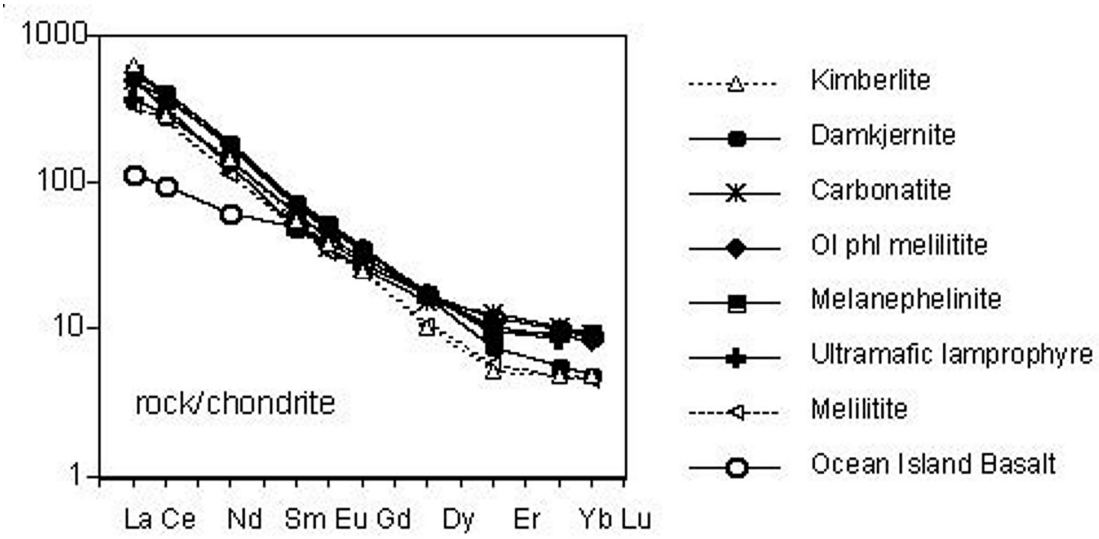

Fig. 5. **REE plots of primitive magma compositions derived from dyke rocks in KACP**

or even four mantle and crustal sources [8, 15, 16, 18, 22, 25]. Pb isotope results for the dyke rocks tend to plot around the Northern Hemisphere Reference Line (Fig. 8) and show the strong influence of an Ocean Island Basalt source. However, one carbonatite dyke shows remarkably high values of $^{207}Pb/^{204}Pb$ and $^{206}Pb/^{204}Pb$ ratios (without a high value of $^{208}Pb/^{204}Pb$). This appears to require formation of an unusually high U/Pb reservoir about 1.75 Ga ago, perhaps linked with metasomatism in the lithospheric mantle.

DISCUSSION

There is no obvious age progression for the various types of magmatic activity. Thus, all of the magma types were formed in the same series of events over a relatively short time span and over a relatively restricted area, and must therefore be related to some extent. The noble gas systematics [21] strongly suggest an origin related to mantle plume activity. Recent experimental results on the melting of carbonated mantle at 6GPa [6] have shown that kimberlites and carbonatites can be formed from the same source during the same melting event, suggesting a strong petrogenetic link between carbonatites, kimberlites and alkaline ultramafic rocks. Therefore the KACP magmatism probably originated in a single event that was triggered by the arrival of a mantle plume beneath the Archaean/Proterozoic lithosphere of the Kola region.

A very important consideration about KACP dyke and pipe rocks is that they show a very strong tendency to low SiO_2 contents, much lower than most common alkaline magmas such as OIB (Fig. 1). This may indicate an extremely low degree

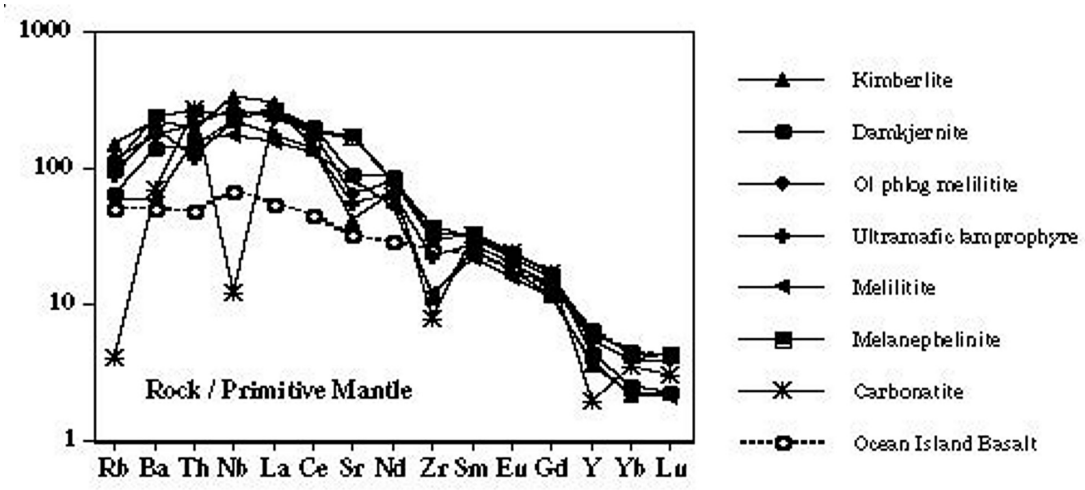

Fig. 6. **Mantle-normalised trace element plot of primitive magma compositions in KACP**

of partial melting in the source mantle. However, the abundance of magmatic carbonate suggests that the primary magmas were derived from a carbonated mantle and the effect of the presence of carbonate in the mantle may enhance the degree of silica undersaturation of the magmas formed from it. The high CaO/Al_2O_3 ratios (Fig. 3) are also strongly indicative of a carbonated mantle source. The dyke and pipe rocks also have much more enriched REE patterns compared to OIB (Fig. 5), again indicating a lower degree of melting than normal. The low HREE abundances of all primitive rock types indicate the presence of residual garnet, and the presence of diamonds in the kimberlites [10] is a clear indication that at least some of the magmas were generated at depths >120km. HREE values of potassic rocks such as kimberlites, melilitites and damkjernites tend to be lower than those of the sodic rocks, probably due to being derived from a deeper source with a higher amount of garnet. This is also in agreement with the negative Zr anomaly shown only by these samples (Fig. 6).

Dyke rocks clearly represent magma compositions, and hence they can be used to investigate the primitive magmas of the KACP (Table 1). Many alkaline ultramafic silicate rocks have high MgO (>12 wt%) and frequently have >500ppm Ni and >1000ppm Cr, and are derived directly from the mantle. It has been suggested [9] that an olivine melilite melanephelinite was the primary magma for the Turiy dyke series. However, some melilitites and melanephelinites have low MgO contents (<10 wt%) and must therefore be the products of fractionated magmas [9]. They also have much lower Ni and Cr contents (4-20ppm Cr; 35-65 ppm Ni), supporting the suggestion that they have experienced fractionation of mafic minerals.

On the MgO-SiO_2 diagram (Fig. 4) some of the dyke rocks show a positive correlation between these oxides, which must relate to mixing between more and less carbonated mantle source regions. Damkjernites fall within this array, having low silica contents (25-27 wt% SiO_2) and only 10-12 wt% MgO. Although they are potassic magmas, they appear to be transitional to true carbonatites as they contain >20% CaO. CaO/Al_2O_3 ratios for silicate dyke rocks range up to 5 (Fig. 3), indicating a very small degree of melting of a carbonated mantle at depth. The damkjernites again have the highest CaO/Al_2O_3, transitional to silicocarbonatites which have ratios >7. Mantle-normalised trace element diagrams for rocks from the dykes and pipes (Fig. 6) show that kimberlite, melilitite and damkjernite have the lowest HREE abundances, indicating a lower degree of melting, more garnet in the mantle source, and probably greater depth of formation.

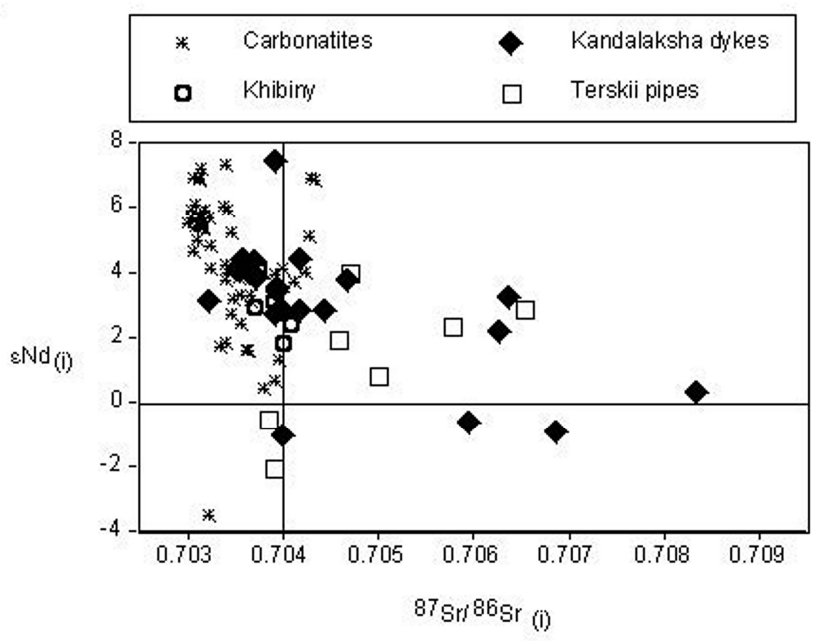

Fig. 7. **Sr-Nd isotope diagram for Kandalaksha dyke rocks, supplemented by data for melilitite and kimberlite pipes from Terskii Bereg and dykes from Khibina massif**

Initial Sr and Nd isotope ratios of most KACP dyke rock-types (Fig. 7) fall in the Depleted Mantle field (εNd_i = 2-4; $^{87}Sr/^{86}Sr$ = 0.7035-0.7045) and the magmas must therefore have been derived from a depleted mantle source. However, some pipes and dykes, particularly the potassic ones, have isotopic compositions that are quite different from those of the majority of the Kola magmas. Several processes could have given rise to these unusual isotopic ratios. One possibility is that they could have been derived from the mantle lithosphere, in which either phlogopite or amphibole was present. Phlogopite has a high Rb/Sr and over time would cause the region of the mantle in which it was situated to have a high $^{87}Sr/^{86}Sr$. However, mantle phlogopite has very low REE contents, and so its effect on the Nd isotope ratio would be limited. In contrast, mantle amphibole has modest Rb/Sr ratios but is often highly LREE-enriched, which would cause low ε_{Nd} values to evolve. The

impact of the mantle plume on the lithosphere may have caused these low-solidus domains to undergo partial melting, thus producing a range of sodic and potassic magmas. An alternative possibility is that samples with low εNd_i values may be contaminated by the granulite facies lower continental crust [11], whereas those with high $^{87}Sr/^{86}Sr$ may result from hydrothermal alteration that has affected Sr but not the REE. Without detailed oxygen and Sr isotope measurements of separated minerals within the samples, this suggestion cannot be verified. However, it is supported by a leaching experiment [1] in which the measured Sr isotope composition of an ultramafic lamprophyre was reduced from 0.711 to 0.709 by leaching in hot acid. No leaching experiments have been carried out prior to Pb isotope analysis, so the effect of alteration on Pb isotopes is as yet unknown. Pb isotope ratios of the dyke rocks cluster around the typical values of modern Oceanic Islands, indicating that much of the Pb is derived from an asthenospheric (plume) source. Nevertheless, a single carbonatite value suggests that ancient metasomatised mantle lithosphere is also a component in the source of Kola magmas.

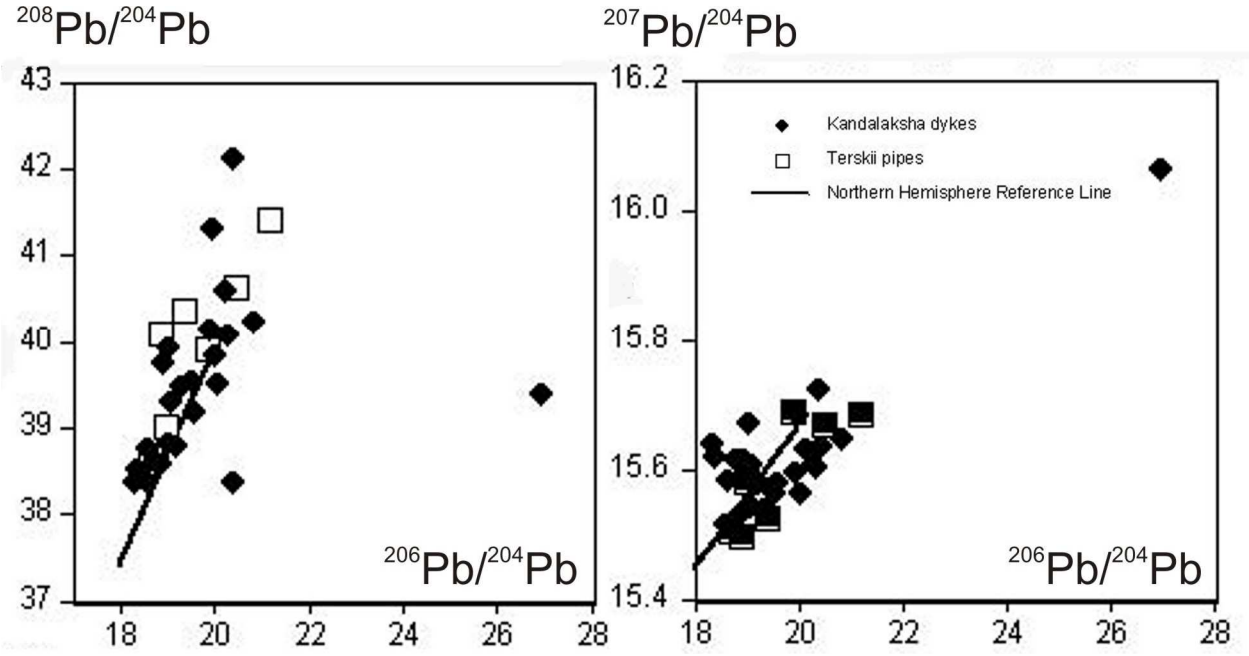

Fig. 8. **Pb isotope compositions (present-day) for dykes and pipes from KACP, compared to the Northern Hemisphere Reference Line (locus of MORB and OIB magmatism)**

Figure 2 shows that there is a spectrum of sodic and potassic magma types within the dykes and pipes. Potassic magmas clearly must have had a different mantle source mineralogy than sodic magmas, and derivation from a phlogopite-bearing lithospheric mantle is one possible explanation. Phlogopite is present in mantle xenoliths from beneath the Kola region [3]. Nevertheless, the REE and trace element patterns of the potassic rocks are very similar to those of the sodic magmatic rocks, indicating a broadly similar source. Although some potassic

magmas have Sr and Nd isotope compositions overlapping with the main field of Kola dyke magmatism (Fig. 7), many show much higher $^{87}Sr/^{86}Sr$ or lower εNd_i values. These unusual values may be derived from the enriched mantle lithosphere. Alternative explanations could be that these rocks are either hydrothermally altered or contaminated by the Archaean/Proterozoic crust.

The evolution and source characteristics of carbonatite magmas in the KACP have been recently reviewed [4]. There is a long-standing debate about whether carbonatite magmas are products of liquid immiscibility or can be derived directly from melting of the mantle (or both). However, many recent experimental studies [5, 20, 23] have demonstrated that carbonatite melts can be formed from carbonated lherzolite at moderate to high pressures (3-10 kb). The presence of carbonatite dykes indicates that carbonate magmas were present as separate entities in the KACP. The similarities of the REE and trace element patterns for ultramafic alkaline silicate rocks and carbonatite dykes indicate that there is a strong relationship between the two magma-types.

CONCLUSIONS

From the data reviewed above, we conclude that most of the primary magmas within the Kola alkaline province were derived from a shallow mantle source although a Devonian asthenospheric mantle plume initiated the magmatism. The influx of heat caused melting of the carbonated garnet peridotite asthenospheric mantle, forming sodic magmas and carbonatites. Pockets of metasomatised lithospheric mantle were also melted and formed potassic magmas. The depth of melting and degree of melting are probably the major factors controlling the precise composition of the melts formed.

A spectrum of primary magmas from carbonatite to damkjernite to melilitite to ultramafic lamprophyre was derived from melting of carbonated garnet peridotite. Most magmas have very similar trace element and isotopic compositions and therefore are derived from a similar mantle source. Potassic magmas may have been derived from enriched mantle lithosphere containing phlogopite, at a deeper level than the sodic magmas.

ACKNOWLEDGEMENTS

We are grateful to colleagues in the SVEKALAPKO project, part of the ESF-funded EUROPROBE project, for useful discussions.

REFERENCES

1. **Beard A.D., Downes H., Vetrin V., Kempton P.D., Maluski H.** Petrogenesis of Devonian lamprophyre and carbonatite minor intrusions, Kandalaksha Gulf (Kola Peninsula) // Lithos, 1996, v. 39, p. 93-119.
2. **Beard A.D., Downes H., Hegner E., Sablukov S.M., Vetrin V., Balogh K.** Mineralogy and geochemistry of Devonian ultramafic minor intrusions of the southern Kola Peninsula,

Russia: implications for the petrogenesis of kimberlites and melilitites // Contrib. Mineral. Petrol., 1998, v. 130, p. 288-303.

3. **Beard A.D., Downes H., Mason P.R.D., Vetrin V.R.** Depletion and enrichment processes in the lithospheric mantle beneath the Kola Peninsula (Russia): evidence from spinel lherzolite and wehrlite xenoliths // Lithos, 2007, v. 94, p. 1-24.
4. **Bell K., Rukhlov A.S.** Carbonatites from the Kola Alkaline Province: Origin, evolution and source characteristics // In: Phoscorites and Carbonatites from mantle to mine. (Eds: F Wall and A N Zaitsev). Mineralogical Society Series, 2004, p. 433-468.
5. **Dalton J.A., Wood B.J.** The composition of primary carbonate melts and their evolution through wall-rock reaction in the mantle // Earth Planet. Sci. Lett., 1993, v. 119, p. 511-525.
6. **Dalton J.A, Presnall D.C.** The continuum of primary carbonatitic-kimberlitic melt compositions in equilibrium with lherzolite: data from the system CaO-MgO-Al_2O_3-SiO_2-CO_2 at 6GPa // J. Petrol., 1998, v. 39, p. 1953-1964.
7. **Downes H., Balaganskaya E., Beard A., Liferovich R., Demaiffe D.** Petrogenetic processes in the ultramafic, alkaline and carbonatitic magmatism in the Kola Alkaline Province: A review // Lithos, 2005, v. 85, p. 48-75.
8. **Dunworth E.A., Bell K.**. The Turiy Massif, Kola Peninsula, Russia: Isotopic and Geochemical Evidence for Multi-source Evolution // J. Petrol., 2001, v. 42, p. 377-405.
9. **Ivanikov V.V., Rukhlov A.S., Bell K.** Magmatic evolution of the melilitite-carbonatite-nephelinite dyke series of the Turiy peninsula (Kandalaksha Bay, White Sea, Russia) // J Petrol., 1998, v. 39, p. 2043-2059.
10. **Kalinkin M.M., Arzamastsev A.A., Polyakov I.V.** Kimberlites and related rocks of the Kola region // Petrology, 1993, № 1, v. 173-180.
11. **Kempton P.D., Downes H., Neymark L.A., Wartho J.A., Zartman R.E., Sharkov E.V.** Garnet granulite xenoliths from the northern Baltic Shield - the underplated lower crust of a Paleoproterozoic Large Igneous Province? // J. Petrol., 2001, v. 42, p. 731-763.
12. **Kogarko L.N.** Alkaline igneous rocks of the Kola Peninsula. In: Alkaline Igneous Rocks // Geol. Soc. Sp. Pub., 1987, v. 30, p. 531-544.
13. **Kogarko L.N., Kononova V.A., Orlova M.P., Woolley A.R.**. Alkaline rocks and carbonatites of the world. Part 2. Former USSR. Chapman and Hall, London, 1995, 225 p.
14. **Kramm U., Kogarko L.N.** Nd and Sr isotope signatures of the Khibina and Lovozero agpaitic centres, Kola Alkaline Province, Russia // Lithos, 1994, v. 32, p. 225-242.
15. **Kramm U.** Mantle components of carbonatites from the Kola Alkaline Province, Russia and Finland: A Nd-Sr study // Eur. J. Mineral., 1993, № 5, p. 985-989.
16. **Kramm U., Kogarko L.N., Kononova V.A., Vartiainen H.** The Kola Alkaline Province of the CIS and Finland: Precise Rb-Sr ages define 380-360 Ma age range for all magmatism // Lithos, 1993, v. 30, p. 33-44.
17. **Kramm U., Sindern S.** Timing of Kola ultrabasic alkaline, alkaline and phoscorite-carbonatite magmatism. In: Phoscorites and Carbonatites from mantle to mine // (Eds: F Wall and A N Zaitsev), Mineralogical Society Series, 2004, p. 75-98.
18. **Mahotkin I, Downes H, Hegner E, Beard A.** Devonian dyke swarms of alkaline, carbonatitic and primitive magma-type rocks from the south Kola peninsula: geochemical and isotopic constraints on plume-lithospheric interaction // Extended Abstract 8th IKC, 2003.
19. **Sindern S., Zaitsev A.N., Demeny A., Bell K., Chakmouraradian A.R., Kramm U., Moutte J., Rukhlov A.S.** Mineralogy and geochemistry of silicate dyke rocks associated with carbonatites from the Khibina complex (Kola, Russia) – isotope constraints on genesis and small-scale mantle sources // Mineral. Petrol., 2004, v. 80, p. 215-239.
20. **Thibault Y., Edgar A.D., Lloyd F.E.** Experimental investigation of melts from a carbonated phlogopite lherzolite: implications for metasomatism in the continental lithospheric mantle // Amer. Mineral., 1992, v. 77, p. 784-794.

21. **Tolstikhin I.N., Kamensky I.L., Marty B., Nivin V.A., Vetrin V.R., Balaganskaya E.G., Ikorsky S.V., Gannibal M.A., Weiss D., Verhulst A., Demaiffe. D.** Gas, rare isotopes and parent trace elements in ultrabasic-alkaline-carbonatite complexes, Kola Peninsula: identifycation of lower mantle plume component // Geoch. Cosm. Acta, 2002, v. 66, p. 881-901.
22. **Verhulst A., Balaganskaya E., Kirnarsky Yu., Demaiffe D.** Petrological and geochemical (trace elements and Sr-Nd isotopes) characteristics of the Paleozoic Kovdor ultramafic, alkaline and carbonatite intrusion (Kola Peninsula, NW Russia) // Lithos, 2000, v. 51, p. 1-25.
23. **Wallace M.E., Green D.H.** An experimental determination of primary carbonatite magma composition // Nature, 1988, v. 335, p. 343-346.
24. **Woolley A.R.** The spatial and temporal distribution of carbonatites // In: Bell, K. (ed.). Carbonatites: Genesis and Evolution. Unwin Hyman, London, 1989. 15-37.
25. **Zaitsev A., Bell K.** Sr and Nd isotope data of apatite, calcite and dolomite as indicators of source, and the relationships of phoscorites and carbonatites from the Kovdor massif, Kola peninsula, Russia // Contrib. Mineral. Petrol., 1995, v. 121, p. 324-335.

UDK 550.42

Mantle plume vs. subduction-related origin of volcanism in Italy: A commentary

Peccerillo A.

Dipartimento di Scienze della Terra, University of Perugia, Piazza Università, 06100 Perugia, Italy pecceang@unipg.it

ABSTRACT

Italy is the site of complex Plio-Quaternary volcanic activity, ranging from mafic to felsic, and from subalkaline to ultra-alkaline. Mafic rocks display variable abundances and ratios of incompatible elements, which cover both orogenic- and anorogenic-type compositions. This testifies to the presence of very heterogeneous upper mantle beneath Italy. Orogenic-type rocks range from calcalkaline to ultrapotassic and are mainly erupted in the Aeolian arc and along the Tyrrhenian border of the Italian peninsula. Anorogenic rocks concentrate in Sicily (Etna, Iblei), Sicily Channel and Sardinia.

When considered collectively, the mafic rocks from Italy show wide variations of radiogenic isotopes, defining continuous trends between distinct mantle compositions, such as FOZO and EM1, and between FOZO and the upper crust. These trends have been interpreted as mixing involving deep reservoirs, emplaced into the upper mantle by uprising plumes. However, the occurrence of abundant rocks in Italy with arc geochemical signatures (i.e., high LILE/HFSE ratios) are best explained by multiple episodes of mantle metasomatism, linked to Oligocene to present subduction processes occurred during convergence between Africa and Europe. Anorogenic magmas represent uncontaminated asthenospheric material that underwent passive ascent and decompression melting in back arc areas or along transfer faults at the boundaries between extruded lithospheric blocks of the African margin.

INTRODUCTION

Plio-Quaternary magmatism in Italy occurs in a relatively restricted area, in and around the Tyrrhenian Sea basin (Fig. 1). Rocks range in composition from calcalkaline and shoshonitic to Na- and K-alkaline and ultra-alkaline, and from mafic to felsic, making up a very complex magmatic setting [33]. Most rocks are intermediate to silicic in composition and were formed by processes of fractional crystallisation, mixing, crustal assimilation and, in some cases, crustal anatexis [33, 34 for a review]. However, there are also significant amounts of mantle-derived mafic rocks that represent parental melts of volcanic suites and provide important information on upper mantle beneath Italy.

Plio-Quaternary mafic magmas in Italy have very variable major, trace element, and radiogenic isotope signatures. Most authors believe that these complexities can be conveniently explained by assuming a genesis of magmas in

mantle sources that were modified by multiple subduction-related metasomatic processes, coupled with melting of uncontaminated asthenospheric material

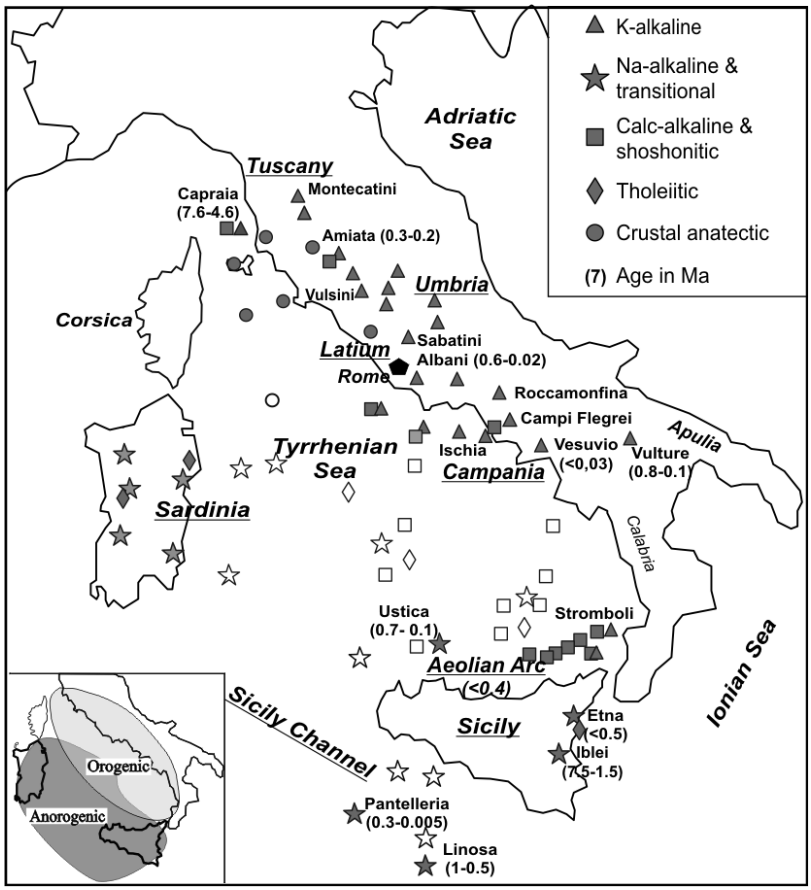

Fig. 1. Schematic map showing location, ages (in parentheses) and petrochemical affinity (indicated by different symbols) of Plio-Quaternary magmatic centres in Italy. Inset: distribution of orogenic (i.e. high LILE/HFSE ratios) and unorogenic (low LILE/HFSE ratios) volcanism.

passively upwelling in zones of lithospheric extension. Both subduction and extension processes would be the effects of the convergence between the European and African plates [e.g., 13, 31, 38]. This has been active from Oligocene to present, during south-eastward rollback of the subduction zone from southern France to southern Tyrrhenian Sea, and the contemporaneous opening of the Balearic and Tyrrhenian back-arc basins [6, 12]. In this context, some magmas (i.e. the calcalkaline to K-alkaline rocks of the Aeolian arc and the Italian peninsula) were generated in the mantle wedge above the subducting slab, whereas other magmas were formed by decompression melting of asthenospheric mantle in back-arc areas (e.g. Plio-Quaternary tholeiitic to Na alkaline volcanism in Sardinia and the Tyrrhenian Sea) or at the margin of the African plate along strike-slip faults (e.g. Sicily Channel Na-alkaline volcanism) generated by block expulsion along geometrically irregular colliding continental margins [24].

Other authors believe that the entire recent Italian volcanism has no genetic link with subduction, and is related to either the ascent and melting of deep mantle plumes or to melting of asthenospheric material in an area of passive rifting [e.g., 5, 21, 45]. Finally, other authors suggest that both subduction and plume components had a role in the genesis of magmatism. In this case, the Na-alkaline volcanism in eastern Sicily would represent almost pure plume material, whereas the calcalkaline to K-alkaline magmas in the southern Tyrrhenian Sea and the Italian peninsula would represent plume material contaminated by subduction-related fluids and melts [16].

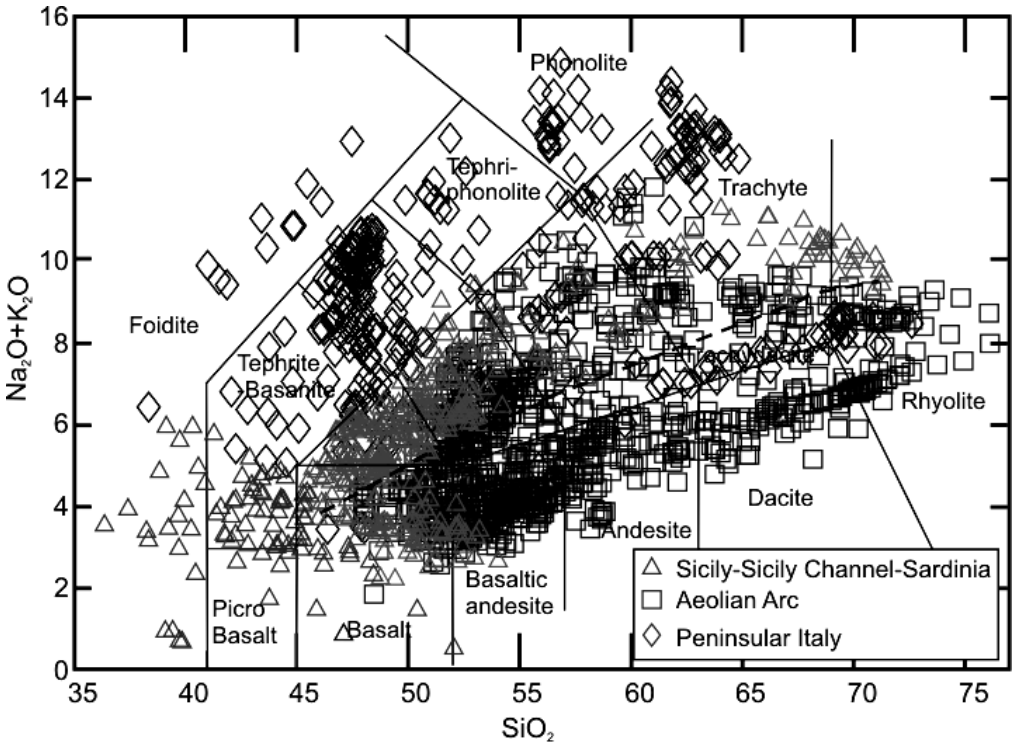

Fig. 2. Total alkalies vs. silica (TAS) classification diagram showing the large compositional variations of Plio-Quaternary volcanism in Italy.

In this paper the most significant petrologic and geochemical data on Italian Plio-Quaternary mafic volcanic rocks are reviewed with the aim of evaluating mantle source characteristics and exploring their bearing on models of geodynamic evolution of the Tyrrhenian Sea area.

MAGMATIC SETTING

Plio-Quaternary volcanic rocks in Italy range in composition from tholeiitic and calcalkaline, to shoshonitic, Na-alkaline, and K-alkaline, and from mafic to felsic covering almost completely the compositional range of rocks occurring at a global scale on Earth (Fig. 2). Data on mafic rocks with variable petrochemical affinity can furnish important information on the upper mantle beneath Italy [27].

Based on incompatible trace element ratios, two broad groups of mafic magmas have been distinguished. A first group, generally referred to as “orogenic”, has high ratios of LILE/HFSE (Large Ion Lithophile elements such as Rb, K, Th, U, LREE, Pb; High Field Strength Elements such as Ta, Nb, Zr, Hf. Ti) and resemble magmas erupted at converging plate margins. Another group, generally referred to as “anorogenic”, has low LILE/HFSE and resemble intraplate OIB-like magmas. Patterns of incompatible elements normalised to primordial mantle compositions for representative samples of the two groups are shown in Fig. 3. It can be noticed that orogenic rocks (Fig. 3a) have fractionated patterns with negative spikes of Ta, Nb and other HFSE, and positive spikes of LILE, especially Cs, Rb, Th, LREE and Pb. By contrast, anorogenic rocks (Fig. 3b) have a bell-shaped pattern with a peak at Ta-Nb, resembling closely typical OIB. Th/Yb vs. Ta/Yb diagram of Italian mafic rocks, discriminating between intraplate and subduction-related compositions, are shown in Fig. 4.

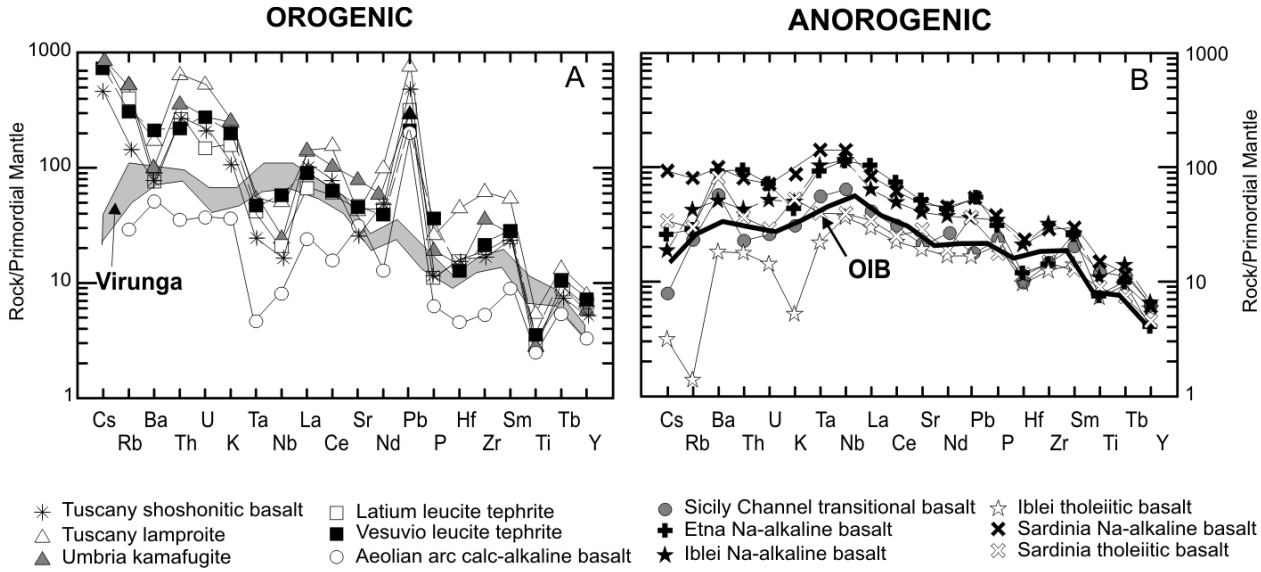

Fig. 3. Incompatible element patterns normalised to primordial mantle composition for mafic (MgO > 5 wt%) orogenic- and anorogenic-type rocks in Italy. The patterns of the Virunga (East Africa) potassic rocks and of average OIB are reported for comparison.

The orogenic rock group is formed by a few arc-tholeiites plus abundant calcalkaline, shoshonitic, potassic and ultrapotassic rocks. These make up several volcanic provinces or districts (e.g. Aeolian arc, Campania Province, Roman or Latium Province, Umbruia, etc.; see Fig. 1 and ref. [33]), and some seamounts (e.g. Marsili, Palinuro, etc.) in the Tyrrhenian Sea (Fig. 1). The second group consists of tholeiitic, transitional and Na-alkaline magmas, mainly occurring in eastern Sicily, Sicily Channel, Sardinia and in some places of the Tyrrhenian Sea (e.g. Ustica). The geographic distribution of Plio-Quaternary orogenic and

anorogenic rocks around the Tyrrhenian Sea basin is schematically shown in the inset of Fig. 1.

The calcalkaline rocks of the Aeolian arc and seamounts are associated with a seismic zone whose earthquake foci increase in depth from Calabria towards the Campania volcanic area (Vesuvio, Campi Flegrei, etc.). This defines a narrow Benioff zone, which is believed to be related to the immersion of the Ionian crust beneath Calabria and the southern Tyrrhenian Sea (e.g., [13, 26], and references therein).

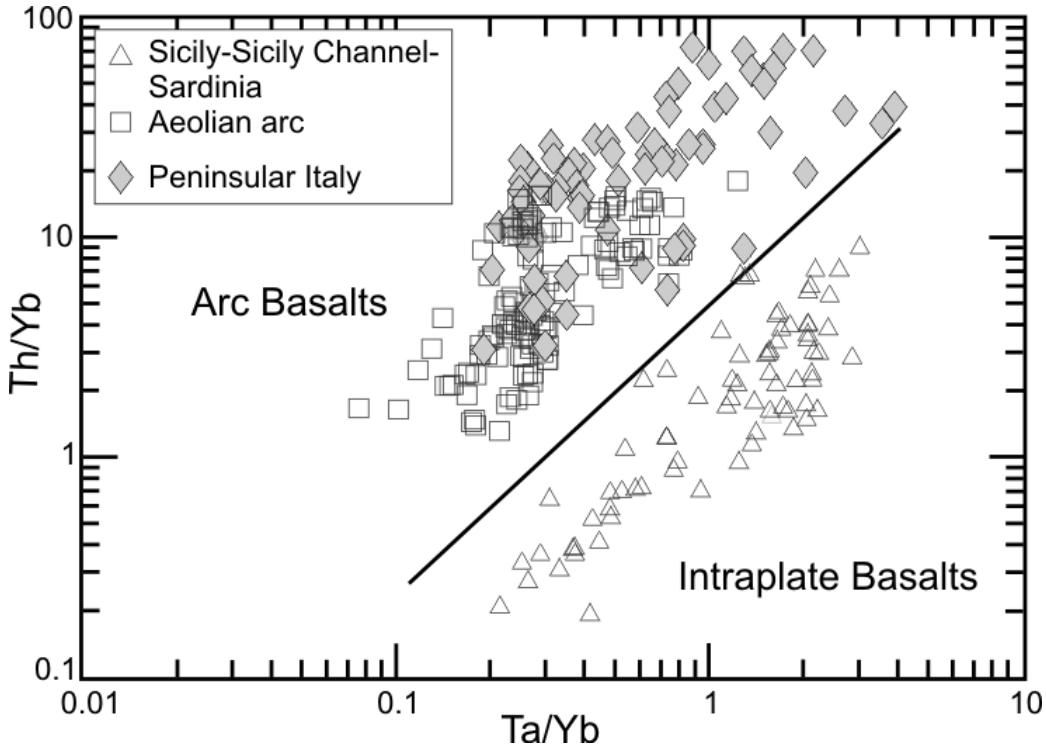

Fig. 4. **Th/Yb vs. Ta/Yb variation of Plio-Quaternary mafic (MgO > 5 wt%) rocks in Italy. The line divides the field of orogenic and anorogenic compositions at a global scale.**

The potassic alkaline rocks represent the most important magma types in central Italy. They show a wide range of potassium enrichment and degree of silica saturation, from nearly saturated shoshonites and ultrapotassic lamproites to strongly undersaturated kamafugites and Roman-type leucite-bearing rocks [32-25]. However, all the potassic alkaline rocks show obvious arc-type trace-element signatures with negative HFSE anomalies and high LILE/HFSE ratios (Fig. 3a). Some mafic ultrapotassic rocks in Tuscany show mantle-equilibrated compositions (Mg# ~ 70-75; Ni ~ 200-300 ppm, Cr ~ 500-700 ppm), and contain mantle xenoliths [8]. However, their incompatible element patterns resemble very closely upper crustal material such as the Tuscany gneiss, S-type granites and average global subducted sediments [e.g., 39, 43] (Fig. 5).

The anorogenic rocks range from tholeiitic to Na-alkaline and nephelinitic, and have low LILE/HFSE ratios. These rocks are located either on the African

plate (e.g., at Iblei, Linosa, Pantelleria and Etna) or in back-arc positions with respect to the Apennine compressional belt (i.e., Tyrrhenian Sea and Sardinia).

Radiogenic isotope compositions show continuous variation of Sr-Nd-Pb isotope ratios from southern Italy to Tuscany and Sardinia. Rocks in the south (Etna, Iblei and the Sicily Channel) have relatively low $^{87}Sr/^{86}Sr$ and high

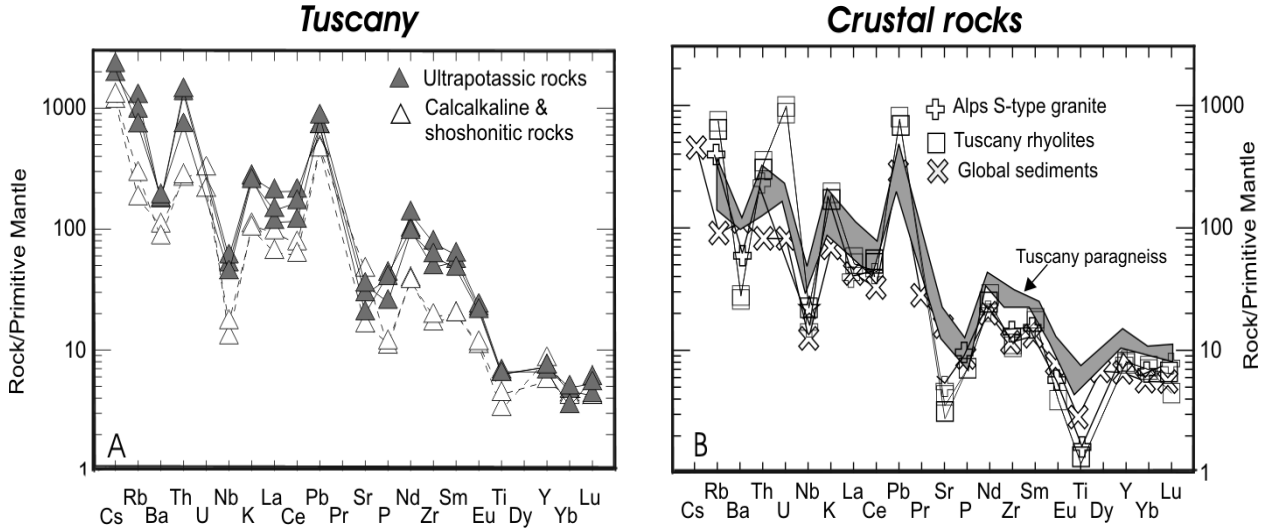

Fig. 5. **Incompatible element patterns normalised to primordial mantle composition for mafic (MgO > 5 wt%) calcalkaline to ultrapotassic rocks**

From Tuscany (A) and for representative upper crustal rocks (B; Tuscany crustal anatectic rhyolites, Tuscany paragneiss, global subducted sediments, S-type granite from Western Alps). Note the close similarity between the mantle-derived Tuscany magmas and the upper crustal rocks.

$^{143}Nd/^{144}Nd$, close to MORB (Fig. 6), and radiogenic Pb isotope ratios (Fig. 7). Overall, these rocks resemble the so-called FOZO mantle reservoir (Focus Zone; [17, 47], and references therein). Rocks in Sardinia have relatively poorly radiogenic Sr- and unradiogenic Pb-isotope composition and resembles the so-called EM1 mantle reservoir. Finally, the magmatism in the Aeolian arc and the Italian peninsula shows intermediate Sr-Nd-Pb isotopic characteristics between Etna and the typical upper crustal rocks, with crustal-like isotopic signatures increasing from south to north [9, 16, 18, 48, 49]. The Tuscany mafic rocks, therefore, have Sr-Nd-Pb isotopic signatures very close to those of S-type granites and metapelites, as also observed for incompatible element patterns (Fig. 5); [39, and references therein].

SUBDUCTION-RELATED VS. PLUME-RELATED HYPOTHESES FOR ITALIAN MAGMATISM

There has been an intense debate on the origin of Plio-Quaternary magmatism in Italy [see ref. 35 for a review]. Most of the discussion has been focused on the dilemma whether this magmatism reflects emplacement of deep mantle plumes or it is the products of shallow mantle processes, such as subduction and passive

asthenospheric upraise and melting [38]. Here, the main evidence in favour and against of the two classes of hypotheses are critically summarised.

Evidence in favour of plume-related models

The idea that the Plio-Quaternary magmatism in Italy results from the emplacement and melting of a deep mantle plume dates back to '70. Vollmer [48] suggested that the entire magmatism along the Italian peninsula, from Vulture to Tuscany, was genetically related to a mantle plume impinging beneath the Italian lithosphere during its south-eastward migration. Such a hypothesis, however, was unable to explain several first-order characteristics of the magmatism, including trace element geochemistry and timing of magma emplacement in the different volcanic districts [see ref. 29]. Recently, the plume hypothesis received new support thanks to seismic tomographic studies of Hoernle et al. [ref. 19, 20]. These authors presented evidence for the occurrence of a low-velocity layer at about 100-300 km beneath the eastern Atlantic, Central Europe and the Western Mediterranean Sea. They interpreted this layer as a plume head and suggested that magmatism in Italy and western-central Europe may be ultimately related to this plume. More specifically, it has been proposed that deep-mantle plume material (indicated as LVC and FOZO; [19, 20]) ascended beneath the eastern Atlantic and Europe, and interacted with different types of resident upper mantle rocks and crustal materials generating the wide range of radiogenic isotopic compositions observed in the eastern Atlantic, Central Europe and Mediterranean volcanic provinces [19].

Based on trace element and radiogenic isotope data, Gasperini et al. [ref. 15] suggested a plume origin for the Quaternary EM1-type magmatism of northern Sardinia, whereas the entire compositional variation of Plio-Quaternary magmatism in central and southern Italy was suggested to results from mixing between a HIMU-like mantle plume and components of subduction origin [16].

Bell et al. [ref. 5] proposed that a plume has lain at a depth of 600 to 400 km for at least 30-35 Ma, beneath the Western Mediterranean area. Although remote from the lithosphere, this plume would have been responsible for most if not all the most important geodynamic and magmatic events occurred in this area from Oligocene to Present.

Sr-Nd-Pb isotope variation is considered as the main evidence in favour of the occurrence of a mantle plume beneath Italy [e.g., 5, 16]. Sr vs. Nd isotope (Fig. 6) and Sr vs. Pb isotope diagrams (Fig. 7) show relatively smooth trends that indicate mixing among at least three distinct and discrete end-members. According to promoters of the plume hypothesis, at least two or three of these components (i.e. FOZO and EM1) originate in plume(s). Some authors (e.g., 7) suggest that also another end-member, represented by the mafic rocks from the Tuscany and Roman (Latium) provinces, could represent a mantle plume. In such a view, the high $^{87}Sr/^{86}Sr$ and low $^{143}Nd/^{144}Nd$ of these magmas would reflect aging and recycling of old subduction-contaminated mantle for at least 2 Ga in the deep earth before being emplaced as a plume at shallow depth to generate potassic magmas.

Other evidence invoked to support the plume hypothesis includes the occurrence of abundant K-alkaline magmatism and the presence of carbonate-rich pyroclastic rocks in central Italy (Umbria-Abruzzi region) and at Mt. Vulture. It has been pointed out that ultrapotassic rocks are typical of intraplate setting [e.g., 2, 21, 45] such as the East Africa rift, which is classically believed to have developed above mantle plumes. Moreover, the carbonate-rich rocks from Vulture and Central Italy are associated with melilitites and are believed to represent carbonatitic magmas. As for the K-rich alkaline rocks, the carbonatite-melilitite association is believed to be typical of plume-related settings such as East Africa [2, 42, 46].

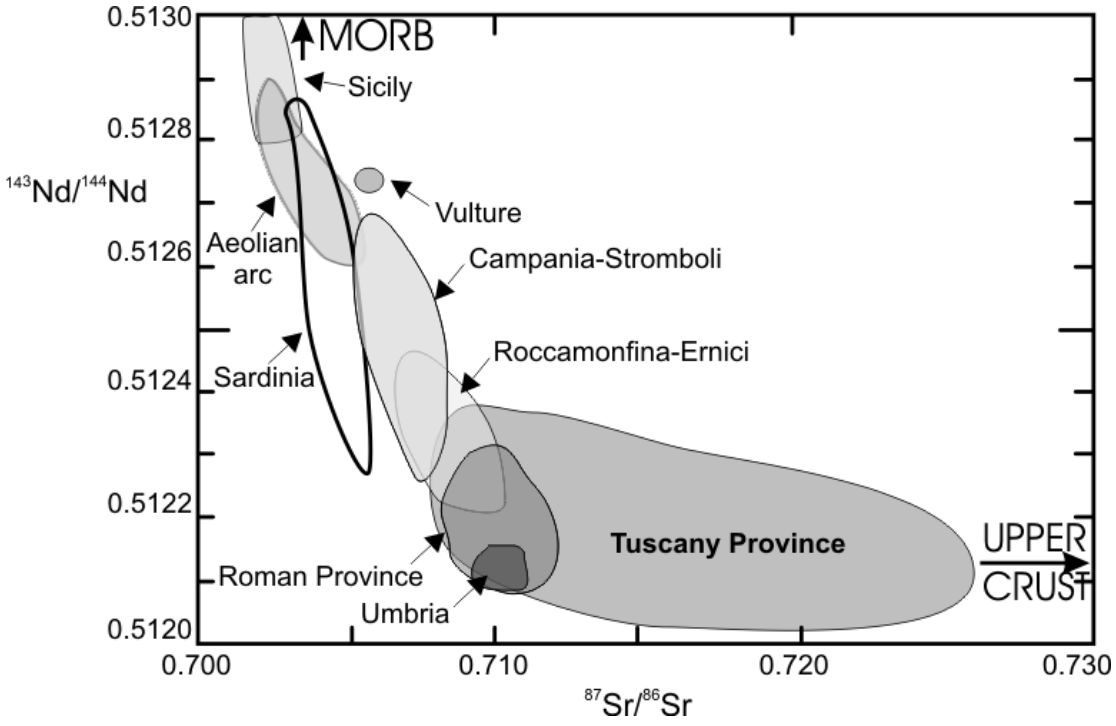

Fig. 6. **Variation of $^{143}Nd/^{144}Nd$ vs. $^{87}Sr/^{86}Sr$ for Plio-Quaternary mafic rocks (MgO > 5 wt%) from the Tyrrhenian Sea area.**

Finally, seismic tomographic images reported by Hoernle et al. [ref. 19] are considered as an important if not decisive evidence in favour of the occurrence of mantle plumes beneath the Western Mediterranean, western-central Europe and the eastern Atlantic.

However, the plume hypothesis conflicts with a number of petrological and geochemical data that represent first-order features of the Italian magmatism. The idea that FOZO or other so-called mantle reservoirs (HIMU, EM1, etc.) represent plumes is based on the concept that geochemical compositions of mantle end-members can be linked to specific geological environments and tectonic settings. This assumption is far from being demonstrated. As discussed in a recent paper by Stracke et al. [ref. 47] FOZO is likely to represent crustal material of various ages introduced into the mantle by subduction processes at various stages of the

evolution of the system Earth. The implication is that FOZO or other mantle compositions do not necessarily represent discrete reservoirs preserved for long periods in the deep mantle and successively emplaced as active plumes [see 25]. In other words, the occurrence of FOZO in Italy or elsewhere by no mean implies, by itself, the presence of a plume.

The Italian ultrapotassic rocks have incompatible element distribution patterns totally different from East Africa potassic volcanic rocks (i.e., Virunga). The latter show enrichment in Ta and Nb and depletion in Rb, Cs, Th and other LILE ([30], Fig. 3a). In contrast, Italian potassic rocks (including carbonate-rich rocks and associated melilitites) show high enrichment in LILE and depletion in HFSE (Figs. 3a, 5a). This suggests different source compositions and, most probably, different tectonic settings for ultrapotassic rocks in Africa and Italy. As discussed earlier, the ultrapotassic rocks from Tuscany have radiogenic isotope signatures and incompatible element patterns very similar to those of upper crustal rocks, such as metapelites and S-type granites. If these magmas derived from a plume sampling material that was recycled through the mantle for billion of years, it should be concluded that the original trace element pattern of incompatible elements were perfectly preserved and did not undergo any significant modification while travelling through the mantle in these billion of years. According to this Author's opinion, such a possibility is extremely unlikely.

The occurrence of carbonatitic magma in central Italy is highly dubious. It has been demonstrated that carbonate-rich rocks in central Italy (Umbria-Abruzzi ultra-alkaline district) represent ultrapotassic magmas similar to those of the Roman Province (Latium) that have suffered secondary addition of carbonate material from the carbonate sedimentary wall rocks. This is evidenced, for example, by the high $\delta^{18}O$ (around +25) of calcite (see discussion in [30, 35]), by the high $\delta^{18}O$ (around +12 to +14) of phenocrystic olivine and clinopyroxenes occurring in the associated melilitites, and by the high MgO content of olivine (Fo up to 99 mol %; [4, 35-37, 42]). All these data indicate strong interaction of silicate magma with carbonate sedimentary rocks, which are present in the region with thickness of several thousand meters. In contrast, the occurrence of carbonatitic material at Mt. Vulture is well demonstrated, but this has little bearing on petrogenesis of other Italian rocks. It must be recalled that Vulture is sited east of the Apennine chain on the edge of the Apulia foreland (i.e. intraplate setting). Vulture is a volcano that shows different petrological, geochemical, isotopic and volcanological characteristics with respect to volcanoes of Umbria-Abruzzi monogenetic centres [33, 34]. It likely derived from subduction contaminated intraplate mantle [10] in a zone of slab breakoff [50]. Suggestion that all these volcanoes belong to a single magmatic province and have similar genesis is against all the available field, petrological, volcanological and geochemical evidences.

As for seismic tomography, V_s and V_P anomalies can be also related to mantle compositional heterogeneity, in addition to thermal anomalies related to plume ascent [e.g., 11, 22]. Tomographic models are strongly dependent on the chosen

reference mantle structure [e.g., 41]. Using different starting assumptions, some anomalies (e.g., mantle plume heads and conduits) may appear strong or disappear entirely [e.g., 1, 41]. Moreover, new S-wave tomography presented by Panza et al. [ref. 28] for the circum-Tyrrhenian mantle has shown that there is no evidence of plumes in this area.

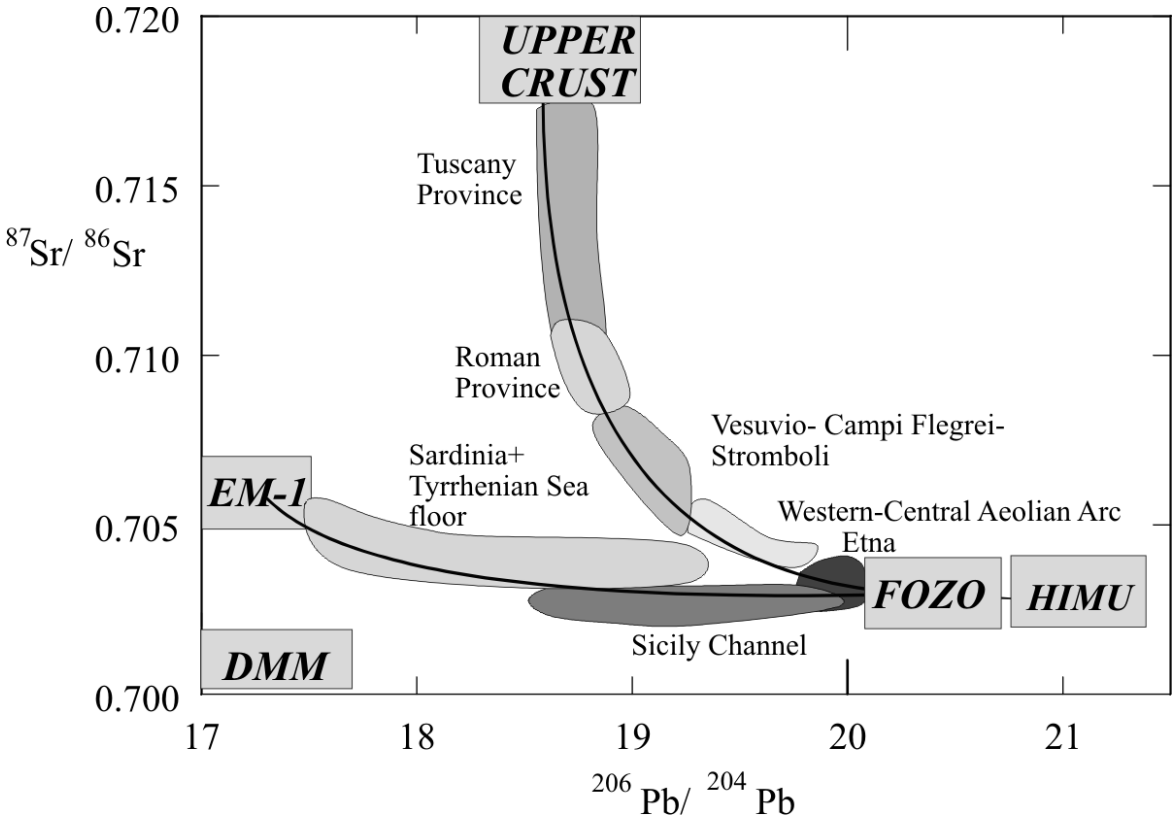

Fig. 7. **Plot of $^{206}Pb/^{204}Pb$ vs. $^{87}Sr/^{86}Sr$ for Plio-Quaternary mafic rocks (MgO > 4 wt%) from Italy.**

The compositions of some mantle end-members (FOZO, DMM, EM1, HIMU; 17, 47) are reported. Hyperbolic lines indicate mixing trends between EM1-FOZO and Upper Crust-FOZO. For further explanation, see text.

Finally, it has to be pointed pout that the Tyrrhenian Sea (i.e., the focus of the proposed mantle plume ascent) is not the site of abundant magmatism as observed in other plume-related Large Igneous Provinces (LIP, e.g. East Africa). It also has undergone strong subsidence in the last 7 Ma (the basin is 3700 m deep) instead of being uplifted as expected for areas of actively uprising asthenosphere and as observed in East Africa.

EVIDENCE IN FAVOUR OF SHALLOW MANTLE PROCESSES

There are several petrological, geochemical and geophysical data that support a subduction-related origin for Italian Plio-Quaternary magmatism. First of all, the bulk of the rocks in the Aeolian arc are calcalkaline to shoshonitic, an association typically related with subduction settings. The incompatible element patterns of

these rocks show high LILE/HFSE ratios, a feature that is typical of subduction-related magmas. These same characteristics are also shown by potassic and ultrapotassic rocks from the Italian peninsula, including those from Umbria-Abruzzi region (Fig. 3).

The isotopic signatures and the incompatible element patterns of Italian mafic ultrapotassic rocks, especially those from Tuscany, resemble closely the upper crust (Figs. 5 and [6; 33, 34]). Such a close compositional matching requires a genesis in a mantle that had been contaminated by upper crustal material. Subduction processes are well able to bring upper crustal rocks into the mantle [e.g., 39]. If this process occurred billion of years ago, as implied by the plume hypothesis, the problem arises of how such a composition could has been preserved with little or no elemental modification after billion of years of recycling through the deep mantle. In contrast, these crustal-like geochemical and isotopic signatures are easily explained if a young contamination of mantle sources is assumed, e.g. by subduction processes occurred form Oligocene to present during Africa-Europe convergence. Finally, the Benioff zone beneath the southern Tyrrhenian Sea is another important evidence in favour of subduction and of its role in the genesis of at least the Aeolian arc and Campania volcanoes. A vertical rigid body cutting the asthenosphere has been also detected by seismic tomography beneath the Apennine. This suggests the occurrence of a remnant of a young subducted slab beneath the Italian peninsula [see 26, 40]. Most if not all these data can be hardly explained by any plume theory.

The FOZO-type composition of some anorogenic Italian rocks (Etna, Iblei) remains difficult to explain. Such a problem applies to a larger scale than the Italian magmatic province [47]. It may represent old subducted crust, or lithosphere contaminated during Mesozoic times [14] or else. Some authors [e.g., 44] suggest that there is not an actively rising plume beneath the Mediterranean but the source of anorogenic magmatism is represented by an old plume head that was emplaced long ago and is now standing beneath the lithosphere. Such a hypothesis cannot be excluded. However, it also cannot be demontrated and, therefore, remains highly speculative.

CONCLUSIONS

Plio-Quaternary volcanism in Italy shows strong compositional variations, which reveal heterogeneous compositions and complex evolution processes of mantle sources. Both subduction-related and intra-plate compositions are observed. These complexities are the heritage of the geodynamic evolution of the circum-Tyrrhenian (and, more widely, of the Western Mediterranean) region during Cenozoic. The mantle sources of the Italian magmatism suffered metasomatic modifications by subduction processes. Melting of these sources gave calcalkaline to ultrapotassic magmas with clear upper crustal geochemical and isotopic signatures. The most recent subduction processes occurred from Oligocene to present by immersion of the Adriatic-Ionian plate (belonging to the African block)

beneath the Tyrrhenian Sea area and the Italian peninsula. Subduction also generated backarc opening, where uncontaminated asthenospheirc mantle passively ascended and melted, giving magmas with anorogenic geochemical signatures. Other OIB-type rocks on the African margin (Etna, Iblei and Sicily Channel) were formed by passive upwelling and melting of upper mantle in zone of transfer faults developed between extruded block along the collision zone [24].

Mantle plume has been invoked by some authors to explain some if not all the Plio-Quaternary volcanism in Italy. However, it fails to account for many key compositional parameters of volcanic rocks, especially those with arc-type trace element signatures. The plume hypothesis is therefore unnecessary and insufficient to explain the compositional characteristics of the igneous rocks in the Tyrrhenian area, although it cannot be excluded that plume emplacement occurred in the past geological history of the area and is still influencing magma compositions, especially beneath the northern margin of the African plate.

ACKNOWLEDGEMENTS.

The authors thanks dr. Nikolay Vladikin for inviting to contribute a paper to the present volume. Research on Italian magmatism has been financially supported by Italian Ministry of University and by the University of Perugia.

REFERENCES

1. **Anderson D.L.** New theory of the Earth. Cambridge University Press, New York, 2007, 384 p.
2. **Bailey D.K., Collier J.D.** Carbonatite-melilitite association in the Italian collision zone and the Ugandan rifted craton: significant common factors // Mineral. Mag., 2000, 64, p. 675-682.
3. **Lustrino M., Wilson M.** The Circum-Mediterranean anorogenic Cenozoic Igneous Province // Earth Sci. Rev., 2007, 81, p. 1-65.
4. **Barker D.K.** Origin of cementing calcite in “carbonatite” tuffs // Geology, 2007, 35, p. 371–374.
5. **Bell K., Castorina F., Lavecchia G., Rosatelli G., Stoppa F.** Is there a mantle plume below Italy? // EOS, 2004, 85, p. 541-547.
6. **Carminati E., Wortel M.J.R., Spakman W., Sabadini R.** The role of slab detachment processes in the opening of the western-central Mediterranean basins: some geological and geophysical evidence // Earth Planet. Sci. Lett., 1998, 160, p. 651-665.
7. **Castorina F., Stoppa F., Cundari A., Barbieri M.** An enriched mantle source for Italy’s melilitite-carbonatite association as inferred by its Nd-Sr isotope signature // Mineral. Mag., 2000, 64, p. 625-639.
8. **Conticelli S., Peccerillo A.** Petrological significance of high-pressure ultramafic xenoliths from ultrapotassic rocks of Central Italy // Lithos, 1990, 24, p. 305-322.
9. **D’Antonio M., Tilton G.R., Civetta L.** Petrogenesis of Italian alkaline lavas deduced from Pb-Sr-Nd isotope relationships // In: Basu A., Hart S.R. (eds.) Isotopic Studies of Crust-Mantle Evolution. Am. Geophys. Un. Mon., 1996, 95, p. 253-267.
10. **De Astis G., Kempton P.D., Peccerillo A., Wu T.W.** Trace element and isotopic variations from Mt. Vulture to Campanian volcanoes: constraints for slab detachment and

mantle inflow beneath southern Italy // Contrib. Mineral. Petrol., 2006, 151, p. 331-351, doi: 10.1007/s00410-006-0062-y.

11. **Deschamps F., Trampert J.** Mantle tomography and its relation to temperature and composition // Phys. Earth Planet. Int., 2003, 140, p. 277-291.
12. **Doglioni C., Gueguen E., Sabat F., Fernandez M.** The western Mediterranean extensional basins and the Alpine Orogen // Terra Nova, 1997, 9, p. 109-112.
13. **Doglioni C., Harabaglia P., Merlini S., Mongelli F., Peccerillo A., Piromallo C.** Orogens and slabs vs. their direction of subduction // Earth Sci. Rev., 1999, 45, p. 167-208.
14. **Esperança S., Crisci G.M.** The island of Pantelleria: a case for the development of DMM-HIMU isotopic compositions in a long-lived extensional setting // Earth Planet. Sci. Lett., 1995, 136, p. 167-182.
15. **Gasperini D., Blichert-Toft J., Bosch D., Del Moro A., Macera P., Télouk P., Albarède F.** Evidence from Sardinian basalt geochemistry for recycling of plume heads into the Earth's mantle // Nature, 2000, 408, p. 701-704.
16. **Gasperini D., Blichert Toft J., Bosch D., Del Moro A., Macera P., Albaréde F.** Upwelling of deep mantle material through a plate window: evidence from the geochemistry of Italian basaltic volcanics // J. Geophys. Res., 2002, 107, B12, 2367, doi:10.1029/2001JB000418.
17. **Hart S.R., Hauri E.H., Oschmann L.A., Whitehead J.A.** Mantle plumes and entrainment: Isotopic evidence // Science, 1992, 256, p. 517-520.
18. **Hawkesworth C.J., Vollmer R.** Crustal contamination vs. enriched mantle: $^{143}Nd/^{144}Nd$ and $^{87}Sr/^{86}Sr$ evidence from the Italian volcanics // Contrib. Mineral. Petrol., 1979, 69, p. 151-165.
19. **Hoernle K., Zhang Y.S., Graham D.** Seismic and geochemical evidence for large-scale mantle upwelling beneath the eastern Atlantic and western and central Europe // Nature, 1995, 374, p. 34-112.
20. **Hoernle K., Behncke B., Schmincke H.-U.** The geochemistry of basalt from the Iblean Hills (Sicily) and the Island of Linosa (Strait of Sicily): evidence for a plume from the lower mantle // Goldschmidt Conf., J. Conf. Abs., 1996, 1, p. 264.
21. **Lavecchia G., Stoppa, F.** The tectonic significance of Italian magmatism: an alternative view to the popular interpretation // Terra Nova, 1996, 8, p. 435-446.
22. **Lee C.-T.** Compositional variation of density and seismic velocities in natural peridotites at stp conditions: implications for seismic imaging of compositional heterogeneities in the upper mantle // J. Geophys. Res., 2003, p. 108.
23. **Lustrino M., Wilson M.** The Circum-Mediterranean anorogenic Cenozoic Igneous Province // Earth Sci. Rev., 2007, 81, p. 1-65.
24. **Mantovani E., Albarello D., Babbucci D., Tamburelli C., Viti M.** Trench-arc-backarc systems in the Mediterranean area: examples of extrusion tectonics // J. Virtual Expl., 2002, 8, p. 131-147.
25. **Meibom A., Anderson D.L.** The statistical upper mantle assemblage // Earth Planet. Sci. Lett., 2003, 217, p. 123-139.
26. **Panza G.F., Pontevivo A., Chimera G., Raykova R., Aoudia A.** The lithosphere-asthenosphere: Italy and surroundings // Episodes, 2003, 26, p. 169-174.
27. **Panza G.F., Peccerillo A., Aoudia A., Farina B.** Geophysical and petrological modelling of the structure and composition of the crust and upper mantle in complex geodynamic settings: The Tyrrhenian Sea and surroundings // Earth Sci. Rev., 2007, 80, p. 1-46.
28. **Panza G.F., Raykova R.B., Carminati E., Doglioni C.** Upper mantle flow in the western Mediterranean // Earth Planet. Sci. Lett., 2007, 257, 200-214.

29. **Peccerillo A.** On the origin of Italian potassic magmas: Comments // Chem. Geol., 1990, 85, p/ 183-196.
30. **Peccerillo A.** Relationships between ultrapotassic and carbonate-rich volcanic rocks in central Italy: petrogenetic implications and geodynamic significance // Lithos, 1998, 43, p. 267-279.
31. **Peccerillo A.** Multiple mantle metasomatism in central-southern Italy: geochemical effects, timing and geodynamic implications // Geology, 1999, 27, p. 315-318.
32. **Peccerillo A.** Geochemistry of Quaternary magmatism in central-southern Italy: genesis of primary melts and interaction with crustal rocks // Geochemistry International, 2001, 39, p. 521-535.
33. **Peccerillo A.** Plio-Quaternary magmatism in Italy // Episodes, 2003, 26, p. 222-226.
34. **Peccerillo A.** Plio-Quaternary volcanism in Italy // Petrology, geochemistry, geodynamics. Springer, Berlin, 2005, 365 p.
35. **Peccerillo A.** On the nature of carbonate-rich volcanic rocks in Central Italy. A reply to comments by Woolley et al // Per. Mineral., 2005, 74, p. 195-204.
36. **Peccerillo A.** Numerical tests and qualitative approach to study of lavas and associated carbonate-rich pyroclastic rocks from the Intra-Apennine volcanoes. A reply to comments by D.K. Bailey // Per. Mineral., 2005, 74, p. 209-212.
37. **Peccerillo A.** Carbonatites vs. carbonated rocks in central italy. a reply to comments by bell and kjarsgaard // per. mineral., 2006, 75, p. 93-100.
38. **Peccerillo A., Lustrino M.** Compositional variations of the plio-quaternary magmatism in the circum-tyrrhenian area: deep- vs. shallow-mantle processes // Plates, plumes, and paradigms. Geol. Soc. Am. Spec. Paper, 2005, 388, p. 421-434.
39. **Peccerillo A., Martinotti G.** The Western Mediterranean lamproitic magmatism: origin and geodynamic significance // Terra Nova, 2006, 18, p. 109-117.
40. **Piromallo C., Morelli A.** P-wave tomography of the mantle under the Alpine-Mediterranean area // J. Geophys. Res., 2003, 108, p. 2065.
41. **Ritsema J., Allen R.M.** The elusive mantle plume // Earth Planet. Sci. Lett., 2003, 207, p. 1-12.
42. **Rosatelli G., Stoppa F., Jones A.P.** Intrusive calcite-carbonatite occurrence from Mt. Vulture volcano, southern Italy // Miner. Mag., 2000, 64, p. 155-164.
43. **Poli G., Peccerillo A., Donati C.** The Plio-Quaternary acid magmatism of Southern Tuscany // Mem. Soc. Geol. It., Vol. Spec., 2002, N. 1, p. 143-151.
44. **Rotolo S. G., Castorina F., Cellura D., and Pompilio M.** Petrology and Geochemistry of Submarine Volcanism in the Sicily Channel Rift // J. Geol., 2006, 114, p. 355–365.
45. **Stoppa F., Lavecchia G.** Late Pleistocene ultra-alkaline magmatic activity in the Umbria-Latium region (Italy): an overview // J. Volcanol. Geotherm. Res., 1992, 52, p. 277-293.
46. **Stoppa F., Lloyd F.E., Rosatelli G.** CO_2 as the propellant of carbonatite-kamafugite cognate pairs and the eruption of diatremic tuffisite // Per. Mineral., 2003, 72, p. 205-222.
47. **Stracke A., Hofmann A. W., Hart S. R.** FOZO, HIMU, and the rest of the mantle zoo // Geochem. Geophys. Geosyst., 2005, 6.
48. **Vollmer R.** Rb-Sr and U-Th-Pb systematics of alkaline rocks: the alkaline rocks from Italy // Geochim. Cosmochim. Acta, 1976, 40, p. 283-295.
49. **Vollmer R., Hawkesworth C.J.** Lead isotopic composition of the potassic rocks from Roccamonfina (south Italy) // Earth Planet. Sci. Lett., 1980, 47, p. 91-101.
50. **Wortel M.J.R., Spakman W.** Subduction and slab detachment in the Mediterranean-Carpathian region // Science, 2000, 290, p. 1910-1917.

UDK 551.22+552.11

Variations of ilmenite compositions from Yakutian Kimberlites and the problem of their origin

Ashchepkov I.V.[1], Vladykin N.V.[2], Pokhilenko N.P.[1], Logvinova A.M.[1], Palessky V.S., Afanasiev V.P.[1], Alymova N.V.[2], Stegnitsky Yu.B.[3], Khmel'nikova O.S.[1], Rotman A.Y. [3]

[1]*United Institute of Geology Geophysics and Mineralogy SD RAS*
[2]*Novosibirsk Institute of Geochemistry SD RAS, Irkutsk*
[3]*Central Scientific Investigation Geological Exploration Institute, ALROSA , Mirny*

ABSTRACT

Picroilmenites from the kimberlites of Siberian platform are the result of polybaric fractionation of protokimberite melts at the stage of the creation of feeder systems. They are formed in three levels in mantle column usually in the interval from 70 to 40 kbar according to the ilmenite thermobarometry (Ashchepkov, Vishnyakova, 2006). Protokimberlites of Siberian platform revel the long trends of the evolution supposed to be the products of the polybaric AFC processes.

The variation tends of Picroilmenites from Hi-Ti to Low –Ti reflect the rising of melts and reveal inflections due to mantle layering and pulsing intrusion, several levels of Cr – enrichment due to contamination and branching in the finishing stage due to the crystallizing in veinand veinlets.

TRE patterns reveal three modes: 1) enriched to 0.1-10 C1 flat, S,W-shaped, or inclined REE patterns with Pb peaks – result of HT melting and channel crystallization, HT metasomatites and pyroxenites (CPMX, IRPS, MARIDS); 2) 10-100C1 – lineal inclined patterns La/Yb_n - 10-25 with HFSE peaks – result of polybaric crystallization of protokimberlite melts mixed with partial melts from peridotites in garnet facies (typical megacrysts); 3) 1000C1 with now peaks of HFSE low degree partial hydrous melting and mixing with highly evolved partial melts (middle –low pressure melts and metasomatics).

Only in Myrninsky field the long trend suggest the relatively close fractionation in long channels to garnet –spinel transition the other demonstrate the extension only to 40 kbars.

INTRODUCTION

Ilmenite is one of the most wide spread mineral in the kimberlites [2, 14, 15, 20-25, 29, 34-36, 39-40, 42-43, 49, 52-53]. Usually it occurs as the discrete rounded nodules and there fragments and more rarely in intergrowth with the other minerals such as phlogopites, olivines and Cr- less (or low) pyropes [44, 46, 55] and clino- and othopyroxenes [14, 15]. Smaller grains in kimberlites refers to the different pyroxenitic [44], MARIDs [18, 22, 28] and metasomatic compositions [4]. The later are enriched in Cr_2O_3 up to 6 %. The small grains common in kimberlite matrix are lower in MgO and of course in NiO and Cr_2O_3

And reflect relatively low pressure kimberlite crystallization

Picroilmenites are the indicators of the kimberlites sources in the placers and are used for the prospecting due to the higher weight and resistance to the alteration [Muggeridge, 1995] in surface conditions.

Number of papers devoted to the picroilmenites their variations of compositions and origin [35, 39, 41, 45, 23, 52]. Nevertheless many questions are not solved yet.

The most MG-rich ilmenite considered to be product of the deepest crystallization in megapyroxenites [15] and in MARID [22] and other metasomatites. Ilmenite megacrysts reveal very close compositions to the host kimberlites [39]. Nevertheless trace element compositions highly very and differ mach from the kimberlites. This fact supposes the high degree of fractionation of the melts responsible for the megacryst creation [23, 35]. Variations from pipe to pipe differ much nevertheless some similarities typical for the picroilmenite from the same region suggest close way of creation.

In this paper we compare the megacryst compositions from 50 pipes from 6 regions of the kimberlite magmatism in Yakutia [3-12]. Here we give the interpretation of the suggesting megacrysts to be formed by the polybaric fractionation of the protokimberlite melts [7, 9].

MINERAL ASSOCIATIONS OF THE PICROILMENITES IN KIMBERLITES

Most common are the megacrystalline nodules which are commonly Cr- poor [24, 45] (<0.5 %). But in Sytykanskaya pipes some large megacrystalline nodules in contacts with the dunites are enriched in Cr_2O_3 (~2%) [3]. Sometimes megacrysts are surrounded by the polycrystalline aggregates and sometime found in a cement in polymict peridotites [53]. Which may be more Cr- rich [46, 55] or an opposite Cr- poor. Cr- enrichment found for many Picroilmenites from N. America are more Cr- rich [46] but in the ilmenites from Prianabarie they are Cr-poor and lower in MgO.

In the megacrystalline garnets with the zonation in CaO contain ilmenites and Cr- low clinopyroxens are found as the intergrowth. Giant grained ilmenite and phlogotites intergrowth are common in micaceous kimberlites. Judging by the contacts megacrystalline associations became finer grained as well as the peridotites [34] and numerous observations in Satykanskaya and Dalnyaya pipes [44]. In pegmatite aggregates they may contain olivine and clinopyroxenes more rarely Cr- poor garnets. In intergranular space rutiles and perovskite are common and more rarely zircons and apatites. Fine and course grained glimmerites are common in group II kimberlites. In turn ilmenite and rutile grains are common in phlogopite megacrysts.

Ilmenites are common in high temperature pyroxenites commonly composed from clinopyroxenes and pyrope-almandine garnets [43]. They are typical in black hot othopyroxenites and websterites suggested to be derivates from the plum magmas as well as in hybrid and anatexic pyroxenites resulting from the remelting of

metasomatites or hydrous remelting of peridotites. [7]. Symplectites of pyroxenes and ilmenites are common in S.Africa and other kimberlites [14] what suppose enrichment of the parental melts in TiO_2.

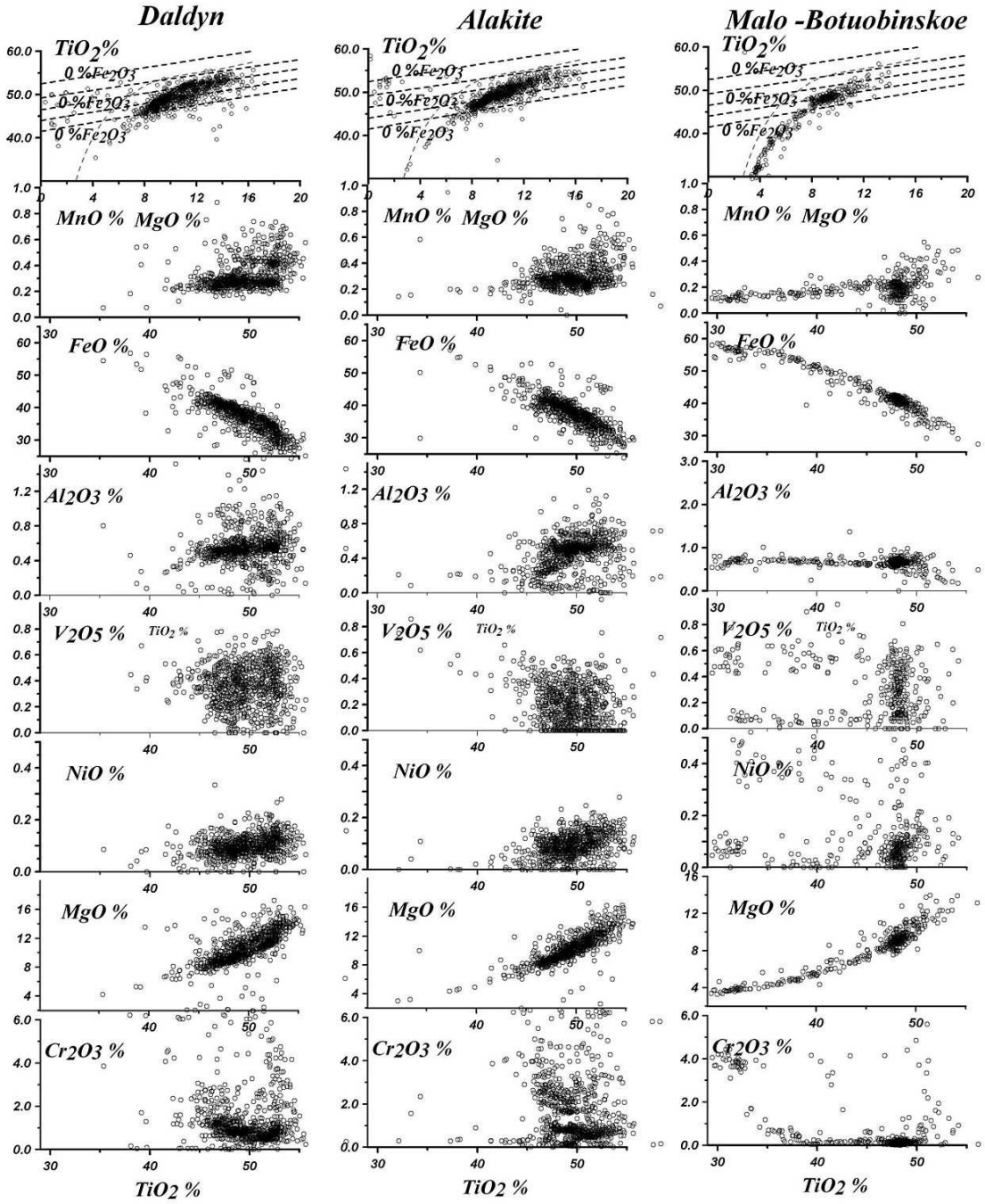

Fig. 1. **Integrated compositional trends for the ilmenites from different kimberlite provinces from Yakutia.**

Picroilmenites are common in the metasomatic associations [20-22; 26, 28] in veins and veinlets in peridotites. Usually in this case they reveal several levels of the enrichments. For example in Sytykanskaya pipe ilmenites in veins contain 2, 4

or close to 6% Cr_2O_3. They are more common in the lherzolites on Cr- websterites in Alakite region in Yakytia then in more depleted compositions. But in Prianabarie depleted mantle peridotites (mainly dunites) often contain Cr- low ilmenites in association with mica. Carbonatite veinlets in peridotites sand pyroxenites commonly contain fine Cr- less picroilmenite grains.

MARID- type of [18] are composed from (mica – amphibole - rutile – ilmenite - clinopyroxenes) suggested to be derivates from the basic hydrous melt and separate group compile the IRPS (ilmenite – rutile – phlogopite - sulphide) rocks which probably are the results.

Ilmenites are common in the contact zones and pyroxenites from Obnazhennaya and other pipes. Ilmenites well as rutile are a common mineral in the eclogites.

Ilmenites are rarely found as diamond inclusions and these are most Cr_2O_3 (8-12 %) and Mg- rich varieties [47], they are similar to those from the ilmenite – bearing peridotites [43]. The others with Cr_2O_3 (~1%) are similar to those from diamonds of [27] and MARID [14].

VARIATIONS OF THE COMPOSITIONS

Ilmenite trends (Fig.1) with lowering of TiO_2, MgO, NiO, and often Al_2O_3 contents and rising FeO и Fe_2O_3, and commonly MnO, V_2O_5, and HFSE components – Nb, Ta, Hf, Y and as a rule REE are resulting from the fractionation in magmatic systems [23, 35], as it was supposed at the base of the lithosphere. Direct contacts [34] suppose nevertheless the vein nature of the fractionation. Geochemistry with the variations in Cr_2O_3, Al_2O_3, V_2O_3 reveal the AFC type of the fractionation [36]. Some rare contacts also reveal the polybaric nature of the fractionation.

In analogy with the megacrytalls of alkali basalts megacrysts should be the result of creation of the feeder at the pre eruption stage and possibly are crystallizing in he channels where the protokimberlite melts were migrated and pulsing several times.

Nearly continuous trends with several inflection points are supposed to be referring to the layering of the mantle columns. Decrease of TiO_2 and MgO in our opinion reflects the pressure decrease during rising which is in accord with the increase of the parameters of the ilmenites crystal cells. This is proved by the pressure calculated using orthopyroxenes [30] and clinopyroxenes [7] in associations with the ilmenites. Thus in the variation diagrams the decrease of TiO_2 - FeO, MgO (fig 1) reflect crystallization during rising of protokimberlite melts from the lithosphere base The fluctuations of MnO and V_2O_5 probably are due to the variations of the oxygen conditions (V_2O_5) and reactions in the contacts (MnO). Probably the admixture of eclogites and subducted material may increase the MnO.

Fe- rich and ilmenites probably are the result of the lowest temperature (and pressure) crystallization in the upper most part of the upper mantle column beneath the kimberlite pipes.

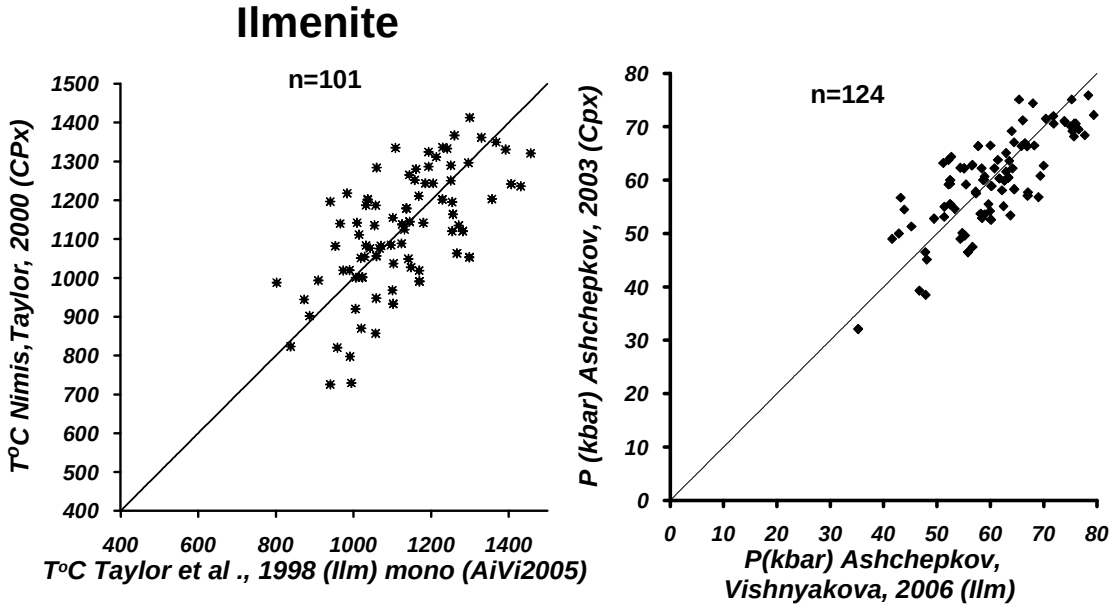

Fig. 2. **Temperature (T ilm [50]– T Cpx [37]) and pressure P correlations between the pressures [4] and P determined by the clinopyroxenes [6].**

Ilmenites with low TiO_2 laying in MgO - TiO_2 diagram within the cratonic conditions [52] reflect according to FeO/Fe_2O_3 the conditions lower QMF buffer [48] and are close to the ilmenite crystallizing from alkali – basalt melts.

MONOMINERAL ILMENITE THERMOBAROMETRY

Monomineral thermobarometry suggest that the cell sizes of the minerals are determined by the TP conditions. For ilmenite it was shown different reaction of the FeFe - MgTi exchange to the pressure and temperatures. Nearly linear behavior for pressure was found for the entire interval but for temperature the linear correlation is determined only for HT conditions [1]. Numerous works where ilmenite was in experimental products [1, 20, 31, 51] do not reveal good correlations for the temperatures and pressures with the compositions but it was found for the cell parameters.

We used the Ol- Ilm thermometer [50] in monomineral configuration to determine the temperatures. The forsterite content it is founding according: Fo=1-0.12-0.00025*P for pressures lower then 30 kbar and Fo=1-0.11-0.00025*P for greater pressures. For Cr- bearing picroilmenites (Cr_2O_3>1%) the correlation Fo=1-0.033*Fe_{Ilm}/Mg_{Ilm}-0.0133-0,0008*P-0.00005*(T^oC_0 -1000) (f.u.) found in ilmenite peridotites (>150 associations) [20] allow to determine forsterite content in olivine using the iteration scheme.

The dependence of geikilite minal from pressure [23, 49] from pressure was used for calibration of pressure. From preliminary formula P= 27+0,4* TiO_2 (%) which was based on the pressure gap from conditions estimated for most deep metasomatites [22] and most shallow mantle ilmenite assemblages from alkali basalts we checked the correlations of the pressures for more then 50 pipes. The

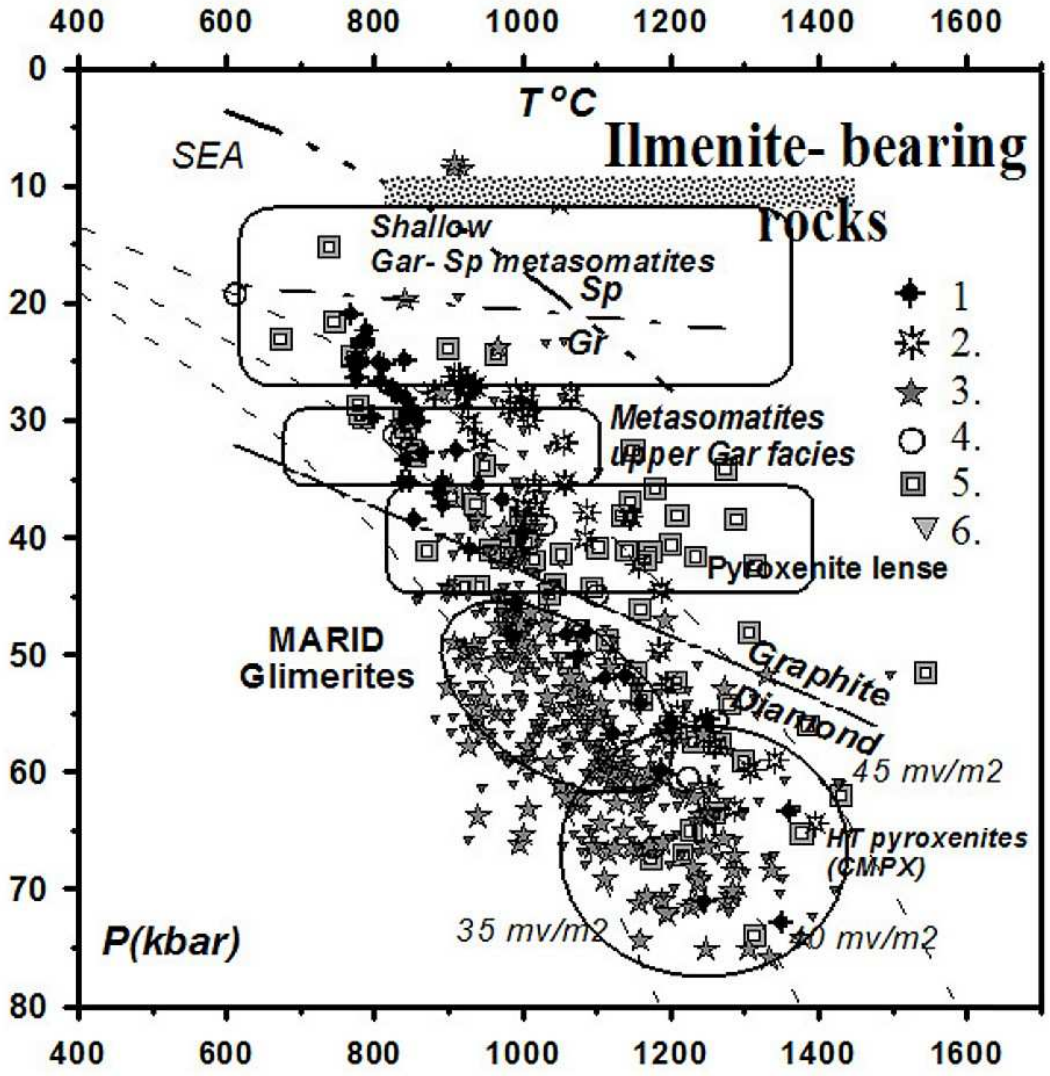

Fig. 3. **TP diagram for the kimberlitic ilmenites and minerals in the association.** Garnet thermobarometry for peridotites [5], garnet thermobarometry for pyroxenites [5]; 3. clinopyroxene thermobarometry [6] ;4. Clinopyroxene thermobarometry [37]; 5. orthopyroxenes thermobarometry [16]-[30]; 6. ilmenite thermobarometry [4].

modified equation obtained by the correlation to the pressure parameters based on clinopyroxenes usinf the data base of [2] and from the journal publication allow to resave a good coincidence of the pressure using the same temperatures (fig. 2).

P_0= (TiO_2-23.)*2.15-(T^oC-700)/20*MgO* Cr_2O_3-1.5*MnO)* T^oC/1273 and further corrections P1=10*(60-Po)/60+P_0

The correlation lines between the methods of mineral thermobarometry and PT diagrams based on pyroxenes and ilmenites reveal very good coincidence. (Fig. 3).

VARIATIONS OF ILMENITE ASSOCIATIONS IN THE MANTLE SECTIONS

The TP conditions according to pyroxene thermobarometry for ilmenite bearing associations are shown on the diagram (Fig.3). The most deep part of the diagram reflect TP conditions of most hot pyroxenites and eclogites (70-60 kbar) tracing convecting branch of the geotherm. Number of the hybrid pyroxenites and hot temperature metasomatites are plotting within the transitional part between lithosphere and asthenosphere from 55 to 60 kbar. More low temperature conditions are traced by phlogopite metasomatic veins with ilmenites and MARID composition from 55 to 40 kbars. Hydrous pyroxenites sometimes are correspondent to the layer which may be found in mantle columns beneath the most pipes. This is due to the accumulation of water in this level due to dehydration of peridotites and metabasaltic part of subducted slab due to the pargasite - hornblendite amphibole decompositions [38] The upper mantle hydrous metasomatic veins and disseminated phlogopites correspond to the 40-25 kbar interval. Relatively rare lherzolites with large primary phlogopites reflect low temperature conditions in the spinel facie.

VARIATIONS OF THE TRENDS WITHIN DIFFERENT REGIONS OF SIBERIAN CRATON

Average MgO contents of ilmenite from the pipes and are used to estimate the probability of the diamonds in the pipes and the placers wich is in accord with the thermobarometry. But most Mg – rich compositions are from the metasomatic associations and do not reflect in reality the most deep seated mantle assemblages.

We also at the diagram (Fig 1) plotted together the compositions of the ilmenites from different pipes to show the most common features of ilmenites in each region.

For *Daldyn* pipes [12, 13, 43, 44] the nearly continuous trend is typical from 55 to 45 TiO_2, FeO – MgO and mor descrete for the others components. Growth of the Fe and incompatible elements is mainly due to olivine fractionation supported by Ni decrease. Nearly constant Al evidences fro the lack of precipitating garnet. The step – rising Cr content in 3 intervals from 0.5 to 2% Cr2O for Zarnitsa pipe suggests the three steps of contamination possibly in during the melt rising what is coinciding with the layering determined by the TP calculations [12]. The 50-55 (70-55 kbar) refer to the mantle metasomatites. And the large inflection 45 and finishing of the major trend refer to the pyroxenite lens where the lherzolites trend for garnet in Cr_2O_3- CaO [48, 49] has an inflection. The abrupt decreasing of TiO_2 content probably refer to the garnet crystallization. Ilmenites from Osennyaya are

shifted to the interval 44-50% interval comparing to more TiO_2 and MgO rich from Udachnaya and Zarnitsa.

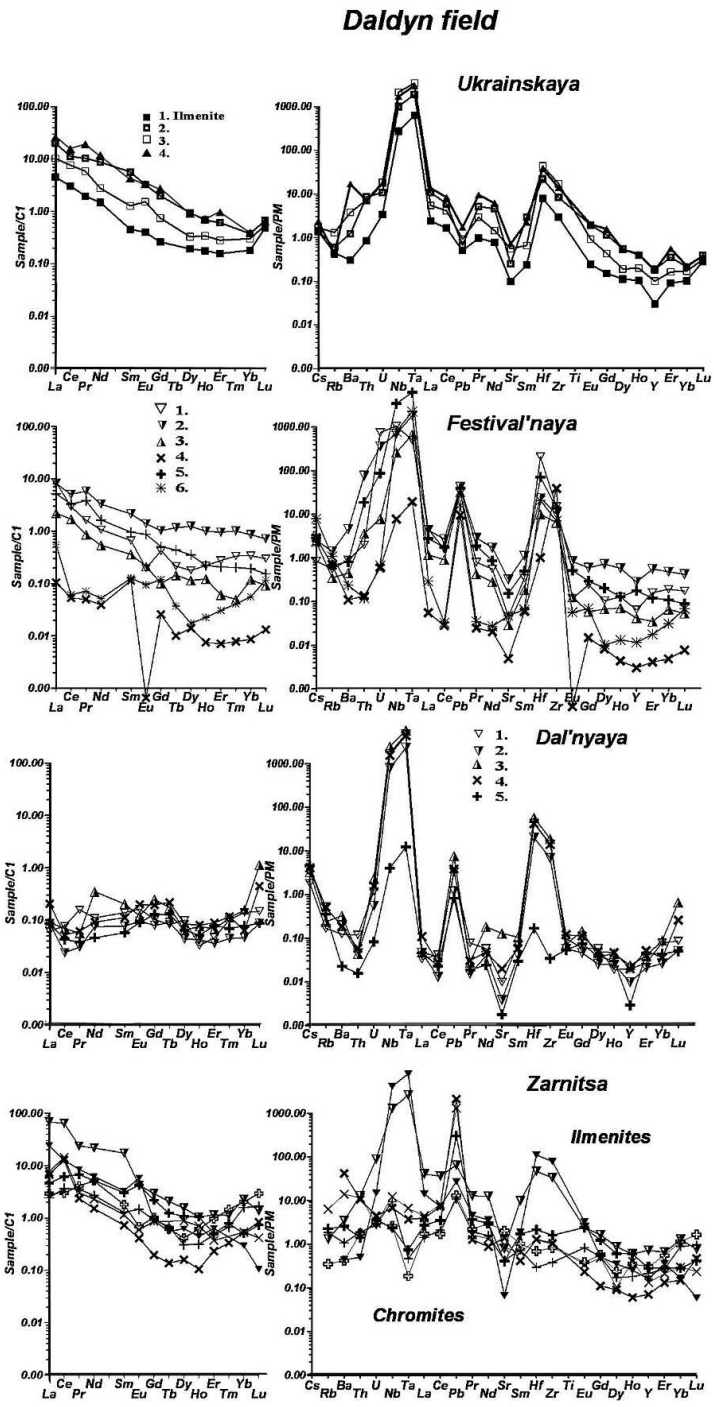

Fig. 4. **REE and trace element spider diagrams for ilmenites from heave mineral separates from Daldyn field kimberlites.**

In MgO- TiO_2 diagram [53], ilmenites from Daldyn are less oxidized then for *Alakite* region In *Alakite* the ilmenite trends the stlitting in Cr_2O_3 are typical. The most low < 0.5 % Cr 2O3 are show decrease and starting from

51% continuous rise of this component. Step rise in 5 intervals is characteristic for Yubileynaya ilmenites. But closely located Ozernaya pipe cutting Yubileinaya already contain only Cr- less ilmenites what refer to the lack of the metasomatic ilmenites in the mantle column of this pipe. Komsomiskaya and Sytykanskaya pipes where metasomatic minerals are common in the mantle column Cr-less compositions aree more rare. Comparison of ilmenites from metasomatic xenoliths and heavy concentrate from Sytykanskaya pipe reveal that the garnet xenoliths from lower part of the mantle section (>55 kbar) mainly drop to the 54-50% TiO_2 interval and those from the upper 40-55 kbar – to the 42-50% TiO_2. For Aykhal pipe ilmenite trend is restricted 46-53% TiO_2. It possible to subdivide it to 7-8 groups. At the end of trend MgO, NiO is lowering fast but Al_2O_3 not so much.

Ilmenite trends for the pipes from *Malo- Botuobinsky* [9] region ilmenite trends for Dachnaya and Mir are very long 31-50% TiO_2 and similar and exponential shape looks like a result of continuous fractionation. They are similar to those from Angola. Low NiO, Cr_2O_3 suggest small degree of exchange and rise of Al_2O_3 suggest olivine as a and ilmenite to be the main prcioitation phases. Ilmenites from Amakinskaya and International'naya reveal 4 intervals, Cr content is very low and became higher in beginning and at the end of crystallization trend.

Crystallization trend of picroilmenites from Deimos *Upper – Muna field* is similar to those from Alakite pipes (fig.1) showing the increasing in Cr at the middle part of the trend. Nearly continuous trend may be separated to 7-8 groups referring to the mantle layering. Similar trend but more long and discrete was determined for Zapolyarnaya pipe. In the others pipes ilmenites are rather rare.

Only in one probe of tuff from Nyurbinskaya pipe picroilmenites are abundand. The trend is restricted from 55 to 48% TiO_2 and consist from three groups. Rapid decrease of NiO, MgO and increase of FeO, V_2O_5, probably is due to the olivine fractionation. Ilmenites from the placer near the pipe reveal more long and fractionated trend.

In kimberlites from Prianabarie ilmenites are more common. The trends commonly are restricted by 55-40% TiO_2 but in several pipes the Fe-ilmenite compositions are found. Cr-content is low from 40 to 50 kbar and rise only for varieties >50% TiO_2. Only in Trudovaya pipe the step wise decreasing from 4 to 1% Cr_2O_3 was determined.

GEOCHEMISTRY OF ILMENITE MEGACRYSTS

Ilmenites analyzed from the left part of the trend enriched in TiO_2 as a rule show low concentration of TRE but the configuration differ. The middle part show lineal inclined patterns fro REE and high peaks of HFSE. The most enriched compositions from the left part of the trends demonstrate the high concentrations

of all the elements up to 1000 C1 but Ta, Nb, Zr, Hf are not higher then the nearest elements on the spider diagrams.

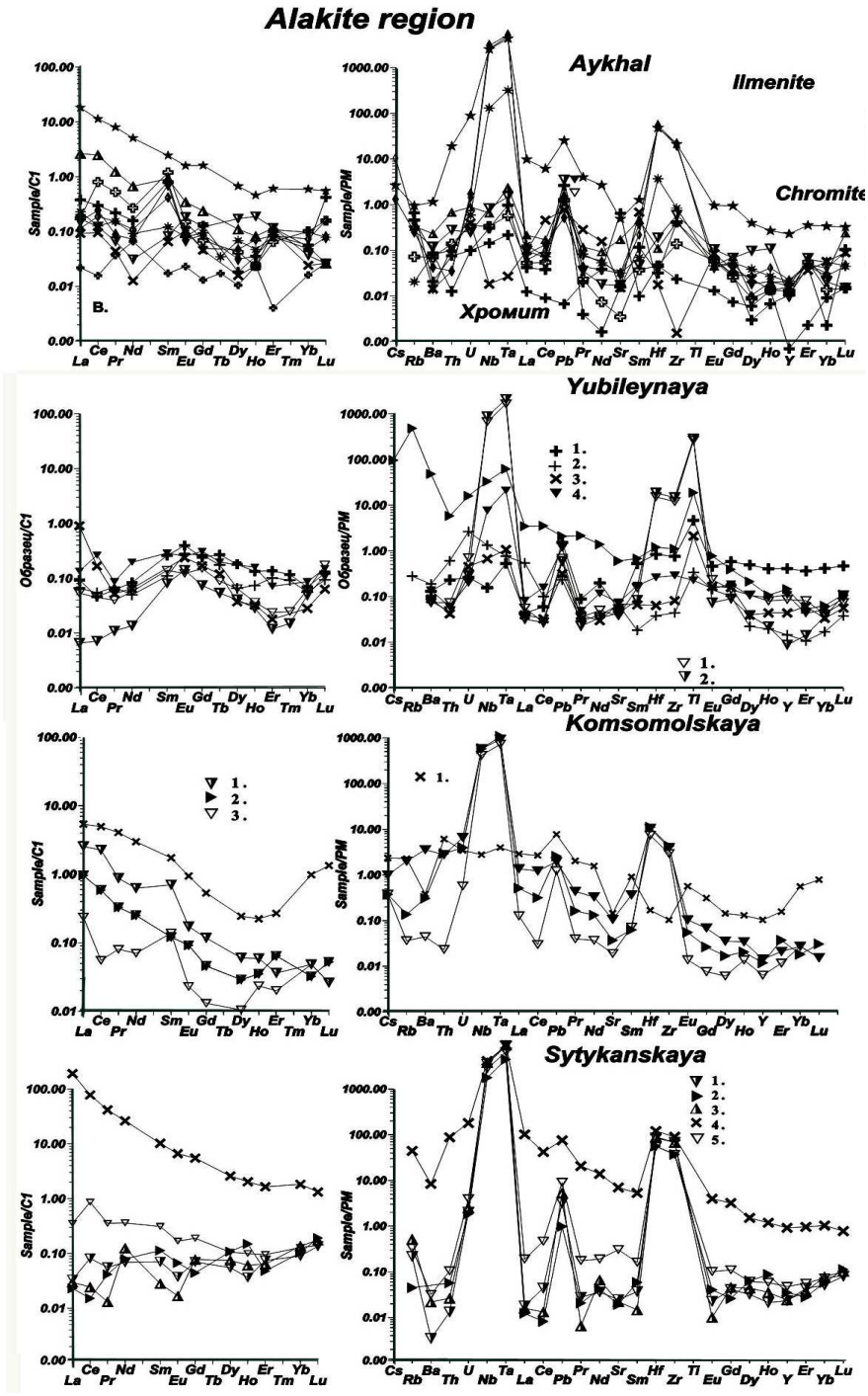

Fig. 5. **REE and trace element spider diagrams for ilmenites from heave mineral separates from Alakite field kimberlites.**

For four pipes from Daldyn region, only ilmenites from Zarnitsa and Ukrainskaya (fig. 4) demonstrate the patterns which may be produced by the melting from the source containing garnets. Small depression in MHREE and Pb

peaks for ilmenites from Zarnitsa suggest the melting origin of the protokimberlite melts. The REE patterns of ilmenites and Chromites are very similar what may mean their close nature of origin. But Ukrainskaya pipe demonstrate PB minima's

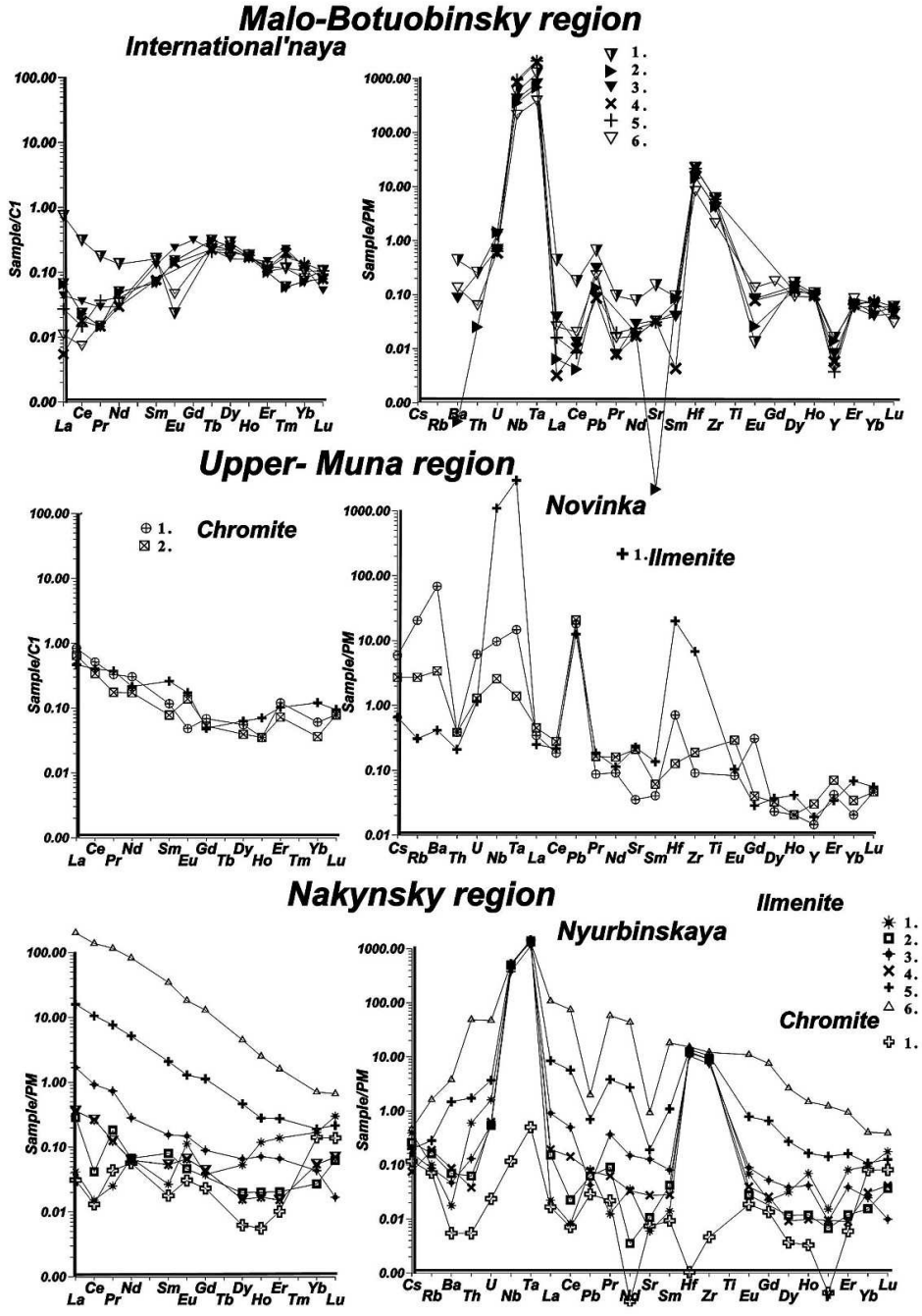

Fig. 6. **REE and trace element spider diagrams for ilmenites from heave mineral separates from Malo-Botuobinsky, Nakynsky, and Uper-Muna fields kimberlites.**

suggesting fractionation of their parental melts. Ilmenites from Festrival'naya pipe also demonstrate melting inclined La/Yb_n patterns with the spreading in the HREE what suggest the melting of garnet in for the enriched compositions. They also demonstrate Hf elevation under Zr quite unusual for the others pipes as well as

enrichment of some compositions in Ba- Th. The lowest in REE show the Eu and two folded patterns. Ilmenites from pipe Dal'nyaya having nearly S- shaped REE distributions.

For the ilmenites from Alakite region the all the ilmenites from different pips reveal the own features. Aykhal ilmenites are show nearly flat REE patterns for the compositions from the Ti reach- most deep compositions (fig. 5). The mildly – enriched compositions of Picroilmenites also reveal the TRE pattern typical for fractionation after melting. And the most enriched demonstrate the patterns which are typical for the very low degree partial melts. The ilmenites from Yubileynaya demonstrate the REE patterns close to S- shaped patterns they are also close to those from chromites. For Ozernaya the shape of the REE distribution is another the more flat, the degree of the enrichment differ and reveal the combination of the melting and fractionation. Nearly flat and even negative inclination REE was found for Sytykanskaya pipe Cr- low ilmenites demonstrating that protokimberlite melts often had flat primitive patterns. But ilmenites from xenoliths and large megacrysts in contact with the peridotites demonstrate the inclined pattern slightly U- shaped in HMREE which possibly formed due to melt percolation as the result of chromatography. Ilmenites from Komsmolskaya pipe demonstrate W- shaped inclined patterns with the inflection on Gd possibly due to the chromatographic effects though the Pb show that probably melting also took place.

Ilmenites from International'naya pipe reveal the pattern similar to garnets from pyroxenitic type. They reveal Y minima typical for diamonds. One of them demonstrate Eu minimum.

In Nakynsky region (fig. 6) the most of high-pressure garnets show nearly flat two folded patterns. But the most enrich demonstrate the lineal distributions similar to alkali basalts and other melt came from garnet facies. Most enriched compositions reveal no peaks in Hf- Zr.

In Prianabarie three populations of ilmenites analyzed demonstrate the different distributions (fig. 7). Those from Nebaibyt have S- shape patterns for REE, TREE patterns show enrichment both in Nb- Ta and Zr-Hf and varying Y. Samples from Khardakh pipe show the enrichment near 10 C1, flat and U – shaped REE distribution or lineal inclined basalt- like REE distributions with peaks in Pb. Ilmenites from Trudovaya pipe reveal the distribution show three different distributions. Those with REE near 1-C1 show slightly U – shape and inclined patterns with Pb peaks in TRE spider diagrams and mild enrichment Zr-Hf and Ta-Nb. Those with distributions near 100C1 for La demonstrate the REE inclination just close to melts produced in garnet. For most enriched ilmenites with the degree of enrichment up to 1000C1 for La reveal La/Yb_n ~15. They show even lower Hf-Zr concentration then nearest elements.

MODEL OF ORIGIN

The main model responsible for the creation of ilmenite is the fractionation of the kimberlites of protokimberlite melts [23]. Nevertheless from our materials it is

seen that there are at least three different types' pf ilmenites with different TRE and REE patters.

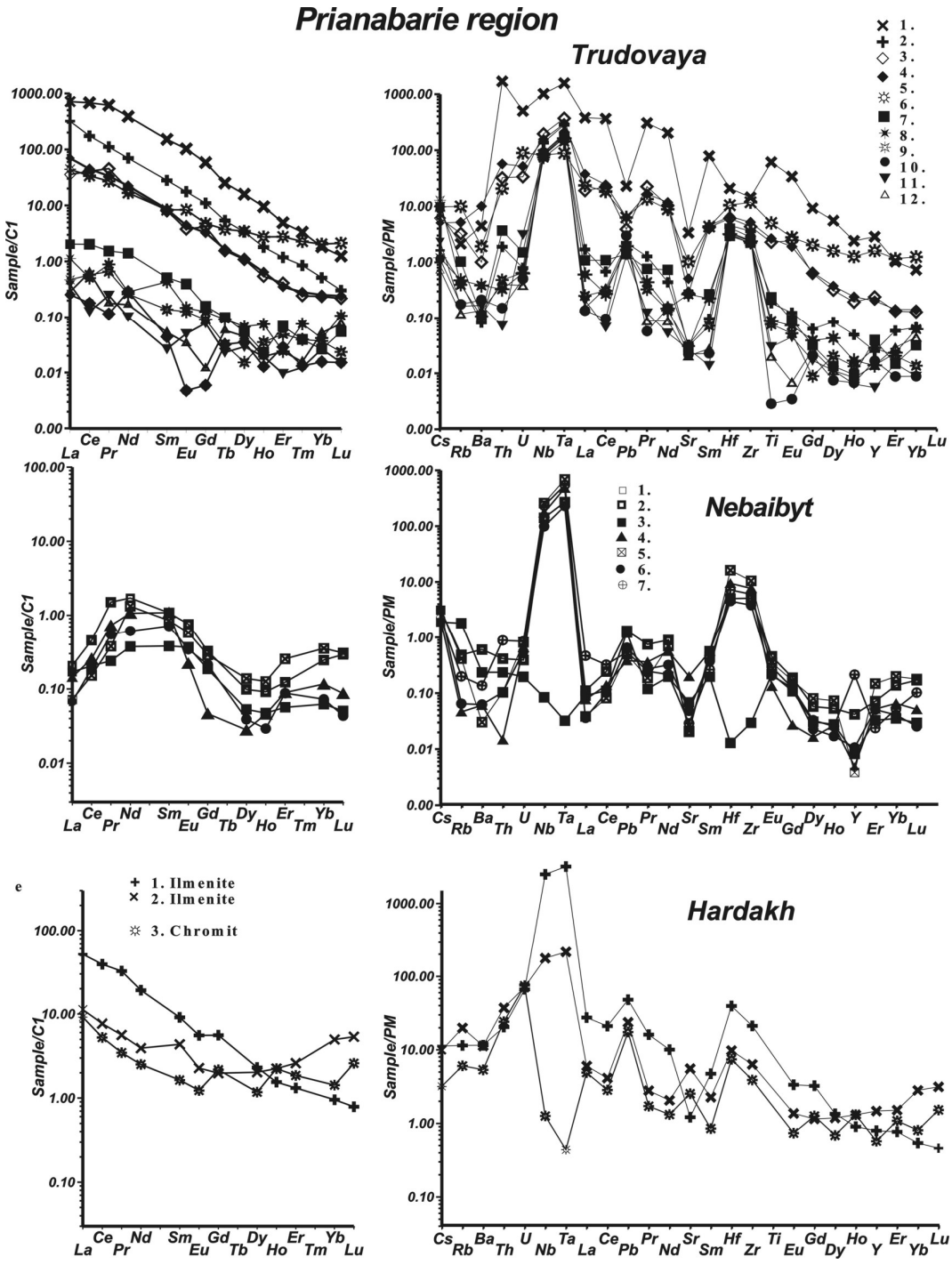

Fig. 7. **.REE and trace element spider diagrams for ilmenites from heave mineral separates from Prianabarie fields kimberlites.**

Those ilmenites with low concentrations of TRE elements demonstrate different Cr- enrichment due to admixture of the partial melts from wall rock lherzolites, those with higher Cr concentration show higher La/Yb_n ratios. But

many of the ilmenite association were formed with very small influence of garnets and thus were produced from very primitive melts and possibly within the essentially dunitic matrix which usually serves the conduit for the melt movements. Each pipe has there own type of TRE patterns fro such a melts which are usually very similar to those for chromites.

The middle part and most common ilmenites demonstrate common enrichment for the fractionation processes and distribution which very close to those of kimberlites. But taking into account low REE KD for ilmenites [54] it should be noted that this must be the melts by the order of 2 or more enriched thus should be the protokimberlite or even carbonatite melts. Calculated liquids show the deficit of HFSE typical for carbonatite liquids, that are of course melts.

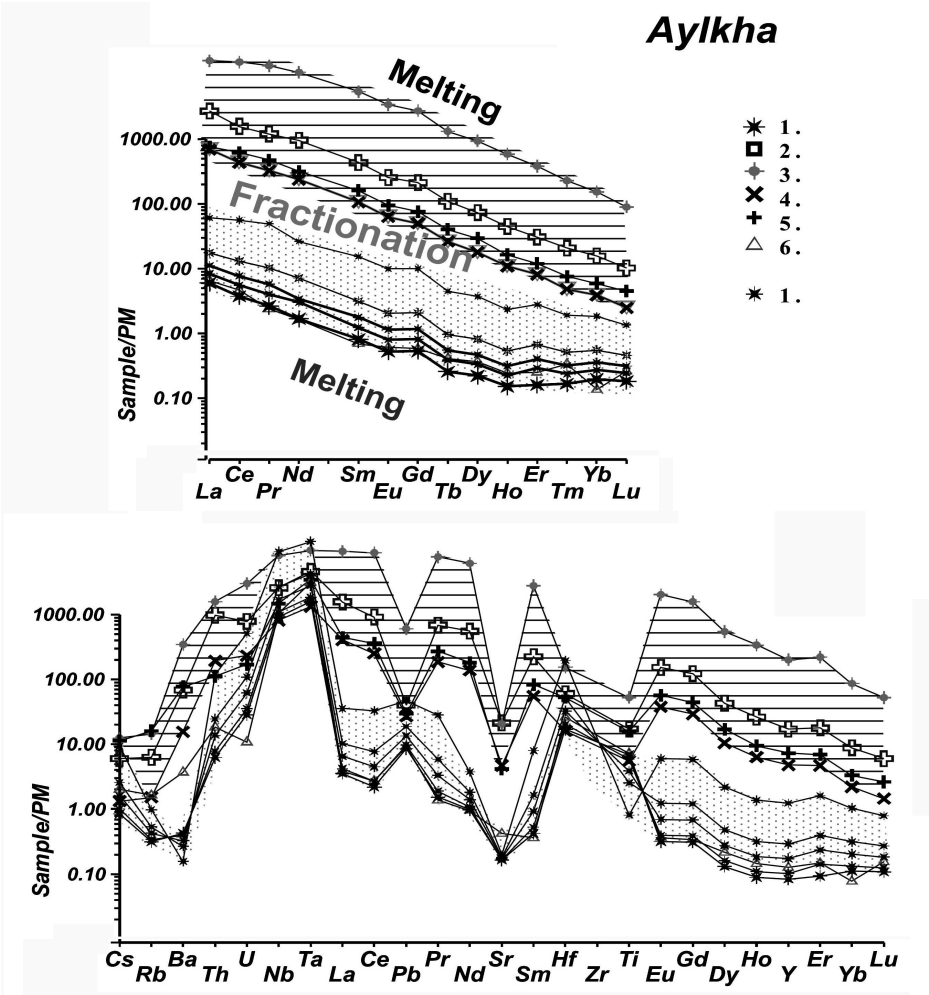

Fig. 8. **Modeling of the TRE for picroilmenites from Aykhal pipe.**

Calculations of the fractionation using as the main precipitates olivine (90%) ilmenites (10%) show that enrichment 2 orders should refer to the nearly complete crystallization of the protokimberlite or carbonatitic melts. Ilmenites with the extreme enrichment to 1000 C1 must be formed from the melts that were resulted from the small degree partial melting of the garnet bearing associations.

Looking at the trends of the main components three or more separate lines of enrichment are detected as a usual. Most probably trends are formed as a result of repeated pulsation of melts in the magmatic feeders with the repeated remelting of primary formed associations. This model may explain the very high enrichment of the melts that formed ilmenites in TiO_2 because the simple fractionation model and origin from the kimberlites hardly ever can explain these phenomena. Remelting of the metasomatic front produced by hydrous or more likely carbonatitic metasomatism near the intruded kimberlites and mixing of this melts with the evolved kimberlites is much more realistic model.

Thus we suppose for he creation of kimberlites three stage model. At the initial stage the ultramafic melts intruded carbonated and hydrated base of lithosphere produce a high temperature Metasomatism with the essential depletion of the base of lithosphere and formation of chromites and ilmenites precipitates (rarely subcalsic garnets within the feeders). The break up of the immiscible liquids during cooling brings to the separation of the major part of TiO_2 in the carbonatitic melts which produced the Ti rich Metasomatism near the feeding system. Next impulses of the melt intrusion was manifested by the remelting of metasomatites and high enrichment of this melts in TiO_2. Step wise process of the melt rising were resulting in continuous enrichment in the Cr and TiO_2 and creation of the megacrysts with step rising of Cr visible for ilmenite trend from many pipes (Yubileynaya, Zarnitsa etc.) [3, 8-13].

Ad the last stage at the top of the magmatic system usually upper then 40kbar the enrichment in water nears this level bring to the branching of the protokimberlite melts and growth of the phlogopites ilmenites veinlets in the peridotites with the very low melting degree which are typical for hydrous metasomatites. Sometimes fluctuations of Hf, Ba, HFSE, Y, Pb, Sr and show that ilmenite crystallization at least at the last low temperature stages were accompanied by the growth and dissolution of zircon, rutile, phlogopite, perovskite and apatite.

Concrete mechanism of the contamination and melt evolution is not determined yet. It should vary between three models. **1.** Polybaric step rising chamber fractionation in the semi closed systems with the dissolutions of the minerals from the roof. **2.** Interaction and dissolutions of the wall rock metasomatites during melt movements with the pumping of the partial melts from the contacts. **3.** Magmatic substitution by the rising melts enriched in volatiles of the large volumes of the host rocks at the front of the rising magmatic systems.

Concrete mechanism may be the combination of this or more complex model. For Mir and Dachnaya pipe the long crystallization line is likely the result of the fractionation in the continuous magma feeder. For Alakite pipes the pulsing rising with the remelting of the metasomatics is more realistic.

CONCLUSIONS

1. Crystallization trends of the ilmenites reflect the polybaric fractionation at the stage of the creation of the feeder systems.
2. TiO_2 - MgO in Picroilmenites increasing with the pressure while entrance of Fe and Mn indicate the temperature decrease.
3. Correlations between the layering and changes of the Picroilmenites components are explained by the exchanges of the magmas responsible for the ilmenite creation with mantle wall rocks.
4. Mantle layering determine the three levels way and possible stages of megacrysts origin: 1) deep HT mantle metasomatites pyroxenites and crystallization in the feeding systems; 2) fractionation of the protokimberlite melts mixed with the partial melt from the wall rocks; 3) low degree partial melting of the hydrous metasomatic fronts and mixing with the evolved protokimberlites.

ACKNOWLEDGEMENTS.

The work was performed with the support of RBRF grands 06-05-64416, 06-05-81016, 05-05-64718.

REFERENCES

1. **Agee J.J., Garrison J.R. and Taylor L.A.** Petrogenesis of oxide minerals in kimberlite Elliott County, Kentucky // Ameican Mineralogist, 1982, v. 67, p. 2842.
2. **Alymova N.A., Kostrovitsky S.I., Ivanov A.S. & Serov V.P.** Picroilmenites from kimberlites of Daldyn field, Yakutia // Transactions of the Russian Academy of Sciences Earth Science Sections, 2004, 395a, p. 444-447.
3. **Ashchepkov I.V., Vladykin N.V., Nikolaeva I.V., Palessky S.V., Logvinova A.M., Saprykin A.I. & Khmel'nikova O.S., Anoshin G.N.** Mineralogy and Geochemistry of Mantle Inclusions and Mantle Column Structure of the Yubileinaya Kimberlite Pipe, Alakit Field, Yakutia // Transactions of the Russian Academy of Sciences Earth Science Sections, 2004, 395(4), p. 517–523.
4. **Ashchepkov I.V. & Vishnyakova E.V.** Monomineral Ilmenite Thermo- And Oxybarometry And It's Application to Reconstruction of Magmatic Systems and Metasomatism within Mantle Columns of Siberian Platform // Geophysical Research Abstracts, 2006, Vol. 8, p. 00921.
5. **Ashchepkov I.V.** Empirical garnet thermobarometry for mantle peridotite // Russian Geology and Geophysics, 2006, 47 (10), p. 1071-1085.
6. **Ashchepkov I.V.** More precise equation of the Jd-Di barometer // Herald of Earth Sciences department Russian Academy of Sciences, 2003, N1 (21)**.**
7. **Ashchepkov I.V., Vladykin N.V., Pokhilenko N.P., Rotman A.Ya., Afanasiev V.P., Logvinova A.M., Kuligin S.S., Saprykin A.I., Kuchkin A.M. & Khemelnikova O.S.** Ilmenite trends from kimberlites of Siberia: Do they represent the mantle feeding vein system? // Geophys. Res. Abs., 2005a, **7**, 00593
8. **Ashchepkov I.V., Vladykin N.V., Pokhilenko N.P., Rotman A.Y., Afanasiev V.P. & Logvinova A.M.** Using of the Monomineral Thermobarometry for the reconstruction of the mantle sections // Problems of sources of deep seated magmatism and plumes, Irkutsk, Institute of Geography SB RAS, 2005b, p. 210-228.

9. **Ashchepkov I.V., Vladykin N.V., Rotman A.Y., Logvinova A.M., Afanasiev V.P., Palessky V.S., Saprykin A.I., Anoshin G.N., Kuchkin A.M., Khmel'-nikova O.S.** Mir and International'naya kimberlite pipes–trace element geochemistry and thermobarometry of mantle minerals // Deep seated magmatism, it's sources and their relation to plum processes, Irkutsk, IG SB RAS, 2004, p. 194-208.
10. **Ashchepkov I.V., Vladykin N.V., Rotman A.Y., Afanasiev V.P., Logvinova A.M., Kuchkin A., Palessky V.S., Nikolaeva I.A., Saprykin A.I., Anoshin G.N., Khmel'nikova O.S.** Variations of the mantle mineralogy and structure beneath Upper - Muna kimberlite field // Problems of sources of deep seated magmatism and plumes, Irkutsk, Geography SB RAS, 2005, p. 170-188.
11. **Ashchepkov I.V., Vladykin N.V., Rotman A.Y., Logvinova A.M., Nikolaeva I.A., Palessky V.S., Saprykin A.I., Anoshin G.N., Kuchkin A. Khmel'nikova O.S.** Reconstructions of the mantle layering beneath the Alakite kimberlite field: comparative characteristics of the mineral geochemistry and TP sequences // Deep seated magmatism. It's sources and their relation to plum processes, Irkutsk, 2004, Institute of Geography SB RAS, 2004d, p. 160-178.
12. **Ashchepkov I., Vladykin N., Pokhilenko N., Sobolev N., Malygina E., Kuligin S., Ovchinnikov Y., Afanasiev N., Mkrtychan G., Rotman A., Kostrovitsky S., Tolstov A., Khmel'nikova J., Pokhilenko L., Logvinova A.** Clinopyroxene geotherms for the mantle columns beneath кimberlite pipes from Siberian craton // 8th International Kimberlite Conference Long Abstract, 2003a, FLA_0355.
13. **Ashchepkov I.V., Vladykin N.V., Amshinsky A.N., Pokhilenko N.P., Rotman A.Y., Nikolaeva I.A., Palessky V.S., Saprykin A.I., Anoshin G.N., Khmel'nikova O.S.** Minerals from Zarnitsa pipe kimberlite: the key to enigma of the mantle composition and construction // Plume and problems of deep sources of alkaline magmatism. Proceedings of Intrernational workshop, Irkutsk State University, 2003b, p. 20-38.
14. **Boyd F.R. and Nixon P.H.** Origin of the ilmenite-silicate nodules in kimberlites from Lesotho and South Africa // Lesotho Kimberlites, Lesotho National Development Corporation, Maseru, Lesotho, 1973, p. 254-268.
15. **Boyd F.R. and Nixon P.H.** Origins of the ultramafic nodules from some kimberlites of northern Lesotho and the Monastery Mine // South Africa. Physics and Chemistry of the Earth, 1975, v. 9, p. 431-454.
16. **Boyd F.R., Pokhilenko N.P., Pearson D.G., Mertzman S.A., Sobolev N.V., Finger L.W.** Composition of the Siberian cratonic mantle: evidence from Udachnaya peridotite xenoliths // Contrib. Mineral. and Petrol., 1997,v. 128, № 2-3, p. 228-246.
17. **Brey G.P., Kohler T.** Geothermobarometry in four-phase lherzolites. II. New thermobarometers, and practical assessment of existing thermobarometers // J. Petrol, 1990, v. 31, p. 1353-1378.
18. **Dawson J.B., Smith J.V.** The MARID (mica –amphibole –rutile –ilmenite –diopside) suite of xenoliths in kimberlite // Geochim. Cosmochim. Acta, 1977, v. 41, p. 309 –323.
19. **Feenstra A,. Peters T.** Experimental determination of activities in $FeTiO_3$ -$MnTiO_3$ ilmenite solid solution by redox reversals // Contrib. Mineral. Petrol., 1996, v. 126, p. 109–120.
20. **Garanin V.K., Kudryavtseva G.P. and Lapin A.V.** Typical features of ilmenite from kimberlites, alkali-ultrabasic intrusions, and carbonatites // International Geology Review, 1979, v. 22, № 9, p. 1025-1050.
21. **Gregoire M., Bell D.R., Le Roex A.P.** Garnet lherzolites from the Kaapvaal craton (South Africa): Trace element evidence for a metasomatic history // J. Petrol, 2003, v. 44, iss. 4, p. 629-657.

22. **Gregoire M., Bell D.R., le Roux A.P.** Trace element geochemistry of glimmerite and MARID mantle xenoliths: their classification and relationship to phlogopite-bearing peridotites and to kimberlites revisited //Contrib. Mineral. Petrol., 2002, v. 142, p. 603–625.
23. **Griffin W.L., Moore R.O., Ryan CG., Gurney J.J., Win T.T.** Geochemistry of magnesian ilmenite megacrysts from southern African kimberlites // Russian Geology and Geophysics, 1997, v. 38, № 2, p. 421-443.
24. **Gurney J.J., Jakob W.R.O., Dawson J.B.** Megacrysts from the Monastery kimberlite pipe, South Africa // In: The mantle sample; Inclusions in kimberlites and other volcanics. Proceedings of the 2nd Inter. Kimber. Conf., 1979, v. 2, p. 265-278.
25. **Gurney, J.J., Moore, R.O. and Bell, D.R.** Mineral associations and compositional evolution of Monastery kimberlite megacrysts // 7 Inter. Kimber. Conf., Extended Abstracts, 1998, p. 290-292.
26. **Harte B.** Metasomatic events recorded in mantle xenoliths: an overview // Mantle Xenoliths. Wiley, Chichester, 1987, p. 625–640.
27. **Kaminsky F.V., Zakharchenko O.D., Griffin W.L., Channer D.M.D., Khachatryan-Blinova G.K.** Diamond from the Guaniamo area, Venezuela // Can Mineralog., 2000, v. 38, p.1347-1370.
28. **Konzett J., Armstrong R.A., Gunther D.** Modal metasomatism in the Kaapvaal craton lithosphere: constraints on timing and genesis from U-Pb zircon dating of metasomatized peridotites and MARID-type xenoliths // Contrib. Mineral. and Petrol., 2000,v. 139, № 6, p. 704-719.
29. **Kostrovitsky S.I., Alymova N.V., Ivanov A.S., Serov V.P.** Structure of the Daldyn Field (Yakutian Province) Based on the Study of Picroilmenite Composition // Extended Abstracts of the 8 Inter. Kimber. Conf., 2003, FLA_0207.
30. **McGregor I.D.** The system MgO- SiO_2-Al_2O_3: solubility of Al_2O_3 in enstatite for spinel and garnet peridotite compositions // Am. Miner., 1974, v. 59, p. 110-119.
31. **Mitchel R.H.** Experimental Studies at 6 - 12 GPa of the Ondermatje Hypabyssal Extended // Abstracts of the 8International Kimberlite Conference, 2003, FLA_0020.
32. **Mitchell R.H.** Kimberlites: Mineralogy, Geochemistry, and Petrology // Plenum Press, New York, 1986, p 442.
33. **Mitchell R.H.** Geochemistry of magnesian ilmenites from kirnberlites in South Africa and Lesotho // Lithos, 1977, v. 10, p. 29-37.
34. **Moore A.E., Lock N.P.** The origin of mantle-derived megacrysts and sheared peridotites-evidence from kimberlites in the northern Lesotho—Orange Free State (South Africa) and Botswana pipe clusters // S. Afr. J. Geol., 2001, v. 104, p. 23– 38.
35. **Moore R.O., Griffin W.L., Gurney J.J., Ryan C.G., Cousens D.R., Sie S.H. and Suter G.F.** Trace elernent geochernistry of ilmenite megacrysts from the Monastery kimberlite // South Africa. Lithos, 1992, v 29, p. 1-18.
36. **Neal C.R., Davidson J.P.** An unmetasomatized source for the Malaitan Alnoite (Solomon Islands); petrogenesis involving zone refining, megacryst fractionation, and assimilation of oceanic lithosphere // Geochim. Cosmochim. Acta, 1989, v. 53, p. 1975-1990.
37. **Nimis P., Taylor W.** Single clinopyroxene thermobarometry for garnet peridotites. Part I. Calibration and testing of a Cr-in-Cpx barometer and an enstatite-in-Cpx thermometer // Contrib. Mineral. Petrol., 2000, v. 139, № 5, p. 541-554.
38. **Nixon P.H.** Kimberlitic xenoliths and their cratonic setting // In: P.H. Nixon (Ed.), John Wiley and Sons, MantIe Xenoliths, Ltd, 1987.
39. **Nowell G.M., Pearson D.G., Bell D.R., Carlson R.W., Smith C.B., Kempton P.D., Noble S.R.** Hf Isotope Systematics of Kimberlites and their Megacrysts: New Constraints on their Source Regions // J. Petrology, 2004, v. 45, p. 1583-1612.

40. **Noyes A.K.** Feasibility Study of U-Pb Ilmenite Geochronology, Monastery Kimberlite, South Africa. // Thesis for degree of Master of Science. University of Alberta A. Edmonton, Alberta Spring, 2000.
41. **O'Neill H.St.C., Pownceby M.I., Wall V.J.** Ilmenite-rutile-iron and ulvospinel-ilmenite-iron equilibria and the thermochemistry of ilmenite ($FeTiO_3$) and ulvospinel (Fe_2 TiO_4) // Geochim.Cosmochim Acta, 1988, v. 52, p. 2065–2071.
42. **Patchen A.D., Taylor L.A., Pokhilenko N.P.** Ferrous freudenbergite in ilmenite megacrysts: A unique paragenesis from the Dalnaya kimberlite, Yakutia // American Mineralogist, 1997, v. 82, p. 991–1000.
43. **Pokhilenko N.P., Sobolev N.V., Kuligin S.S., Shimizu N.** Peculiarities of distribution of pyroxenite paragenesis garnets in Yakutian kimberlites and some aspects of the evolution of the Siberian craton lithospheric mantle // Proceedings of the VII Inter. Kimber. Conf., 2000, p. 690-707.
44. **Rodionov A.S., Sobolev N.V., Pokhilenko N.P., Suddaby P., Amshinsky A.N.** Ilmenite-bearing peridotites and megacrysts from Dalnaya kimberlite pipe, Yakutia // 5 Intern. Kimber. Conf.: Extended abstracts, United States, 1991, p.339-341.
45. **Schulze D.J., Valley J.R., Bell D.R., Spicuzza M.J.** Oxygen isotope variations in Cr-poor megacrysts from kimberlite // Geochim. Cosmochim. Acta, 2001, v. 65, iss. 23, p. 4375-4384.
46. **Schulze D L., Anderson P.F.N., Hearn Jr.B.C., Hetman CM.** Origin and significance of ilmenite megacrysts and macrocrysts from kimberlite // International Geology Review, 1995, v. 37, p. 780-812.
47. **Sobolev N.V., Kaminsky F.V., Griffin W.L., Yefimova E.S., Win T.T., Ryan C.G., Botkunov A.I.** Mineral inclusions in diamonds from the Sputnik kimberlite pipe, Yakutia. // Lithos., 1997, v. 39, p. 135-157.
48. **Sobolev N.V.** Deep-Seated Inclusions in Kimberlites and the Problem of the Composition of the Mantle // Amer. Geophys. Union, Washington, DC, 1977, p. 279.
49. **Sobolev N.V., Yefimova E.S.** Composition and petrogenesis of Ti-oxides associated with diamonds // Int. Geol. Rev., 2000, v. 42, p. 758– 767.
50. **Taylor W.R, Nimis P.** A single-pyroxene thermobarometer for lherzolitic Cr-diopside and its application in diamond exploration // 7th Int Kimb Conf. Abstract Volume, Cape Town, 1998, p 897-898.
51. **Wechsler B., Prewitt C.T.** Crystal structure of ilmenite ($FeTi0_3$) at high temperature and at high pressure // American Mineralogist, 1984, v. 69, p. 176-185.
52. **Wyatt B.A., Baumgartner M., Anckar E., Grutter H.** Compositional classification of ''kimberlitic'' and ''non-kimberlitic'' ilmenite // Lithos, 2004, v. 77, p. 819– 840.
53. **Wyatt B.A., Lawless P.J.** Ilmenite in polymict xenoliths from the Bultfontein and De Beers Mines, South Africa. // In: Komprobst, J. (Ed.), Kimberlites II: Their Mantle and Crust Mantle Relationships. Proc. 3rd Int. Kimb. Conf. Elsevier, Amsterdam, 1984, p. 43–56.
54. **Zack T., Brumm R.** Ilmenite/liquid partition coefficients for 26 trace elements determined through ilmenite/clinopyroxene partitioning in garnet pyroxenites // 7th International Kimberlite Conference. Extended abstracts. Cape Town, 1988, p. 702-704.
55. **Zhang H.F., Menzies M.A., Mattey D.P., Hinton R.W., Gurney J.J.** Petrology, mineralogy and geochemistry of oxide minerals in polymict xenolits from the Bultfontein kimberlites, South Africa: implication for low bulk-rock oxygen isotopic ratios // Contrib Mineral. Petrol., 2001, v. 141, iss. 3, p. 367-379.

UDK 552.48; 552.321.6

The nature of indicator minerals in kimberlites: a case from the mantle xenoliths studying

Spetsius Z.V.

YaNIGP CNIGRI, ALROSA Co. Ltd, Mirny, Yakutia, Russia; spetsius@cnigri.alrosa-mir.ru

ABSTRACT

The studying of indicator minerals from kimberlites and mantle xenoliths allowed to conclude that main kimberlitic minerals such as garnet, olivine and partly chromite and ilmenite are xenocrysts from the desintegrated mantle rocks as well as diamonds itself.

In this paper are described associations with the diamond from the Nyurbinskaya and Sytykanskaya pipes that combine three different groups: inclusions in diamonds, intergrowth of diamonds with megacrystic minerals and diamondiferous xenoliths. Chemistry of minerals and peculiarities of diamonds are discussed. Garnet inclusion compositions from diamonds of the Sytykanskaya pipe suggest that peridotitic paragenesis predominate in this pipe but in intergrowth with diamonds are found eclogitic garnets. The distribution of eclogitic diamonds is confirmed by the finding of 11 diamondiferous eclogites. According the wide distribution of partial melt products and other features not excluded the metasomatic origin of diamonds in some xenoliths.

Presented in this paper data are important considering their implication to this problem at least in three aspects: 1) first of all, because of their wide variations in composition of studied samples, 2) in connection with the unusual peculiarities of kimberlites and mantle associations of these pipes, and 3) as samples containing diamonds.

It is possible to speculate from these evidences that many eclogitic and part of pyroxenitic xenoliths are experienced a strong metasomatic influence. There is ample evidence that this statement is confident and that is confirmed by wide distribution of zoned garnet in investigated parcel of diamondiferous samples from the Nyurbinskaya pipe and intensive development of phlogopite and other metasomatic minerals in eclogites of both pipes.

Keywords: kimberlites, indicator minerals, xenoliths, eclogites, diamonds, garnet

INTRODUCTION

At present possible consider and it is enough motivated by different facts that suppressing part of kimberlitic indicator minerals is formed due to disintegration of mafic and ultramafic mantle xenoliths [1-40]. That, in the first place is a main indicator mineral - garnet, amongst the broad variety composition of which possible only some separate megacrysts present itself derivate of the kimberlitic magma or sooner have a related relationship with kimberlites. To such, as judged by given fine geochemical and isotopic of the studies, can be referred low

chromium and somewhat high titanium garnets, which are considered as formation related kimberlites or having with them united source [19]. At least, even precise isotopic of the study do not allow to select amongst megacrystic garnets certain types of garnet, which could be considered as derived due to magmatic differentiation of the kimberlitic magma. More probably that the overwhelming part of megacrysts is also formed due to breakdown of ilmenite bearing ultramafites or others mantle rocks. Xenogenic nature all others pyropic garnet as high chromium, so and low chromium to account peridotitic and pyroxenitic or eclogitic xenoliths does not cause the doubts.

The most ambiguous is a question of the chrome spinels source and recognition amongst them xenogenic grains from the mantle ultramafites and strictly kimberlitic chromites. To the last, certainly, can be referred spinel microcrystals from the kimberlitic ground mass, however evident criterion of the difference their composition and principle of the separation clear paragenic types all do not exist, in spite of it is enough detailed designed categorization that developed in works [3, 8, 27].

Before recent time was considered that main part of olivine in kimberlites is a direct derived of the kimberlitic magma, but what have shown the detailed studies Re-Os systems of the in situ sulfides in large grains of olivine from the Udachnaya pipe [9], overwhelming quantity of large more than 3-4 mm olivines, is also xenogenic.

Ilmenite, in the opinion of some researchers in majority its crystallized right in kimberlitic substratum that is motivated its geochemical particularity and in the first place that exists specifics a composition given mineral, as in respect of different kimberlitic fields, so and somewhat separate kimberlitic pipe [14]. The possibility to crystallizations ilmenite right in kimberlitic substratum is confirmed beside detailed geochemical and experimental studies given mineral and does not cause of the considerable doubts. However we shall note that ilmenite the less wide-spread mineral in comparison to spinels in groundmass of majority of kimberlites. Garanin V.K. is distinguished 11 genetic groups of ilmenite for kimberlites of the Archangelsky province, that are parallelize as well as with ilmenite groups in kimberlites of the Yakutian province [3]. It is shown that in the high grade diamondiferous pipes of Yakutia (Mir, Udachnaya and other) is noted consistent narrow and clearly directed evolution trend of the ilmenite composition from the peridotites through ilmenite-pyroxene to garnet-ilmenite intergrowths with increase in this direction geikelite component in ilmenite. From brought statement, obviously that genesis of ilmenite links with the mantle ultramafites. Moreover the composition varieties of ilmenite in xenoliths practically completely overlap the spectrum of this mineral in kimberlites [3, 8, 14, 33].

Thereby, we can not deny the fact of the presence of ilmenitebearing mantle xenoliths and hence the presence of two different groups of this mineral in kimberlites. However on present stage of the studies, clear toolbox on division of the origin given mineral in kimberlites is not installed, since if consider only

chemical particularities of ilmenites from kimberlites and mantle xenoliths, that exists enough big field of their composition overlapping. Using the geochemistry also does not give the clear criterion of division these two in principal different genetic groups of one mineral type and given problem requires undertaking the additional studies and generalizations.

ANALYTICAL METHODS

The study of the garnets and others minerals composition predominantly was realized by means of x-ray microprobe Superprobe JXA-8800R of "ALROSA" Co. Ltd. (Mirny) and partly with electron microprobe Cameca (IGIG, Novosibirsk) and Institute of Geology diamond and precious metals (Yakutsk) in reference conditions. In separate cases analysis of secondary phases of partial melting products and some other minerals was executed with using Link ISIS - 300.

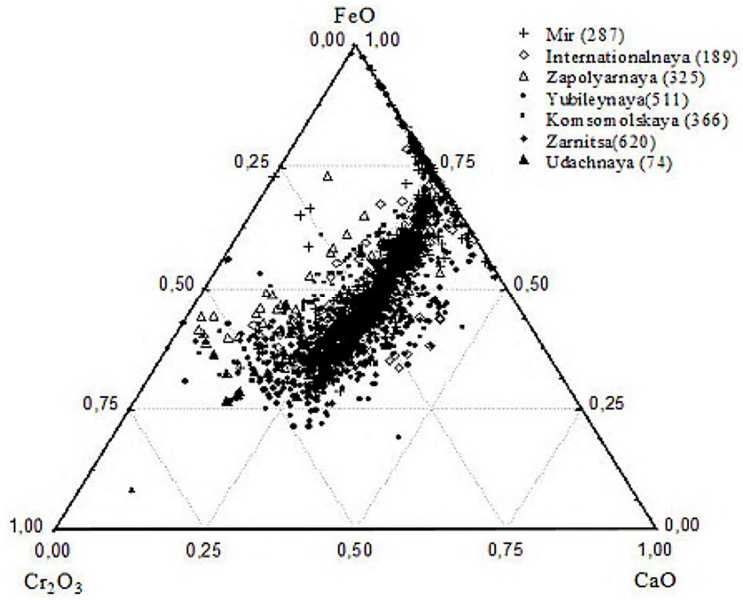

Fig. 1a. **Plot of the garnet compositions in the kimberlites of main industrial diamondiferous pipes in coordinates on Cr-Fe-Ca.**

Analytical conditions included an accelerating voltage of 15 keV, a beam current of 20 nA, beam size of 5 µm, and 20 seconds counting time for all elements. In all cases natural minerals and synthetic were used as standards. Predominantly certificated in IGIG (Novosibirsk) natural minerals were used as the standards. All analyses underwent a full ZAF correction.

RESULTS

Studies of the chemistry of indicator mineral were executed during of the last four years from the Yakutian kimberlite pipes with different productivity. As a whole, indicator minerals in association with diamond from high-grade kimberlites

have a following particularities: for garnet, aside from high contents of chromium and comparatively low - calcium, characteristic of raised content sodium and lowered content of titanium; chrome spinels differ the lowered contents TiO_2, MgO and raised - Fe; in olivine noted lowered amount ferric oxide and titanium, but in clinopyroxenes - lowered concentrations Al, Fe, Ti, Mn and raised - Mg, Ca, Cr and Na.

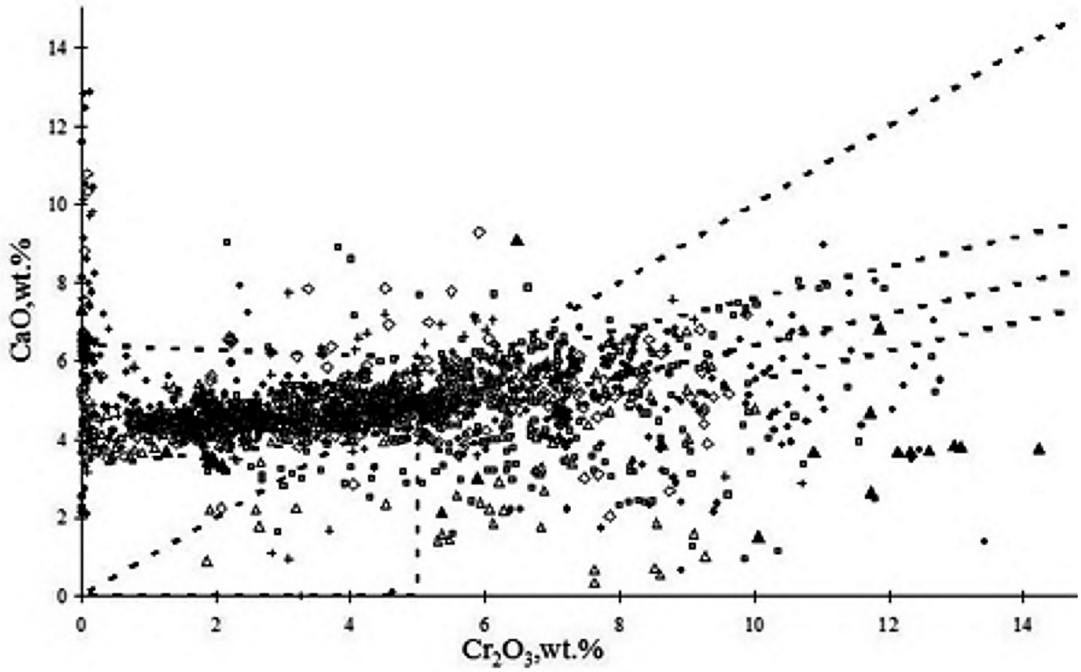

Fig. 1b. **Plot of the garnet compositions in the kimberlites of main industrial diamondiferous pipes on diagram of N.V.Sobolev [27].**

Major portion of these regularities it is enough obvious from data given on garnet from different kimberlitic pipe, which are submitted on triple diagram CaO-FeO-Cr_2O_3 and are illustrated also on the known diagram of N.V. Sobolev [27], reflecting distribution of garnet in association with diamond (Fig. 1a,b). From presented illustrations it is enough obviously that the compositions of garnet population from the industrial diamondiferous pipe practically are completely overlapped, to say at least, in ratio of Ca, Cr and Fe that is indicative of resemblance composition variations of main indicator mineral - garnet, within not only separate field, but also different fields. Naturally that these regularities can be kept only under it is enough representative amounts of grains in analysed garnet sets from each pipe.

The small differences are fixed on diagram CaO-Cr_2O_3, in particular, raised calcium content differ the garnets from pipes Mir, Komsomolskaya and Zarnitsa, but garnet compositions from pipes Jubileynaya and Udachnaya are wide-spread in area of raised Cr-content (Fig. 1b). With standpoint defining influences of the composition mantle source on the composition of indicator mineral kimberlites of

interest discuss the results, got in process of the study of diamondiferous xenoliths collections from the Nyurbinskaya and Sytykanskaya pipes.

MINERAL ASSOCIATIONS WITH DIAMOND IN THE NYURBINSKAYA KIMBERLITE PIPE

Paragenetic associations with diamond in kimberlites can be split into 3 main types: a) association different mineral, being kept as inclusions in diamond crystals, b) minerals intergrowth with diamonds, c) xenoliths of diamondiferous mantle rocks. The picked types, in that or other amount are discovered in all kimberlitic pipes with the industrial content of diamonds. These associations always attracted the stare attention of the researchers since they contain the most reliable information about condition of the diamond origin in the nature and information on particularity of the environment at the time of diamond formation i.e. petrologycal particularity of the upper mantle of given region.

As any new object, kimberlites of relatively recently discovered pipes Botuobinskaya and Nyurbinskaya were a subject of the intensive studies in the last decade. In spite of this short term, study of the geology and mineralogy kimberlites and the other particularity of the composition of these pipes is dedicated series of publications [1, 4, 13, 16, 31, 34]. In these works is demonstrated singularity of kimberlites of the new field, as on isotopic features, that approaches them with the 2-nd group of kimberlites and on particularity of the composition of indicator minerals, in the first place garnet and chrome spinels. They are revealed also essential differences of the lithospheric mantle underneath the Nakynsky field, both on set of petrographic types of the mantle rocks, and tectono-magmatic evolution in comparison with nearby Malobotuobinsky and Daldyno-Alakitsky regions [31].

Already first information on study of the diamonds external morphology from kimberlites given field have shown that they are also different on spectrum and ratio of the morphological groups from the diamond populations of the others kimberlitic pipes of Yakutian province [4, 34]. In diamond population raised amount round crystals was fixed from kimberlites Nakynsky field, diamond "in coat" and diamond with cavity, channel of the pickling and the other sign of the natural dissolution and resorption. Under visual study of the mineral inclusions in diamond from kimberlites of this field, was noted raised contents in them orange garnet and the other mineral supposedly eclogitic association [4, 34, 40]. This conclusion was confirmed by microprobe study results of the inclusions in diamonds from the Botuobinskaya pipe, which have shown that more than 50 % crystal belongs to the eclogites paragenesis that pointed to the high abundance of eclogites crystals amongst diamonds of this pipe [16]. That makes obvious the specificity of the new region and importance of the study of the particularities mantle xenoliths, especially with the diamonds in them.

The material for given studies have included the mantle rocks or monomineral garnet megacrysts containing single diamond intergrowth or in rare cases several

crystals on their surfaces. Xenoliths and megacrysts with diamonds (more than 160 samples) were extracted from kimberlite ore in process of its enrichment by means of X-ray separators. Since sample are presented by the garnetbearing xenoliths, in which of primary mineral only garnet was fresh remain or nearly monomineral garnet megacrysts, given mineral alongside with diamonds was a main object of the studies. The microprobe study of its composition was done for all samples and morphological study of diamonds was executed.

Table 1.

Average composition of garnet groups of diamondiferous xenoliths from the Nurbinskaya pipe, after [38].

Sort 8	G1	G2	G3	G4	G5	G6	G7	G8
	Eclogite Group B	**Eclogite** Group B	**Eclogite** Group B	**Eclogite** Group B	**Eclogite** Group C	**Websterite + Eclogite**	**Wehrlite-Lherzolite**	**Dunite-Harzburgite**
SiO_2	39.3 (7)*	39.7 (5)	40.2 (4)	40.5 (14)	40.2 (4)	40.6 (1)	40.5 (4)	40.7 (5)
TiO_2	0.27 (9)	0.45 (12)	0.29 (6)	0.38 (14)	0.40 (11)	0.30 (10)	0.37 (13)	0.15 (6)
Al_2O_3	21.2 (3)	21.2 (5)	21.8 (3)	22.0 (10)	21.9 (3)	22.1 (4)	22.0 (18)	15.4 (13)
Cr_2O_3	0.07 (5)	0.08 (5)	0.08 (6)	0.10 (7)	0.10 (5)	0.11 (6)	0.17 (7)	9.87 (16)
MgO	9.38 (20)	10.2 (14)	12.4 (4)	14.1 (12)	9.00 (97)	15.5 (10)	20.6 (33)	19.1 (9)
CaO	5.09 (75)	8.27 (84)	5.05 (79)	10.2 (22)	16.3 (15)	3.82 (83)	3.37 (95)	6.12 (11)
MnO	0.48 (12)	0.39 (7)	0.38 (6)	0.19 (7)	0.14 (4)	0.37 (8)	0.34 (12)	0.47 (9)
FeO	23.1 (21)	18.2 (23)	18.8 (9)	10.8 (35)	11.0 (45)	16.4 (34)	10.7 (37)	7.46 (42)
Na_2O	0.10 (4)	0.16 (6)	0.12 (2)	0.22 (6)	0.17 (3)	0.12 (2)	0.12 (5)	0.04 (2)
NiO	<0.03	<0.03	<0.03	<0.03	<0.03	<0.03	<0.03	<0.03
Total	98.99	98.65	99.12	98.49	99.21	99.32	98.17	99.31
#samples	7	13	40	6	10	30	8	7
Relative %	**5.8**	**10.7**	**33.1**	**5.0**	**8.3**	**24.8**	**6.6**	**5.8**

Note: *- Numbers in ( ) represent the 1 sigma precision of the analysis in terms of the least unit cited.

The representative samples collection is presented by round form xenoliths or monomineral garnet, containing visible diamonds. In row of samples is discovered on the surface 2 and more diamond crystals. This given collection of xenoliths and megacrysts with diamond is unique in having multiplicity of samples and that they are found in kimberlites recently open pipe. In spite of a many years industrial mining of such known pipe as the Mir and Udachnaya, the whole amount discovered in them xenoliths with diamond, as a rule, does not exceed 100 samples in each pipe. This is rightly for xenoliths with diamonds collected from studied in detail kimberlitic pipe, as of Yakutia, and South Africa [5, 10, 17, 18, 23-29, 33].

Not stopping in detail on features of diamonds being present in xenoliths, shall note only that in most cases they are presented by octahedral crystals. In the whole, on collection the following morphological diamond groups are in the ratio: octahedrons - 65%, transient forms - 22%, intergrowth - 8%, different twins types - 5%. In several studied samples the diamonds are present in amount five and more crystal. Herewith in some xenoliths noted accumulation of diamonds, those form the separate chains and veins. In rare samples the diamonds are presented by coated crystals, which usually have yellow-green coloration. The size of diamonds

varies from 0.5 mm to 4-5 mm on long axis. It is necessary to emphasize that many diamonds contains the channels of the pickling and the other signs to corrosions, amount such like crystal on collection as a whole forms ≈ 30%.

As was it already noted, in all xenoliths garnets were analysed on subject of the determination main rock type, moreover in most cases, was realized determination of the composition central and peripheral garnet zones for the reason of possible zonation discovery. On this base almost 10% of studied garnets reveal zonation in respect of the main element - Ca, Mg and Fe. The results of microprobe analysis composition this mineral in explored xenoliths were recalculated by means of factorial analysis that has allowed selecting 8 groups garnet; it is enough clearly differing on that or other main component [31]. There were given amount of analyzed samples and percent contents of the separate groups in the studied xenoliths parcel (Table 1). Chosen as a result of cluster analysis the garnet groups are correspond enough close upon their composition to that garnet types in varieties of mafic or ultramafic mantle xenoliths. In particular, group G-8 completely corresponds to the garnet of dunite-harzburgite paragenesis, according to high chrome (> 8.0 wt.% C_2O_3) and magnesium and answer the group G10 of Dawson-Stephens classification [6]. The garnets of the group G-7, with similar high magnesium, are differing much more low contents C_2O_3 and CaO and link with garnet of lherzolite or wehrlite xenoliths. The garnet group G-6 corresponds to this mineral from garnet websterites, which much less magnesian in contrast with garnet two previous groups, but also has low CaO contents. Is not excluded that separate sample from this groups xenoliths can belong to the magnesian eclogites. The garnet group G-5 corresponds completely the mineral from the high aluminous eclogites, including grospydites, kyanite and coesite eclogites, as well as samples of this group with corundum. High CaO in garnet is a criterion for separation of these type xenoliths [29]. The garnets of 4th group close previous on magnesian, but differ the smaller contents CaO and upon their composition can belong to the different types Mg-Fe-eclogites [31]. Cluster groups garnet G-1, G-2 and G-3 for that typical low Cr raised Fe and varying CaO contents correspond to the garnets from varieties of magnesian and Mg-Fe eclogites. It is necessary to note that garnets of the group G-6 with raised Mg# and lowered Ca can belong to both xenoliths types' as magnesian eclogites and garnet websterites. Close on composition of main oxides garnets can be found also in megacrysts association from kimberlites [6]. Somewhat ambiguous also mineral cluster group G-7, that differ the raised Cr and Mg and low contents calcium. The similar garnets meet as in composition of lherzolites and pyroxenites xenoliths, and also can be correlated with garnet megacrysts association, probably, it is reasonable to select those in a group of transient rocks. In any case, the first five cluster groups, that unite the garnets with moderate Mg, raised Fe and low Cr, with high degree of probability, answer the varieties of mantle rocks predominantly of eclogitic composition. On share of this type diamondiferous xenoliths happens to more than 60% sample in given parcel of diamondiferous samples. It should be emphasized that samples,

certainly, of dunite-harzburgite paragenesis form less 10% from the whole population of diamondiferous xenoliths (see table 1).

The analysis of the inclusions in diamonds of the Botuobinskaya pipe of the same Nakynsky field have shown that eclogite paragenesis forms not less 50% of the whole diamond population of this pipe [16]. Such a high content of eclogitic paragenesis diamonds never was noted earlier amongst diamond populations of any kimberlitic pipes of the Yakutian province. These data are persuasively confirmed by our results of studies of diamondiferous xenoliths from the Nyurbinskaya pipe. As it was shown above, the main part of samples amongst

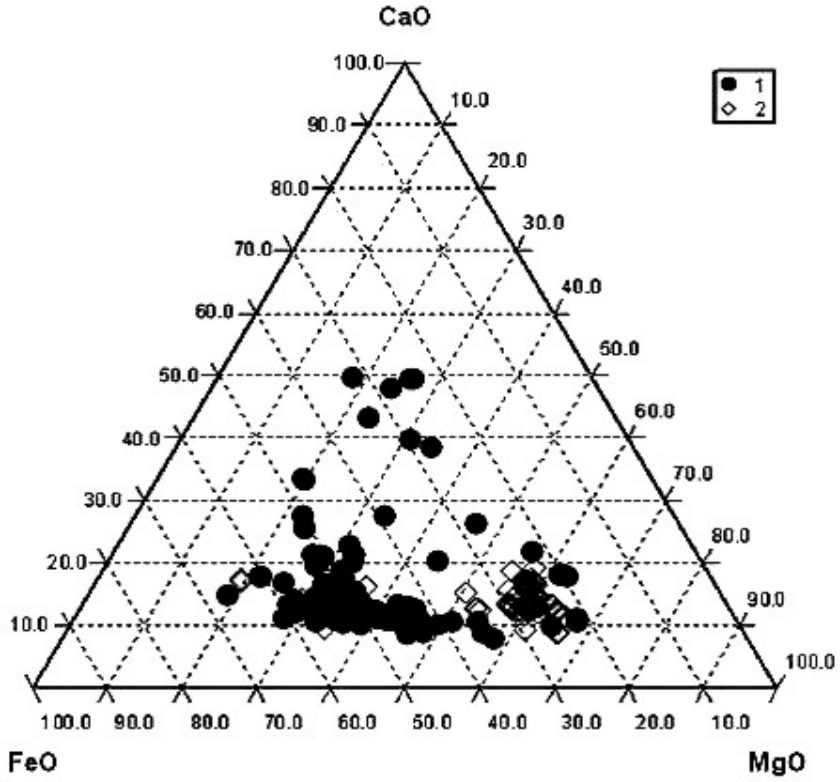

Fig. 2. **Plot of the composition of garnets in diamondiferous xenoliths and in kimberlite concentrate from the Nyurbinskaya pipe.**

1 - garnet from diamondiferous xenoliths and 2 - garnet from the kimberlite concentrate (level 612-687, AKB).

diamondiferous xenoliths consists of garnet being responsible by its composition for different type's eclogites or less garnet websterites. The portion of ultramafic paragenesis samples: dunit-harzburgites or in some cases, probably, lherzolites or pyroxenites of the composition amongst the whole collections forms < 10%. Herewith necessary to note that percent content of diamondiferous eclogitic associations can be even above since in given collections practically were absent xenoliths containing diamonds of cubic form. As judged by author's material, the amount of those crystals in diamond populations both pipe forms not less than 3-5%. Since all xenoliths were recovered with the luminescent separator, naturally

that xenoliths containing cubic diamonds, could not be extract due low intensity of X-ray luminescence of these crystals. At the same time, as it was noted earlier, kyanite eclogites are a maternal source of this sort of diamonds [29]. Thereby, is not excluded that portion of eclogitic substratum, having been a source ambience for diamond formation in the subcontinental lithospheric mantle under this kimberlitic field, was else above.

All received results on garnets chemistry from studied xenoliths and megacrysts with diamond are shown on triangular diagram of the garnet composition in coordinate Mg-Ca-Fe (Fig. 2). As follows from presented data, garnets field from diamondiferous xenoliths of the Nyurbinskaya pipe occupies the broad range on all main component. Moreover on composition variety garnets from xenoliths and megacrysts with diamond overlay the field of diamondiferous xenoliths from pipes Mir and Udachnaya [28]. On variations of the contents CaO range garnet in associations with diamond from pipe Nyurbinskaya broader, than in xenoliths with diamond from the Mir pipe. Necessary to note that garnets composition in Nyurbinskaya xenoliths turned out to be broader, than on separate horizons and in concentrate from bore holes of this pipe. The comparison of garnets composition variations from concentrate and diamondiferous associations shows that field of the garnet associated with diamonds several broader, than field of garnet from concentrate (see Fig. 2). That points on the necessity of the more careful selection of garnets in test when undertaking search and exploratory work on territory of the Nakynsky kimberlite field. The orange garnets of eclogite type, sometimes close on external look to almandine garnet of metamorphic rocks and in some cases can be rejected and be not included in sampling of indicator kimberlite minerals associating with diamond.

The received data indicate a specific composition of the ambience diamond formed and accordingly that the lithospheric mantle in region of new Nakynsky kimberlite field. Probably, this explains high grade of diamonds in kimberlites of both pipe, which is in this instance provided by high content of diamonds in mantle xenoliths, in the first place in eclogites. We can not confirm on all 100% - is this result of selective seizure or effect of the anomalous composition to mantles in given region. However, the results, received in process of the study xenoliths with diamond from the Nyurbinskaya pipe, indicate of raised widespread of diamondiferous eclogite xenoliths and pyroxenites in kimberlites of this pipe. This allows considering the more probable reason for dominant of eclogites paragenesis diamond - raised spreading eclogites substratum in the lithospheric mantle composition under Nakynsky kimberlite field. Aside from this, such indirect signs as broad spreading of round dissolved forms of diamonds and crystals with channel and the other signs of corrosions are indicators of raised influence the processes metasomatism and partial melting on diamonds formation [28, 36, 38]. These processes, probably, have not only defined the presence of the separate types of crystals and specificity diamond population, but also, probably, have provided the arrival of sufficient amount carbon, due to intensive penetration of fluid

components. The participation of metasomatic processes and accompanying fluids in origin of diamonds is emphasized by the presence of phlogopite in rims around diamonds in xenoliths and by the zonation in garnet of diamondiferous xenoliths of this pipe [28].

It is well known that garnets in the majority of eclogite and websterite xenoliths from kimberlites uniform on composition within sample and homogeneous in separate grain [18, 31], but in garnet from diamondiferous xenoliths of the pipe Nyurbinskaya this regularity is not a case. Performing microprobe analysis has discovered the presence of possible garnet zonality in many samples. Special attention was done and results of microprobe study of chemistry of central and peripheral parts garnet grains from many samples are presented in [38], where it is enough obviously denominated inhomogeneity of this mineral on that or other component. This is expressed in changing of contents Ca, Mg and Fe, and in more rare cases of titanium and chromium. It should be emphasized that zonation in garnet can result from, at least, two different processes: 1) magmatic crystallization or subsolidus transformation and 2) zonation can be a result of metamorphic transformations [35].

If garnet or other mineral zonations were formed as a result magmatic crystallizations, that usually define the falls of magnesian and increases the contents a ferric from the centre to peripheries of garnet grains. Zonation of garnet in studied xenoliths, on the contrary, is expressed in growth of magnesian, as well as, in contents CaO to the rim of grains. The content of FeO, opposite, falls to periphery garnet grains in the majority of samples. Such behavior of the row of petrogenic elements indicate that the most probable scenario was a change the contents Mg, Ca and Fe under influence of metasomatic fluids. The conclusion about forming zonation in the process of metasomatose is emphasized also by the emplacement rims around zonal grains and veins executed by metasomatic minerals, in the first place by phlogopite.

MINERAL ASSOCIATIONS WITH DIAMOND IN THE SYTYKANSKAYA KIMBERLITE PIPE

The Sytykanskaya pipe, opening in 1955 and is located in 27 km to the northeast from the Ayhal town. Almost 98% of its area was overlapped by terrigenous-carbonate sediments with thickness 0 - 22 m and traps 5 to 72 m [29].

Diamondiferous eclogites from this pipe were described in four separate publications [12, 15, and 24], however compositions main minerals garnet and clinopyroxene are brought only on two samples. Exactly also episodic and fragmentary is brought information on morphologies and other particularity of diamonds in xenoliths. Analyses of minerals practically are absent in literature on composition of diamond inclusions from this pipes. Considering that at present the developing of the Sytykanskaya pipe practically is completed, we have considered expedient to characterize as minerals, associating with diamond in intergrowth, inclusions and diamondiferous eclogites, and mineralogical particularities diamond

themselves from these association on author's material with attraction of the literary information.

The Sytykanskaya pipe consists of two independent bodies: northeast (main) and south-west. The pipe is built by three phases of the kimberlite intruding. As a whole for kimberlites of the Sytykanskaya pipe is characteristic of raised amount of pyropic garnet and picroilmenite. Herewith breccia of northeast part of the main body is characterized by smaller contents pyrope and more high - picroilmenite, than breccia of central part. In south-west body pyrope contents are lower than in both parts of the north-eastern body, but picroilmenite occupies the intermediate position between amount of this mineral in central and north-eastern parts. The content of the mantle xenoliths varies from rare in south-west body to 3.5% volume in the central. Characteristic is the sharp prevalence of ultramafic types for central part. Except of presence of cataclastic lherzolites and diamondiferous eclogites, central ore pole differs from north-eastern by raised amount of dunites, garnet-spinel lherzolites, lowered - an ilmenite ultrabasites and equal-grained garnet lherzolites. The Sytykanskaya pipe pertains to deposits with sharp difference in diamond grade and different typomorphic features of diamonds of separate ore poles. Content of diamonds in porphyritic kimberlites of north-eastern body is less, but in autolitic kimberlite breccia - in 7 times less in contrast with autolitic kimberlite breccia of the north-eastern body [40].

Previously than give the short description of xenoliths with diamond it should be noted that all of these samples were displayed from products of the enrichment of the exploratory tests Amakinskaya expedition that has conditioned the small size of xenoliths or mineral-intergrowth with diamond. The consolidated features of the modal composition of samples, amount crystal in them and sketch description of diamonds were provided in [32]. From brought data turns attention on itself that diamonds are discovered in xenoliths not only in xenoliths and as intergrowths with pyrope of peridotitic or eclogitic type, but counter also in associations with ilmenite or with orange titan-pyrope typical of xenoliths ilmenitebearing ultramafites. This, certainly, is due to raised and wide-spread content of the ilmenitebearing mantle xenoliths in given pipe.

*The petrographic features of xenoliths and megacryst*s. The size of studied sample varies within 1-5 sm on long axis of xenoliths that as noted above, is to a considerable extent conditioned by selection product sample enrichments. As a rule, they have an oval form. In principal can be stand out two groups of diamondiferous samples. The first group is presented by monomineral megacrysts, containing inclusion of the diamond. In most cases, megacrysts minerals are presented by garnets mainly peridotites or eclogites of the composition [32]. The garnets of these two types could be enough certain divide even by visual study under binocular microscope upon their typical coloration: violet Cr-pyropes from peridotites and orange from eclogites. It is necessary to note that in one of the sample garnet on its composition can be referred to type of lherzolite or pyroxenite paragenesis, that is characterized by high magnesian and lowered contents of the

chrome component (< 4 wt.% Cr_2O_3). Amongst these formations also megacryst-intergrowths with diamonds have been met, where mineral-host is presented by the ilmenite [32].

The xenoliths of diamondiferous eclogites differ by lengthened oval form, and small size (< 30 mms on long axis). The coarse-grained samples with granoblastic or poikilitic structure are predominating. The majority of them are cataclastic. Two groups of xenoliths stand out: bimineralic and kyanitebearing. As that, so and other are contain visible products of intensive process of the partial melting, metasomatism and later secondary transformations [32].

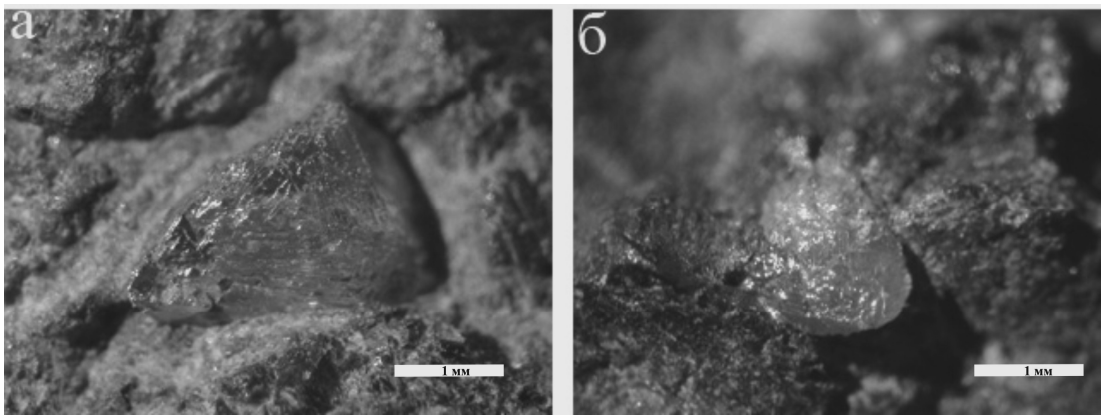

Fig. 3. **Diamonds in xenoliths from pipe Sytykanskaya.**

a) Oktahedron with polycentric construction of the facets in bimineral eclogite, sample S-16; b) Round form octahedron in magnesian eclogite, sample S-17.

The garnet is a main mineral and forms from 50 to 80% and even 90% modal composition of the samples. The mineral possesses orange or pale-orange color, composing main fabrics of the sample in the form of irregular grains with the sizes 2-4, and sometimes 6 mm. The clinopyroxene forms irregular grains 1 to 5 mm and is intensively changed by amorphization that stipulated its porcelaneous look and pale-green or sometimes bluish coloration. Primary omphacite is present as rare relicts in separate samples.

At presence in samples of kyanite, he forms lengthened grains, usually, colorless transparent, sometimes with bluish tone by size 1-2 mm. In quantitative attitude kyanite forms less than 5 % of rock. Aside from these minerals the sulfides are present in most of xenoliths and ilmenite is noted as ore mineral in 2 samples.

The diamonds characteristic. In accordance with separation of two groups associations with diamond it is reasonable to discuss crystal particularities in these two types. The diamonds being present in the form of intergrowths and inclusions in megacrysts are presented in most cases by single crystals mainly of octahedral habit, with size 1-3 mm [32]. Usually, those are octahedrons with polycentric rising facets that answer the I varieties of Yu. L. Orlov [20]. In one of the garnet megacrysts the diamonds forms intergrowth of crystals and in the other, like on

garnet composition, the diamond is present in the form of globous sulphur of the unit of the type board (variety III according [20]).

In xenoliths of diamondiferous eclogites the diamonds are presented by three main varieties [12, 24, and 32]. Diamonds of octahedron habit are installed in three samples with polycentric construction of the facets and belong to I variety [20]. The examples of diamonds in eclogites are given on Fig. 3.

Table 2.

Composition of minerals in association with diamonds from the Sytykanskaya pipe (after [32])

№	Sample	SiO_2	TiO_2	Al_2O_3	Cr_2O_3	FeO	MnO	MgO	CaO	Na_2O	Total
1	ТС-75	41,3	0,17	23,3	0,07	6,92	0,09	12,2	16,3	0	100,35
2	ТС-145	41,1	0,14	23,3	0,08	7,04	0,12	11,3	17,6	0,05	100,73
3	S-15	41,23	0,23	22,63	0,18	8,56	0,19	13,08	13,74	0	99,92
4	S-16	40,5	0,45	22,95	0,08	8,74	0,18	12,63	13,66	0,14	99,33
5	S-17	40,44	0,22	23,11	0,11	8,1	0,19	13,12	13,61	0,06	98,98
6	S-14	38,63	0,35	23,82	0,05	11,18	0,2	6,58	18,66	0,15	99,69
7	ТС-146	41,2	0,16	23,1	0,07	6,79	0,1	10,3	18,8	0,05	100,56
8	ТС-6а/2	41,2	0,2	23,1	0,08	6,74	0,12	11,3	17,6	0,03	100,4
9	ТС-16/2	40,9	0,27	22,8	0,06	11,8	0,23	11,6	12,9	0,06	100,62
10	ТС-16/1	40,9	0,14	23,2	0,03	7,05	0,12	10,9	18	0,03	100,37
11	ТС-145	40,9	0,13	22,1	0,06	5,34	0,53	12,1	18	0,08	99,24
12	ТС-146	40,9	0,12	23,4	0,08	5,76	0,75	11	18,3	0,07	100,38
13	102/14	42,2	0,16	17,9	8,33	6,54	0,27	22,5	2,53	0	100,43
14	ТС-56/2	40,5	0,12	15,11	10,8	7,78	0,44	19,2	5,21	0,02	99,18
15	ТС-2а/2	41,4	0,96	19,6	3,51	9,56	0,33	19,6	5,28	0,03	100,58
16	ТС-16/3	41,3	0,03	16,3	9,92	7,34	0,39	23,4	0,66	0,01	99,35
17	ТС-41	40,1	0,76	21,4	0,16	13,9	0,38	11,7	11	0,11	99,51
18	С-42/92	41,07	0,02	16,22	9,8	6,86	0,38	22,39	2,22	0	98,96
19	С-40/87	41,49	0,03	16,45	9,83	6,38	0,29	23,4	1,27	0	99,14
20	С-42/97	41,22	0	15,56	10,28	7,24	0,3	23,52	0,78	0	98,9
21	С-42/9	41,24	0,06	15,5	10,6	7,09	0,3	22,86	1,7	0	99,35
22	С-16а	41,89	0,03	15,47	10,65	7,97	0,35	22,28	1,96	0	100,6
23	С-21 б	41,61	0,05	15,28	10,83	6,68	0,34	22,62	2,04	0	99,45
24	С-42/91	41,65	0,07	15,27	10,8	7,39	0,31	22,12	2,26	0	99,87
25	С-42/8	41,29	0,01	15,4	11,04	6,5	0,29	23,71	0,99	0,02	99,25
26	С-56	40,62	0,15	14,57	11,31	7,42	0,42	19,56	5,19	0,2	99,44
27	С-32	41,61	0,03	14,87	11,44	6,49	0,32	23,2	1,86	0	99,82
28	С-1 б	41,08	0,08	14,79	11,62	6,73	0,34	21,86	2,52	0	99,02
29	64/1	41,91	0,03	14,87	11,04	6,37	0,31	23,27	1,37	0	98,45
30	69/4	41,09	0,9	16,58	6,1	6,83	0,27	21,09	6,57	0	98,43
31	110/6	41,66	0,47	18,3	6,17	6,46	0,26	21,71	3,43	0	98,46
32	С-15 а	42,12	0,02	17,62	8,12	7,42	0,27	23,5	1,31	0	100,38
33	С-12 б	41,31	0,08	16,82	8,6	7,23	0,36	21,02	3,92	0	99,34
34	С-21 а	41,93	0,01	17,01	8,7	6,91	0,32	23,12	1,42	0	99,42
38	S-14	55,3	0,524	8,98	0,08	4,29	0,03	9,77	14,7	5,92	99,76
39	S-15	54,15	0,16	8,83	0,18	1,97	0,05	11,03	17,83	3,42	98,16
40	ТС-145	56,2	0,45	9,02	0	5,83	0,04	10,1	12,6	6,91	101,26
41	ТС-145	55,01	0,61	5,85	0	1,72	0	14,33	21,7	0,75	100
42	ТС-146	54,46	0,34	5,42	0	1,78	0,08	15,06	22,35	0,43	100

Note: Analyses: 1-37 - garnets (1-12-from xenoliths, 13-17-from intergrowths, 18-37-from inclusions), 38-42-clinopyroxenes from xenoliths.

The diamonds of the transient form and laminar rhombic dodecahedrons are the most wide-spread in xenoliths of the eclogites from the Sytykanskaya pipe, as well as intergrowths of the lasts. Only in one xenolith of kyanitic eclogite are installed 2 crystals of the cubic form of the yellow color of IV variety [20]. To say the least, in three samples (S-14, 15, 17) is clearly tracked that diamonds are related to product of the partial melting developed between garnet and clinopyroxe grains that witnesses in favor of their more late metasomatic origin [36, 28, 38]. Not excluded similar genesis of crystals in sample TS-145 and -146, where detailed are characterized secondary phases of the products of the partial melting, presented new-forming clinopyroxene of phassaite composition, sanidine and spinel [15].

If consider the morphological particularities of diamonds from xenoliths and mineral-megacrysts as a whole, it is possible to note that on wide-spread and variety of the morphological forms they are close to diamond population from kimberlites of this pipe. Either as amongst diamond being present in kimberlites [40], amongst diamond from xenoliths and intergrowths with garnet and the other minerals, dominate transient, round or close to rhombic dodecahedrons crystals.

Chemistry of minerals associating with diamonds. The main mineral as in intergrowth with diamond, so and in eclogite xenoliths is a garnet. The garnets from imtergrowths with diamond (Table 2) are characterized comparatively broad variations composition as on correlation main oxides Mg, Fe, and Ca, and on contents Cr and Ti. The presence of garnet with high contents Cr_2O_3 (more than 8 wt.%) allows to select dunit-harzburgite paragenesis amongst megacrysts containing diamonds. In explored collection are present also garnets with comparatively moderate contents Cr_2O_3 (1.0-4.0 wt.%), which can be referred with lherzolite garnet. At the least, two samples of megacrysts in intergrowth with the diamond (see tabl. 2) differ the low contents (< 4 wt.%) Cr_2O_3 that allows considering them as garnets of pyroxenitic or eclogitic paragenesis.

The garnets from some intergrowth samples are characterized by high contents TiO_2 and, probably, can belong to the associations Ilm-Gt peridotites. The presence of given paragenesis is confirmed also by the presence amongst samples diamond in intergrowth with ilmenite.

The garnets of eclogitic type as from intergrowths with diamond, so and from xenoliths are characterized essential variations composition in respect of three main components Ca, Mg, and Fe (Table 2). Moreover it is necessary to emphasize that garnet with high contents Ca is fixed not only in kyanite eclogites, but also in intergrowth with diamond, where this mineral, as judged by given chemical analysis, contains 54% of grossular component and corresponds to the grospydite garnet type.

Primary clinopyroxene of the omphacitic composition that present only as a rare relicts, is fixed in 3 eclogite samples moreover in 2 cases he is installed in kyanite eclogites. On its composition mineral is a typical omphacite with high contents Na_2O (see table 2). Only in sample of bimineralic eclogite he is differ the

lowered content of sodium oxide and Al_2O_3. For omphacites is typical comparatively low contents (≈10 wt.%) oxides Mg and Ca, as well as small quantity of FeO (< 6 wt. %). In clinopyroxene one of the sample is installed raised content of titanium (0.45 wt.% TiO_2). For all omphacites is typical unessential admixture or absence (below limit of sensitivity) of chromium and manganese oxides.

We can not to discuss in detail the condition of the formation all xenoliths since relicts of primary clinopyroxenes are found only in three samples. Based on given experimental studies results of equilibrium of mantle mafic rocks minerals [7] the temperatures of their formation are valued in interval 1200-1300°C under fixed pressure of the order 30 кбар.

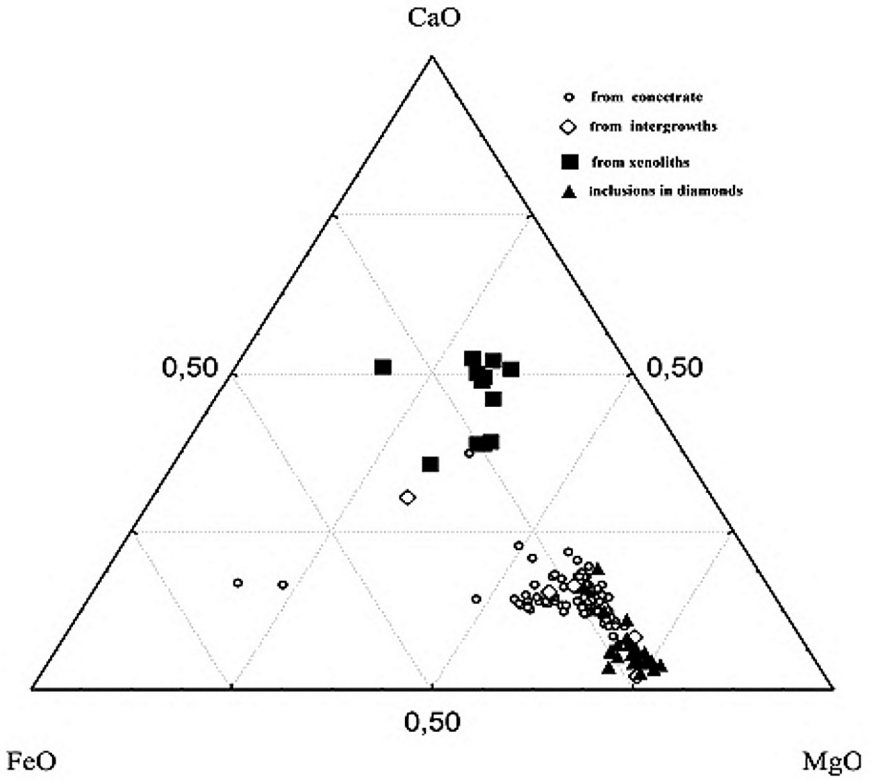

Fig. 4. **Plot of garnets associating with diamond in kimberlites of the pipe Sytykanskaya**.

(1) – garnet from the diamondiferous xenoliths, (2) – garnet from megacrysts in intergrowth with diamond, (3) - garnet from inclusions in diamonds.

In two samples of eclogites authors of the work [15] are analysed phases of the products of the partial melting, and amongst them clinopyroxene of fassaite composition, which are wrongly considered by them as possible primary phases. The analyses of these mineral are provided in [15] and, as it is shown in works [33, 36], low contents sodium in their composition and development them on primary omphacite, as well as the other particularities uniquely witnesses in favor of their more late formation in process of the partial melting and metasomatose. To

associations of the products of the partial melting belongs also noted in that sample sanidine, which analyses are given in [15]. As ore mineral in sample of disthen eclogite is installed ilmenite, which is once in a while noted amongst accessories in eclogites [33]. In this instance it, either as usually, is presented by high iron and nearly without Mg mineral that is close to titanomagnetite with the high admixture of pyrofanitic component [15].

The carry out studies have shown that associations with diamond in kimberlites of the Sytykanskaya pipe are presented by comparatively varied formations, which can be split into three main groups: diamondiferous xenoliths, monomineral megacrysts different on garnet composition in intergrowth with diamond and inclusions in diamonds (Fig. 4). To the second group are pertain also comparatively rare intergrowths of diamond with ilmenite and olivine. Such a set of the mantle formations associating with diamonds is usual for kimberlitic of the majority pipes of the Yakutian province. Does not differ on composition and garnet from inclusions in diamond from given pipe, in comparison with mineral of the inclusions from diamond other pipes, for instance Udachnaya as well as garnets from the diamondiferous xenoliths of Mir and Udachnaya pipes [23, 26. 27].

If judge about distribution of eclogitic and peridotitic paragenesis in diamond population of this pipe on the ground of available for us 30 mineral inclusions [32], peridotitic diamonds sharply dominate, since on chemistry all garnets belongs to the dunite-harzburgite paragenesis. If value on the ration of different paragenesis diamonds is done on the ground of the distribution of intergrowths of diamonds in mineral-megacrysts, in the first place on garnets, that picture is greatly changed. Alongside with presence diamond in intergrowth with garnet of lherzolite and, probably, pyroxenite composition, more than a half of all explored samples are presented by diamonds in intergrowth with the orange eclogitic garnet. Unusual and rare are discoveries of diamond in the form of intergrowth with ilmenite megacrysts. Raised distribution of ilmenitebearing diamond associations in given pipe is confirmed by the presence of high titanium low-Cr pyrope in intergrowth with diamond [32]. If we are going to discuss the particularities of diamondiferous xenoliths, shall in the first place note that amount of discovery these unique and rare xenoliths in given pipe is 11 samples and four of them are kyanite eclogites. On its petrographic particularity and the other features, they are similar with the kyanite eclogites from the Udachnaya pipe, which are characterized in detail [23, 29]. The bimineral eclogites of the Udachnaya and Sytykanskaya pipes are close also; those correspond to the magnesian variety on garnet composition and the other features.

Resuming results on this paragraph, possible to emphasize that the study of associations with diamond in kimberlites of the Sytykanskaya pipe allows selecting amongst them three types that are usual for other pipes of the Yakutian province: inclusions in diamonds, mineral-megacrysts in intergrowth with diamond and diamondiferous xenoliths. Inclusions in diamond are presented in the first place by garnet; moreover on result of the study of their composition amongst them sharply

dominate dunite-harzburgite paragenesis. The particularity of diamond, residing in the form of intergrowth in megacrysts, is more high distribution of eclogitic paragenesis and ilmenite that is fixed by host-minerals, as evidenced as well by the presence of high-Ti pyropes, associating with diamond.

CONCLUSION

The raised portion of diamonds, formed in eclogitic ambience, is emphasized comparatively broad distribution amongst mantle xenoliths of Nyurbinskaya and Sytykanskaya pipes of diamondiferous eclogites, which particularity is the presence amongst them of highly aluminous varieties of kyanite eclogites and grospidites. It should be pointed out as it is obviously from brought data that estimated paragenesis of diamond populations from any kimberlite pipe on base of inclusions in diamonds does not fully correlate with diamond association of as mantle xenoliths and megacrysts either as with composition of indicator kimberlite minerals. This in turn, points to possibility that it could be enough principle difference in distribution and ratio of mantle xenoliths of given composition, indicator mineral and source ambience forming diamond populations in separate pipes.

Another remark concern that according results of diamondiferous xenoliths investigations in eclogites of both pipes are fixed the features of intensive partial melting and metasomatose that altogether with peculiarities of diamonds allowed to conclude about the possibility of diamond growths under influence of metasomatic fluids and connected partial melting as was demonstrate for some xenoliths from the Udachnaya pipe [36].

REFERENCE

1. **Agashev A.M., Pokhilenko N.P., Tolstov A.V., Polyanichko V.V., Mal'kovets V.G., Sobolev N.V.** New Age Data on Kimberlites from the Yakutian Diamondiferous Province // Dokl. RAN, 2004, V. 399, p. 1142-1145 (in Russian).
2. Bobrievich A.P., Bondarenko M.N., Gnevushev M.A, Krasov A.M., Smirnov G.I., Yurkevich R.K. The diamond deposits of Yakutia. Moscow: Gosgeoltekhizdat, 1959, 527 p (in Russian).
3. **Bogatikov O.A., Garanin V.K., Kononova V.A., Kudryavzeva G.P. et al.**. Arkhangelskaya diamondiferous province (geology, petrography, geochemistry and mineralogy). MGU, 2000, 522 p.
4. **Cherny S.D., Fomin A.S., Yanygin Ju.T., Banzeruk V.I., Kornilova V.P.** Geology and composition of the Nakyn field kimberlite pipes and diamond properties (Yakutia) // Ext. Abstracts. Cape Town, 1998, p. 147-148.
5. **Dawson J.B.** Kimberlites and their xenoliths. Berlin: Springer-Verlag, 1980, 252 p.
6. **Dawson J.B., Stephens W.E.** Statistical classification of garnets from kimberlite and associated xenoliths // J. Geol., 1975, v. 83, p. 589-607.
7. **Ellis D.I., Green D.N.** An experimental study of the effect of Ca upon garnet - clinopyroxene Fe-Mg exchange equilibria // Contrib. Miner. and Petrol., 1979, v. 71, p. 13-22.

8. Garanin V.K., Kudryavzeva G.P., Marfunin A.S., Mixaylichenko O.A. 1991. Inclusions in diamond and diamondiferous rocks. M., MGU, 240 p. (in Russian).
9. **Griffin W.L, Spetsius Z.V., Pearson N.J., O'Reilly S.Y.** In-situ Re-Os analysis of sulfide inclusions in kimberlitic olivine: new constraints on depletion events in the Siberian lithospheric mantle // Geochemistry, Geophysics, Geosystems, 2002, v. 1, № 11. GC000287.
10. **Gurney J.J.** Diamonds // In: Ross J. et al. (eds) Diamonds, Kimberlites and Related Rocks, Geol. Soc. Aust. Spec. Publ., 14, Blackwell Scientific Publications, Melbourne, 1989, v. 2, p. 935-965.
11. **Ireland T.R., Rudnick R.L, Spetsius Z.V.** Trace elements in diamond inclusions from eclogites reveal link to Archean granites // Earth and Planetary Science Letters, 1994, v. 128, p. 199-213.
12. **Koptil V.I., Lazko E.E., Serenco V.P.** Diamondiferous disthen eclogites from the kimberlite pipe Sytykanskaya – the first find in SSSR // Dokl. AN SSSR, 1975,v. 225, № 4, p. 924–927 (in Russian).
13. **Kornilova V.P., Fomin A.S., Zaitsev A.I.** New type of diamondiferous kimberlite rocks on the Siberian platform // Regional Geology and Metallogeny, 2001, v. 13, p. 105-117 (in Russian).
14. **Kostrovitsky S.I., Alymova N.V., Yakovlev D.A., Serov I.V., Ivanov A.S., Serov V.P.** Peculuarities of ilmenite typochymism from diamondiferous fields of Yakutian province // Dokl. RAN, 2006, v. 406, № 3 (in Russian).
15. **Lazko E.E., Serenco V.P., Koptil V.I., Rudnizkaya E.S., Zepin V.I.** Disthen diamondiferous eclogites from the kimberlite pipe Sytykanskaya (Yakutia) // Izvestiya AN SSSR, 1982, Ser. geol., № 7, p. 55-69 (in Russian).
16. **Mityukhin S.I., Spetsius Z.V.** Paragenesis of inclusions in diamonds from the Botuobinckaya pipe (Nakyn field, Yakutia) // Russian Geology and Geophysics, 2005, v. 46, p.1246-1258.
17. **Navon O.** Diamond formation in the Earth's mantle // The 7th IKC proceeding 2, 1999, p. 584-605.
18. **Neal C.R., Taylor L.A., Davidson J.P., Holden P., Halliday A.N., Paces J.B., Clayton R.N., Mayeda T.K.** Eclogites with oceanic crustal and mantle signatures from the Bellsbank kimberlite, South Africa, Part 2: Sr, Nd, and O isotope chemistry // Earth Planet. Sci. Lett., 1990, v. 99, p. 362-379.
19. **Nowell G.M., Pearson D.G., Bell D.R., Dowall D.P., Carlson R.W., Kempton P.D., Noble S.R., Smith C.B., Zartman R.E.** Hf isotopic systematics of kimberlites and their megacrysts: New constraints on kimberlite source regions and implications for mantle evolution // Journal of Petrology, 2004, v. 45, p. 1583-1612.
20. **Orlov Yu.L.** The Mineralogy of Diamond. John Wiley and Sons, New York, 1977, 235 p.
21. **Pearson D.G., Shirey S.B., Carlson R.W., Boyd F.R., Pokhilenko N.P., Shimizu N.** Re-Os, Sm-Nd and Rb-Sr isotope evidence for think Archaean lithospheric mantle beneath the Siberia craton modified by multistage metasomatism. Geochim. Cosmochim. Acta, 1995, v. 59, p. 959-977.
22. **Pearson D.G., Shirey S.B., Bulanova G.P., Carlson R.W., Milledge H.J.** Re-Os isotopic measurements of single sulfide inclusions in a Siberian diamond and its nitrogen aggregation systematics // Geochim. Cosmochim. Acta 1999, v. 63, p. 703-711.
23. **Ponomarenko A.I., Sobolev N.V., Pokhilenko N.P.** Diamondiferous grospydite and diamondiferous disthen eclogites from kimberlite pipe Udachnaya, Yakutia // Dokl. AN SSSR, 1976, v. 226, p. 927-930 (in Russian).
24. **Ponomarenko A.I., Spetsius Z.V.** Diamondiferous eclogites from the kimberlite pipe Sytykanskaya // Geology and Geophysics, 1976, № 6, p. 103–106 (in Russian).

25. **Shirey S.B., Harris J.W., Richardson S.H., Fouch M., James D.E., Cartigny P., Deines P., Viljoen F.** Regional patterns in the paragenesis and age of inclusions in diamond, diamond composition, and the lithospheric seismic structure of Southern Africa // Lithos, 2003, v. 71, p. 243–258.
26. **Snyder G.A., Taylor L.A., Crozaz G., Halliday A.N., Beard B.L., Sobolev V.N., Sobolev N.V.** The diamond-bearing Mir eclogites, Yakutia: Nd and Sr isotopic evidence for the continental crustal imput in an Archean oceanic environment // Ext. Abstracts of 7th Intern. Kimb. Conf., Cape Town, South Africa, 1998, p. 826-828.
27. **Sobolev N.V.** Deep-seated inclusions in kimberlites and the problem of the composition of the upper mantle. American Geophys. Union, Washington, DC, 1977, 279 p.
28. **Spetsius Z.V.** Metasomatism and partial melting in xenoliths from the kimberlites of Yakutia: implication to the origin of diamonds // Proceedings of Intern. Workshop: Deep-seated magmatism, its sources and their relation to plume processes, Irkutsk - Ulan-Ude, p. 128-159.
29. **Spetsius Z.V.** Petrology of highly aluminous xenoliths from kimberlites of Yakutia // Lithos, 2004, v. 77, p. 525–538.
30. **Spetsius Z.V., Belousova E.A., Griffin W.L., O 'Reilly S.Y., Pearson N.J.** Archean sulfide inclusions in Paleozoic zircon megacrysts from the Mir kimberlite, Yakutia: implications for the dating of diamonds // Earth Planet. Sci. Lett., 2002, v. 199, p. 111-126.
31. **Spetsius Z.V., Ivanov A.S., Mityukhin S.I.** Xenoliths and megacrysts with diamonds from the Nyurbinskaya pipe (Nakyn field, Yakutia) // Dokl. RAN, 2006, v. 408, № 6, p. 810-814 (in Russian).
32. **Spetsius Z.V., Koptil V.I.** Associations with the diamond from the kimberlite pipe Sytykanskaya, Yakutia // Geologiya I Razvedka, 2007, in press (in Russian).
33. **Spetsius Z.V., Serenko V.P.** Composition of continental upper mantle and lower crust beneath the Siberian platform. Moscow: Nauka, 1990, 272 p (in Russian).
34. **Spetsius Z.V., Serenko V.P.** Lithosphere of the Middle-Marxinsky kimberlite field // In: Geology and Tectonics of Platforms and Orogenic Regions in Northeastern Asia. Siberian Brunch RAS, Yakutsk, 1999, v. 2, p. 104—108 (in Russian).
35. **Spetsius Z.V., Spetsius V.Z.** Exsolution textures and minerals inhomogeneity in xenoliths from Yakutian kimberlites: evidence for the mantle evolution // Proceedings of Intern. Workshop: Plumes and problems of sources of deep magmatism and plumes. Petropavlovsk-Kamchatsky, 2005, p. 148-169.
36. **Spetsius Z.V., Taylor L.A.** Partial Melting in Mantle Eclogite Xenoliths: Connection with Diamond Paragenesis // In'l. Geology Review, 2002, v. 44, p. 973-987.
37. **Spetsius Z.V., Taylor L.A.** Metasomatic diamonds in eclogite xenoliths: petrologic and photographic evidence // Ext. Abstracts of 8th Intern. Kimberlite Conf., Victoria, Canada, 2003.
38. **Spetsius Z.V., Taylor L.A., Valley J.V, Ivanov A.S., Banzeruk V.I., Spicuzza M.** Garnets of anomalous oxygen isotope compositions in diamondiferous xenoliths (Nyurbinskaya pipe, Yakutia) // Proceedings of 6th Intern. Workshop: Deep-seated magmatism, its sources and plumes. Mirny-Irkutsk, 2006, p. 59-79.
39. **Taylor L.A., Milledge H.J., Bulanova G.P., Snyder G.A., Keller R.A.**. Metasomatic eclogitic diamond growth: evidence from multiple diamond inclusions // Int. Geol. Rev., 1998, v. 40, p. 663-676.
40. **Zinchuk N.N., Koptil V.I.** Typomorphizm of diamonds of the Siberian Platform. M.: Nedra, 2003, 603 p. (in Russian).

UDK 550.42

CO_2 magmatism in Italy: from deep carbon to carbonatite volcanism

Stoppa F.

Dipartimento di Scienze della Terra- Università G.d'Annunzio, Chieti, fstoppa@unich.it

ABSTRACT

The importance of CO_2 in the Italian mantle and magmatism is supported by the presence of Middle-Upper Pleistocene carbonatites along the Italian Apennine graben-systems. Carbonatites are co-eruptive and chemically conjugate to kamafugites (kalsilite melilitite or foidite). Immiscibility phenomena largely explain the genetic relationship between the two rock-types. Their peculiar geochemistry reflects the differing solubility of the high field strength elements in rocks which have different peralkalinities. Dolomite and calcite dominated inclusions occur in mantle nodules and plutonic rocks such as soviets and melilitolites, which have been brought up by extrusive carbonatites. Nyerereite was found in melilite and apatite inclusions although the Italian extrusive carbonatites are always calcitic. Sequestration by abundant leucite, kalsilite, haüyne and nepheline, and dispersion of alkalis in subvolcanic aqueous fluids, may explain the low alkaline character of Italian carbonatites.

The high Ca, CO_2, F, S, Cl content of primitive melt inclusions in high pressure crystals suggests that these elements were not assimilated by the magma from the crust during its ascension towards the surface. In addition, the high radiogenic isotopic composition and compatible element content are regarded as primary magmatic characteristics. Veined mantle nodules show pervasive reaction with carbonatitic melts as illustrated by the presence of amphibole, fassaitic cpx and phlogopite phases. Metasomatising carbonatitic melts are thought to be released from a deep plume. The geodynamic and geochemical setting of Italian carbonatites implies a very deep source for heavy Carbon and it has even been speculated that this Carbon could be originated from the Earth's core.

Keywords: Italy, Pleistocene, carbonatites, kamafugites, mantle metasomatism.

INTRODUCTION

Carbonate inclusions in mantle nodules, large volumes of mantle CO_2 discharges at the surface, and the eruption of carbonatites are a large scale geological window on deep geodynamic processes which are active underneath the central southern Italian peninsula. This area has a complex mixture of peculiar geological features among which is an outstanding magmatic association of leucitites, melilitites, kamafugites and carbonatites (Tab. 1 and Fig. 1). Carbonatites occur in Middle-Late Pleistocene continental grabens in an approximately 100 km wide belt and have been discontinuously traced for 450 km along the Apennines of Italy, called the IUP (Intra-Appenine Ultra-Alkaline Province [19, 20, 45].

Italian carbonatites are mostly extrusive and add significantly to the number of worldwide occurrences. Both their importance and the way they differ from intrusive carbonatites have been recently stressed [58]. Carbonatite volcanism in Italy and its intriguing association with kamafugites, became internationally known after that Polino (Umbria) carbonatite was described [48]. Other carbonatites were found in the following 4 years at Cupaello (Latium), San Venanzo (Umbria) and at Vulture [39, 42, 50, 54]. More recently, the geographical gap between the northern outcrops and the Vulture area has been partially filled by the discovery of the Grotta del Cervo and Oricola (Abruzzo) carbonatite occurrences [52, 55]. Other carbonatitic rocks occur in Italy [57] but are much older and not related to the Pleistocene examples and so will not considered here.

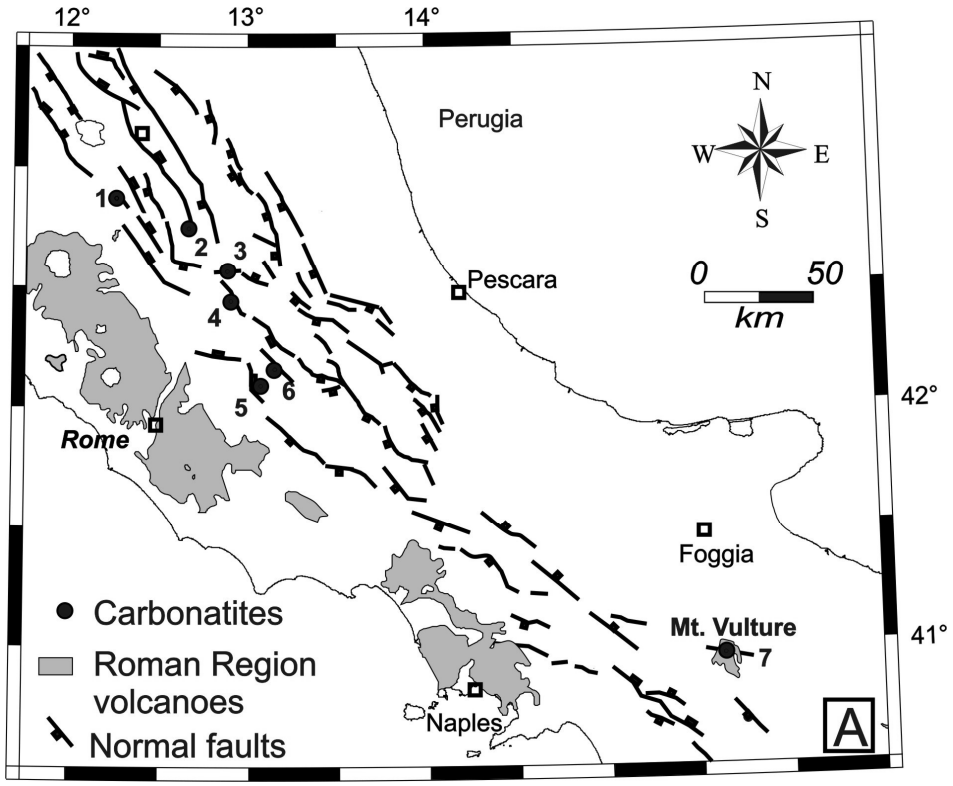

Fig. 1. **Geological map and tectonic sketch map of table 1 rocks, mofetes and active volcanoes.**

Much data have been published on the volcanology, mineralogy, petrology, geochemistry and the tectonic setting of the carbonatite-kamafugite association. D.K. Bailey, K. Bell and A.R. Woolley were all involved in the research from the beginning and contributed greatly to the study of the Italian carbonatite. Other outstanding contributions came from A. Cundari, concerning the relationship with leucite-bearing rocks, and from F. Lloyd for studies relating to tufissitisation and diatreme formation. Russian scientists also provided expert contribution relating to mafic/ultramafic alkaline rocks associated with Italian carbonatites, notably their mineralogy, inclusion studies and petrogenesis of these complex rocks [25, 37, 38].

Apatite was studied in detail in collaboration with Liu Y. of Fuzhou University, China. Several field trips at IUP volcanoes and conferences, notably EUROCARB 2002, during the last 15 years have revealed these fascinating rocks to hundreds of international geologists. However, the importance of Italian carbonatites may be still underestimated as they are not easily accommodated in the long established

Table 1.

Italian extrusive carbonatites and conjugate rocks considered in this work.

Location	*Age ka*	*Occurrence*	*Lithology*	*Conjugate rocks*	*Mineralogy (alphabetical)*	*Mantle debris*
San Venanzo	~265	Maar, tuff ring, agglomerate, airfall	Ca-carbonatite	Kamafugitic ol melilitite	Ankerite, calcite, perovskite, Si-CO-OH-apatite, Ti-magnetite,	Micronodules (scarce): forsterite, Cr-diopside, chromite
Polino	~265	diatreme, tuffisite,	Ca-carbonatite	none	Cr-phlogopite, Fe-monticellite, forsterite, Sr-Ba-calcite, Ti-magnetite, Th-perovskite, Zr-schorlomite	<2 cm nodules (abundant): dunite, glimmerite
Cupaello	~491	Lapilli ash tuff and agglomerate	Ca-carbonatite	kalsilitite	apatite, calcite, perovskite, Zr-schorlomite, Kybinskyte, Kymzeinite	Xenocrysts (abundant): Cr-phlogopite, Cr-clinopyroxene
Grotta del Cervo	<300	vent not localised, lapilli ash tuffs	Carbonatitic kamafugite	Kamafugitic foidite	Calcite, diopside, haüyne, kalsilite, leucite, melanite, phlogopite, Sr-REE-rich apatite, Ti-magnetite,	Micronodules (frequent): clinopyroxenite
Oricola	~531	tuff rings and lapilli ash tuffs	Ca-carbonatite	Kamafugitic foidite	Mn- Calcite, Si-Sr-S-rich fluorapatite, Ba-Sr-rich sanidine, Melanite, Cpx, Ba-rich phlogopite, Ti-magnetite	Xenocrysts (rare): forsterite, chromite
Vulture	~132	maars and lapilli tuffs	Ca-carbonatite	Ol melilitite/foidite	apatite, calcite, clinopyroxene, Nb-Ba-perovskite neyrereite, Ti-magnetite	Large nodules (abundant): lherzolite, wherlite, amph-peridotite,

subduction models adopted for Italy. Carbonatites have not been found in any subduction environment either oceanic or continental [58]. This is too much of a coincidence to be ignored. The assumption, made by some, that Italian carbonatites occur purely in a subduction environment is axiomatic as there is no geophysical evidence for a slab beneath IUP [10]. Theories concerning the generation of carbonatite in a subduction environment would need a more robust cause-effect demonstration. Therefore, it is felt that Italian carbonatites need to be interpreted in a larger geological context which can include the recent discovery of large extrusive carbonatites in Spain and France [1] which are remote from subduction in time and space.

CARBONATE MANTLE NODULES, METASOMATISM AND MINERAL INCLUSIONS

Spinel lherzolite, wherlite and phlogopitite nodules described in a number of IUP outcrops [16, 31, 48, 54] are re-equilibrated to lithospheric mantle pressures but contain rare relicts of Cr-Mg garnet, indicating a deeper origins. Detailed analyses on 300 xenoliths from Mt. Vulture have confirmed that 20% contain carbonate [31]. Mantle debris from Polino, San Venanzo and Vulture contains a large number of carbonate melt inclusions [25, 38, 48]. Mantle nodules host calcite globules often linked by menisci-necks and are composed of a mosaic of 2-20 μm crystals, with varying optical orientation. Some of these globules contain liquid/gaseous CO_2 bubbles and are pierced by quenched microphenocrysts of silicate phases. The carbonate composition varies from calcite to Mg-calcite (3.8-5.0 wt% MgO) both within the carbonate globules and from globule to globule. The Sr-Nd isotope ratios of the carbonate in the xenoliths are similar to the extrusive carbonatite and silicate rocks of Mt. Vulture supporting derivation from the same mantle source [5, 6]. These features are consistent with formation from a quenched calciocarbonatite melt suggesting that the enrichment of the lithospheric mantle in incompatible trace elements and LREE may be caused by the infiltration of such a melt. Reaction between carbonatite melt and peridotite have been studied in detail in the Vulture nodules and it has been suggested that this could be produced by a percolating alkaline-carbonatite metasomatising a previous pyrope harzburgite mantle [31]. Formation of the immiscible silicate-carbonatite liquids within mantle xenoliths occurred via disequilibrium immiscibility during their exhumation.

VOLCANIC CO_2 AND MOFETES

Central-southern Italy and Etna emit $2.5\text{-}5 \times 10^{11}$ mol. a^{-1} of deep CO_2 contributing to a worldwide total of $1.5\text{-}8.3 \times 10^{12}$ mol a^{-1}. The IUP area has an average deep CO_2 discharge of 3-10 x 10^6 mol. a^{-1} km^{-2}, with Vulture volcano alone producing 3.7 x 10^6 mol a^{-1} km^{-2} of CO_2, and is one of the biggest producers of continuous deep-seated CO_2 degassing in the world [12]. Others impressive occurrences known as mofetes or mefites, emit CO_2 in amounts only slightly less than volcanoes. The mefite d'Ansanto is located 30 km W-SW of Vulture in a non volcanic area and emits ~300,000 ton/year of CO_2 [29]. Several casualties have occurred in Italy due to rapid CO_2 discharge or accumulation in both volcanic and non volcanic areas. Most of the Italian CO_2 has a $\delta^{13}C_{Ctot}$ between 2 and -2‰ vs PDB indicating a mantle/magmatic contribution. Unaltered Italian carbonatites has $\delta^{13}C_{(‰)PDB}$ between -8 and -4 [30, 32]. This is also confirmed by He isotopes that displays varying R/Ra values but can be up to a maximum 7.33, nearly a plume-type values [29]. Due to a complex water-rock interaction most of the CO_2 released from the Italian mantle is sequestered in non magmatic systems and confined to ground waters and in travertine, a rock of frequent geological occurrence in Italy.

In the last 2 m.y., the IUP lithosphere has experienced a rapid thinning, decreasing from a thickness of >100 km to <60 km. However, thermal flow is low indicating adiabatic mantle cooling. Rapid adiabatic mantle decompression is more suggestive of volatile expansion as opposed to a high degree of partial melting. This also fits well with the presence of such a great CO_2 flux and the carbonatitic/ultrapotassic magmatism.

MAARS, DIATREMES AND TUFFISITES

There is abundant physical evidence of CO_2 eruptions produced by rapid localised transfer of CO_2 to the surface. Intense CO_2 flowing in a conduit (diatreme) leaves a distinctive tuff produced by fluidisation of carbonatitic (and/or silicate) melt, ultramafic rocks and other solid debris. The highly explosive release at the surface of such an amalgam produces a distinctive volcanic morphology, the maar. A maar is a crater deeply excavated in the substratum, surrounded by a thin apron of lapilli ash tuff. The lapilli are peculiar often displaying spin, layered or cored internal structures made of concentric melilitite and carbonatite [47]. Most of the tuff-ring strata are outward dipping around the vent and are inclined between 10-15°. This is typical for air-fall deposits whose resting angle have been modified by surges. The surge deposits can have impressive dune-layers and in some cases there is a laterally continuous, layered blanket of welded agglutinated lapilli ash tuff (San Venanzo in Umbria, Oricola in Abruzzo, Vallone Toppo del Lupo and Lago Piccolo at Vulture). This distinctive “flaggy” tuff mantles the previous morphology and lies unconformably either on the previous tuffs or substratum and may even mantle the inside of previous craters. High-angle layers show reomorphic structures such as plastic folds and slickensides. Such features were also observed in the large carbonatitic field of Fort Portal, Uganda [2]. They are related to high temperature deposition in a near plastic state which also explains the agglutination, compaction and welding of lapilli, which previously led some to confuse pyroclastic layers with lava flows [49]. However, most of the Italian carbonatites have typical pyroclastic features such as large concentric and/or nucleated lapilli, interlapilli empty spaces, layering and gradations and cross lamination (Plate 1).

DIAMONDS

No discrete large sized diamonds have yet been found in Italian ultramafic rocks. However, the occurrence of lamproites, melilitites and carbonatites containing chromite, pyrope and Cr-diopside are suggestive of their possible presence. Nanodiamonds are reported at Etna and, also possibly, in Iblei, Sicily. Carbonatites are a interesting new source for diamonds and the mystery of the origin of some large diamond placers could be due to weathering and dissolution of extrusive carbonatites.

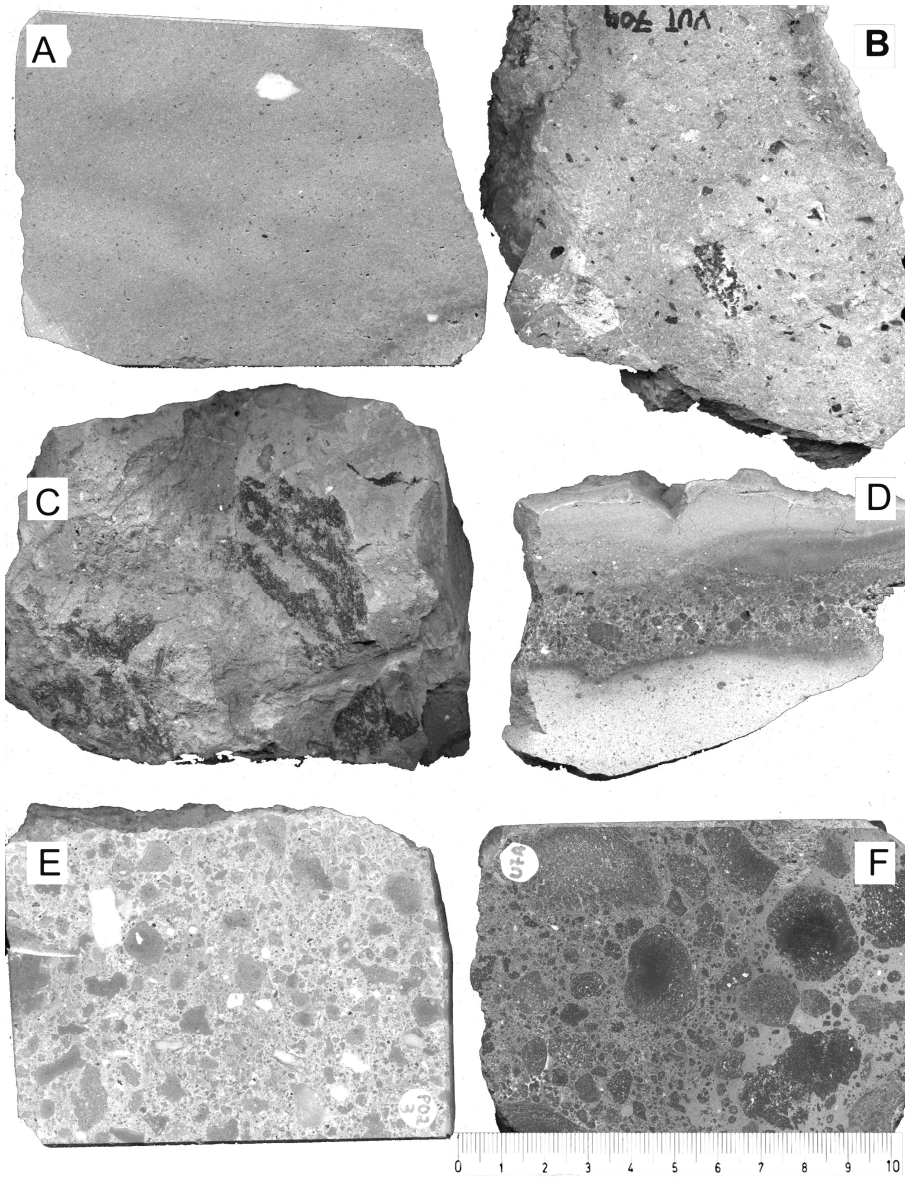

Plate 1. **Polished hand-scale samples.**

A= Polino carbonatite massive block in the tuffisite; B=Vulture carbonatite from Vallone Toppo del Lupo, lapilli ash tuff with mafic xenocrysts and ijolite lithics; C= Oricola carbonatite lapilli ash tuff; D= Cupaello carbonatite ash tuff with kalsilitite lapilli; E= Polino tuffisite, carbonatite lapilli and lithics in carbonatite matrix; F= San Venanzo carbonatitic tuffisite, olivine melilitite in carbonatite ash matrix.

CARBONATITES

These are calcite-carbonatites carrying abundant silicate ultramafic debris. The compatible element content of the carbonatites is a function of the amount of chromite, Ni-forsterite, Cr-phlogopite, Cr-diopside and Cr-amphibole which reflects the main mantle mineral phases of the IUP carbonatite source. Primary calcite has a variable composition in both inter- and intra-outcrops, but it generally contains high amounts of Mn, Sr, Ba, LREE of up to two orders of magnitude with respect to bulk rock and silicate fraction (Tab. 3, Fig. 2). This is due to the presence of cements which are virtually pure calcite in the bulk carbonatite rock.

Calcite from different carbonatites has distinctive chemical composition which allow for a definite association with individual outcrops. Nyerereite and dolomite are rarely reported and when found are only preserved in mineral inclusions [30, 34]. Sr-Ba carbonates are frequent and generally considered to not have a primary

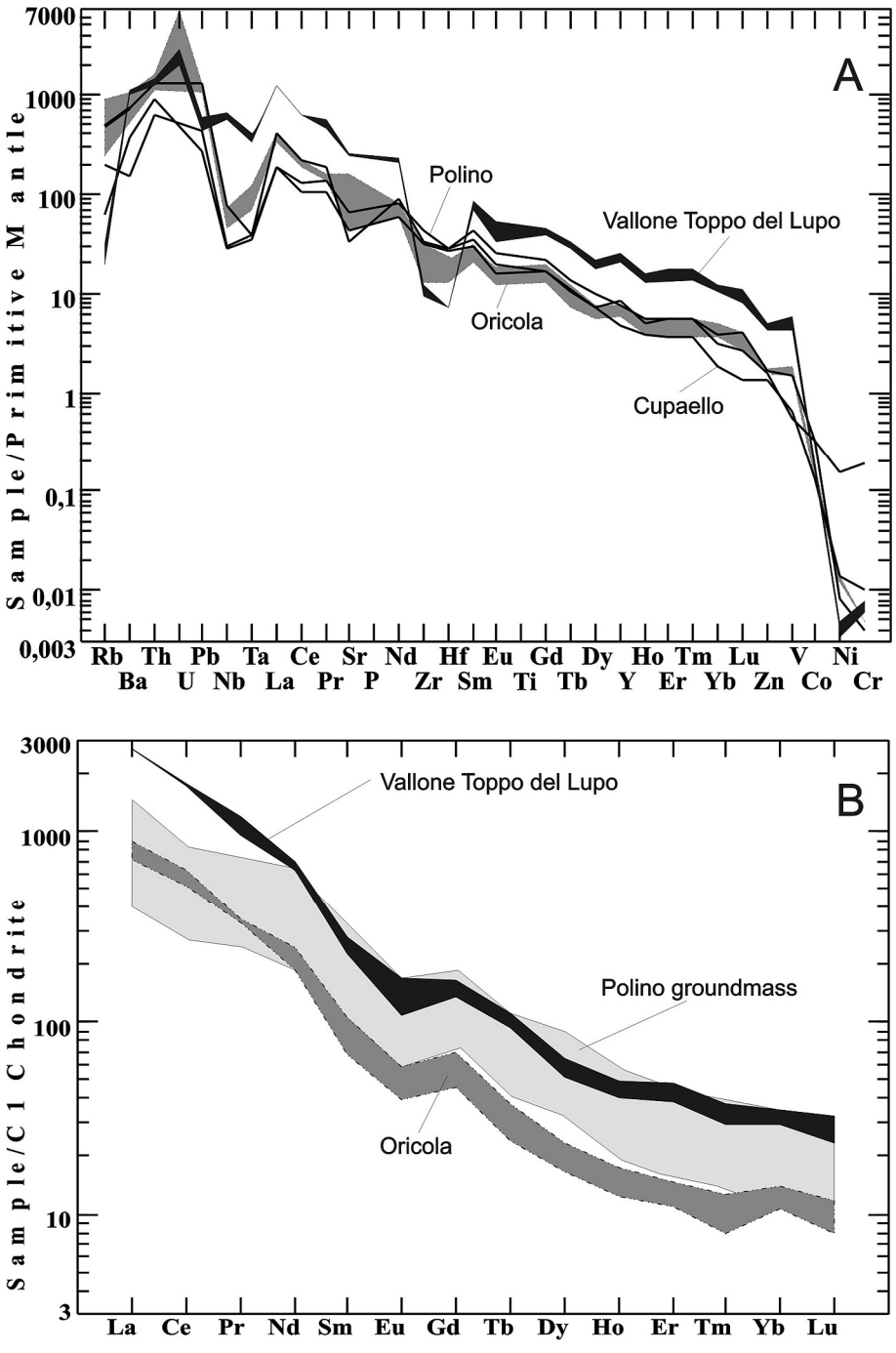

Fig. 2. **A=Mantle normalised LILE, HFSE and compatible elements; B= C1-chondrite normalised REE**

origin but have exolved from a primary Sr-Ba-rich calcite during its alteration to secondary, almost pure calcite. Olivine and its reaction product, Fe-monticellite, are frequent hitherto demonstrating recombination of carbonatite melt to form Ca-

silicates. Some other recombination products found are ghelenite, wollastonite and rankinite. Silicate ground mass minerals in Italian extrusive carbonaties have a very specific composition and often work as $HFSE^{3+4+}$ (Ti and Zr group) scavengers, for example Zr-schorlomite [21]. Non-silicates, perovskite and apatite concentrate LILE and $HFSE^{2+3+}$ and may be competitors of calcite [46]. Most of the other minerals, which can be present in substancial amounts, are likely to be xenocrysts incorporated mechanically from co-eruptive silicate rocks during volcanic activity or during the period of melt immiscibility.

Table 2.

Representative analyses of IUP carbonatites (lab. SGS Canada Inc, Toronto, XRF, NA, ICP-MS).

Locality	Polino	Cupaello	Oricola	Vulture*	Locality	Polino	Cupaello	Oricola	Vulture*
SiO_2	16	18.1	24.7	16.8	Ce	232	166	316	1095
TiO_2	0.51	0.37	0.38	0.54	Sr	1824	1295	2395	6955
Al_2O_3	3.9	2.51	10.45	5.81	Pr	28.2	21.1	30.7	104
Fe_2O_3	3.65	2.25	4.91	6.28	Nd	113	71.5	88.4	310
FeO	1.31	0.12	1.3	1.3	Sm	22.2	12.3	10.4	40.1
MnO	0.07	0.04	1.19	0.48	Zr	345	201	104	96.8
MgO	7.31	7.83	1.12	1.52	Hf	8	7.95	6	2
CaO	38.3	34.3	27.5	36.6	Eu	4.7	2.305	2.7	9.11
Na_2O	0.05	0.03	1.47	0.42	Gd	15.8	12.2	9.5	31.5
K_2O	0.49	1.01	4.18	0.29	Tb	1.7	0.9	1.1	3.9
P_2O_5	0.59	0.82	0.28	2.3	Dy	7.5	5.6	5	15.2
CO_2	24	25.6	19.6	19.55	Y	38	14	20	82.7
LOI	2.93	6.59	-	5.25	Ho	1	0.7	0.7	2.6
Total	99.1	99.6	97.1	97.2	Er	2.6	1.7	1.9	7.2
Rb	26	81.5	186	18.7	Tm	0.3	0.2	0.2	0.9
Pb	31	50	129	65.5	Yb	1.5	0.79	1.9	5.7
U	9	5.3	76.5	51.9	Lu	0.2	0.09	0.3	0.7
Th	59	41	72.8	86.7	Ni	308	29	27	4.4
Ba	3181	789	2945	6050	Cr	501	33.5	16	22
Nb	20	17	25	349	Sr/Sr	0.71041	0.71007	0.7109	0.70615
Ta	0.9	0.9	0.9	9.4					0.70598
La	111	88.9	170	637	Nd/Nd	0.51207	0.51188	0.51207	0.51258
									0.51265

Note: Data from [54] and * unpublished analysis (2007).

The chemical composition of Italian carbonatites is given in Tab. 2. Major oxides show high silica (16-24wt%) which is largely due to xenocrystic content. High MgOwt% is generally associated to forsterite and/or diopside containg often chromite inclusions. Mantle-normalized bulk rock geochemistry shows negative spikes of HFSE (e.g. Nb-Ta an Zr-Hf) and high LREE/HREE fractionation (Fig. 2 A and B). Negative spikes of Nb-Ta and Zr-Hf are very typical of worldwide carbonatites, both intrusive and extrusive [58] and cannot be considered a hallmark

of subduction [7, 43]. More evolved carbonatites with lower Mg# ($Mg/Mg+Fe^{2+}$ at.), lower compatible element contents and few mantle debris (e.g Vallone Toppo del Lupo and Oricola), have higher LREE/HREE and greater $HFSE^{4+}/HFSE^{3+}$ fractionation (i.e. Nb-Ta/Zr+Hf). HFSEs having larger ionic radius are lesser fractionated but U and Th values are particularly high at Oricola and Vallone Toppo del Lupo. These features suggest that some carbonatites are more differentiated than others and concentrate light HFSE and LILE in the final stages of melt evolution. Some other minor differences observed among HFSE ratios may be the result of the slightly different solubilities of HFSE in the parental magma [9], which is most likely to be a carbonatitic foiditic/melilititic melt [25, 38]. In fact, Italian carbonatites are chemically conjugated and are often co-eruptive with kamafugitic melilitites and foides.

Intrusive carbonatite examples are limited to sövite and alvikite ejecta [30, 51]. These rocks have a different composition in comparison with extrusive carbonatites as they contain substancial amounts of K-feldspar and sphene. Rare olivine, cpx and Ti-garnet form the cafemic fraction. This is probably a result of differentiation that occurred with slower cooling.

UMBRIA CARBONATITES

Umbrian carbonatites were initially identified by F. Stoppa at the end of the 1980^{s}. They are in newly discovered outcrops sometimes or associated with well known occurrences of kamafugitic rocks (kalsilite-bearing melilitites or foidites).

The Polino carbonatite occurs in a diatreme as a typical, shallow level tuffisite breccia exhibiting both crater facies and massive facies (Plate 1). Its high content of xenocrystics forsterite and Cr-phlogopite explain the relatively high silica content, as well as very high content of compatible elements (Ni+Cr>1000 ppm), which is similar to that of kimberlite; however, the minerals in the groundmass are typical of carbonatites: Sr-Ba-calcite, Th-perovskite, Zr-shorlomite, Ti-magnetite, Si-CO-OH apatite [21, 46, 48]. There are no directly associated silicate rocks, but chemical composition, age and tectonic setting suggest a conjugate nature with the San Venanzo kamafugites [43].

San Venanzo comprises a large maar, a tuff ring and a small diatreme-tuff cone. The volcano is composed of 80% vol. of kamafugite and phonolitic foidite including two lava flows of olivine leucite kalsilite melilitite (local name: venanzite). The remaining 20% is carbonatitic and carbonatite tuffs form indurated beds of agglutinate lapilli and a mixed carbonatite-melilitite breccia of thin ash fall layers (Plate 1). The mineralogy and geochemistry of the San Venanzo carbonatites have been somewhat neglected; it is complicated by the comminution of kamafugite and carbonatite component of the eruptive melt, a mechanical processes due to the movement of the grains, drops and bubbles into a range of ash particle sizes which in turn is influenced by explosive activity. Other causes are

agglomeration, immiscibility and mingling of the carbonatite and melilitite liquids as well as alteration of primary carbonate in calcite cement.

Table 3.

Primary calcite in lapilli groundmass from Polino and Oricola (EMPA and LA-ICP-MS)

Locality	Polino					Oricola					
EMPA											
SiO_2	0.66	3.30	0.03	2.28	3.32	0.01	0.05	0.07	0.24	0.05	0.01
FeO*	0.26	0.47	0.18	0.31	0.42	0.22	0.17	0.21	0.17	0.16	0.22
MgO	0.34	1.35	1.13	1.04	1.85	0.34	0.31	0.31	0.33	0.32	0.34
MnO	0.02	0.01	0.05	0.03	0.04	1.67	1.58	1.57	1.42	1.60	1.67
CaO	53.40	49.58	53.40	50.82	49.90	55.96	55.53	55.59	55.63	56.51	55.96
P_2O_5	0.28	0.19	0.19	0.29	1.35	0.25	0.22	0.20	0.19	0.32	0.25
Total	54.96	54.9	54.98	54.77	56.88	58.45	57.86	57.95	57.98	58.96	58.45
LAICPMS											
Rb	20.36	4.04	9.16	6.33	7.92	118	184	412	224	122	118
Pb	106	40.4	25.1	14.4	19.8	56.1	198	253	328	219	56.1
U	10.5	10.8	5.94	3.52	4.88	62.1	168	209	182	211	62.1
Th	2.97	3.09	8.45	4.18	1.11	41.9	81.0	113	142	97.4	41.9
Ba	2186	1864	818	1660	1368	2620	4491	2596	5463	4286	2620
Nb	6.51	6.10	4.82	3.53	3.79	22.3	45.4	52.0	75.3	49.4	22.3
Ta	<0.08	<0.1	<0.2	<0.1	<0.2	0.9	1.9	2.6	3.2	2.3	0.9
La	147	128	107	56.7	65.8	116	196	252	335	217	116
Ce	229	184	155	78.1	90.7	179	324	413	595	380	179
Sr	3440	4592	2090	6046	4691	3070	3939	4489	6238	6528	3070
Pr	28.0	23.4	19.6	9.9	10.8	18.6	32.7	42.5	56.6	36.9	18.6
Nd	109	77.3	74.8	36.0	39.6	59.7	101	119	164	108	59.7
Sm	20.5	12.8	13.1	5.5	6.4	6.7	11.2	15.1	21.0	14.9	6.7
Zr	69.9	102	71.9	31.3	80.6	134	240	293	372	270	134
Hf	1.96	5.21	2.48	0.95	3.58	1.5	3.1	5.5	5.5	4.1	1.5
Eu	4.26	2.23	2.07	1.16	1.33	1.5	2.3	2.8	4.2	2.6	1.5
Gd	14.7	6.2	11.8	5.4	4.6	10.2	13.2	15.0	18.1	13.2	10.2
Tb	1.33	0.47	0.72	0.43	0.38	0.6	1.0	0.9	1.6	0.9	0.6
Dy	7.45	1.66	3.27	1.82	1.53	3.1	4.2	5.0	7.3	4.2	3.1
Y	34.2	6.88	13.4	8.9	7.9	16.1	24.6	25.2	39.1	23.8	16.1
Ho	1.07	0.21	0.49	0.29	0.24	0.4	0.8	0.7	1.2	0.8	0.4
Er	2.55	<0.6	0.73	0.59	0.80	1.3	2.1	2.1	2.9	1.9	1.3
Tm	0.21	<0.1	0.13	0.09	<0.08	0.1	0.3	0.2	0.4	0.2	0.1
Yb	1.56	<1	<0.9	<0.7	<0.7	<2.1	<1.9	<2.1	2.6	2.3	<2.1
Lu	0.16	<0.1	0.10	<0.1	<0.1	0.2	<0.2	0.2	0.4	0.2	0.2

Note: FeO* = Total iron; data from [31, 32].

Cupaello is a thin kalsilitite lava flow, which has preserved fine-grained carbonatite tuff and mixed kalsilitite / carbonatite agglomerate beneath the flow [39]. Concentric or massive carbonatite lapilli and tear-drop shaped juvenile fragments show porphyritic texture with calcite laths in a very fine grained calcite groundmass.

ABRUZZO CARBONATITES

The Oricola carbonatite is a widespread surge deposit of fine grained Mn-calcite containing large concentric lapilli and calcite laths. There is a notable amount of kamafugitic-foiditic silicate glass shards mixed within the carbonates which were probably produced by highly explosive activity [52]. Apatite is the only non carbonate mineral detected although abundant silicate debris including cpx and phlogopite are also found. The chemistry of this rock indicates possible conjugation with the near kamafigutic foidite of Grotta del Cervo.

Less information is available about Grotta del Cervo occurrence due to its poor exposure. The rock is a carbonatitic tuff which includes some kamafugitic foidite blocks. The calcite forming the tuff matrix has high Sr and Ba content. The kamafugitic foidite blocks contain kalsilite, haüyne, leucite and nepheline plus cpx, melanite and spinel [55]. The apatite contains up to 6.73wt% of REE_2O_3 and 2.17wt% SrO [11].

VULTURE CARBONATITES

The Vulture volcano there are at least 7 major maars or diatremes which are related to carbonatitic tuffs (or tuffisite) that are composed of carbonatite/melilitite concentric lapilli immersed in a carbonatite matrix of Sr and LREE rich carbonates. These form a swarm which extends beyond of the main volcanic edifice and are about 130 ka old. The main outcrops are Casa Rossa/Mulino Vecchio, near Masseria Cuscito, Piano Comune, Lago Piccolo, Lago Grande, Vallone Toppo del Lupo and Serra di Braida [13-15, 27, 28, 33]. The structure and composition of Vulture carbonatites differ from outcrop to outcrop due to the effects of diatremic transport and volcanic mechanisms which can modify the carbonatite/melilitite volume ratio and granulometry of the deposit [41, 47]. Welded-ash and lapilli layers that are true carbonatite (modal carbonate >50vol%) have been reported from Lago Grande, Lago Piccolo and Vallone Toppo del Lupo. Also mantle nodules are variably concentrated; their maximum frequency and size are found at Casa Rossa and Lago Grande. Ultramafic debris are widespread in Vulture carbonatites as attested by relatively high proportion of SiO_2, which is very similar to the Umbria and Abruzzo carbonatites. In general, the larger concentrically shelled lapilli have inner layers made of melilitite and outer layers made of agglutinated, smaller porphyritic carbonatite lapilli which also form most of the blanket tuffs that are widespread around the vents. In addition, small melilititic spin-lapilli are sprayed into the carbonatite droplet-ash matrix of the tuffs. The accretion of carbonatite droplets around a more viscous melilitite, or a solid kernel has been described in detail in several papers [41-43]. Depth of accretion is suggested by the kernels coring the lapilli: peridotites and mega-xenocrysts indicate mantle lithosphere origin; melilitolite, clinopyrossenite and felsic rocks indicate crustal depths. Vulture carbonatites contain clinopyroxene, apatite, zoned Ti-magnetite with Mn-Mg-rich rim and perovskite with Nb-Ba-rich

rim. Secondary phases are ettringite, barite, hematite and Fe-hydroxides often replacing sulphide. Large crystals found in carbonatite matrix are xenocrysts or cognate macrocrysts of forsterite, Cr-hastingsite, Cr-phlogopite, Cr-diopside showing a reaction rim.

Intrusive coarse calcite-carbonatite (sövite) and fine grained (alvikite) ejecta from the plutonic complex are associated with ne-syenite, melilitolite (uncompahgrite and ultramelilitolite), ijolite and clinopyrossenite and have been reported from the Monticchio Lakes syntheme and from other older volcanic units [30, 51].

Vulture sövite is coarse grained and shows some textural and mineralogical layering. It is mainly formed by calcite (1.5 to 3.5wt% MgO, up to 0.24wt% SrO) and much lower amounts of dolomite (18wt% MgO, up to 1.21% SrO), spinel (60wt% Al2O3, 26.5wt% MgO, 10.7wt% FeO), forsterite, perovskite and apatite. $^{143}Nd/^{144}Nd$ (0.512648 +/- 15) and $^{87}Sr/^{86}Sr$ (0.705978 +/- 10) ratios are similar between soëvite and the Vulture alkali mafic silicate rocks. $\delta_{13}C$ (-4.8) is in the range for mantle derived carbonatites. $\delta^{18}O$ has values which plot within a broad range of worldwide carbonatites and is believed to have been slightly affected by fractionation as well as deuteric alteration [30]. Compared with world average sövite compositions, the Vulture sövite has high Th, U and Sr. LREE/HREE fractionation is also typical of carbonatites having a value around 100.

Vulture alvikite is equigranular fine-medium grained rock formed of rare large euhedral Ti-garnet in a groundmass of mosaic textured calcite and cpx. Calcite contains abundant small rounded inclusions of K-feldspar. Wollastonite forms patches. Accessory euhedral sphene, Ti-magnetite and apatite constitute the remainder. Modal composition is calcite 85%, cpx 9.6%, K-feldspar 3.9%, Ti-garnet 0.5%, sphene 0.4%, apatite 0.3%, wollastonite 0.3%, magnetite 0.1%. Calcite has a very low MgO, with a typical SrO content between 0.15 and 0.25wt% and FeO up to 0.3wt%. Garnet has TiO2 up 4.7wt% and is a solid solution of 87-89mol% andratide, 9-12mol% grossular and 0.5-1mol% pyrope. K-feldspar is sanidine in composition with limited Ab molecular solid solution between 15 and 17%, FeO has a concentration up to 0.52wt%.

FOIDITE, MELILITITE AND MELILITOLITE

This complex rock suite can have types which are virtually carbonate free of also types which are carbonate-rich, in both cases they are strictly associated with carbonatites in tectonic setting, age, trace elements and isotope geochemistry. They are rarely vented physically separated from carbonatites and are often finely comminuted into carbonatite by explosive activity (San Venanzo, Cupaello, Oricola, Grotta del Cervo, Vulture). Only Polino carbonatite occurs in isolation. Thus makes Italian carbonatites and kamafugitc melilitite/foidites a very typical conjugate pairs [52]. The extrusive mafic rocks associated with Italian carbonatites have been exhaustively described in a number of papers and not repeated here. For

those readers who may be unfamiliar with their specific literature we would mention that the rocks are melilitites or foidites, with more potassic variants being kamafugites or even kalsilitites (tab. 1). Mineralogy is extremely complex owing to the etheromorphic nature of the rocks and crystallisation under variable composition and pressure of volatiles. In some cases up to 4 different types of foids are present (e.g. Grotta del Cervo kamafugitic foidite). In melilitites, ghelenitic molar proportion is possibly correlated with the CaO content of the rock. Distinctive Ti-Zr-Ca-silicate, Zr-cuspidine, kybinskite, kymzeinite, Zr-cuspidine and götzenite occur as a response to the high peralkaline nature of some of these rocks [35, 36]. The diversity of mineral compositions suggests a complex history of crystallization for the IUP kamafugitic rocks. The investigation of melt and fluid inclusions indicate that the earliest magmatic minerals of these rocks are olivine and clinopyroxene, which form large and rather homogeneous phenocrysts. The high maximum Mg# of olivine phenocrysts (up to 0.91) suggest that the magma was almost undifferentiated and close to a primary mantle melt.

Coarse intrusive rocks are much less well known and are the subject of a minority of papers [36, 44, 53]. They are found as either discrete subvolcanic bodies or, more frequently, as ejecta or blocks in carbonatites or melilitite/foidite. They are generally leucite-calcite melilitolite and ultra-melititolite or uncomphagrite which are virtually olivine-free and containing wollastonite and rankinite instead of monticellite. Other accessory minerals are haüyne, nepheline, Ti-garnet, Ti-magnetite, phlogopite and Ti-magnetite. Melilitolites have a much higher CaO contents of melilitites and have variable peralkalinity, in some case it is extreme (AI>20). They can contain variable amounts of carbonates up to >20%vol.. However, when they are carbonate-free still preserve contents of CaO (>35wt%) usually found only in carbonatites. Their essential mineralogy, further modified by phenomena typical of intratelluric differentiation, is largely explicable by decarbonatation reaction between carbonatite melt and silicate phases [40, 44]. These rocks are associated with sövite and alvikite ejecta and indicate plutonic differentiation of the parental carbonate ultramafic magma which, when erupts, is able to preserve much better primitive or near primary characteristics.

GEOCHEMICAL AND GEODYNAMIC CHARACTERISTICS AND PLUME ACTIVITY

Italian carbonatite and melilitite/foidite are co-eruptive conjugate pairs [38-40, 52] and it has been demonstrated that there is no dilution by sedimentary limestone or any other crustal assimilation [3, 4]. The geochemistry of Zr-Hf, Ta-Nd, Ti depends on the differing solubility of these elements in alkaline/peralkaline melts and therefore have different geochemical behaviour with respect to basaltic melts [9]. This was already noted and others, who discredited the tectonic classification ability of popular diagrams based on HFSE ratios for non basaltic, cratonic and potassic rocks [24].

Italian carbonatites and conjugate silicate rocks have C, O and B isotope ratios ranging from typical mantle values to enriched heavy isotope values which disprove the derivation of carbonatitic melts from a crustal reservoirs. However, by plotting Sr, Nd and Pb isotopic ratios for IUP rocks it is possible to detect a relationship between two separate mantle end-members: FOZO and ITEM [3, 4, 5, 6]. Any involvement of sedimentary limestones can be discharged, as those are much less radiogenic than ITEM. Furthermore, addition of crustal material is in disagreement with high Cr+Ni content, strongly silica undersaturated character, peralkalinity and, in general, with the geochemistry of comagmatic kamafigite-carbonatitte pair [52]. Mantle melts associated with subduction do not have an ITEM or FOZO component, which appears to dispose the hypothesis of an origin of IUP carbonatitites by subduction adopted by some [26]. ITEM is a highly radiogenic reservoir which may be located outside the main convective mantle. It is accepted that the deep mantle that remains isolated for a time scale of over a billion years would allow for the radioactive decay of light nuclides such as K. Light nuclides are a likely, volatile component which exsolves slowly during cooling and contraction of the outer core. Several observations suggest it is likely that C (and other light elements) were incorporated into the Earth's core during accretion [56]. Graphite and carbides are commonly present in iron meteorites and this is consistent with the dissolution of C into Fe-Ni liquids. The carbon isotopic composition of graphite in iron meteorites exhibits a uniform value of -5‰ identical to the mode in the distribution found in diamonds, carbonatites and oceanic basalts [23]. If there is C (and K-Rb) in the core, which is not reached by subduction there is no point making the deep C evolution more complex by involving shallower Earth layers [8]. Movement of heavy carbon towards the surface is simple when differentiation of the inner part of the planet takes place over billions of years. If FOZO is representative of a common asthenospheric reservoir then the ITEM isotopic characteristics can be related to the hypothesised ‘D’ layer of the mantle as on the Earth it doesn’t exist any other similar reservoir. To date, Italian carbonatites and melilitites have always been associated with continental lithospheric thinning [17, 18, 20]. However, plume models have long been proposed for Italy but plume size and composition have as yet been poorly addressed [22]. More recently, the existence of a very large plume confined to the transition layer beneath the Central Mediterranean Sea, Azores-Canary area and continental Europe, has been suggested [4-6]. Plume head expansion in the mantle would produce an asynchronous mosaic of extending areas and extensive mantle metasomatism driven by a general eastward mantle flow. Most of the rare ultralkaline rocks found in the Central Mediterranean sea and the active volcanoes can be explained from fingers emitted by the degassing plume head or simply by metasomatised sub-lithospheric mantle melting during lithosphere thinning.

DISCUSSION AND CONCLUSIONS

The high Ca contents and carbonate inclusions in most Mg-rich olivine phenocrysts found in Italian carbonatites and kamafugites indicate that high Ca is a primary characteristic of Italian mantle melts. The composition of mantle melts has been characterized by primary high K_2O, Na_2O, F, Cl and S contents, which are inherited by all later derivatives. This rules out any crustal assimilation of carbonate, chlorides or sulphates. The conditions of the initial magma crystallization during its ascension towards the surface has been estimated from the results of thermometric experiments with melt and fluid inclusions and mantle nodules as proxy geobarothermometers. The highest crystallization temperature recorded by melt inclusions in olivine is 1240° - 1360°C [25, 38]. The occurrence of associated lherzolites indicates that the primary magma segregated from the source at about 22 kbar [16]. The complex rock mineralogy results from primary mantle magma crystallization under open-system conditions, with strong variations in H_2O/CO_2, and probably oxygen, potential. The parental magma was clearly a carbonated melilitite/foidite which becomes immiscible with carbonatite at some point in this process [25, 37-40, 51]. Primary silicate–carbonate inclusions in calcite were also reported from the Mt. Vulture sövite [30]. Their carbonate component is dominated by dolomite. The carbonate melt coexisting with alkaline silicate melt should contain substantial amounts of alkalis and neyrereite has been found in melilite and apatite inclusions [34]. However, considering the rarity of alkali carbonates in IUP carbonatites we postulate that alkalies could be consumed at crustal pressure by the crystallization of foids in kamafugites and potassium feldspar in phonolites and/or be dissolved in aqueous fluid separating during eruption.

In our opinion there is nothing about Italian carbonatites and their tectonic setting to lead us to consider them as exceptional to other worldwide carbonatites. There is very strong evidence that Italian mantle was invaded by carbonatitic melts (alkaline?) and that mantle minerals reacted to form a complex metasomatic assemblage. Fluid inclusion studies indicate that pristine parental magma was rich in CaO and CO_2 and that carbonatite-silicate immiscibility occurred over a wide range of T/P conditions [52]. Co-eruption of physically separated but chemically conjugated kamafugite and carbonatite is a clear demonstration of immiscibility. Silicate-carbonate immiscibility is considered to be the most effective evolutionary process in the kamafugitic/carbonatitic melts, but, open system conditions and a variable volatile ratio can explain the complex mineralogy of kamafugite/carbonatite association. In addition, variation in the solubility of HFSE in alkaline/peralkaline liquid explains HFSE changes. Sövite/melilitolite formation relates to slow differentiation and decarbonatation in plutonic conditions.

Italian carbonatites cannot be linked to subduction processes and it is more likely that a continental lithosphere extension, coupled by a deep plume expansion, may relate to the more general Mediterranean geologic setting and the location of central Europe carbonatites.

REFERENCES

1. **Bailey D.K., Garson M., Kearns S.,Velasco A.P.** Carbonate volcanism in Calatrava, central Spain: a report on the initial findings // Mineral. Mag., 2005, v. 69, p. 907-915.
2. **Bailey K., Lloyd F., Kearns S., Stoppa F., Eby N., Woolley A.R.**. Melilitite at Fort Portal, Uganda: Another dimension to the carbonate volcanism // Lithos, 2005, v. 85, p. 15-25.
3. **Baily D.K.**. Carbonate volcanics in Italy: numerical tests for the hypothesis of lava-sedimentary limestone mixing // Periodico di Mineralogia, 2006, v. 74, p. 205-208.
4. **Bell K., Kjasgaard B.** Discussion of Peccerillo (2004). Carbonate-rich pyroclastic rocks from Central Apennines: carbonatites or carbonate-rich rocks? Periodico di Mineralogia, 2006, v. 75, p. 85-92.
5. **Bell K., Castorina F., Lavecchia G., Rosatelli G., Stoppa F.** Is there a mantle plume beneath Italy? // EOS, 2004, v. 85 (50), p. 541, 546-547.
6. **Bell K., Castorina F., Rosatelli G., Stoppa F**. Largescale, mantle plume activity below Italy: Isotopic evidence and volcanic consequences // Geophys. Res. Abs., 2003, v. 5, № 14217.
7. **Bell K., Lavecchia G., Stoppa F.** Reasoning and beliefs about Italian geodynamics // Boll. Soc. Geol. It., Volume Speciale, 2005, № 5, p. 119-127.
8. **Brenker F. R., Vollmer C., Vincze L., Vekemans B., Szymanski A., Janssens K., Szaloki I., Nasdala L., Joswig W., Kaminsky F.**. Carbonates from the lower part of transition zone or even the lower mantle // Earth and Planetary Science Letters, 2007, v. 260, p. 1-9.
9. **Chakhmouradian A. R.** High-field-strength elements in carbonatitic rocks: Geochemistry, crystal chemistry and significance for constraining the sources of carbonatites // Chemical Geology, 2006, v. 235, p. 138-160.
10. **Chiarabba C., Jovane L., di Stefano R.**. A new view of Italian seismicity using 20 years of instrumental recordings // Tectonophysics, 2005, v. 395, p. 251-268.
11. **Comodi P, Liu Yu, Stoppa F and Woolley R.A.** A multi-method analysis of Si-, S- and REE-rich apatite from a new find of kalsilite-bearing leucitite (Abruzzi, Italy) // Mineralogical Magazine, 1998, v. 63, p. 661-672.
12. **Gambardella B., Cardellini C., Chiodini G., Frondini F., Marini L., Ottonello G., Vetuschi Zoccolini M.** Fluxes of deep CO2 in the volcanic areas of Central-Southern Italy. Journal of Volcasnology and Geothermal Research, 2004, v. 136, p. 31-52.
13. **Giannandrea P., La Volpe L., Principe C, Schiattarella M.** Unità Stratigrafiche a Limiti Inconformi (UBSU) e storia evolutiva del vulcano medio-pleistocenico di Monte Vulture (Appennino meridionale, Italia) // Boll Soc Geol It, 2006, v. 125, p. 67-92.
14. **Giannandrea P., La Volpe L., Principe C., Schiattarella M.** Carta geologica del Mt. Vulture alla scala 1:25.000. Litografia Artistica Cartografica Srl., Firenze, 2004.
15. **Giannandrea P., Principe C., La Volpe L., Schiattarella M.** Note illustrative alla nuova carta geologica alla scala 1: 25.000 del Monte Vulture – The new geological map 1:25.000 of Monte vulture volcano. In C Principe (ed): Geologia del Monte Vulture. Monografia geologica, Regione Basilicata Dipartimento Ambiente e Territorio. Finiguerra, Lavello, 2006, p. 25-49.
16. **Jones, A.P., Kostoula, T., Stoppa, F., Woolley, A.R.** A geotherm estimated from mantle xenoliths in Mt. Vulture volcano, Southern Italy // Mineralogical Magazine, 2000, v. 64, p. 593-613.
17. **Lavecchia G., Boncio P.** Tectonic setting of the carbonatite-melilitite association of Italy // Min. Mag., 2000, v. 64, p. 583-592.
18. **Lavecchia G., Creati N.** The Intramountaine ultra-alkaline Province (IUP) of Italy: a brief review with consideration on the thickness of the underlying lithosphere // Boll. Soc. Geol. It, 2002, 1, 87-98.

19. **Lavecchia G., Stoppa F.** The tectonic significance of Italian magmatism: an alternative view to the popular interpretation.Terra Nova, 1996, v. 8, p. 435-446.
20. **Lavecchia G., Stoppa F., Creati N.** Carbonatites and kamafugites in Italy: mantle-derived rocks that challenge subduction // Annals of Geophysics, 2006, 49/1, 389-402 ISSN.
21. **Lupini L., Williams C.T., Woolley R.A.** Zr-rich garnet and Zr- and Th- rich perovskite from the Polino carbonatite, Italy // Min. Mag., 1992, v. 56, p. 581-586.
22. **Macera P., Gasperini D., Piromallo C., Blichert-Toft J., Bosch D., del Moro A., Martin S.** Geodynamic implications of deep mantle upwelling in the source of Tertiary volcanics from the Veneto region (south-eastern Alps) // J. Geodyn., 2003, v. 36, p. 563–590.
23. **Mattey, D.P.**. Carbon isotopes in the mantle // Terra Cognita, 1987, № 7, p. 31-37.
24. **Muller D., Rock N.M., Groves D.I.** Geochemical discrimination between shoshonitic and Potassic volcanic rocks in different tectonic settings: A pilot study // Mineral. Petrol., 1992, v. 46, p. 259-289.
25. **Panina L.I., Stoppa F., Usoltseva L.M.** Genesis of Melilitite Rocks of Pian di Celle Volcano, Umbrian Kamafugite Province, Italy: Evidence from Melt Inclusions in Minerals // Petrology (Petrologiya), 2003, v. 11, p. 365-382.
26. **Peccerillo A.**. Plio-Qaternary volcanism in Italy: petrology, geochemistry, geodinamics. Sprnger, Berlin, 2005, 365 p.
27. **Principe C. (ed)** Geologia del Monte Vulture. Regione Basilicata Dipartimento Ambiente e Territorio. Monografia geologica. Finiguerra, Lavello, 2006, p. 227.
28. **Principe C., Giannandrea P.** Storia evolutiva del Monte Vulture – Monte Vulture volcano evolutive history. In C Principe (ed): Geologia del Monte Vulture. Monografia geologica, Regione Basilicata Dipartimento Ambiente e Territorio. Finiguerra, Lavello, 2006, p. 49-55.
29. **Rogie J.D., Kerrick D.M., Chiodini G., Frondini F.** Flux measurements of non volcanic CO_2 emission from some vents in central Italy // Journal of Geophysical Research, 2000, v. 105, p. 8435-8445.
30. **Rosatelli G., Stoppa F., Jones A.P.** Intrusive calcio-carbonatite occurrence from Mt. Vulture volcano, southern Italy // Min. Mag., 2000, v. 64, p. 615-624.
31. **Rosatelli G., Wall F., Stoppa F.** Calcio-carbonatite melts and metasomatism in the mantle beneath Mt. Vulture (Southern Italy). Lithos, 2007, in press.
32. **Rosatelli G, Wall F., Stoppa F., Brilli M.** Spatially-resolved LAICPMS analysis of carbonates: Polino carbonatite, calcite cements and limestone. 2008. In prep.
33. **Schiattarella M., Beneduce P., Di Leo P., Giano S.I., Giannandrea P., Principe C.** Assetto strutturale ed evoluzione morfotettonica quaternaria del vulcano del Monte Vulture (Appennino lucano) // Boll Soc Geol It, 2005, v. 124, p. 543-562.
34. **Sharigin V.V., Stoppa F., Jones A.P.** Mantle metasomatism and alkali carbonatite silicate phase reaction as inferred by Nyerereite inclusion at Vulture Volcano carbonatite rocks // 9th IKC, Frankfurt, 2008, short abstracts.
35. **Sharigyn V.V., Stoppa F.** Zr-Ti disilicates from the Pian di Celle volcano, Umbria, Italy // Eur. J. Min., 1996, v. 8, p. 1199-1212.
36. **Sharigyn V.V., Stoppa F., Kolesov B.A.** Cuspidine in melilitolites of San Venanzo // Doklady AN RAN, 1996, v. 348, p. 800-804.
37. **Sharygin V.V.** Silicate-carbonate liquid immiscibility in melt inclusions from melilitolite minerals: the Pian di Celle volcano (Umbria, Italy) // Memórias, 2001, № 7, p. 399-402.
38. **Solovova I.P., Girnis A.V., Kogarko L.N., Kononkova N.N., Rosatelli G., Stoppa F.** Compositions of magmas and carbonate-silicate liquid immiscibility in the Mt. Vulture alkaline igneous complex, Italy // Lithos, 2005, v. 85, p. 113-128.
39. Stoppa F., Cundari A. A new Italian carbonatite occurrence at Cupaello (Rieti) and its genetic significance // Contrib. Mineral. Petrol., 1995, v. 122, p. 275-288.

40. **Stoppa F., Cundari A.** Origin and multiple crystallization of the kamafugite-carbonatite association at S.Venanzo - Pian di Celle, Umbria, Italy // Min. Mag., 1998, v. 62, p. 273-289.
41. **Stoppa F., Woolley A.R.** The Italian carbonatites: field occurrence, petrology and regional significance // Mineralogy and Petrology, 1997, v. 59, p. 43-67.
42. **Stoppa F.** The San-Venanzo maar and tuff ring, Umbria, Italy: eruptive behaviour of a carbonatite-melilitite volcano // Bull. Volcanol., 1996, v. 57, p. 563-577.
43. **Stoppa F.** Consensus and open questions about Italian CO_2 –driven magma from the mantle // Periodico di Mineralogia, Special Issue Eurocarb, 2003, v. 72, p. 1-8.
44. **Stoppa F., Cundari A., Rosatelli G., Woolley A. R.** Leucite melilitolites in Italy: genetic aspects and relationship with associated alkaline rocks and carbonatites // Periodico di Mineralogia, Special Issue Eurocarb, 2003, v. 72, p. 223-251.
45. **Stoppa F., Lavecchia G.** Late Pleistocene ultra-alkaline magmatic activity in the Umbria-Latium region (Italy): an overview // J. Volcanol. Geotherm. Res., 1992, v. 52, p. 277-293.
46. **Stoppa F., Liu Y.** Chemical composition and petrogenetic implications of apatites from some ultra-alkaline Italian rocks // European J. of Mineralogy, 1995, v. 7, p. 391-402.
47. **Stoppa F., Lloyd F., Rosatelli G.** CO_2 as the virtual propellant of carbonatite-kamafugite conjugate pairs and the eruption of diatremic tuffisite // Periodico di Mineralogia, Special Issue Eurocarb, 2003b, v. 72, p. 205-222.
48. **Stoppa F., Lupini L.** Mineralogy and petrology of the Polino monticellite calciocarbonatite (Central Italy) // Mineral. Petrol., 1993, v. 49, p. 213-231.
49. **Stoppa F., Principe C., Giannandrea P.** Comments on: Carbonatites in a subduction system: the Pleistocene alvikites from Mt. Vulture (southern Italy) by d'Orazio et al. // Lithos, 2007, in press.
50. **Stoppa F., Principe C.**. Eruption style and petrology of a new carbonatitic suite from the Mt. Vulture, Southern Italy: the Monticchio Lake formation // Journal of Volcanology and Geothermal Research, 1997, v. 80, p. 137-153.
51. **Stoppa F., Rosatelli G., Principe C.** Classificazione modale delle vulcaniti del Monte Vulture - Modal classification of Monte Vulture volcanics // In C Principe (ed): Geologia del Monte Vulture. Monografia geologica, Regione Basilicata Dipartimento Ambiente e Territorio. Finiguerra, Lavello, 2006, p. 87-105.
52. **Stoppa F., Rosatelli G., Wall F., Jeffries T.**. Geochemistry of carbonatite - silicate pairs in nature: a case history from Central Italy // Lithos, 2005, v. 85, p. 26–47.
53. **Stoppa F., Sharygin, V.V., Cundari A.**. New mineral data from the kamafugite-carbonatite association: the melilitolite from Pian di Celle, Italy // Mineral. Petrol., 1997, v. 61, p. 27-45.
54. **Stoppa F., Woolley A.R.** The Italian carbonatites: field occurrence, petrology and regional significance // Mineral. Petrol., 1997, v. 59, p. 43-67.
55. **Stoppa F., Woolley A.R., Cundari A.** Extent of the central Appenine melilitite-carbonatite province: new evidence from kamafugite at Grotta del Cervo, Abruzzo // Min. Mag., 2002, v. 66, p. 555-574.
56. **Tingle T.N.**. Accretion and differentiation of carbon in the early Earth // Chemical Geology, 1998, v. 147, p. 3-10.
57. **Vichi G., Stoppa F., Wall F.** The carbonate fraction in carbonatitic Italian lamprophyres // Lithos, Special Issue Eurocarb, 2005, v. 85, p. 154-170.
58. **Woolley A.R., Church A.A**. Extrusive carbonatites: A brief review. Lithos, 2005, v. 84, p. 1-14.

UDK 552.321.6

Kimberlite and carbonatite exploration in southern West Greenland; Summary of previous activities and recent work by the kimberlite research group at the Geological Survey of Denmark and Greenland

Sand K.K.[1], Nielsen T.F.D.[1], Secher K.[1] and Steenfelt A.[1]

[1]*Geological Survey of Denmark and Greenland, Øster Voldgade 10, DK-1350 Copenhagen, Denmark*

ABSTRACT

The Archaean craton in southern West Greenland comprises numerous occurrences of ultramafic alkaline rocks including kimberlite (senso lato), ultramafic lamphrophyre, lamproite and carbonatite. The kimberlite research group at GEUS has since 2001 been concerned with the task of studying known and tracing new occurrences using geochemical and geophysical tools. A study of geochemical and geophysical surface signatures of these rocks has been successful and resulted in many new occurrences. The work conducted by the research group includes storing and systematising information and data reported by exploration companies and field data obtained by GEUS. In addition, the data is used to study the origin of the alkaline magmas, and to assess the diamond potential of West Greenland. Presently, the origin of the alkaline magmas is addressed by mineral chemistry and melt characterisation. A significant diamond potential has been established for southern West Greenland based on the physical regime in the lithospheric mantle and by indicator mineral chemistry.

INTRODUCTION

The Archaean craton and adjacent Proterozoic terranes of West Greenland host a variety of ultramafic alkaline rocks including dykes of kimberlite (senso lato), lamproite, ultramafic lamphrophyre and carbonatite complexes (Fig. 1). The alkaline and carbonatite magmas were emplaced in specific time windows in the geological evolution, which can be related to major episodes of continental break-up [13]. The oldest episodes are Archaean and the youngest dated are Palaeogene. Mantle xenoliths and xenocrysts, including diamond (see Fig. 2), are known from many dykes and have for decades encouraged diamond exploration.

The present kimberlite research group at the Department for Economical Geology at GEUS has existed since 2001 and includes 4-8 scientists, technicians and students. This group has mainly been concerned with the study of kimberlitic rocks in the Sarfartoq and Maniitsoq regions, but ultramafic alkaline rocks from all parts of Greenland are included in the investigation. This paper focuses on work

conducted in the Sarfartoq and Maniitsoq regions (Fig. 2). The primary aim of the group has been to find new occurrences, to conduct studies related to the origin of

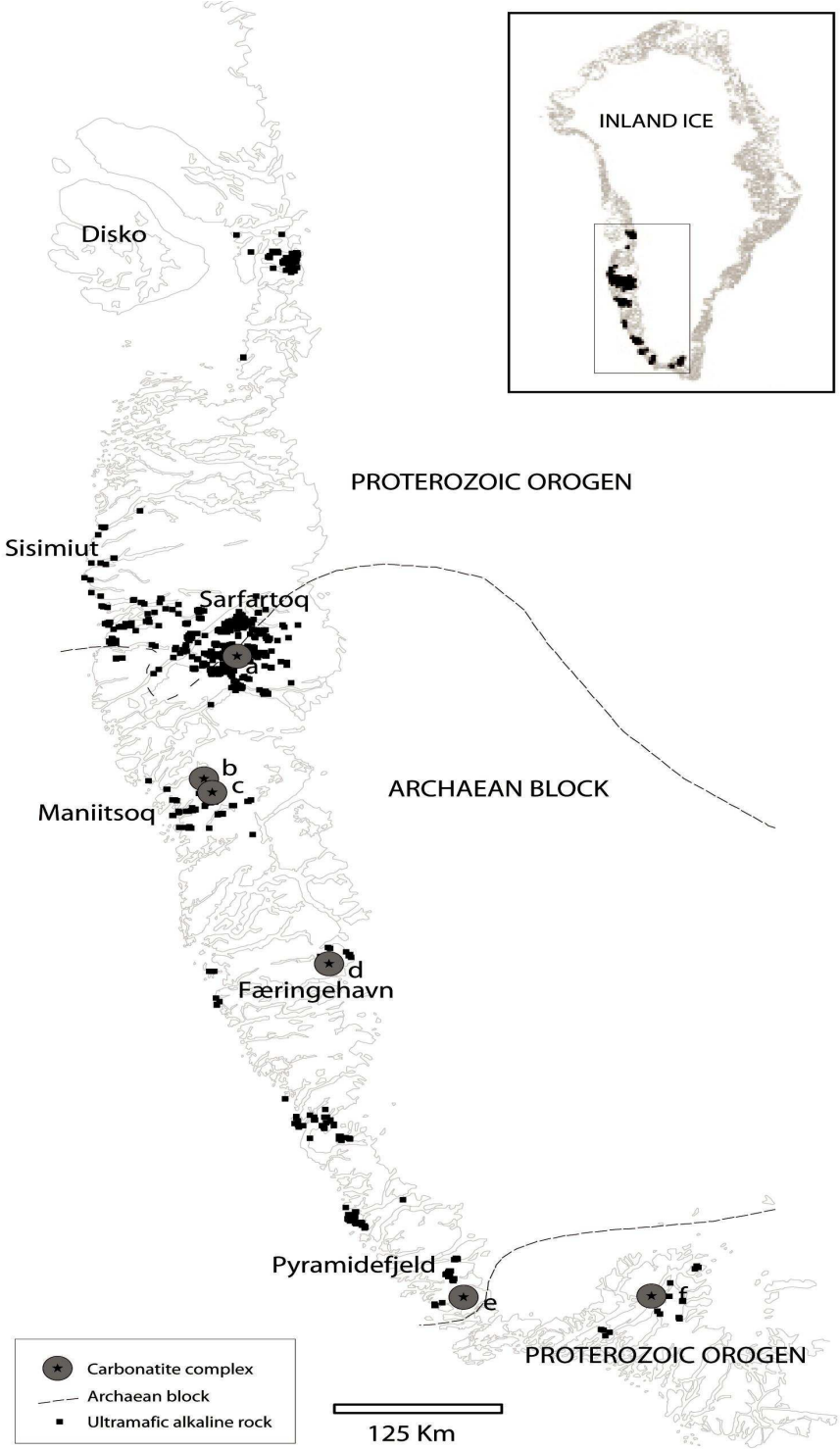

Fig. 1. **Distribution of ultrabasic alkaline rocks in southern West Greenland.**

Carbonatite complexes: a) Sarfartoq, b) Tupertalik, c) Qaqarssuk, d) Tikiusaaq, e) Grønnedal-Ika, f) Qassiarsuk.

the ultramafic alkaline magmas, the lithosphere structure, and to assess the diamond potential of West Greenland. The investigations are carried out in corporation with the Bureau of Minerals and Petroleum (BMP), Government of Greenland.

GENERAL GEOLOGY

A review of known occurrences of ultramafic alkaline rocks and carbonatites in West Greenland is published in 1992 by [13]. Since then, more dykes have been discovered in the northern part of the Archaean craton, and a Jurassic carbonatite and ultramafic lamprophyre (UML) dykes centrally in the craton, see below. The northernmost occurrence is a group of c. 1700 Ma UML dykes intruded into Archaean basement east of Disko [13]. Three clusters of ultramafic alkaline dykes have been recognized within the northern part of the craton (see Fig 1). The Sisimiut swarm comprises 1284-1203 Ma old lamproitic dykes and c. 590 Ma old kimberlitic dykes, which generally have a vertical E-W to SE-NW striking orientation [22, 24, 29]. The Sarfartoq swarm consists mainly of 560-600 Ma kimberlitic and UML dykes with several orientations, however, the northern part is dominated by a N-S trend. The 560 Ma old kimberlitic and UML dykes of the Maniitsoq swarm have orientations in a predominantly ENE-SSW direction. A carbonatite complex is known from the Sarfartoq region; the 600 Ma old Sarfartoq carbonatite complex (Fig.1a). Further south in the Maniitsoq region the ca. 3 Ga old Tupertalik carbonatite complex (Fig. 1b) [2], and the 165 Ma old Qaqarssuk carbonatite complex (Fig 1c) [24] are located. Until the discovery of the 158 Ma Tikiusaaq carbonatite complex (Fig. 1d) east of Færingehavn in 2005 [26], only a few UML dykes were known from the central part of the Archaean craton. Towards the southern edge of the craton, the abundance of alkaline dykes increases, and they comprise UML, monchiquite, carbonatite and a few occurrences of kimberlite. The southern occurrences are Mesozoic in age, and a presently interesting occurrence, the Pyramidefjeld comprises a small swarm of diamond bearing kimberlite sheets. Further south, within the Palaeoproterozoic orogen around 61ºN latitude, the large Mesoproterozoic Gardar rift and related alkaline igneous province [31] comprises UML dykes and intrusive complexes including a carbonatite body within the Grønnedal-Ika (Fig. 1e) complex and carbonatite lavas at Qassiarsuk (Fig. 1f). For more information on the occurrences east of Disko please refer to [1].

EXPLORATION

West Greenland has attracted diamond exploration since the early 1970s. (Fig. 2. shows the known diamond occurrences in southern West Greenland). The first diamonds from kimberlitic/UML rocks recovered in West Greenland were two microdiamonds and one macrodiamond from UML dykes at Pyramidefjeld. After

that followed regional kimberlite prospecting covering large parts of West Greenland resulting in the recovery of two microdiamonds from bulk stream sediment samples from the broad Sarfartoq valley [19]. Field campaigns by exploration companies from 1994 onwards have involved regional till and stream

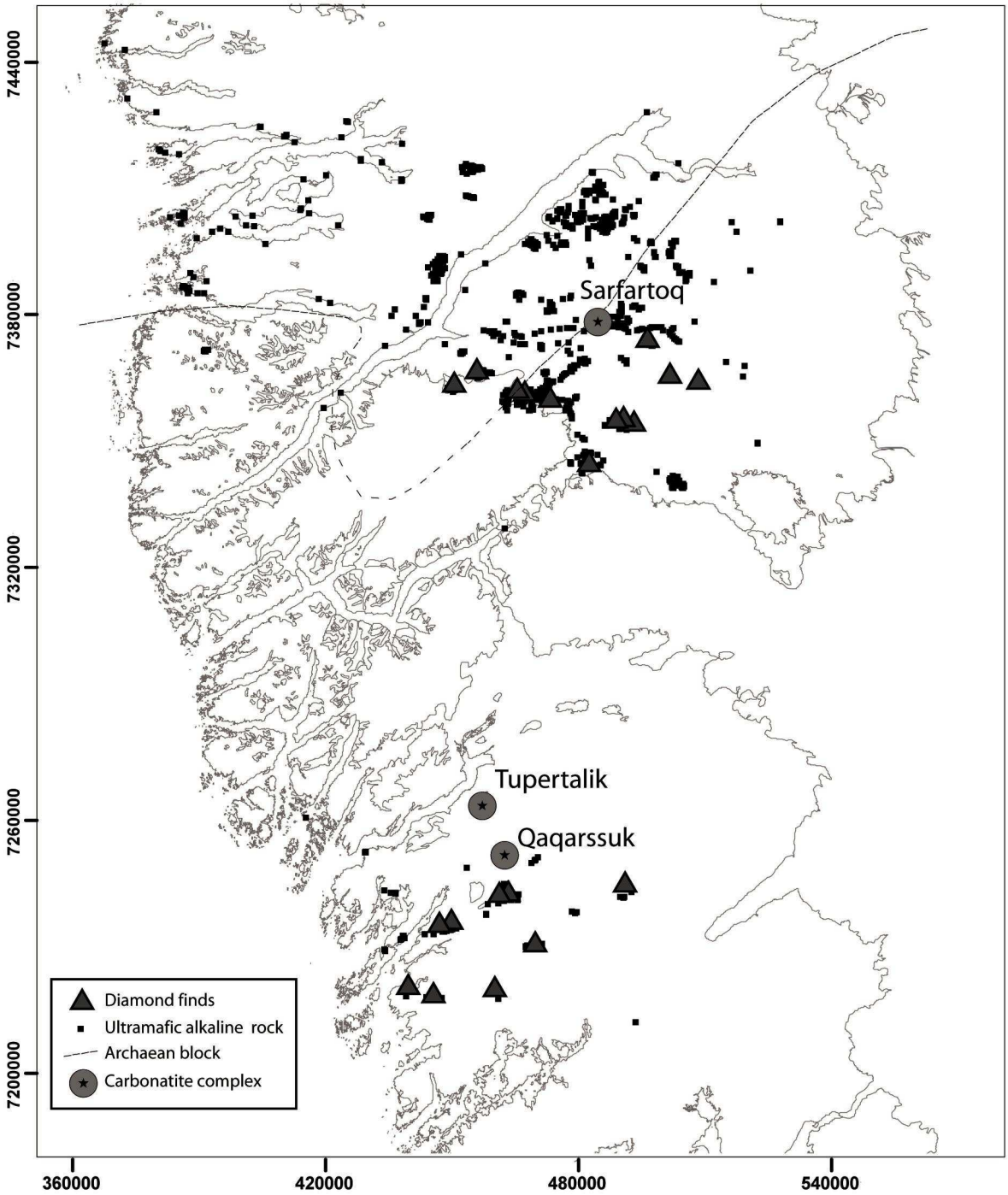

Fig. 2. **Focus area of the kimberlite research group at GEUS. Diamondiferous Neoproterozoic kimberlite and UML dykes in the northern part of the Archaean craton of West Greenland.**

sediment sampling programs aiming to locate kimberlite indicator minerals, airborne magnetic and electromagnetic surveys and drilling on frozen lakes for possible diatremes. In 1997, diamonds were extracted from in situ kimberlitic/UML dykes east of Maniitsoq, where one 792 kg sample of a large dyke yielded 25 microdiamonds <0.5 mm) and 16 macrodiamonds (all 0.5<1 mm). The focus subsequently shifted north to the Sarfartoq region, where a large number of microdiamonds were recovered from a single kimberlitic/UML occurrence (sub-cropping sill returning 474 microdiamonds and 5 macrodiamonds). In 2004, a diamondiferous dyke was located in the Sarfartoq region by the company Hudson Resources Inc. The company recovered 151 diamonds in 107.9 kg of host rock [6]. Since then the company has increased its activities each year completing establishing an excavation site and a Dense Media Separation plant setup in 2007 [7]. In 2006 Crew Minerals ASA collected 20 samples of 50 kg of five kimberlitic dykes in the Maniitsoq area and discovered that 18 of the 20 samples returned diamonds with two to eight stones in every sample [5].

PETROLOGICAL AND GEOCHEMICAL RESEARCH

Most of the first known alkaline dykes were found in the well-exposed coastal zones during reconnaissance related to general geological mapping. Inland occurrences, particularly dykes, are much more difficult to locate because they weather more extensively than the country rock gneisses and form vegetated depressions in the landscape. In addition, large parts of the inland areas are partially covered by till. A few inland occurrences were found by exploration companies looking for base metal mineralization.

In recent years exploration companies and the GEUS research group have made use of geochemical and geophysical exploration methods to find new occurrences of alkaline, kimberlitic and carbonatite rocks. Presently, the exploration data comprise: reconnaissance scale stream sediment geochemistry, regional and local scale abundance and chemistry of kimberlite indicator minerals in samples of till and stream sediment, a hyper spectral survey [30], and regional and local scale aeromagnetic and electromagnetic surveys. Much of the data have been acquired by companies and successfully used by them to locate new occurrences of kimberlite dykes, including the one with the presently known best diamond grade (see below). All acquired exploration data are archived at GEUS, and the research group has the benefit of making use of the comprehensive dataset compiled over the years [8, 11]. In addition, GEUS maintains a comprehensive sample archive (sediment samples, ultramafic alkaline rocks, and crustal and mantle xenoliths) from which samples can be extracted for examination and analysis as methods and ideas develop.

At present the data and the collections are used for studies of the structure and properties of the West Greenland lithosphere, and to gain knowledge of the origin and genesis of kimberlites, ultramafic lamprophyres and carbonatites. The regional

distribution patterns of many chemical and petrographic parameters provided by the exploration data are studied by the research group. The studies indicate that high Nb in stream sediment and abundance of garnet (peridotitic and eclogitic) in tills outline areas with occurrences of kimberlites and UML. These research themes aims at assessing the diamond potential by establishing where in West Greenland favourable conditions for the formation, preservation, and transport of diamonds to upper crustal levels can be expected.

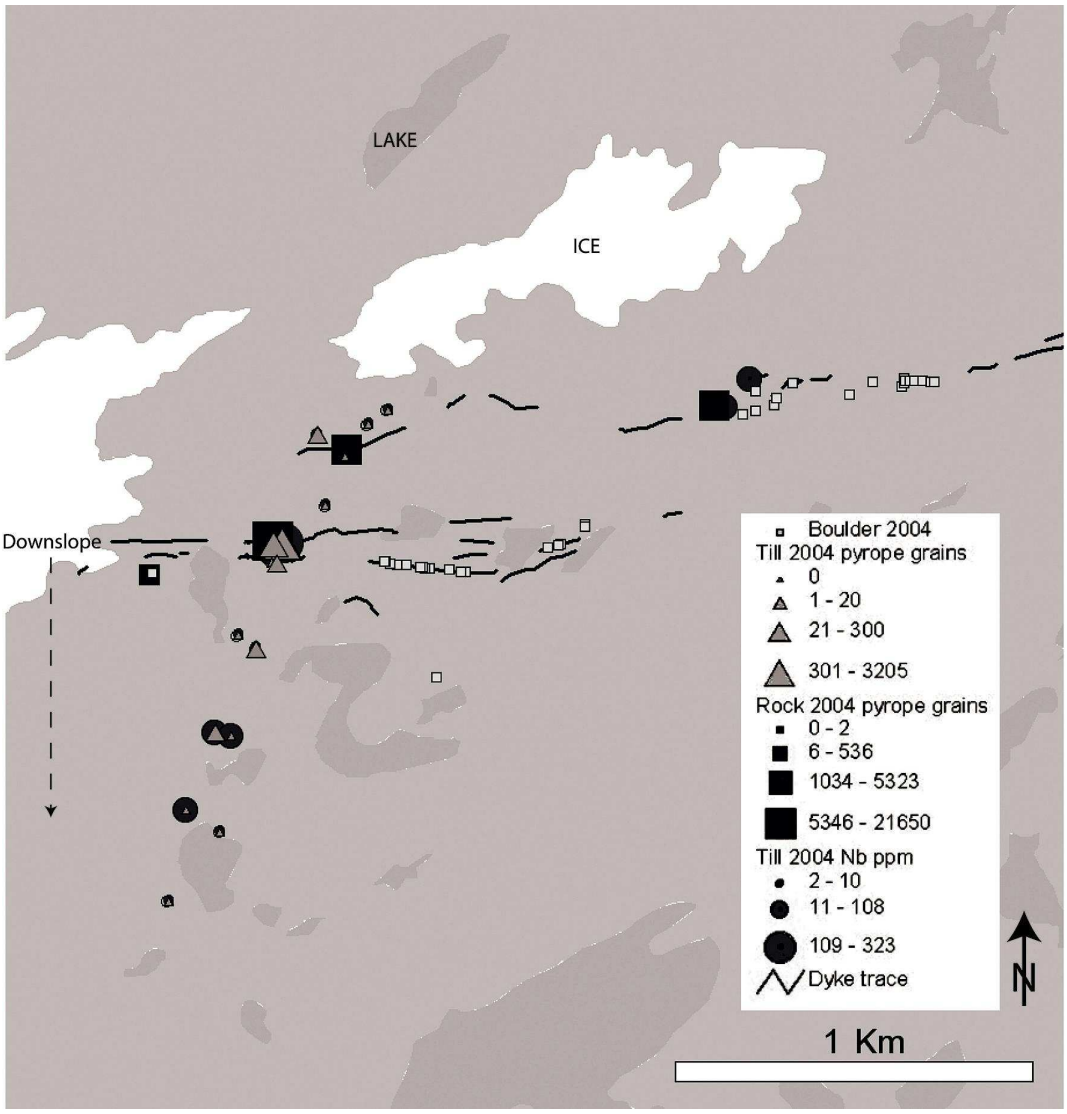

Fig.3. **Local distribution of Nb in till sample, and pyrope in rock and till samples. It is evident that the concentration decreases downslope of the occurrences.**

On a regional scale, the abundance and chemistry of KIM outline the known areas with kimberlite and UML intrusions well, and show that the chemistry of the indicator minerals is very useful in the evaluation of diamond potential of the regions [8, 9, 11, 27]. However, on a local scale it is the experience that tracing KIM in till back to a kimberlitic or UML sources is not straightforward due to disturbances related to glacier movements. A study conducted by the kimberlite

research group in 2004 concluded that the abundance of KIMs is high close to kimberlitic and UML dykes (sills) or among kimberlitic and UML boulders, but the number decreases significantly within a short distance down-ice or downslope from the occurrence [9, 27] (Fig. 3). The use of published discrimination diagrams for identification of mineral phases derived from the diamond window has been an efficient discrimination tool in the evaluation the information from the surface samples [9].

The main accomplishments in exploration by the group has been: 1) to find new occurrences of kimberlite in the Sarfartoq and Maniitsoq regions and to emphasise the diamond potential of the regions [9,17,21] ; 2) to describe the dispersion of KIM from kimberlite dykes [27]; and 3) to locate a new Jurassic carbonatite complex and associated UML dykes in the central part of the Archaean craton [26].

A CASE STORY: SUCCESSFUL RESULT OF COMBINED GEOCHEMICAL AND GEOPHYSICAL EXPLORATION FOR ULTRAMAFIC ALKALINE ROCKS; THE TIKIUSAAQ CARBONATITE COMPLEX

A stream sediment sample collected during the geochemical mapping of West Greenland [25] had a chemical composition that strongly indicated the presence of carbonatitic rocks similar to those at Sarfartoq [23] and Qaqarssuk [12]. The anomaly occurred in an area where there were no previous records of carbonatites or alkaline ultramafic rocks. A small-sized but strong magnetic anomaly displayed by the aeromagnetic map of West Greenland (see e.g.[20]) was located upstream from the a anomalous stream sediment sample supported the suggestion for a new carbonatite occurrence. In addition, KIM in till samples showed a small cluster of picked peridotitic garnet, which suggested the occurrence of kimberlitic/UML rocks (Fig. 4)

During fieldwork (2005), the field visit on these locations resulted in the discovery of a new carbonatite complex (named Tikiusaaq) and ultramafic lamprophyre dykes. The complex appears to be centred where *in situ* massive carbonatite was found in the walls of a creek cutting through a gentle slope covered by gravel and vegetation. The preliminary field observations indicate that the emplacement of the carbonatite has affected an area of more than 100 km^2 within highly metamorphosed and strongly deformed Archaean basement. Field observations indicate that parts of the intrusion were explosive [26]. The dimensions and internal structure of the core zone have not yet been fully established. However, by analogy with other carbonatite complexes in West Greenland, it is expected that the core zone is in the order of 1–2 km wide [26].

U-Pb isotope compositions of zircons and perovskite constrain the age of ultramafic lamprophyres and carbonatite to the time span from 165 to 152 Ma, i.e. Late Jurassic [26, 28]. The age makes the new carbonatite near-coeval with the

Qaqarssuk carbonatite complex [164 Ma, 24] and with UML dykes located at Færingehavn on the coast west of Tikiusaaq [13].

TERMINOLOGY AND GENESES OF THE GREENLANDIC ULTRAMAFIC ALKALINE ROCKS

The 600 Ma old ultramafic alkaline dykes were called 'kimberlitic' by [13], but [15] concluded that they were best referred to a 'carbonatite ultramafic lamprophyre suite (aillikites or melnoites [15]). It was further suggested that the West Greenland province represents "one of the few bona fide examples of ultramafic lamprophyre which contain diamonds". Reports on indicator mineral assemblages [11] and diamond contents [e.g. 6] have re-opened the discussion on the classification of the dykes. This has lead to an investigation by the GEUS

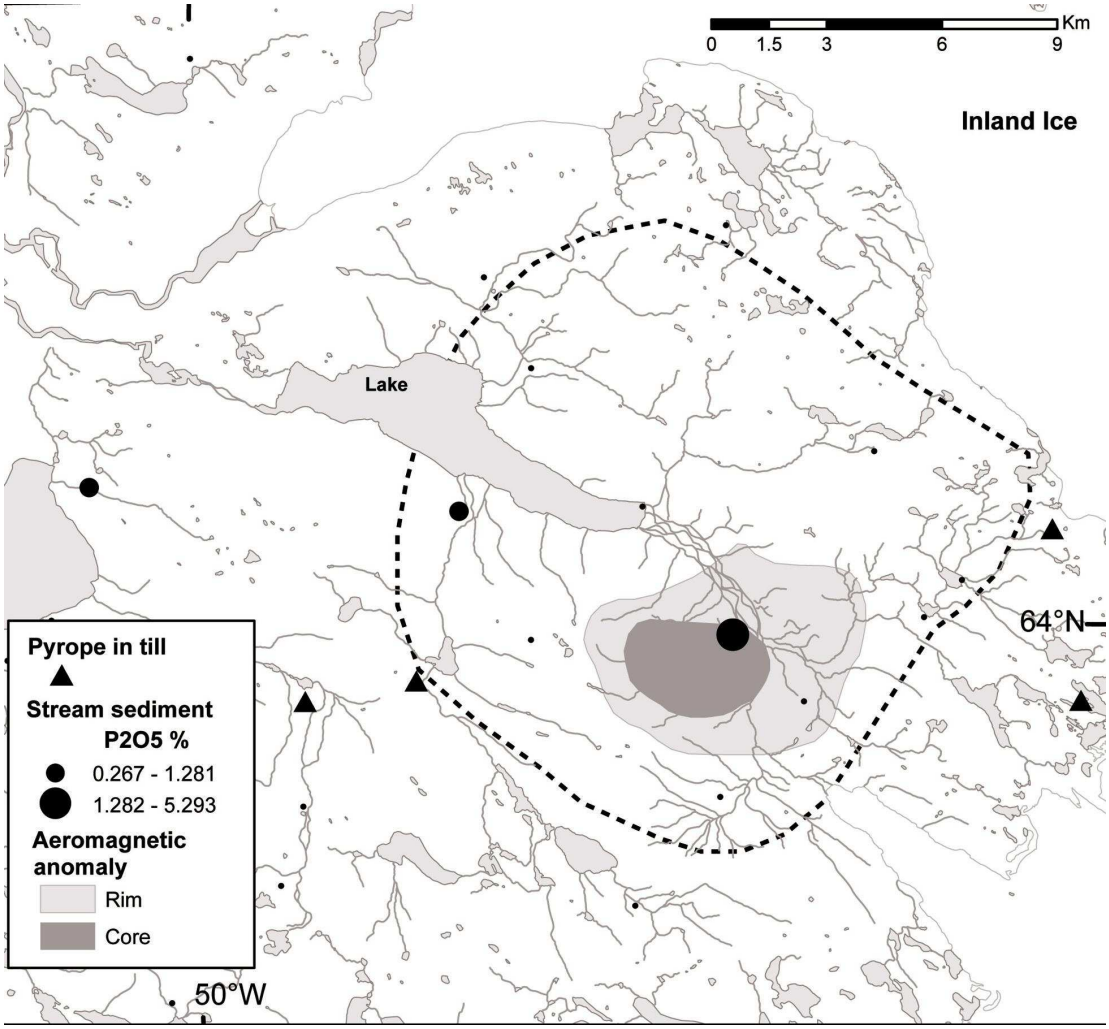

Fig. 4. **The area of the Tikiusaaq complex.**

Phosphorus (P_2O_5) anomalies in stream sediment and mantle-derived garnet grains in till in combination with the magnetic anomaly reveal the presence of a carbonatite and UML dykes in poorly exposed terrain. Massive carbonatite was located within the extent of the magnetic anomaly, while fracturing and veining related to the intrusion of the carbonatite magma as well as UML dykes were recorded within the area of the dashed line.

research group of the groundmass mineralogy and characterisation of these rocks. The investigation was initiated by a detailed study of the Majuagaa dyke in the Maniitsoq area [17], together with preliminary results of a regional investigation of the groundmass minerals of the dykes [16].

The Majuagaa dyke is 2.5 km long and up to 2 m wide and diamondiferous [10]. It is located c. 50 km SSE of Maniitsoq (Fig. 1) and strikes WSW–ENE. The dyke is dark grey with many olivine-rich fragments (up to 10 cm) and rounded megacrysts of ilmenite (up to 4 cm). It contains the classic kimberlitic suites of megacrysts and mantle nodules, including eclogite [10]. The groundmass is fine-grained and composed of olivine fragments, calcite, dolomite, serpentine, ilmenites and minor Mg-rich spinel. Phlogopite and apatite are rare. Mineral data from groundmass, megacrysts and nodules, the bulk chemistry, and analytical techniques are reported in [17]. It is further concluded that the Majuagaa dyke is a calcite-kimberlite with significant similarities to well established kimberlites [17]. In addition it was concluded that dykes in the Maniitsoq region bear strong resemblance to archetypal, South African, on-craton, Type 1 kimberlites.

DIAMOND POTENTIAL OF THE SOUTHERN WEST GREENLANDIC LITHOSPHERIC MANTLE

The diamond potential of the southern West Greenlandic lithospheric mantle has been assessed in a master thesis [21] using geothermobarometry mainly applied to 4-phase mantle peridotitic xenoliths (garnet, olivine, clinopyroxene, orthopyroxene) from ~600 Ma old kimberlitic (senso lato) dikes and sills. In addition, lithological and major element geochemical observations have been used to construct a model mantle transect [Not shown, see 21]. The xenoliths included in the study originate from 13 localities in the central, northern and marginal region of the Archaean craton Fig. 2.

The mineral chemistry of the southern West Greenlandic xenoliths resembles in general that of the Slave and Kaapvaal cratons. Detailed testing of different thermobarometer combinations allowed an evaluation of which combination is most applicable to the West Greenlandic peridotites. Because of problems relating to lack of equilibrium in the clinopyroxenes in these rocks, the favoured thermometer is a Ca-in-orthopyroxene formulation ($T_{Ca\text{-}in\text{-}opx}$) [4]. For harzburgites and wehrlites, a formulation based on the Fe-Mg exchange between olivine and garnet [18] is favoured. Three Al-in-orthopyroxene barometers yield radically different xenolith-geotherms, resulting in three distinct models for mantle evolution in southern West Greenland. Fig. 5 show the variation displayed by lherzolites between the Brey and Köhler barometer P_{BKN} [4] and the McGregor formulation P_{MC} [14], both at the $T_{Ca\text{-}in\text{-}opx}$ temperature formulation. The P_{MC} barometer, based on the chemically simple MAS-system [14], is favoured and it is argued that barometers requiring correction for minor elements propagate

analytical errors into the P/T estimates, when applied to the present suite of peridotites.

The combined results suggest a layered mantle below southern West Greenland displaying increasing fertility with depth, in agreement with previous studies [e.g. 3]. No lateral variation in pressure, temperature or heat flow at mantle depths can be identified in the investigated sub-areas despite variable crustal histories. Using the favoured pressure and temperature combinations, twenty-seven of thirty-one samples are from the diamond stability field, whereas the Brey and Köhler [4] formulation depresses pressures and yields a weaker diamond potential.

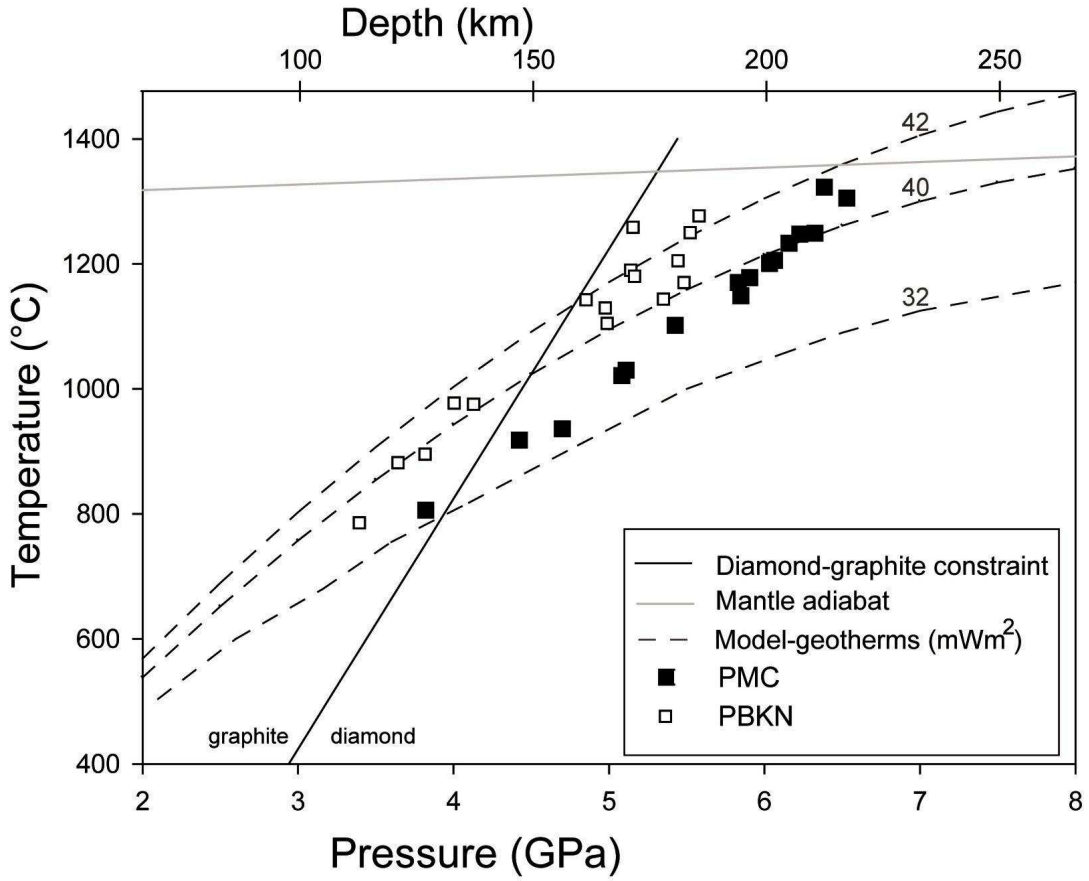

Fig. 5. **Comparison of the P/T distribution of lherzolites from eight localities in southern West Greenland (For simplicity only P/T estimates for lherzolites are shown).**

Temperatures are calculated using the $T_{Ca\text{-}in\text{-}opx}$ (favored for lherzolitic rocks in the present study) in combination with P_{MC} and P_{BKN}. Two distinct apparent xenolith geotherms are evident. The P_{MC} formulation defines a near-linear trend and the P_{BKN} display a convex trend. The P/T array based on each of the barometers results in a distinct interpretation of mantle evolution and diamond potential. The P_{MC} formulation is preferred in the present study.

Based on the thermal conditions established by [21] it is concluded that a significant diamond potential existed in the lithospheric mantle at the time of kimberlite/UML eruption ca. 600 Myr ago. This is supported by the conclusions of [17] that based on mineralogy of the host rock propose that all regions of the West

Greenland province of ultramafic magmatism are favourable for diamond exploration.

CONCLUDING REMARKS

The research group at GEUS has successfully applied geochemical and geophysical tools in order to locate new occurrences of ultramafic alkaline rocks in southern West Greenland. The knowledge and data collected during this process has been used to improve the techniques of geochemical and geophysical exploration and to conduct studies on diamond potential and magma characterization and nomenclature. Based on thermal constraints in the lithospheric mantle in southern West Greenland it is argued that a considerable diamond potential exists in the Sarfartoq and Maniitsoq regions. This is supported my mineralogical studies of and by recent diamond finds in these regions.

FUTURE WORK

In the coming years the kimberlite research group will continue the study of samples of West Greenland alkaline rocks and carbonatites including their mantle xenoliths. The group will make use of advanced methods to obtain new isotope data and chemistry in minerals and melt-inclusions with the objective of improving our understanding of where conditions are favourable for diamond occurrences. Using the experience gained in the Sarfartoq and Maniitsoq regions, the area of interest will be extended to include the southern part of the Archaean craton with the objective of creating a model for the entire West Greenland subcontinental lithosphere.

REFERENCES

1. **Bernstein S., Knudsen C., Beard D.K., Bruun M.** Placer diamonds in unconsolidated sands of the Cretaceous Atâne Fm, Disko Island, West Greenland // Danmarks og Grønlands Geologiske Undersøgelse Rapport, 2007, v. 13, 18 pp, 18 app.
2. **Bizzarro M., Simonetti A., Stevenson R.K., David J.** Hf isotope evidence for a hidden mantle reservoir // Geology, 2002, v. 30, p. 771-774.
3. **Bizzarro M., Stevenson R.K.** Major element composition of the lithospheric mantle under the North Atlantic craton: Evidence from peridotite xenoliths of the Sarfartoq area, southwestern Greenland // Contrib. Miner. Petrol., 2003, v. 146, p. 223-240.
4. **Brey G.P., Köhler T.** Geothermobarometry in 4-Phase Lherzolites .2. New Thermobarometers, and Practical Assessment of Existing Thermobarometers // Jour. Petrol., 1990, v. 31, p. 1353-1378.
5. **Crew Minerals ASA, M.A.** 2007, Press release of 15 January, http://www. crewminerals. com/news.cfm?id=10.
6. **Hudson Resources Inc.** 2004, Press Release. http://www.hudsonresources. ca/files/NR2004-11.pdf
7. Hudson Resources Inc,2007, http://www.hudsonresources.ca/files/NR2007-10.pdf.
8. **Jensen S.M., Lind M., Rasmussen T.M., Schjøth F., Secher K.** Diamond exploration data from West Greenland // Danmarks og Grønlands Geologiske Undersøgelse Rapport, 2003, v. 21, 50 p.

9. **Jensen S.M., Sand K.K., Steenfelt A.** Regional distribution and chemistry of indicator minerals from in situ rocks and surficial deposits in the Maniitsoq and Sarfartoq regions // Extended abstracts vol., Workshop on Greenland´s diamond potential, Copenhagen, 2005, 7-9 November, p 43.
10. **Jensen S.M., Secher K.** Investigating the diamond potential of southern West Greenland // Geological Survey of Denmark and Greenland Bulletin, 2004, № 4, p. 69-72.
11. **Jensen S.M., Secher K., Rasmussen T.M.** Diamond exploration data from West Greenland: 2004 update and revision // Danmarks og Grønlands Geologiske Undersøgelse Rapport, 2004, v. 117, 90 p.
12. **Knudsen C.** Petrology, geochemistry and economic geology of the Qaqarssuk carbonatite complex, southern West Greenland // Monograph Series of Mineral Deposits, 1991, v. 29, p.110.
13. **Larsen L.M., Rex D.C.** A review of the 2500 Ma span of alkaline-ultramafic, potassic and carbonatitic magmatism in West Greenland, Lithos, 1992, v. 28, p. 367–402.
14. **McGregor I.D.** The system MgO-Al_2O_3-SiO_2: Solilubility of Al_2O_3 in enstatite for spinel and garnet compositions // American mineralogist, 1974, v. 59, p. 110-119.
15. **Mitchell R.H., Scott Smith B.H., Larsen L.M.** Mineralogy of ultramafic dikes from the Sarfartoq, Sisimiut and Maniitsoq areas, West Greenland // in: Gurney, J.J., Gurney, J.L., Pascoe, M.D., Richardson, S.H., (Eds), Proceedings of the 7th IKC 2, Red Roof Design cc, Cape Town, 1999, p. 574–583.
16. **Nielsen T.F.D., Jebens M., Jensen S.M., Secher K.** Archetypal kimberlite from the Maniitsoq region, southern West Greenland and analogy to South Africa // Geological Survey of Denmark and Greenland Bulletin, 2006, № 10, p. 45–48.
17. **Nielsen T.F.D., Jensen S.M.** The majuagaa calcite-kimberlite dyke, Maniitsoq, southern West Greenland // Danmarks og Grønlands Geologiske Undersøgelse Rapport, 2005, v. 43, p. 59.
18. **O´Neil H.S.C., Woo B.J.** Experimental-Study of Fe-Mg Partitioning between Garnet and Olivine and Its Calibration as a Geothermometer // Contrib. Mineral. Petrol., 1979, v. 70, p. 59-70.
19. **Prast W.G.** Greenland - mines and prospects // Mining Magazine, 1973, v. 128, v. 25-30.
20. Rasmussen T.M. Aeromagnetic survey in central West Greenland: project Aeromag 2001 // Geology of Greenland Survey Bulletin, 2002, v. 191, p. 67–72.
21. **Sand K.K.** A geotherm for the cratonic lithospheric mantle in southern West Greenland: thermal implications for diamond potential // University of Copenhagen, 2007.
22. **Scott B.H.** Kimberlite and lamproite dykes from Holsteinsborg, West Greenland, Meddelelser om Grønland // Geoscience, 1981, № 4, 24 p.
23. **Secher K., Larsen L.M.** Geology and mineralogy of the Sarfartôq carbonatite complex, southern West Greenland // Lithos, 1980, v. 13, p. 199–212.
24. **Secher K., Nielsen T.F.D., Heaman L., Jensen S.M., Schjøth F.** Emplacement of kimberlites and UMLs in an alkaline province located 64º–67ºN in southern West Greenland – Evidence from 40 new robust age analyse // 9IKC, Frankfurt, 2008.
25. [25] Steenfelt, A.,2001, Geochemical atlas of Greenland - West and South Greenland, Rapport Grønlands Geologiske Undersøgelse 46.
26. **Steenfel A., Hollis J.A., Secher K.** The Tikiusaaq carbonatite: a new Mesozoic intrusive complex in southern West Greenland // Geological Survey of Denmark and Greenland Bulletin, 2006, № 10, p. 41-44.
27. **Steenfelt A., Jensen S.M., Sand K.K.** Distribution of kimberlite indicator minerals in till within the Neoproterozoic Sarfartoq-Maniitsoq province of kimberlite and ultramafic lamprophyres, southern West Greenland // Workshop on Greenland´s diamond potential, Copenhagen, 2005, 7-9 November, p 43.

28. **Tappe S.** Unpublished data.
29. **Thy P., Stecher O., Korstgård J.A.** Mineral chemistry and crystallization sequences in kimberlite and lamproite dikes from the Sisimiut area, central West Greenland // Lithos, 1987, v. 20 391–417.
30. **Tukiainen T., Krebs J.D.** Mineral resources of the Precambrian shield of central West Greenland (66° to 70°15' N). Part 4. Mapping of kimberlitic rocks in West Greenland using airborne hyperspectral data // Danmarks og Grønlands Geologiske Undersøgelse Rapport, 2004, v. 45, 39 p. + appendices and 1 DVD.
31. **Upton B.G.J., Emeleus C.H.** Mid-Proterozoic alkaline magmatism in southern Greenland: the Gardar Province // in: Fitton, J.G., Upton, B.G.J., (Eds), Alkaline Igneous Rocks, Blackwell Scientific, Boston, MA, 1987, p. 449–471.

УДК 553.81

Lithospheric mantle characteristics of the Nakyn field in Yakutia from datas on mantle xenoliths and basaltsin the Nyurbinskaya pipe

Sablukov S.M. [1], Sablukova L.I. [1], Stegnitsky Yu.B.[2], Banzeruk V.I. [3]

[1] "RUSGEO" Limited, Moscow;
[2] YaGEER&D CNIGRI, ALROSA Co. Ltd., Republic Yakutia (Sakha), Mirny;
[3] Nyurbinskaya Mine, ALROSA Co. Ltd., Republic Yakutia (Sakha), Mirny)

ANNOTATION

Mantle xenoliths (nodules), occurring in abundance in rock related to all plausible intrusion phases in the Nyurbinskaya pipe, vary in size from 2-6 cm to 21 cm. In all, more then 240 nodules have been examined. Petrologically, the xenoliths are dominated by various garnet peridotite and clinopyroxenite rocks and chrome spinel peridotite, with a minor proportion of spinel peridotite and eclogite (groups A and B). There also occur rare megacrysts of Ti-association orange garnet and macrocrystals of orange and red garnet of eclogite suite. Mantle xenoliths have a granular structure, with an almost complete absence of cataclastic ("sheared") peridotite, although fragments of banded (layered) rocks and rocks with unbalanced mineral paragenesis are abundant. About 10% of garnet peridotite and clinopyroxenite xenoliths contain picroilmenite with a peculiar composition appearing atypical of kimberlitic ilmenite, and their clinopyroxene also features a quite uncommon mineral chemistry. The behavior of TP parameters characterizing the examined nodules fits the 40 mW/m^2 conductive geotherm. The kimberlite pipes of the Nakyn field appear to be older than the other diamondiferous kimberlite pipes of Yakutia. Their peculiar geochemistry and mineralogy might reflect the early state of the lithospheric mantle, which appears to be more primitive, i.e., unaffected by Fe-Ti mantle metasomatic processes triggered by a Late Devonian asthenospheric diaper (mantle plume) so intense as obviously was case with the younger kimberlite rocks in the Malo-Botuobinsky, Daldyn-Alakitsky and Verkhne-Munsky provinces. A similar shift in rock chemistry (a sharp increase in Ti and Fe content along with a decrease in Al content) is also shown by the relatively young (post-kimberlite) mafic rocks in the Nyurbinskaya pipe with respect to the relatively old (pre-kimberlitic) mafic rocks occurring in the same pipe.

INTRODUCTION

Diamondiferous kimberlite rocks of the Nakyn field discovered in 1994 appear solitary with respect to diamond-bearing kimberlites from other Yakutian districts, not only in location but also in the majority of compositional characteristics. In particular, the Nakyn kimberlites are characterized by a predominance of chrome spinel and pyrope among the high pressure minerals (with almost total absence of picroilmenite), an essentially phlogopitic rock matrix,

and a peculiarly low concentration of all incompatible elements except for K and Rb [6, 9, 11, 23, 25 and many others].

Particular high-pressure mineral species from Nakyn field pipes (primarily garnet and chrome spinel and, mare rarely, clinopyroxene and picroilmenite) have been (and still are) the subject of quite extensive literature [2, 9, 11, 13, 23], while the information about mantle xenoliths in Nakyn field kimberlite rocks is a yet scanty. A very detailed research was devoted to the unique diamondiferous mantle xenoliths and mineral intergrowths encountered in the course of kimberlite concentration during mining at the Nyurbinskaya pipe [21, 22]; along with this, the presence of mantle nodules in this pipe was mentioned in these reports just in passing. Some attention was given to the presence of small single inclusions of serpentinite, garnet serpentinite, kyanite eclogite and glimmerite [7]. A somewhat more detailed description has been given to mantle xenoliths from the Botoubinskaya pipe [20], which is very similar in composition to the Nyurbinskaya pipe. This is why mantle rock xenoliths of the Nyurbinskaya pipe are worthy of thorough investigation, which undoubtedly would help gain more information on the structure and composition of lithospheric mantle for the whole Nakyn kimberlite field and establish the reasons for the already notified peculiarity of the Nakyn kimberlites.

A prominent feature of the Nyurbinskaya pipe consists in the presence of a pre-pipe dolerite intrusion (xenoliths of which occur in pipe kimberlites) and a post-pipe (penetrating) dolerite intrusion [8, 11]. Analysis of compositional peculiarities for the igneous rock bodies with differing age from the Nyurbinskaya pipe would contribute to revealing the peculiar features of temporal evolution of the upper mantle in the study area.

RESEARCH TARGETS AND ANALYTICAL METHODS

Description of core samples (800 meters run) and visual examination of quarry walls and ore yard stock-piles during a period a period since August 2006 till September 2007 revealed that mantle xenoliths occur in sizable amounts in rocks related to all intrusion phases evident in the Nyurbinskaya pipe; in some drill core intervals, their concentration ranges up to 6.3 xenoliths per 10 m run. In all, more than 240 mantle xenoliths were identified. These xenoliths are generally quite large, with a prevailing size between 4 and 6 cm (Fig. 1), and the biggest one proved to be as large as 21.2 cm (weighing as much as 3.5 kg). Nothing of the kind (neither in quantity nor by size) was ever encountered in our analysis of more than 20,000 m run of drill core samples examined altogether for kimberlite pipes of the Lomonosov deposit (Arkhangelsk district), to which the Nyurbinskaya pipe is commonly compared [6]. Along with thia, xenoliths size like this is quite common with kimberlite pipes from other Yakutian districts.

Most of the examined xenoliths are oval, very strongly (sometimes in a zoned fashion) altered (serpentinized, saponitized, carbonatized or silicified), with only

garnet and opaque minerals remaining unaltered and sporadically occurring relict of phlogopite, clinopyroxene and amphibole.

The mantle xenoliths were examined both visually and instrumentally (in transparent thin sections). Mineral chemistry (327 analyses) was analyzed using a Camebax SX-50 X-ray spectral microanalyzer (U = 15 kV; I = 15 nA) (Analytical Laboratory of GINTsVETMET; analyst: A.I. Tsepin).

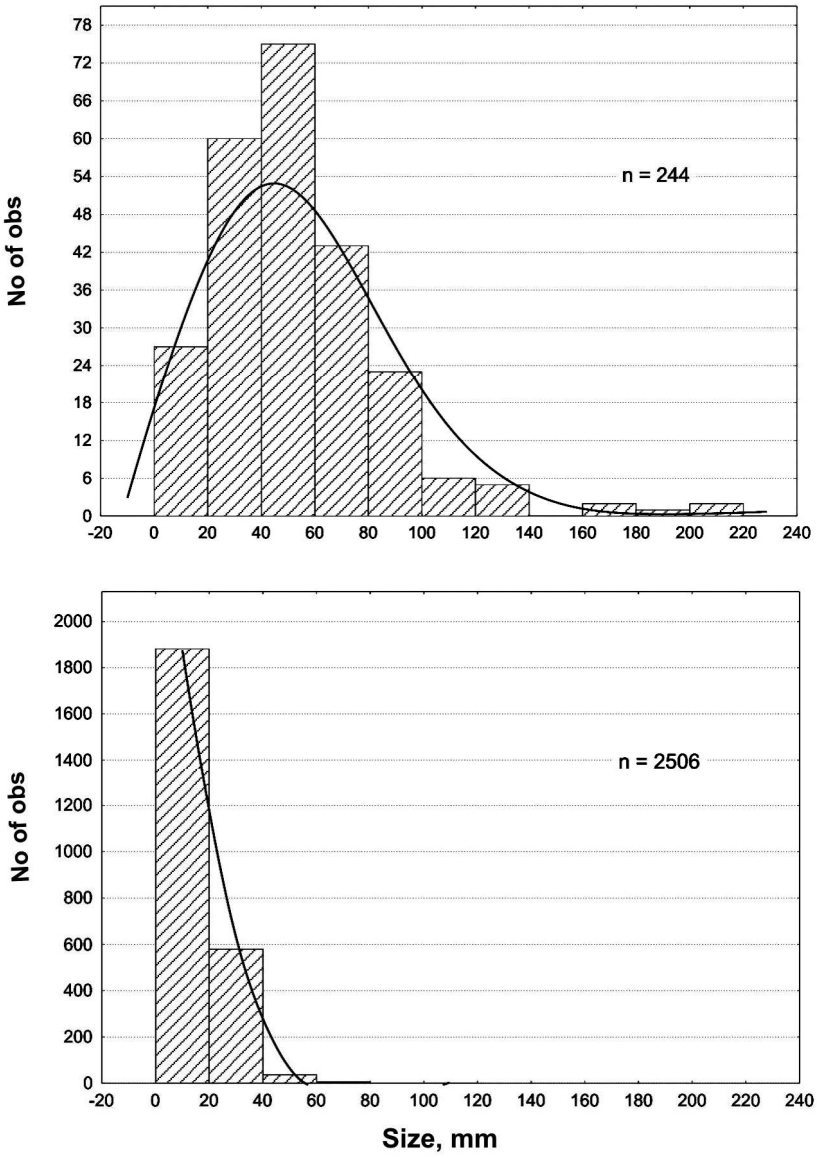

Fig. 1. **Histogram for the sizes of mantle xenoliths in the kimberlite rocks from Nyurbinskaya pipe (top) and Lomonosov deposit pipes, Zimni Bereg, Arkhangelsk province (botom)**

Pre-pipe dolerite xenoliths and post-pipe dolerite samples were examined in thin sections, by silicate analysis (Analytical Laboratory of GIN RAS), by ICP-MS analysis (Analytical Laboratory of IMGRE MNR RF), and lastly, by Nd-Sr isotope analysis (Analytical Laboratory of IGGD RAS).

MANTLE NODULES: PETROGRAPHY

To typify the mantle nodules, we used a number of classification schemes and criteria proposed by different researches [5, 12, 19, 26, 30]. Deep-seated inclusions can be generally subdivided into *deep-seated rock inclusions* (including their disintegration products, e.g., xenoliths, microxenoliths, intergrowths, oikocrysts, xenocrysts) and *megacrysts* (macrocrystals).

Classification of mantle xenoliths from the Nyurbinskaya pipe proved to be quite difficult due to intense alteration of the rocks involved, peculiar composition of some essential minerals, and significant compositional variability often shown by different grains of a common mineral species within a common sample (in some cases, these variations have a zoned distribution), probably pointing to certain deviation from equilibrium in respective mineral suites. At the present-day stage of investigation, the subdivision of the identified mantle xenolits into definite types or varieties can be just *preliminary*.

The spectrum of mantle inclusion varieties occurring in Nyurbinskaya pipe kimberlites is rather rich, including various ultramafics (with some combined, complexely structured rocks among them), mafic and megacrysts (or macrocrystals).

Mantle xenoliths are sharply dominated by ultramafic varieties (predominantly garnet-containing, with a minor proportion of chrome spinel ones) with relatively equigranular (allotriomorphic and hypidiomorphic granular) structures and some evidence of dynamo-metamorphism only present as small zones and bands of recrystallized olivine, whereas typical cataclastic ultramafics are almost totally absent. Metasomatic features, namely, phlogopitization of garnet and clinopyroxene, occur quite frequently.

Garnet-free ultramafics are represented essentially by spinel-bearing and chrome spinel peridotite varieties.

Spinel peridotite xenoliths occur rather rarely (in all, they are eight in number, which is 4.8% of the identified mantle xenoliths). They have a fine-grained crystalline texture (with some sideronitic elements) and a massive structure. Small, irregularly shaped chrome spinel grains are homogeneously dispersed in an olivinic ground-mass and fill the interstices between olivine grains.

Chrome spinel peridotite xenoliths are more abundant (16 in number, which is 9.6% of the identified mantle xenoliths). These rocks consist predominantly of altered olivine, with pseudomorphs after clinopyroxene occurring in amounts of 1-3% (occasionally, up to 10%) in some samples. Chrome spinel concentration is also quite low, varying from single grains to 1%. In addition, coarse-grained laths of chloritized mica also occur sporadically. These rocks have a fine-to-medium-grained crystalline texture and a massive structure. Chrome spinel occurs as small (0.1 - 0.2 mm) grains with varying habit: flat-faced octahedral, combination-type crystals, myriohedral crystals and xenomorphic grains; chrome spinel grains with differing morphology often occur together in a common sample.

Most of the Nyurbinskaya pipe mantle xenoliths are garnet-containing rocks.

Granular, massive garnet peridotite is the most abundant and diversified group of mantle xenoliths in the examined collection (it includes 106 xenoliths, which is 63.9% of the total number of mantle xenoliths identified). Although the proportions of the main rock-forming minerals in these xenoliths vary, most of them are characterized by an essentially olivinic composition (70-99% olivine). Clinopyroxene occurs in most of the samples but in moderate amounts (usually less than 5%, rarely up to 10-30%). Segregations of this mineral are irregularly shaped (quite commonly appearing as interstitial). Most of the clinopyroxene grains are altered, but relicts of emerald-green grains also occur. Ortopyroxene pseudomorphs are difficult to identify; they occur in a few samples in amounts of not more than 1-2%. Pyrope, like clinopyroxene, occur in amounts from single grains to 20-25%. Pyrope grains vary in color very widely, from orange-red, red and crimson to violet and lilac, with varying depth of coloration. Some samples of this group contain chrome spinel grains (similar in morphology to chrome spinels from chrome spinel peridotite xenoliths), rare picroilmenite grains of size about 0.5 mm, and coarse-grained laths of (usually chloritized) phlogopite and, rarely, bright green amphibole. The texture of these garnet peridotites is fine-to-medium-grained crystalline, allotriomorphic or hypidiomorphic granular, occasionally with some polygonal (protogranular) elements. The structure of these rocks is massive or, more rarely, with certain oriented elements appearing as subparallel, discontinuous chains of garnet grains in the olivinic groundmass.

Granular, banded garnet peridotite xenoliths are less abundant (in all, these are seven in number, which is 4.2% of the identified mantle xenoliths). These rocks are complexely structured and heterogeneous. Their texture is medium-to-grained crystalline, panidiomorphic or allotriomorphic granular, and the structure of these rocks is taxitic. Rocks of this group are banded, with band-shaped zones enriched with clinopyroxene and garnet (up to 30-50%) and, rarely, with orthopyroxene. All their rock-forming minerals (except for garnet) are altered, with relicts of emerald-green chrome-diopside occurring in just a few samples. Pyrope varies in color from red and crimson to violet, most of the grains being pale colored. In some of the samples, pyropes with differing color shades (pale crimson and pale violet, pale pink and pale red) occur together in garnet-rich zones, being therewith quite similar in composition.

In some samples of granular garnet peridotite, subparallel banding is very clearly defined, such that alternating layers of garnet peridotite and garnet pyroxenite are evident. These samples are somewhat transitional between garnet peridotite and garnet pyroxenite, both in structure and garnet composition (usually low-Cr). Rocks of this type quite commonly contain interstitial picroilmenite segregations.

Garnet clinopyroxenite (17 xenoliths, which is 10.2% of mantle xenoliths analyzed) are characterized by a medium-to-coarse-grained crystalline, hypidiomorphic granular texture, a massive structure and approximately equal

proportions of garnet and clinopyroxene. Some of the samples show large zones of fusion (or metasomatic working) manifested as zones of clinopyroxene replacement by a fine-grained scaly aggregate of chloritized phlogopite. Garnet shows a variety of color shades: orange, pale yellow-orange, pale yellowish-pink, pale reddish-crimson. In some samples, garnet grains with differing color and composition occur together. Relicts of clinopyroxene are of pale green color. About one third of clinopyroxenite samples contain irregularly shaped picroilmenite segregations; in some cases, rutile is present instead of ilmenite. Some of garnet clinopyroxenite samples could be classified as very high-Mg Group A eclogite [26], in spite of their low-Fe clinopyroxene and olivine composition (see below).

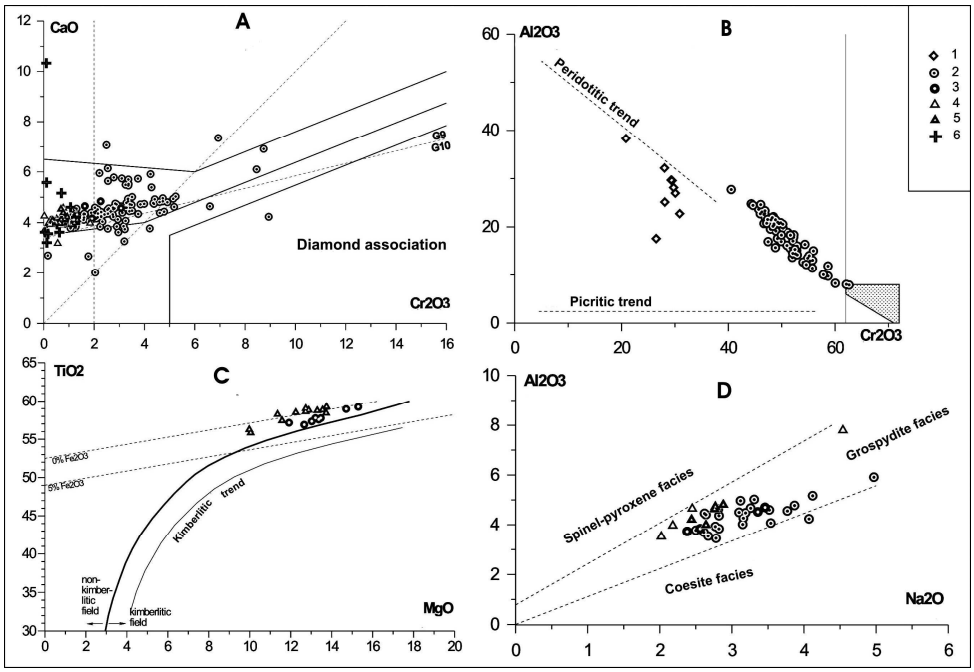

Fig. 2. **Chemical composition of mantle xenolith minerals from Nyurbinskaya pipe on diagrams (wt. %): A - garnets [19], B – chrome spinel [19], C - picroilmenite [32], D - clinopyroxene [15, 16]**

Symbols: minerals from xenoliths: 1 – spinel peridotites, 2 – chrome spinel and garnet peridotites, 3 – garnet peridotites with picroilmenite, 4 – garnet clinopyroxenites and eclogites, 5 - garnet clinopyroxenites and eclogites with picroilmenite, 6 – garnet megacrysts

Garnet megacrysts (macrocrystals) are rare (in all, 12 inclusions of this sort were identified, which is 7.2% of the xenoliths studied). These garnet grains vary in size from 0.8 to 3 cm and in color from orange to red.

MINERAL CHEMISTRY

Chrome spinel from *chrome spinel peridotite* samples is characterized by a vide variation in mineral chemistry (Fig. 2B). It is represented by high-Cr varieties

(45-62% Cr_2O_3) with lower than average FeO (below 20 wt. %) and TiO_2 contents (below 1 wt. %). Much the same composition is typical of chrome spinel from *garnet peridotite,* with only TiO_2 content occasionally ranging up to 1.56 wt. %. Judging from the compositional similarity of chrome spinel grains with a characteristic $Cr^{3+} \Leftrightarrow Al^{3+}$, isomorphism, these xenolith types are related to different dept facies, from grospydite (C_2) and coesite (C_3) to diamond-pyrope facies (D), therewith belonging to a common, syngenetic population of nodules. Along with this, chrome spinel from spinel peridotites corresponds in composition (below 30% Cr_2O_3, about 30% Al_2O_3, and 26-44% FeO) to the low-pressure spinel-pyroxene depth facies B [5, 15, 16], therewith differing drastically from chrome spinel from the other two nodule groups. This suggests that spinel peridotite xenoliths might represent a peculiar, individual nodule type (not necessarily of mantle origin), in contrast to mantle xenoliths from the Lomonosov deposit (Arkhangelsk district), where chrome spinels from different nodules form a continuous compositional sequence from picotite (facies B) to chromite (facies D)[15, 16].

Garnet from *massive garnet peridotite* is characterized by a rather widely varying Cr_2O_3 content (0,5 – 9 wt. %), with a predominance of low-Cr and medium-Cr garnet varieties of lherzolite suite, and only a few garnet grains of wehrlite and dunite-harzburgite suite (Fig. 2A). Note that garnet grains with relatively high Cr_2O_3 (5-9 wt. %) and TiO_2 contents (0.2-0.6 wt. %) occur in those nodules that contain no chrome spinel. All the analyzed garnets from *banded garnet peridotite* nodules represent a low-Cr (0.6-3.74% wt. % Cr_2O_3) garnet variety of lherzolite suite with higher than average FeO content (8-10%).

Garnet clinopyroxenite xenoliths can be subdivided into two groups based on garnet chemistry. The first, high-Mg garnet variety with low Cr_2O_3 (0,07-0,18 wt. %) and higher than average FeO contents (9.9-11.7 wt. %) corresponds to garnet from Group II(A) eclogites (according to the classification scheme of Schulze [30]), being similar in composition to G7 cluster group garnets from diamond-bearing rock xenoliths of the Nyurbinskaya pipe [21, 22], whereas the high-Mg garnets with higher than average Cr_2O_3 (1.84-2.24%) and lower than average FeO contents (7.6-9.1 wt. %) are similar to garnet from peridotite and clinopyroxenite, both of these garnet varieties occurring together in some of the analyzed nodules.

Garnets from *ilmenite-containing peridotite and clinopyroxenite* nodules are characterized by a medium Cr_2O_3 content (up to 2 or, rarely, 3 wt. %) and, in some cases, higher than average TiO_2 content (up to 0.25-0.5 wt. %).

Orange garnet *macrocrystals* are characterized by a low Cr_2O_3 content (0.11-0.17 wt. %) and higher than average FeO (9.68-20.66 wt. %) and, in some cases, TiO_2 (0.40-0.76 wt. %) and CaO contents (up to 10.33 wt. %). Red garnet macrocrystals show a higher Cr_2O_3 content (0.71%) and lower FeO (8.74 wt. %) and TiO_2 contents (0.15 wt. %). According to the classification scheme proposed in [30], orange garnets correspond to Ti association megacrysts and Group A and Group B eclogites, and the red garnets to group A eclogite.

Picroilmenite from different mantle xenoliths is characterized by higher than average TiO_2, MgO and Cr_2O_3 contents, being almost free of hematite component. In the classification diagram (Fig. 2C), its composition falls outside of the compositional field of typical kimberlitic picroilmenite [32]. Along with this, picroilmenite from *peridotite* nodules, when compared to that from the *clinopyroxenite* ones, is generally characterized by higher MgO (11.9-15.3% against 9.98-13.75 wt. %) and, especially, Cr_2O_3 contents (1.12-1.82 wt. % against 0.25-0.89%).

Clinopyroxene from different nodules in the Nyurbinskaya pipe rocks (Fig. 2D) are unexpectedly similar in composition, being generally characterized by a high #Ca index (47.6-50.6, with an average of 49.9), higher than average Na_2O (2-5 wt. %) and Al_2O_3 contents (3.5-5.5 wt. %) and lower than average FeO (1.3-2.4 wt. %) and MgO contents (12.6-15.0 wt. %), with a varying Cr_2O_3 content (0.07-3.85 wt. %). Only in a few samples does clinopyroxene chemistry fall outside these narrow ranges. This being so, clinopyroxenes from garnet-containing and chrome spinel peridotites are very similar in composition; clinopyroxenes from peridotite and clinopyroxenite (including eclogite) nodules differ only in Cr_2O_3 content (respectively, below 1 wt. % and more than 1 wt. % Cr_2O_3); lastly, picroilmenite-containing rocks only slightly differ in clinopyroxene chemistry from respective ilmenite-free rockvarieties. In general, nodules from the Nyurbinskaya pipe differ significantly in clinopyroxene composition from similar nodules hosted in Zimni Bereg kimberlites, both those of the Al-series (the Lomonosov deposit) and the Fe-Ti series ones (the V. Grib deposit)[14, 16, 18], and, probably, from nodules of the same type hosted in kimberlite pipes of other kimberlite fields in the Yakutian province.

Generally speaking, minerals of mantle nodules from the Nyurbinskaya pipe vary in composition rather widely, some of them (particularly, clinopyroxene and picroilmenite) showing compositional features atypical of respective kimberlite-hosted mineral species occurring in other regions. Along with this, the presence or absence of picroilmenite in the nodules has no effect on the composition of other minerals involved (namely, clinopyroxene and garnet) as is typical of ilmenite peridotite xenoliths (Fe-Ti series mantle rocks after Marakushev [12]). With this in mind, almost all the examined xenoliths can be tentatively classified as Mg-Al series mantle rocks (after [12]), while only some Ti-garnet macrocrysts (megacrysts) can be (also tentatively) classified as Fe-Ti series mantle rocks. In addition, the significant dissimilarity in composition sometimes shown by different grains of a common mineral species (primarily garnet) in a common sample, i.e., some deviation from equilibrium in their mineral suites, is also worthy of note.

NODULE FORMATION: TP PARAMETERS

To establish the TP parameters that governed the formation of the examined mantle xenoliths, we used mineral chemistry data for the clinopyroxene+garnet

(Cpx+Ga) mineral paragenesis, which is most common to different nodule types. The temperature was determined from the NS94T geothermometer, and the pressure from the NS94P barometer [28], with the analytical method respectively modified for peridotite and eclogite. The moderate dispersion of the results obtained and the fact that they are not contradictory to petrographic characteristics of the examined xenoliths confirm the correctness of using this method in this study (Fig. 3).

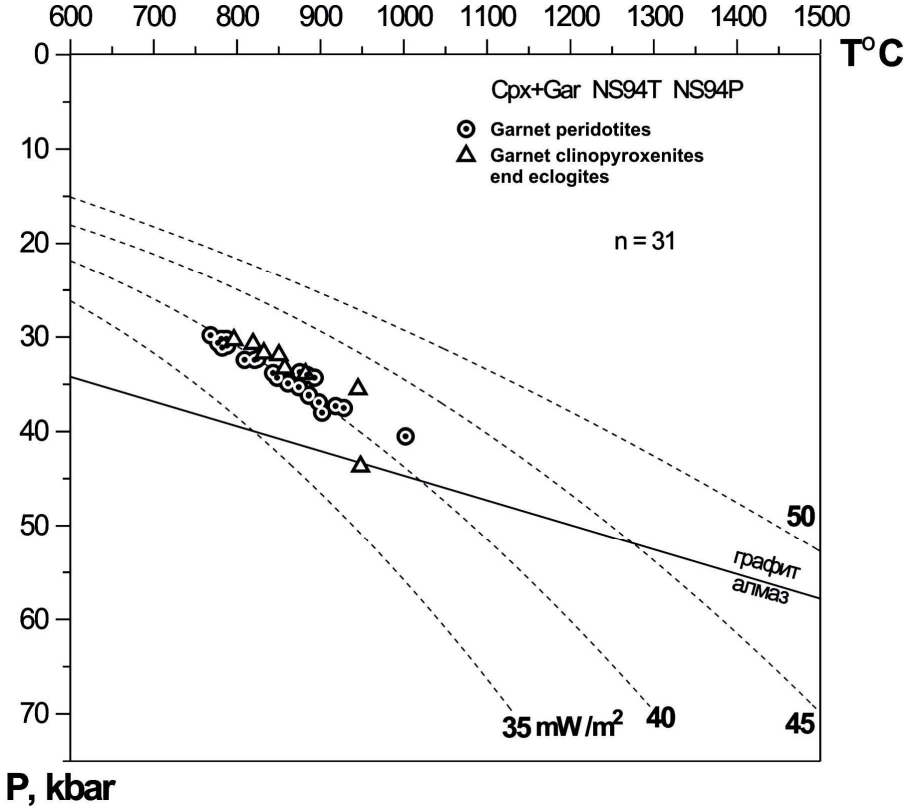

Fig. 3. **TP parameters of formation of mantle xenoliths from Nyurbinskaya pipe kimberlites**

The temperature and pressure are calculated on paragenesis garnet-clinopyroxene [28]. A line graphite - diamond on [27]; lines a conductive geoterm on [29].

Garnet peridotite (23 samples) is characterized by a very restricted range of TP forming parameters: 768-928 ^{o}C (up to 1002 ^{o}C) and 29.8-37.5 kbar (up to 40.5 kbar), and it is interesting that different petrological varieties of peridotite (including the ilmenite-containing ones) are similar in these parameters. Nearly the same TP parameters are characteristic of different garnet clinopyroxenite and eclogite varieties (eight samples): 796-945 ^{o}C (up to 948 ^{o}C) and 30.3-35.5 kbar (up to 43.7 kbar). Only one eclogite sample falls into the field of diamond stability [27] (essentially at the graphite-diamond boundary), while all the remaining nodules correspond to grospydite and coesite depth subfacies [5]. In general, the behaviour of forming parameters for the examined nodules and different types of peridotite and eclogite fits well to the 40 mW/m^2 [29].

RESULTS AND DISCUSSION

Mantle xenoliths of the Nyurbinskaya pipe are dominated by various garnet peridotite and clinopyroxenite rocks and chrome spinel peridotites, with a minor proportion of spinel peridotite and Group A and Group B eclogites [26]. In addition, rare megacrysts of Ti-assiciation orange garnet and orange and red garnet of eclogite suite also occur. The analyzed mantle xenoliths have a granular structure, with almost total absence of cataclastic peridotite and certain abundance of banded (laminated) rocks and rocks with unbalanced mineral suites. About 10% of garnet peridotites and clinopyroxenite xenoliths contain picroilmenite with peculiar mineral chemistry (atypical of kimberlitic ilmenite), and clinopyroxene chemistry is also somewhat uncommon.

Judging from mineral chemistry data calculated TP forming parameters, the examined mantle xenoliths are related just to the middle part of the sequence of mantle rocks captured by kimberlite magmas. However, some high-pressure minerals from kimberlite concentrate samples tend to characterize a somewhat wider range of penetrated mantle rocks.

In general, the Nyurbinskaya pipe kimberlites are more similar in abundance and size of mantle xenoliths and in sharp predominance of garnet peridotite xenoliths to kimberlites from other Yakutian kimberlite fields and to Group 1 kimberlites than to geochemically similar kimberlites of the Lomonosov deposit in the Arkhangelsk province [6]. Along with this, the kimberlite rocks of the Nyurbinskaya pipe differ drastically from other Yakutian kimberlites by their high chrome spinel peridotite xenolith content, by the presence of picroilmenite with atypical composition in the xenoliths, and by a complete absence of characteristic picroilmenite megacrysts.

It is conceivable that the prominent compositional peculiarity of Nakyn field kimberlites may be related to lateral heterogeneities in mantle substrate of the Yakutian province. Of course, it is also not improbable that the revealed sharp distinctions in rock composition may be just related to nonsynchronous intrusion of kimberlite magmas, which “recorded” the specific state of mantle characterizing different periods of its evolution. However, the profound scatter of available radiogeochronological dating results for Nakyn field kimberlites, as broad as form 332 to 450 Ma [1, 24, 31], leaves this suggestion without any support.

Having subjected a common set of Nyurbinskaya pipe kimberlite samples to K-Ar dating (three samples: 396+/-8 Ma, 404.5+/-9,0 Ma, 399+/-8 Ma, with an average of 399.8+/-8 Ma) and to Rb-Sr dating (isochrone age: 399.6+/-4.6 Ma; N=5; initial $^{87}Sr/^{86}Sr$ = 0,70522+/-0,00019; MSWD=1,3), we established the intrusion age for the Nyurbinskaya pipe (and, probably, for the other pipes of the Nakyn field) as 399.6+/-4.6 Ma, which is Early Devonian, Emsian (D_1em) [17]. This age is more than by 40 Ma older than the Late Devonian to Early Carboniferous (340-350 Ma) age of kimberlites from other Yakutian districts [3].

It is conceivable that it is precisely the older age of the Nyurbinskaya pipe as compared to kimberlites in other Yakutian diamond-bearing kimberlite fields that is responsible for its compositional peculiarity.

The Nyurbinskaya kimberlite pipe is a complicated volcanic complex, which formed as a result of multiple local volcanic events (multi-stage volcanic activity). In addition to several magmatic rock bodies related to different phases of essentially kimberlite intrusion, this complex incorporated a pre-pipe dolerite intrusion (xenoliths of which occur in the kimberlites) and a post-pipe dolerite intrusion penetrating the kimberlites [8, 11].

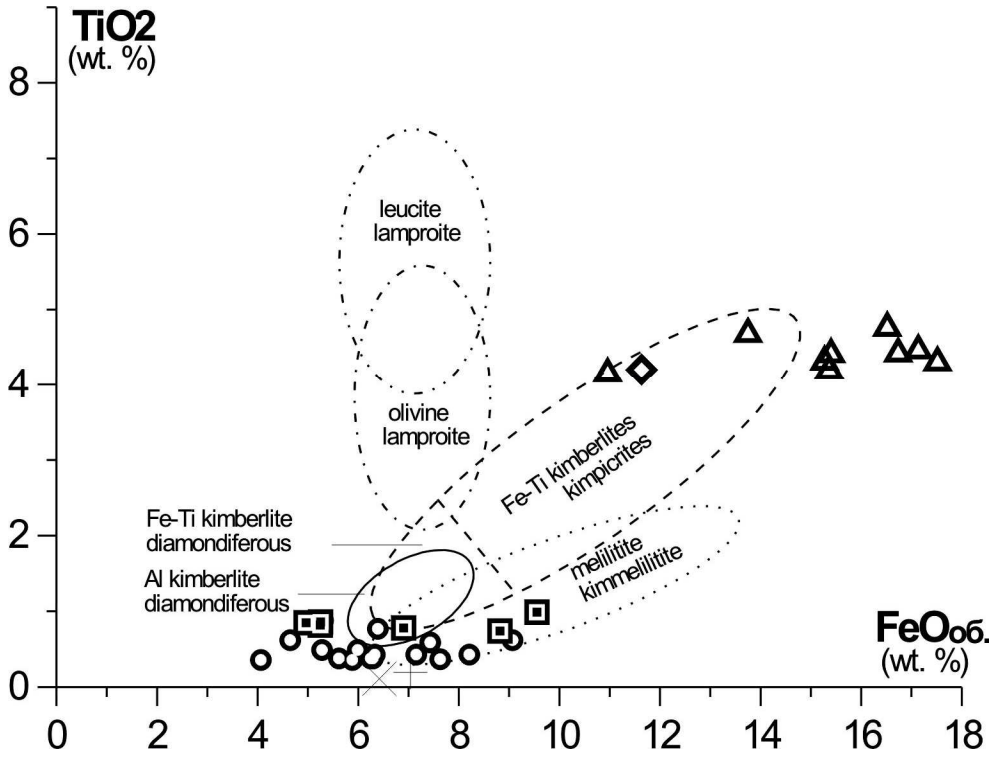

Fig. 4. **Chemical composition of volcanic rocks from the Nyurbinskaya pipe in coordinates: FeO_{tot} - TiO_2**

Circles – kimberlites of different types; a square – xenolits of the pre-pipe dolerits; triangles - post-pipe dolerite intrusions; a rhombus - a body of basalts in 160 m to the east from Nyurbinskaya pipe (skv 4/660).

Our preliminary investigation (a comprehensive study of mafic rocks is now still on run, such that only first, tentative results are presented here) revealed that petrographically similar but obviously nonsynchronous mafic volcanic rock bodies (separated from each other by the kimberlite intrusion stage) show not simply dissimilar but radically differing geochemical characteristics. Only SiO_2, Na_2O, K_2O and Co contents of pre-kimberlite and post-kimberlite dolerites are somewhat similar. Pre-kimberlite dolerites are 1.5 times higher in Al_2O_3 and MgO, 2 to 3 times higher in Ba and Pb, 5 times higher in Ni and 15(!) times higher in Cr as compared to post-kimberlitic dolerites. Along with this, post-kimberlitic dolerites

are richer than the pre-kimberlitic ones in the overwhelming majority of elements: FeOtot, CaO, Be, V, Ga, Rb, Cs, Sr, (by a factor of 1.5-2.5), TiO_2, MnO, P_2O_5, Cu, Zn, Y, Zr, Hf, REE, Th, U, (by a factor of 3 to 6), and more than ten times richer in Nb and Ta(!). The most prominent geochemical features of the pre-kimberlitic ("old") mafic rocks of the Nyurbinskaya pipe are their significantly lower Ti and Fe contents and higher Al content as compared to those of the post-kimberlitic ("young") mafic rocks of this pipe (Fig. 4). Geochemically, the pre-kimberlitic dolerites are likely to be related to some geochemically depleted source, whereas the inferred source of post-kimberlitic dolerites must be sharply geochemically enriched.

This radical geochemical dissimilarity between dolerites with differing age in the Nyurbinskaya pipe may be indirect evidence of their differing mantle origin and profound difference in time of intrusion. Along with this, in most of the published literature these dolerites are all deemed to be Devonian (Middle Paleozoic), and to have mantle sources similar to each other and to those of Nakyn field kimberlites, including the almost common protolith model age for kimberlite and mafic rocks with respect to depleted mantle: $T_{Nd}(DM)$ = 1100 Ma [8].

Our preliminary isotopic dating of different volcanic bodies incorporated in the Nyurbinskaya pipe complex (kimberlites, pre-kimberlite and post-kimberlite dolerites) revealed a drastic dissimilarity in their age and Nd-Sr characteristics (including the model age $T_{Nd}(DM)$). The Rb-Sr dating gave an inferredly Late Riphean age for pre-kimberlitic dolerites (isochrone age 703+/82 Ma; N=3; initial $^{87}Sr/^{86}Sr$ = 0.70750+/-0.00015; MSWD=1.9) and a supposedly Late Carboniferous to Early Permian age post-kimberlitic dolerites (isochrone age 269+/-12 Ma; N=3; initial $^{87}Sr/^{86}Sr$ = 0.70817+/-0.00039; СКВО=1,01). The K-Ar age of one of the pre-kimberlitic dolerite samples (656 Ma) agrees well with its age determined from the Rb-Sr isochrone (703 Ma). The K-Ar age of two other samples with a higher than average K_2O content (326-346 Ma) might be "juvenated" by the action of post-kimberlitic dolerites (328-356 Ma). For post-kimberlitic dolerites, the age of a basalt glass sample appears to be the most trustworthy as this sample represents a rock that most adequately reflects the composition of the primary basaltic melt (328 Ma). Based on K-Ar and Rb-Sr dating results considered together, there is reason to believe that the pre-kimberlitic dolerites are of Late Riphean age (700 Ma), while the post-kimberlitic dolerites appear to be Middle Carboniferous (328 Ma). This sharp difference in dating for the three distinct stages of magmatic activity in the Nyurbinskaya pipe agrees well both the sharp boundaries between the rock bodies related to the three different intrusion stages and with their profound geochemical dissimilarity. The Nd-Sr isotope characteristics of the rocks related to the three different intrusion stages are also drastically dissimilar, as can be seen from the eSr – eNd diagram (Fig. 5). Pre-kimberlite dolerites are related to old enriched lithospheric mantle (EM II, eNd = - 12.2, eSr = +54.6) with a model age $T_{Nd}(DM)$ = 2450 Ma, probably with some old lower crust material involved.

Post-kimberlitic dolerites originated from depleted mantle (eNd = +4.7, eSr = +43.7) with a model age $T_{Nd}(DM)$ = 770 Ma, inferredly with some participation of young upper crust material. The mantle source of Nyurbinskaya pipe kimberlites appears to be close to BSE and enriched with radiogenic Sr (eNd = +1.0, eSr = +25.2; model age $T_{Nd}(DM)$=1100 Ma), which fits well to previously reported data [6, 10].

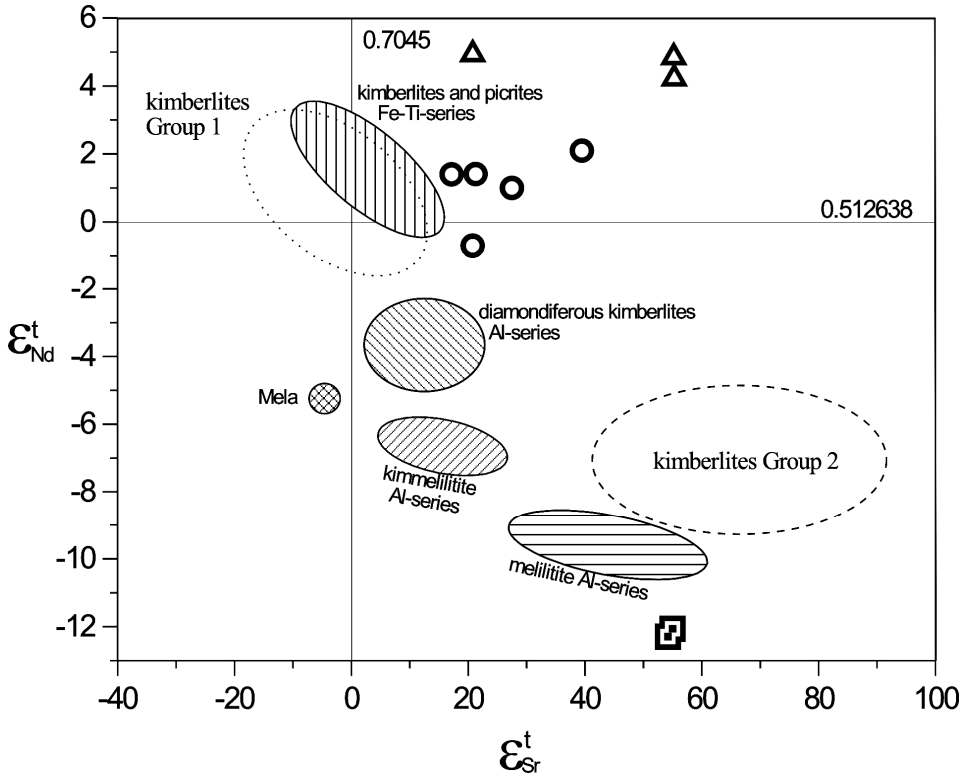

Fig. 5. **Sr and Nd isotope composition of the volcanic rocks from the Nyurbinskaya pipe in comparison by volcanic rocks of Zimni Bereg (Arkhangelsk province) [4].**

Symbols - see figure 4.

To summarize, the rock bodies related to three distinct stages of magmatic activity in the Nyurbinskaya pipe differ drastically both in intrusion age and in essentially all geochemical and isotope characteristics. The most profound geochemical distinction consists in that the pre-kimberlitic ("old") mafic rocks involved in the examined volcanic complex are significantly lower in Ti and Fe and higher in Al as compared to the post-kimberlitic ("young") mafic rocks in the same pipe (Fig. 4). It is interesting that the most prominent petrochemical difference between Nakyn field kimberlites (relatively old, Early Devonian) and kimberlites from other Yakutian kimberlite fields (relatively young, Late Devonian and Mesozoic rocks) also consists in comparatively low Ti and Fe contents and a relatively high Al content of the "old" Nakyn kimberlites (Fig. 4). In addition, protolith model age of the "young", post- kimberlitic, Fe- and Ti-enriched dolerites of the Nyurbinskaya pipe ($T_{Nd}(DM)$ = 770 Ma) proved to be close to that of the

relatively young (as compared to Nyurbinskaya pipe kimberlites), also Fe- and Ti-enriched, kimberlites in other Yakutian kimberlite fields (T_{Nd}(DM) = 0.7-0.6 Ga)[10].

It is not inconceivable that these characteristic geochemical distinctions between the "old" and "young" mafic rock bodies in the Nyurbinskaya pipe and the geochemical difference of quite the same type between the relatively old Nyurbinskaya pipe kimberlites and relatively young kimberlites from other Yakutian districts (Figure 4) are due to the action of some similar geological processes which exerted a similar effect on corresponding zones in upper mantle, i.e., zones of magma generation for mafic rocks and kimberlites.

The role of a global geological factor that could have such a profound impact on (an least) upper mantle geochemistry and cause intensive Fe-Ti mantle metasomatism could be played by an asthenospheric diaper, intrusion, or mantle plume. The relatively old rocks (both mafic and kimberlites) that intruded prior to the plume effect might have bearing on the composition of old, geochemically depleted lithospheric mantle, while the relatively young rock bodies (both mafic and kimberlite) that intruded after the action of the mantle plume might reflect the composition of geochemically enriched (by the plume) upper mantle with varying degree of metasomatic transformation. This difference manifests itself both in geochemical peculiarities of respective rock varieties with differing age and in peculiar characteristics of "directly" mantle rock fragments, i.e., deep-seated xenoliths, which could be treated as "records" of the state of mantle in different periods of its evolution (prior to the plume intrusion and after this event).

The relatively old (pre-plume) magmatic rocks, i.e., Early Devonian kimberlites of the Nyurbinskaya pipe and the mafic rocks penetrated by the pipe, are characterized by low Fe and Ti contents and by a total absence of picroilmenite in kimberlites, along with the atypical, "non-kimberlitic" composition of picroilmenite in rare mantle xenoliths. The relatively young (post-plume) magmatic rocks, i.e., the mafic rocks penetrating the kimberlites of the Nyurbinskaya pipe, as well as the Late Devonian and Mesozoic kimberlites in other Yakutian kimberlite fields, are characterized by higher than average Fe and Ti contents and a ubiquitous presence and/or very high concentration of picroilmenite in kimberlite rocks, along with the typical "kimberlitic" composition of picroilmenite both in kimberlites and in mantle xenoliths.

The post-plume, metasomatized state of upper mantle is reflected in different rock characteristics in the majority of Yakutian kimberlite fields, whereas the pre-plume, "relict" state of geochemically depleted upper mantle is only inferred for Nakyn field kimberlites. This is why the direct examination of mantle rock fragments from kimberlites of the Nakyn field is undoubtedly of interest as an investigation of relict rocks characterizing the zones that previously existed in the upper mantle but than vanished as a result of complete transformation in later geological events. This ***direct*** examination of mantle rock fragments is no less

(and, maybe, even more) important and interesting than the *indirect* study of mantle rocks through the medium od geochemical and isotopic characteristics of their host kimberlites.

CONCLUSIONS

In general, kimberlite rocks of the Nyurbinskaya pipe are more similar in abundance and size of mantle rock xenoliths in sharp predominance of garnet peridotite xenoliths to kimberlite rocks from the other Yakutian kimberlite fields and to Group 1 kimberlites than to geochimically similar kimberlites of the Lomonosov deposit in the Arkhangelsk province [6]. Along with this, the abundance of chrome spinel peridotite rocks, the presence of picroilmenite with atypical composition in rock xenoliths and the absence of characteristic picroilmenite megacrysts make the Nyurbinskaya pipe sharply different from other Yakutian kimberlites. Judging from mineral chemistry and calculated TP forming parameters, the examined mantle xenoliths characterize just the middle part of succession of mantle rocks captured by kimberlite magmas.

The Nyurbinskaya pipe, like all known kimberlite pipes of the Nakyn field, might be older than the other Yakutian kimberlite pipes. Its geochemical and mineralogical peculiarity might reflect the early state of the mantle, somewhat more primitive, yet unaffected by a Fe-Ti mantle metasomatism under the action of a Late Devonian asthenospheric diaper (mantle plume) so intence as was the case with mantle substrate of relatively younger kimberlites of the Malo-Botuobinsky, Daldyn-Alakitsky and Verkhne-Munsky district.

ACKNOWLEDGEMENTS

The autors are grateful to all the geologists and engineers affiliated in the Nyurbinsky Mine, Mirnenskaya geological prospecting expedition and YaGEER&D CNIGRI, ALROSA Co. Ltd., who not only presented us with a possibility of examining the quarry walls, ore yard stockpiles and drillcore samples but also rendered us the utmost help and assistance in our field work.

REFERENCES

1. **Agashev A.M., Pohilenko N.P., Tolstov A.V., Poljanichko V.V., Mal'kovets V.G., Соболев. Н.В.** New data on age of the kimberlites from the Yakutia diamond province // Doklady RAS, 2004, v. 399, № 1, p. 95-99.
2. **Ashchepkov I.V., Vladykin N.V., Rotman A.J. etc.** Features of a structure lithospheric mantle of the Nakyn kimberlite fields and on xenoliths and xenocrysts Nyurbinskaya pipe // Works of IV International Seminar «Deep magmatism, its sources and connection with plume processes ». Irkutsk - Ulan-Ude, 2004, p. 145-165.
3. **Brahfogel' F.F.** Geological aspects of the kimberlite magmatism of Northeast of the Siberian platform. Yakutsk, 1984, p. 128.
4. **Verichev E.M., Sablukov S.M., Sablukova L.I., Zhuravlev D.Z.** New type diamondiferous kimberlites of the Zimni Beregt (Arkhangelsk province) // Reports of the RAS, 1999, v. 368, № 2, p. 226-229.

5. **Deep seated xenoliths and the upper mantle** / under Red. Sobolev. V.S., Dobretsov N.L., Sobolev N.V. Novosibirsk: Nauka, 1975, p.272.
6. **Golubeva J.J., Pervov, V.A., Kononova V.A.** Low-titanium diamondiferous kimberlites – a new petrogeohemical type. Comparison Nakyn (Yakutia) and Zolotiza (the Arkhangelsk area) versions // Regional geology and metallogeny, 2006, v. 27, p. 15-25.
7. **Zankovich N.S., Zinchuk N.N.** Petrographical and mineralogical characteristics of the kimberlitye pipes of different phases of Nakyn fields // Problems of diamond geology and some ways of their decision. Voronezh, 2001, p. 54-72.
8. **Zemnuhov A.L., Zajtsev A.I., Kopylova A.G., Tomshin M.D., Janygin J.T.** Basaltic magmatism Khannja-Nakyn district // Geology of diamond - the present and the future. Voronezh, 2005, p. 482-494.
9. **Zinchuk N.N., Aljabjev T.E., Banzeruk V.I., Stegnitsky Ju.B., Rotman A.J., Egorov K.N., Koptil' V.I.** Geology, material structure and diamond potential of the kimberlites from the Nakyn kimberlite fields of Yakutia (on an example of Nyurbinskaya pipe). // Geology of diamond - the present and the future. Voronezh, 2005, p. 807-824.
10. **Kononova V.A., Golubeva J.J., Bogatikov O.A., Nosova A.A., Levskij L.K., Ovchinnikova G.V.** Geochemical (ICP-MS geochemistry, isotopy Sr, Nd, Pb) heterogeneity kimberlites from Yakutia: questions of genesis and diamond potentiale. // Petrology, 2005, v. 13, № 3, p. 227-252.
11. **Kornilova V.P., Fomin A.S., Zajtsev A.I.** New type diamondiferous kimberlites on the Siberian platform // Regional geology and metallogeny, 2001, v. 13-14, p. 105-117.
12. **Marakushev, A.A.** Peridotite nodules in kimberlites and basalts as indicators of deep litosphere structure // Proc. 27th IGC, Petrol., Sect. S.09, Moscow, Nauka, 1984, v. 9, p. 153-161 (in Russian).
13. **Pohilenko N.P., Sobolev N.V., Zinchuk N.N.** Anomaly kimberlites the Siberian platform and Slave craton, Canada, their major features in connection with a problem of forecasting and searches // Diamonds and diamond potential of the Timan-Ural region. Materials of the All-Russia meeting. Syktyvkar, 2001, p. 19-21.
14. **Sablukov S.M.** Petrochemical series of the kimberlite rocks // Dokl. AN SSSR, 1990, v. 313, № 4, p. 935-939 (in Russian).
15. **Sablukov S.M., Budkina L.I.**) Deep inclusions and features of a chemical compound of coexisted minerals // Works TsNIGRI, 1988, v. 229, p 16-23.
16. **Sablukov S.M., Sablukova L.I., Shavirina M.V.** 2000. Mantle xenoliths in the Zimny Bereg kimberlite deposits of rounded diamonds, Arkhangelsk diamondiferous province // Petrologiya, v. 8, № 5, p. 466-494.
17. **Sablukov S.M., Banzeruk V.I., Sablukova L.I., Stegnitskij J.B., Bogomolov E.S., Lebedev V.A.** Ancient age of the Nakyn field kimberlites (Yakutia) - one of the reasons of an originality of their material structure // VIII Inter. conf. «New ideas in sciences about the Earth». Moscow, Reports, 2007, v. 5, p. 209-212.
18. **Sablukova L.I., Sablukov S.M., Verichev E.M., Golovin N.N.** Petrography and chemistry of minerals mantle xenoliths and xenocrysts from Grib kimberlite pipe, Zimni Bereg, Russia. // Works of III Inter. Sem. «Plumes and a problem of deep sources alkaline magmatism» (Khabarovsk). Irkutsk, 2003, p. 159-187.
19. **Sobolev, N.V.**. The deep seated inclusions in kimberlites and the problem of the upper mantle composition. Publishing House “Nauka”, Siberian Branch, Novosibirsk, 1974 (in Russian).
20. **Spetsius Z.V., Serenko V.P.** Deep seated xenoliths from Nakyn kimberlite fields // Geological aspects of a mineral base of joint-stock company " ALROSA ", a modern condition, prospects, decisions. Additional materials. Peace, 2003, Pp. 191-195.

21. **Spetsius Z.V., Mitjuhin S.I., Ivanov A.S., Banzeruk S.V.** Associations with diamond in kimberlite pipes of the Nakyn field: the appendix to a technique of searches // Geology of diamond - the present and the future. Voronezh, 2005, p. 1083-1095.
22. **Spetsius Z.V., Тейлор L., Валей D.** Chemy and $d^{18}O$ garnets in diamondferous xenoliths from Nyurbinskaya pipe // Works of VI International Seminar « Deep magmatism, its sources and plume». Irkutsk, 2006, p. 71-95.
23. **Tomshin M.D., Fomin A.S., Janygin J.T. etc.** Features of magmatic formations Nakyn kimberlite fields of the Yakutia province // Geol. and geophys., 1998, v. 39, № 12, p. 1693-1703.
24. **Agashev A.M., Fomin A.S., Watanabe T., Pokhilenko N.P.** Preliminary age determination of recently discovered kimberlites of the Siberian kimberlite province // 7-th IKC. Exstented Abstracts. Kape Town, 1998, p. 9-10.
25. **Cherny S.D., Fomin A.S., Yanygin Ju.T., Banzeruk V.I , Kornilova V.P.** Geology and composition of the Nakyn field kimberlite pipes and diamond properties (Yakutia) // 7-th IKC. Exstented Abstracts. Kape Town, 1998, p. 9-10.
26. **Coleman R.G., Lee D.E., Beatty L.B., Brannock W.W.** Eclogites and eclogites: their differences and similarities // Bull. Geol. Soc. Amer., 1965, v. 76, № 3, p. 483-508.
27. **Kennedy C.S., Kennedy G.C.** The equilibrium boundary between graphite and diamond // J. Geophys. Res., 1976, v. 81, p. 2467-2470.
28. **Nikitina L.P. and Simakov S.K.** TERRA nova. Fifth International EMPG Symposium, 1994, v. 6. p. 34.
29. **Pollack H.N. and Chapman D.S.** On the regional variation of heat flow, geotherms, and lithospheric thikness // Tectonophysics, 1977, v. 38, p. 279-296.
30. **Schulze, D.J.** A classification scheme for mantle-derived garnets in kimberlite: a tool for investigating the mantle and exploring for diamonds // In: Jones, A.G., Carlson, R.W. and Grutter, H. (Eds.), A Tale of Two Cratons: The Slave-Kaapvaal Workshop. Lithos, 2003, v. 71, № 2-4, p. 195-213.
31. **Shamshina E.A., Zaitsev A.I.** New age of Yakutian kimberlites // 7-th IKC. Exstented Abstracts. Kape Town, 1998, p.783-784.
32. **Wyatt, B.A, Baumgartner, M., Ancar, E. and Grutter, H.** Compositional classification of “kimberlitic” and “non-kiberlitic” ilmenite // 8th Inter. Kimb. Conf., Selected Papers, Lithos, 2004, v. 2, v. 77, p. 819-840.

UDK 550.42+552.111

RHÖNITE IN SILICA-UNDERSATURATED ALKALI BASALTS: INFERENCES ON SILICATE MELT INCLUSIONS IN OLIVINE PHENOCRYSTS

Sharygin V.[1], Kóthay K.[2], Timina T.[1], Szabó C.[2], Pető M.[2], Török K.[2, 3], Vapnik Y.[4], Kuzmin D.[1, 5]

[1] *Institute of Geology and Mineralogy SD RAS, Koptyuga pr. 3, 630090 Novosibirsk, Russia*
[2] *Lithosphere Fluid Research Lab, Department of Petrology and Geochemistry, Eötvös University, Pázmány Péter sétány 1/C, H-1117 Budapest, Hungary*
[3] *Research Group for Environmental Physics and Geophysics of the Hungarian Academy of Sciences, Department of Geophysics, Eötvös University, Pázmány Péter sétány 1/C, H-1117 Budapest, Hungary*
[4] *Department of Geological and Environmental Sciences, Ben-Gurion University of the Negev, P.O. Box 653, 84105 Beer-Sheva, Israel*
[5] *Max Planck Institute for Chemistry, Geochemistry Division, 55020 Mainz, Germany*

ABSTRACT

Silicate melt inclusions containing rhönite **$Ca_2(Mg,Fe^{2+})_4Fe^{3+}Ti[Al_3Si_3O_{20}]$** were studied in olivine phenocrysts from alkali basalts of six different volcanic regions: Udokan Plateau, North Minusa Depression, Tsagan-Khurtei Ridge (Russia), Bakony-Balaton Highland, Nógrád-Gömör Region (Hungary) and Makhtesh Ramon (Israel). Rhönite-bearing silicate melt inclusions are relatively common phenomena in alkali basalts and usually coexist with inclusions containing no rhönite. Inclusions with rhönite generally occur in the core of the olivine phenocrysts. According to heating experiments and CO_2 microthermometry, all the rhönite-bearing inclusions in core of the olivine phenocrysts were trapped as silicate melt at T>1300°C and P>3-5 kbar. Rhönite crystallized in a narrow temperature range (1180-1260°C) and P<0.5 kbar. The petrography and thermometry of rhönite-bearing silicate inclusions show a general crystallization sequence: ± sulfide → Al-spinel → rhönite → clinopyroxene → apatite → ± amphibole, Fe-Ti oxide (ilmenite or Ti-magnetite) → glass.

There are no essential differences in chemistry among rhönites from olivine-hosted silicate melt inclusions from phenocryst, ocelli and groundmass of alkali basalts, from alteration products of kaersutitic amphibole mega/xenocrysts and of kaersutite in deep-seated xenoliths in alkali basalts. The rare occurrence of rhönite as regular constituents in rocks may be explained from its microstructural peculiarities. This mineral is an intermediate member of the polysomatic spinel-pyroxene series. Possibly, the structural feature of rhönite does explain why it is an unstable mineral in under changing crystallization conditions.

Keywords: Rhönite; Clinopyroxene; Spinel; Silicate melt inclusions; Olivine phenocryst; Alkali basalts

INTRODUCTION

Rhönite is a rare Ti-bearing aluminosilicate, which belongs to the aenigmatite group. Its simplified formula can be written as $\mathbf{Ca_2(Mg,Fe^{2+})_4Fe^{3+}Ti[Al_3Si_3O_{20}]}$ [49]. This mineral principally has been described to occur in silica-undersaturated mafic to intermediate igneous rocks (e.g., alkali basalt, phonolite, tephrite, nepheline syenite) in which the rhönite can be associated with several minerals (e.g., olivine, clinopyroxene, plagioclase, feldspathoids, and spinel) [66, Johnston, Stout, 1985; 73, 42 and others]. The first detailed descriptions of rhönite appear at the beginning of 20th century from nepheline-bearing basalts of Scharnhausen, Rhön district, Germany [79] and from Puy de Saint Sandoux, Auvergne, France [53]. Since that discovery, rhönite has been found in various localities and different geological environments, but particularly in alkali basalts as groundmass or as ocelli mineral and as a product of alteration of amphibole, which occur as mega/xenocrysts or as a constituent in ultramafic and mafic xenoliths. Origin and occurrences of rhönite are summarized in Table 1. Moreover, recent studies on silicate melt inclusions have shown that rhönite is a common daughter phase in the silicate melt inclusions of olivine phenocrysts in most alkali and subalkali basalts and in their xenoliths [3, 51, 29, 44-46, 39, 81, 87, 88, 28, 83]. This work is a compilation of the data on rhönite from silicate melt inclusions in olivine phenocrysts from alkali basalts of six different volcanic fields from Russia, Hungary and Israel.

EXPERIMENTAL AND ANALYTICAL TECHNIQUES

Olivine phenocrysts with rhönite-bearing silicate melt inclusions and coexisting fluid and crystal inclusions were carefully selected from doubly polished thin sections of rocks and individual olivine grains, which were specially handpicked under stereomicroscope from different fractions of crushed rocks.

Experimental study on individual melt inclusions were performed using high-temperature heating stage (up to 1600^{o}C) in argon atmosphere with visual monitoring technique developed by Sobolev and Slutsky [77] and installed at the Institute of Geology and Mineralogy (IGM) in Novosibirsk, Russia. This technique was used to evaluate homogenization temperatures for melt inclusions and ranges of melting for specific daughter phases (Al-spinel, rhönite, clinopyroxene). Additionally, we used a heating stage designed by Petrushin et al. [67] in the IGM for heating of inclusion “in blind”. Separated and groundmass-free olivine grains (30-100 pieces) with inclusions were put in alundum capsule with graphite cover and then in platinum capsule, and were heated in argon atmosphere up to a given high temperature. Grains had been held at this temperature for 20-30 minutes and then quenched.

Low temperature experiments on the fluid phase of melt inclusions and coexisting fluid inclusions were made using FLUID INC-USGS low temperature heating/freezing stage equipped with a Leitz (Laborlux S) microscope at the

Lithosphere Fluid Research Lab (LRG), Department of Petrology and Geochemistry, Eötvös University, Budapest (ELTE) and at the IGM.

Rock-forming minerals and solid phases of the silicate melt inclusions were performed at the IGM using a Camebax 50X electron microprobe (accelerating voltage 20 kV, probe current 30 nA, beam 2-3 μm, measuring time 40 s) and at the

Table 1.

Summary of rhönite occurrences and origins

Association	Appearance/Origin	Locality	Reference
Si-undersaturated mafic to intermediate rocks (alkali basalt, phonolite, tephrite, etc.)	phenocrystal, microphenocrystal or groundmass mineral	Rhön and Eifel district, Germany	[79, 20, 72, 48, 8]
		Central France	[53, 32, 60]
		Sakhalin, Russia	[86]
		Greenland	[79, 41]
		Trinidade hotspot	[22]
		Texas, USA	[11]
		Eastern Austria	[35-37]
		Hawaii, USA	[40]
		Southern Sweden	[66]
		Iceland plume	[68]
		Western Romania	[73, 16]
		Hungary	[64]
		Antarctica	[52, 85]
		Cape Verde	[42]
		Cameroon	[65]
	daughter phase of silicate melt inclusions in olivine	Kamchatka, Russia	[3]
		Transbaikalia, Russia	[55, 51]
		Khakasia, Russia	[29, 81]
		Hungary	[44-46, 87, 88]
		Southern Israel	[83]
		Central France	[39]
Kaersutitic amphibole macro/xenocrysts in basalts	product of complete or partial alteration of kaersutite	Oki Islands, Japan	[82]
		New Zealand	[52]
		Central France	[4, 60]
		Armenia	[33]
		Cameroon	[65]
		Ustica Isl., Etna, Italy	[1, 58]
Amphibole-bearing and amphibole-free mafic xenoliths in basalts	interstitial mineral or alteration product of kaersutite	Central France	[4]
		Eifel district, Germany	[74]
		Antarctica	[26, 31]
		Hungary-Slovakia	[88, 38]
		Canada	[12, 23]
		Australia	[71]
		Khakasia, Russia	[28, 30]
Diamonds in kimberlites	phase of inclusions in diamonds	South Africa	[43]
Metasomatic	on the basalt-coral contact	Isle of Réunion	[34]
Technogenic combustion metamorphism (burned spoil-heaps, fields of charcoal preparation, etc.)	high temperature annealing of petrified wood pieces	Chelyabinsk coal basin, Russia	[14]
	phase in basic paralavas		[13]
	charcoal preparation	Etna, Italy	[15]
	pyrometallurgy		[47]
Extraterrestrial (meteorites)	phase of refractory inclusions in chondrites	Allende, Efremovka and Axtell meteorites	[21, 24, 25, 61, 62, 75, 76]
Synthetic	melting experiments with basalts, xenoliths and meteorites		[7, 6, 48, 50, 55, 57]

ELTE using an AMRAY 1830 I/T6 type scanning electron microprobe (accelerating voltage 15 kV, probe current 1-2 nA, beam 2-7 μm, measuring time 100 s). The accuracy of major element determination was better than 1-2 % of total value.

GENERAL CHARACTERISTICS OF STUDIED ALKALI BASALTS

Rhönite from olivine phenocryst hosted silicate melt inclusions were studied at six Si-undersaturated alkali basaltic volcanic fields from Russia, Hungary and Israel. These volcanic regions developed in highly different ages and slightly different geodynamical environment (Table 2). Udokan Plateau volcanic field (UPVF) occurs in the northeastern Baikal rift system (Transbaikalian region, Russia) and its development is related to late Cenozoic magmatic activity [69, 70]. Tsagan-Khurtei Ridge volcanic field (TKRVF) is located in the central part of the Mongolo-Transbaikalian province of alkaline granitoids and bimodal basalt-comendite volcanic series (Transbaikalian region, Russia). The formation of TKRVF is connected to late Triassic rifting process in the Transbaikalian portion of the province [56]. North Minusa Depression volcanic field (NMDVF) is located in the southwest part of the Siberian craton at the Salair segment of the Altai-Sayan fold belt (Khakasia, W-Siberia, Russia). The appearance of NMDVF is related to short-time Cretaceous magmatic activity due to rifting of continental lithosphere [2, 9]. Bakony-Balaton Highland volcanic field (BBHVF) is situated in the central Pannonian Basin (W-Hungary), whereas the Nógrád-Gömör Volcanic Field (NGVF) occurs at the northern edge of the Pannonian Basin (N-Hungary/S-Slovakia). Development of both volcanic fields is related to extensional-postextensional processes, which formed the Neogene Pannonian Basin [80, 17, 18 and references therein]. Makhtesh Ramon volcanic field (MRVF) located in southern Israel was developed by pre-rifting magmatism corresponding to a Late Jurassic-Early Cretaceous event which is also known in the Middle East in Samaria-Galilee fields in Central Israel, Jordan, Lebanon, and Syria [27, 83].

Source materials of these volcanoes are assumed to derive from the asthenosphere, which produced alkali basalts geochemically similar to OIB. Compositions of the studied rocks vary from olivine melanephelinite to basanite, hawaiite and trachybasalt. The total amount of olivine ± clinopyroxene ± plagioclase phenocrysts usually does not exceed 15 vol.%. Forsteritic olivine (Fo_{87-63}) is the major phenocryst, whereas clinopyroxene and anorthitic plagioclase are not abundant. The groundmass consists mostly of olivine ($Fo_{<70-60}$), Ti-Al-rich clinopyroxene, Ti-magnetite, plagioclase and/or feldspathoids (nepheline, leucite), and minor glass, apatite, phlogopite, ilmenite (Table 2). All of these basaltic rocks contain no rhönite as phenocryst, microphenocryst or groundmass mineral. However, rhönite can be observed as a phase of partial or complete replacement after kaersutite or pargasite occurring as mega/xenocrysts and as metasomatic constituents in mafic and ultramafic xenoliths in basalts of the studied volcanic fields [30, 28, 88].

Table 2.

Location, ages and mineralogy of investigated alkali basalt rocks

Locality	Rock	Age, Ma	Phenocrysts	Groundmass	Reference
Udokan plateau volcanic field (UPVF), Transbaikalia, Russia					
volcano Pravyi Lurbun	Ol nephelinite	14	Ol+Cpx	Ol+Cpx+Mag+Ap+Ne+Lc+Phl+Ilm+Cc+Kfs	[55]
extrusion Nizhnii Lurbun	Ol nephelinite	14	Ol+Cpx	Ol+Cpx+Mag+Ap+Ne+Lc+Phl+Ilm+Cc+Kfs	[69, 70]
lava flow Verkh. Ingamakit	basanite	2.5	Ol+Cpx+Pl	Ol+Cpx+Mag+Pl+Ap+Ilm+Kfs+Ne+Lc	
volcano Kislyi Klyuch	hawaiite	1.8	Ol+Cpx+Pl	Ol+Cpx+Mag+Pl+Ap+Ilm+Kfs	
Tsagan-Khurtei ridge volcanic field (TKRVF), Transbaikalia, Russia					
Tsagan-Khuntei suite	trachybasalt	212	Ol+Cpx+Pl	Ol+Cpx+Mag+Pl+Ap+Phl+Ilm+Kfs	[51, 56]
North Minusa depression volcanic field (NMDVF), Khakasia, Russia					
pipe Bele	basanite	79	Ol+Cpx+Pl	Ol+Cpx+Mag+Pl+Ap+Ilm+Kfs	[9]
dike Bele	basanite	79	Ol+Cpx+Pl	Ol+Cpx+Mag+Pl+Ap+Ilm+Kfs	[29]
pipe Tergesh	hyalobasanite	77	Ol+Cpx	Ol+Cpx+Mag+Pl+Ap+Ilm+Gl	[81]
Bakony-Balaton Highland volcanic field (BBHVF), Western Hungary					
volcano Badacsony	basanite	3.6	Ol+Cpx+Pl	Ol+Cpx+Mag+Pl+Ap+Phl+Ilm+Kfs+Ne	[5]
volcano Kabhegy	basanite	4.6	Ol+Cpx+Pl	Ol+Cpx+Mag+Pl+Ap+Phl+Ilm+Kfs+Sod+Anc	[17, 18]
volcano Zalahaláp	basanite	2.9	Ol+Cpx+Pl	Ol+Cpx+Mag+Pl+Ap+Ilm+Kfs+Sod+Ne	[80]
volcano Hegyestű	Lc basanite	6	Ol+Cpx+Pl	Ol+Cpx+Mag+Pl+Ap+Lc+Ilm+Ne+Sod	[45, 46]
Nógrád-Gömör volcanic field (NGVF), Northern Hungary-Southern Slovakia					
Eresztvény, Medves plateau	basanite	2.6	Ol+Cpx+Pl	Ol+Cpx+Mag+Pl+Ap+Kfs+Ne	[5]
Magyarbánya, Medves plateau	basanite	2.6	Ol+Cpx+Pl	Ol+Cpx+Mag+Pl+Ap+Phl+Ilm+Kfs+Ne	[17, 18]
Terbelét (Terbelény)	basanite	2.6	Ol+Cpx+Pl	Ol+Cpx+Mag+Pl+Ap+Phl+Ilm+Kfs	[80]
Pécskő	hawaiite	4.5	Ol+Cpx+Pl	Ol+Cpx+Mag+Pl+Ap+Kfs	[44]
Makhtesh Ramon volcanic field (MRVF), Southern Israel					
S. Qarnei Ramon	basanite	110-125	Ol+Cpx+Pl	Ol+Cpx+Mag+Pl+Ap+Ne+Phl	[59]
Mt. Arod	bas.nephelinite	110-125	Ol+Cpx±Pl	Ol+Cpx+Mag+Ap+Ne+Pl±Phl±Ilm+Anc	[19, 83]

Note: Ol=olivine; Cpx=clinopyroxene; Pl=plagioclase; Mag=Ti-magnetite; Ap=apatite; Ilm=ilmenite; Lc=leucite; Ne=nepheline; Kfs=K-feldspar; Phl=phlogopite; Cc=calcite; Gl=glass; Sod=sodalite; Anc=analcite; bas. = basanitic.

DESCRIPTION OF RHÖNITE-BEARING SILICATE MELT AND COEXISTING INCLUSIONS IN OLIVINE PHENOCRYSTS

Rhönite-bearing silicate melt inclusions were commonly found in the core of olivine phenocrysts from all the studied regions. Usually, rhönite-bearing inclusions coexist with rhönite-free inclusions within the single olivine grain. However, rhönite-free silicate melt inclusions, which were not considered in this study, are generally confined to the outer zones of olivine phenocrysts. All inclusions, either rhönite-bearing or rhönite-barren, are primary in origin. Distribution of silicate melt inclusions in olivine is different: they are single inclusions or sometimes groups of inclusions outlining growth zones. The shape of inclusions is oval, rounded or negative crystal shaped. The sizes vary up to 200 μm (Fig. 1-2). All silicate melt inclusions studied may contain daughter phases such as rhönite, clinopyroxene, Al-spinel, Ti-magnetite, apatite, phlogopite, kaersutite, ilmenite, nepheline, feldspars, sulphate and sulphide bleb. A CO_2-bearing bubble is also always present in the inclusions. Sometimes Cr-spinel occurs as xenogenic,

accidentally trapped mineral in the silicate melt inclusions. In some cases, halos of minute silicate melt and fluid inclusions (size of 1-5 µm) occur around the large melt inclusions (>50 µm) suggesting partial leakage after entrapment (Fig. 1-2). Besides the silicate melt inclusions, olivine phenocrysts also contain coexisting sulphide blebs, CO_2 fluid inclusions and single Cr-spinel crystals.

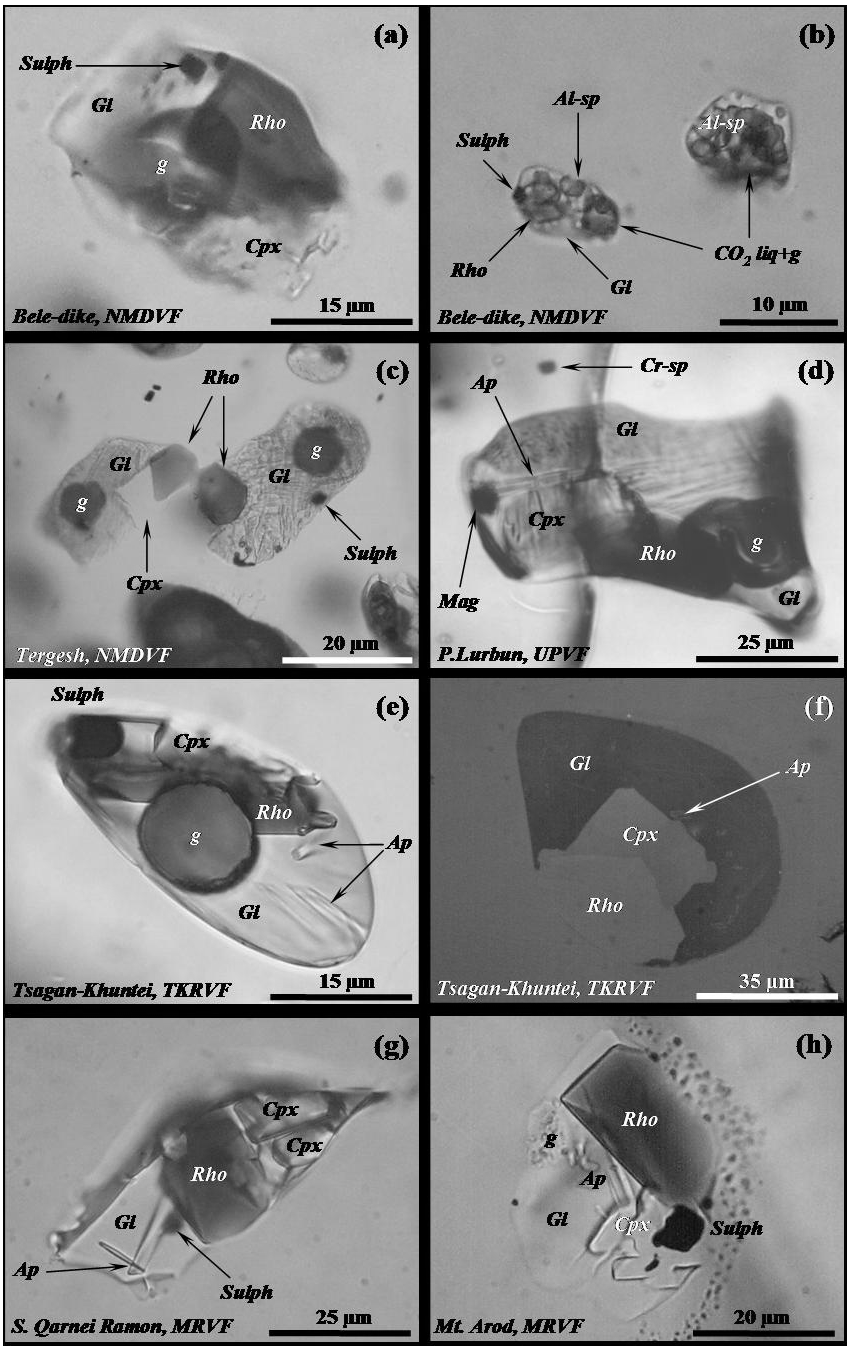

Fig. 1. **Photomicrographs of primary rhönite-bearing silicate melt inclusions in phenocrystal olivine from alkali basalts of NMDVF, UPVF, TKRVF and MRVF.**

Ordinary and reflected lights. Symbols and analyses see Tables 2-4.

NMDVF, Khakasia, Russia

Bele

Olivine-hosted silicate melt inclusions with rhönite were occasionally found in basanites from the major body of the Bele pipe [29]. Besides rhönite, the inclusions also contain clinopyroxene and apatite as daughter minerals. Rhönite-bearing inclusions have also been recognized in olivine of the Bele dyke (0.5 km

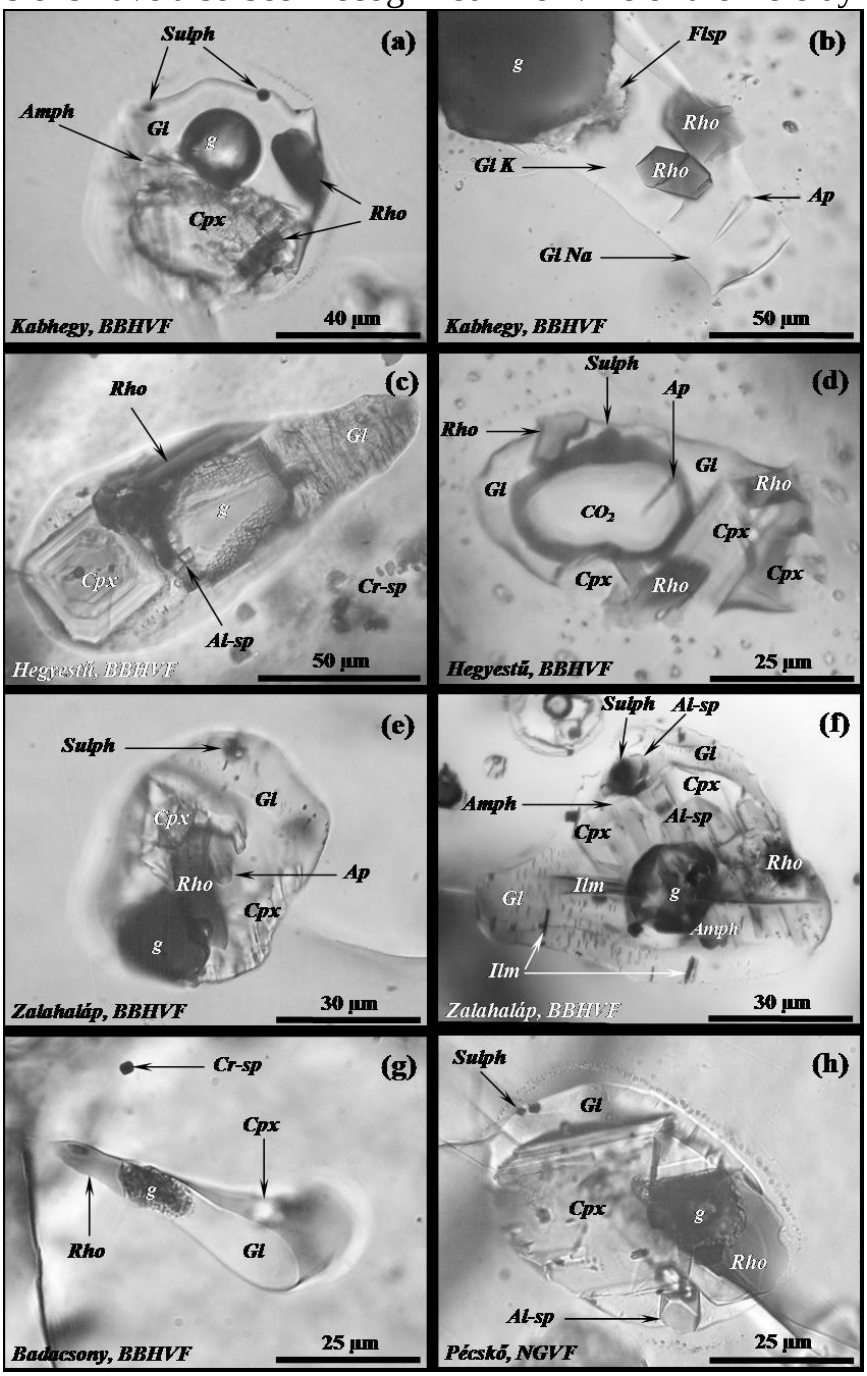

Fig. 2. **Photomicrographs of primary rhönite-bearing silicate melt inclusions in phenocrystal olivine from alkali basalts of BBHVF and NGVF, ordinary light.**

Halo of very small melt and fluid inclusions exist around some large inclusions evidencing about partial leakage after their entrapment. Analyses see Table 5.

rhönite + clinopyroxene + sulphide bleb + fluid bubble ± Al-spinel (Fig. 1a-b). The petrography of inclusions shows that rhönite is the second crystallized daughter phase after Al-spinel. The fluid bubble in the silicate melt inclusions is two-phased at room temperature and is almost pure CO_2. Homogenization of the fluid into the liquid happened at >+20^oC, which corresponds to density near of ca. 0.75 g/cm^3, assuming pure CO_2.

Tergesh

Abundant silicate melt inclusions were found in the olivine phenocrysts of the Tergesh hyalobasanite [Timina et al., 2006]. They occasionally decorate the growth zones of the host olivine and are associated with single Cr-spinel crystals and CO_2 fluid inclusions. Phase composition of the silicate melt inclusions in olivine is glass + fluid bubble ± daughter crystals ± sulphide bleb ± accidentally trapped Cr-spinel. In some inclusions glass is devitrified. Rhönite and clinopyroxene are the principal daughter phases, whereas apatite, ilmenite and Ti-magnetite occur very rarely (Fig. 1c). The relationships between minerals within the olivine-hosted inclusions show that rhönite is the earliest-crystallized daughter phase. The single fluid inclusions coexisting with the silicate melt inclusions are almost pure CO_2. The melting point varies from -57.0 to -58.0^oC, homogenization into the liquid happened at +24^oC, which corresponds to density near of ca. 0.7 g/cm^3, assuming pure CO_2.

UPVF, Transbaikalia, Russia

Rhönite-bearing silicate melt inclusions were occasionally found in olivine phenocrysts of olivine melanephelinite (Pravyi Lurbun volcano, extrusion Nizhnii Lurbun), basanite lava flow (Verkhnii Ingamakit) and hawaiite (Kislyi Klyuch volcano). In the olivine melanephelinites the silicate melt inclusions sometimes coexist with CO_2 fluid inclusions and individual solid inclusions of Cr-spinel. The silicate melt inclusions consist of glass + bubble + daughter minerals. Rhönite, Ti-Al-rich clinopyroxene and apatite are common daughter phases (Fig. 1d), whereas Ti-magnetite, Ba-Ti-phlogopite, nepheline and leucite, which are typical constituents in the groundmass of the rocks, occur rarely. The petrography of the silicate melt inclusions shows that rhönite is the earliest daughter phase. The fluid phase in the silicate melt, as well as single fluid inclusions is almost pure CO_2. The melting point of the fluid phase varies from -56.6 to -58.0^oC. The homogenization into the liquid happened at +21-22^oC, which corresponds to density of ca. 0.75 g/cm^3, assuming pure CO_2.

BBHVF, Western Hungary

Silicate melt inclusions containing rhönite were found in olivine phenocrysts of basanites and trachybasalt from several volcanoes in the central Pannonian Basin. The first petrographic and thermometric studies for some BBHVF melt inclusions were provided by Sobolev et al. [78].

Kabhegy

Rhönite is a common daughter phase of large silicate melt inclusions from the

cores of olivine phenocrysts [46]. Assemblages of such inclusions are glass + rhönite + clinopyroxene + amphibole + apatite + fluid bubble + sulphide bleb ± K-Na feldspar ± Al-spinel (Fig. 2a-b). Accidentally trapped Cr-spinel is also rarely seen. The relationship of phases in the silicate melt inclusions suggests the following crystallization sequence: sulphide bleb → Al-spinel → rhönite → clinopyroxene → apatite → amphibole → K-Na feldspar → glass. There are no microthermometry data of single CO_2 fluid inclusions and the CO_2 phase in the silicate melt inclusions.

Haláp

Rhönite is an extremely rare phase in the olivine-hosted silicate melt inclusions of the Haláp alkali basalt. The inclusions also contain glass, sulphide bleb, clinopyroxene, Al-spinel, apatite, ilmenite, amphibole and bubble (Fig. 2e-f) [44, 46]. Rhönite is the earliest daughter mineral crystallized within inclusions. Note that rhönite-free silicate melt inclusions are more common and their phase composition is glass + Al-spinel + clinopyroxene + ilmenite + sulphide bleb + bubble. According to microthermometry and Raman spectroscopy, gas bubbles in silicate melt inclusions is pure CO_2, but in some case with small amount of CO and CH_4 [46].

Badacsony

In the Badacsony alkali basalts rhönite occurs also scarcely in the silicate melt inclusions. The most typical phase composition of such inclusions is glass + rhönite + clinopyroxene ± sulphide bleb ± Ti-magnetite + bubble (Fig. 2g). Rhönite can be considered as the earliest crystallized mineral. Rhönite-free inclusions contain such daughter crystals as clinopyroxene, apatite, ilmenite, leucite, phlogopite. Xenogenic accidentally-trapped Cr-spinel frequently attached to these inclusions. There are no microthermometry data of single CO_2 fluid inclusion and the CO_2 phase in the silicate melt inclusions.

Hegyestű

Olivine phenocrysts in the Hegyestű alkali basalt contain primary silicate melt inclusions, CO_2 fluid inclusions, individual Cr-spinel inclusions and sulphide blebs [44, 45]. Usually, silicate melt, fluid and sulphide inclusions are grouped in the way that outlines the growth zones in the core of the host olivine phenocrysts. The common mode for melt inclusions is glass + bubble + silicate daughter minerals ± sulphide globule. Accidentally trapped Cr-spinel is also observed in the silicate melt inclusions. Clinopyroxene and rhönite are the major daughter minerals. Some inclusions also contain apatite, ilmenite, Al-spinel, K-Na-feldspar and nepheline. Halos of minute silicate melt and fluid inclusions (size - 1-5 μm) occasionally occur around the largest melt inclusions (>50 μm) suggesting partial leakage after entrapment (Fig. 2c-d). The relationship of phases in the melt inclusions suggests the following sequence of crystallization: sulphide bleb → Al-spinel → rhönite → clinopyroxene → apatite → (ilmenite, K-Na-feldspar, nepheline) → glass.

Freezing experiments on bubbles in silicate melt inclusions and coexisting fluid inclusions in olivine phenocrysts show that bubbles contain almost pure CO_2.

The melting points for fluid from silicate melt inclusions vary from –56.8 to -60.9°C. This CO_2–rich fluid is expected to have low density. However, the existence of halos around large inclusions (Fig. 2d) assumes partial leakage after entrapment in the host olivine, which, in turn, indicates that the initial density of fluid was higher. Fluid inclusions coexisting with silicate melt inclusions show two phases (CO_2 liquid + CO_2 vapour) at room temperatures with homogenization into

Table 3.

Compilation of thermometric data for rhönite-bearing inclusions in olivine of some alkali basalts.

Locality	Region	Rock	Phase composition of inclusions	T melting for main phases,°C			T hom, °C	P, kb est.	Reference
				Cpx	Rho	Al-sp			
Kamchatka	FERussia	high-Al basalt	Gl+Opx+Al-sp± Rho+Cpx±Amph+g				1250-1350	>2-3	[3]
Ingamakit, Munduzhyak	UPLF	Ol nephe-linite	Gl+Rho+Cpx+ Ap+Mag±Ne+g	1180-1200	>1200		>1250	>4.5	[55] data of author
Tsagan-Khuntei suite	TKRVF	Trachy-basalt	Gl±Al-sp+Rho+Cpx Ap±Mag±Ilm+Kfs+g				1280-1320	>0.8-1	[51]
Bele	NMDVF	basanite	Gl+Rho+Cpx+ Ap±Mag+g				>1250	>2	[30]
Tergesh	NMDVF	hyalobasanite	Gl+Rho+Cpx+Ap± Mag±Ilm+Sulph+g	1130-1190	>1200		1270-1310	>3	[81]
Hegyestű	BBHVF	Lc basanite	Gl±Al-sp+Rho+Cpx+ Ap±Ne+Sulph+g	1190-1210	1220-1245		1270-1310	>4	[45]
Kabhegy	BBHVF	basanite	Gl+Al-sp+Rho+Cpx+ Amph+Ap±Ilm+Sulph+g				1280-1300		author's data
Zalahaláp	BBHVF	basanite	Gl+Rho+Cpx±Amph+ Ap+Ilm+Sulph+Cal+g				1220-1270		[46]
Pécskő	NGVF	hawaiite	Gl+Al-sp+Rho+Cpx± Amph+Ap±Ilm+Sulph+g	1165-1235	>1200	1255-1275	1300-1350	>3	[44]
Nagy-Salgó	NGVF	Ol-Cpx cumulate xenoliths in basanite	Gl+Al-sp+Rho+Cpx+ Amph±Ap±Sulph+g	1190-1240	1220-1265	1260-1320	<1350	>4	[87, 88]
S. Qarnei Ramon	MRVF	basanite	Gl+Rho+Cpx+ Ap±Ilm+Sulph+g	1140-1180	1180-1230		1310-1355	7.0-7.2	[83]
Mt. Arod	MRVF	Ol-Cpx cumulate in bas. nephelinite	Gl+Rho+Cpx+Ap+ Sulph+g				>1250	7.0-7.2	[83]
Puy Beaunit	C.France	alkali basalt	Gl+Rho+Cpx+Pl+ Sp+Sulph+g	1225-1245			1260		[39]

Note: Rho=rhönite; g=gas bubble; Al-sp=Al-rich Cr-poor spinel; Amph=Ti-kaersutitic/pargasitic amphibole; Cal=calcite filling gas bubble; Sulph=sulphide bleb; est=estimated. Other symbols see Tab. 2.

the liquid phase (at about +25°C) and with melting point at –57.8°C. It suggests density of ca. 0.7 g/cm^3 assuming pure CO_2 composition. According to Raman studies, fluid bubble in the silicate melt inclusions is also recognized as low-density CO_2 with small amount of CO and CH_4 [46].

NGVF, Northern Hungary-Southern Slovakia

Rhönite-bearing silicate melt inclusions were observed in olivine phenocrysts of alkali basalts from several localities of the NGVF. However, only the Pécskő hawaiite are well studied with respect to silicate melt inclusions [44]. It is more interesting that silicate melt inclusions with rhönite also occur in olivine from cumulate xenoliths (olivine-clinopyroxene-spinel ± amphibole) in the Nagy-Salgó basanite [87, 88] and in spinel and olivine from spinel lherzolite in the Terbeléd (Trebel'ovce) basanite [38] of the NGVF.

Pécskő

Rhönite-bearing silicate melt inclusions frequently occur in olivine phenocrysts. Such inclusions are commonly greater in size than the rhönite-free inclusions and show random distribution in the host phenocryst. Their phase composition is glass + Al-spinel + rhönite + clinopyroxene ± Ti-amphibole ± sulphide bleb + bubble. Accidentally trapped xenogenic Cr-spinel are also observed attached to the silicate melt inclusions. In some inclusions the bubble is filled by carbonate minerals. The petrography of inclusions shows that rhönite crystallized after Al-spinel. The silicate melt inclusions in olivine coexist with individual crystals of Cr-spinel, rounded Cr-rich diopside xenocrysts and sulphide blebs. Halos of coexisting minute silicate melt and fluid inclusions (size <1 μm) occasionally occur around the largest melt inclusions indicating partial leakage after entrapment (Fig. 2h).

Medves plateau and other outcrops

In these rocks rhönite was occasionally identified in some olivine-hosted inclusions from Eresztvény, Magyarbánya and Terbeléd. Usually it coexists with clinopyroxene, apatite and sulphide bleb, sometimes with phlogopite.

TKRVF, Transbaikalia, Russia

Rhönite was previously described in some olivine-hosted silicate melt inclusions of the Tsagan-Khuntei suite trachybasalts [51]. The phase composition of inclusions is glass + rhönite + clinopyroxene + apatite + sulphide bleb + bubble (Fig. 1e-f). Daughter Al-spinel, amphibole and K-Na-feldspar occur occasionally in the silicate melt inclusions. Xenogenic accidentally trapped Cr-spinel sometimes can also be seen attached to the inclusions. The mineral relation within inclusions shows that rhönite is one of the earliest daughter minerals, which crystallized after Cr-spinel. Sometimes the glass is devitrified or altered. In these cases late stage carbonate mineral fills up the bubble. The silicate melt inclusions coexist with individual Cr-spinels, sulphide blebs and rarely fluid inclusions. The fluid inclusions show heterogeneity (CO_2 liquid + CO_2 vapour) at room temperatures with homogenization into the gas phase at about +26°C and melting at –56.8°C. These values suggest low density of ca. <0.1 g/cm^3 assuming pure CO_2. According to Raman studies, fluid bubble in the silicate melt inclusions is also recognized as low-density CO_2.

MRVF, Southern Israel

Rhönite-bearing silicate melt inclusions were found in olivine phenocrysts from the S. Qarnei Ramon basanite [83]. Their common composition is glass + rhönite + clinopyroxene + sulphide bleb + bubble ± apatite. (Fig. 1g). Rhönite is the earliest-crystallized phase. Accidentally trapped Cr-spinel was also recognized in the

Table 4.

Representative analyses of phases from rhönite-bearing inclusions in olivine from alkali basalts of the UPVF, TKRVF, NMDVF and MRVF

Comp. of inclus.	Phase	*n*	SiO_2	TiO_2	Cr_2O_3	Al_2O_3	FeO	MnO	MgO	CaO	Na_2O	K_2O	P_2O_5	Cl	Sum	H. in Fo
ol nephelinite, volcano Pravyi Lurbun, UPVF																
Gl+Rho+Cpx+	Gl	2	55.19	0.87	0.00	23.75	0.84	0.01	0.10	0.91	6.07	11.38	0.23	0.23	99.58	76.9
Ap+Mag+g	Rho	3	25.78	11.86	0.10	15.26	17.87	0.11	14.56	11.63	1.19	0.00	0.08	0.00	98.44	-
	Cpx	2	41.82	5.27	0.05	9.56	6.15	0.08	11.60	22.70	0.66	0.00	0.94	0.00	98.83	-
	Mag	1	-	17.16	10.13	16.80	43.72	0.53	6.70	-	-	-	-	-	95.04	-
ol nephelinite, extrusion Nizhnii Lurbun, UPVF																
Gl+Rho+	Gl	1	59.70	0.25	0.01	25.70	1.56	0.01	0.28	0.10	7.97	3.47	0.07	0.20	99.32	75.9
Cpx+g	Rho	1	24.31	12.20	3.30	16.63	15.00	0.10	15.00	10.60	1.65	0.00	0.00	-	98.79	-
basanite, lava flow Verkhnii Ingamakit, UPVF																
Gl+Rho+	Gl	1	55.64	0.97	0.01	26.34	1.24	-	0.43	2.60	6.57	2.27	1.00	-	97.07	85.4
Cpx+g	Rho	2	24.56	10.07	0.40	16.73	17.21	-	14.26	12.51	0.86	0.03	0.03	--	96.66	-
	Cpx	1	45.24	3.02	0.01	8.13	6.87	-	11.99	23.34	0.59	0.00	0.16		99.35	-
hawaiite, volcano Kislyi Klyuch (Polyakov), UPVF																
Gl+Rho+	Gl	1	65.50	0.17	-	22.90	0.54	-	0.06	1.74	2.43	4.13	0.87	0.12	98.46	70.7
Cpx+g	Rho	1	25.70	8.64	-	16.91	23.01	-	10.59	10.93	1.49	0.05	0.25	-	97.57	-
	Cpx	1	41.95	3.90	-	11.58	8.08	-	10.24	22.44	0.64	0.00	0.17	-	99.00	-
trachybasalt, Tsagan-Khuntei suite, TKRVF																
Gl+Rho+	Gl	5	64.58	0.32	0.01	23.53	1.05	0.02	0.18	1.19	5.56	2.38	0.32	0.06	99.20	74.8
Cpx+Ap+	Rho	1	27.03	8.46	0.01	17.24	22.34	0.18	12.27	11.04	1.34	0.00	0.00	-	99.91	-
Sulph+g	Cpx	1	44.44	1.99	0.00	10.63	8.81	0.15	10.60	21.82	0.68	0.00	0.81	-	99.92	-
Gl+Rho+	Gl	4	62.17	0.65	0.01	23.79	1.05	0.01	0.28	1.85	6.55	2.34	0.49	0.06	99.24	78.0
Cpx+g	Rho	1	24.87	9.12	0.34	17.96	22.49	0.08	12.71	11.24	1.04	0.00	0.00	-	99.85	-
	Cpx	1	43.22	3.90	0.00	9.94	8.24	0.07	11.43	21.77	0.63	0.00	0.76	-	99.96	-
Gl+Al-sp+	Gl	3	61.55	0.69	0.02	23.19	1.33	0.02	0.62	2.17	6.09	2.34	0.69	0.07	98.78	77.7
Rho+Cpx+	Al-sp	1	0.00	0.31	0.02	63.23	19.63	0.15	16.31	0.00	0.00	0.00	0.00	-	99.65	-
Ap+g	Rho	4	24.29	9.56	0.12	18.64	22.43	0.10	12.20	11.27	0.92	0.00	0.00	-	99.53	-
	Cpx	1	43.88	3.73	0.00	10.65	7.74	0.09	11.87	21.15	0.66	0.00	0.00	-	99.77	-
basanite, pipe Bele, NMDVF																
Gl+Rho+	Gl	1	55.53	0.24	0.02	24.57	1.13	0.02	0.36	0.22	14.04	1.60	0.00	0.01	97.74	70.7
Cpx+Ap+g	Rho	1	26.45	11.21	0.32	15.26	21.61	0.18	10.27	11.59	1.20	0.00	0.00	0.00	98.09	-
basanite, dike Bele, NMDVF																
Gl+Rho+	Gl	1	57.04	0.24	0.00	26.97	0.98	0.00	0.35	0.78	6.78	4.81	1.12	0.25	99.31	79.6
Cpx+Sulph+g	Rho	1	25.71	10.26	0.11	16.09	20.67	0.10	13.11	11.35	1.22	0.00	0.02	0.00	98.65	-
	Cpx	1	42.68	3.97	0.00	11.33	7.36	0.08	10.38	22.85	0.77	0.00	0.54	0.00	99.96	-
hyalobasanite, pipe Tergesh, NMDVF																
Gl+Rho+g	Gl	1	54.42	1.18	0.00	23.25	3.16	0.08	0.38	3.62	4.40	3.21	1.48	-	95.18	75.7
	Rho	1	26.27	11.38	0.02	15.70	19.58	0.12	13.99	11.36	1.28	0.00	0.00	-	99.70	-
Gl+Rho+	Gl	1	52.79	1.68	0.00	22.99	3.90	0.07	0.17	3.46	5.26	5.35	1.29	-	96.95	76.7
Cpx+g	Rho	1	24.89	10.54	0.92	17.02	19.73	0.14	12.37	11.49	0.94	0.00	0.00	-	98.04	-
	Cpx	1	41.61	5.99	0.00	11.41	7.15	0.11	9.76	21.91	0.71	0.00	1.16	-	99.81	-
basanite, S. Qarnei Ramon, MRVF																
Gl+Rho+	Gl	2	60.35	0.29	0.02	23.69	1.73	0.04	1.48	0.58	5.64	4.99	0.52	0.32	99.73	83.8
Sulph+g	Rho	2	23.77	11.44	1.64	19.48	12.64	0.10	17.32	10.02	2.25	0.00	0.00	-	98.65	
Gl+Rho+	Gl	2	61.06	0.24	0.00	24.49	0.91	0.01	0.41	0.57	5.26	5.73	0.31	-	99.05	81.5
Cpx+Sulph+g	Rho	1	27.38	10.72	0.49	17.59	14.51	0.11	14.73	12.45	1.21	0.00	0.00	-	99.19	-
	Cpx	1	43.60	4.40	0.02	10.60	5.85	0.06	11.97	21.93	0.75	0.00	0.61	-	99.79	-
Ol-Cpx cumulate xenolith in basanitic nephelinite, Mt. Arod, MRVF																
Gl+Rho+Cpx+	Gl	1	59.24	0.02	0.01	25.23	0.86	0.00	0.07	0.41	7.53	5.93	0.09	0.28	99.66	74.6
Ap+Sulf+g	Rho	1	26.90	8.76	0.04	19.82	18.31	0.10	12.62	11.23	1.37	0.00	0.00	0.00	99.15	-
	Cpx	1	43.90	0.10	0.00	17.43	6.42	0.09	8.88	21.78	1.12	0.00	0.19	0.00	99.91	-
Gl+Rho+Cpx+	Gl	2	60.07	0.07	0.00	25.29	0.70	0.01	0.13	0.58	5.62	4.19	0.15	0.41	97.21	74.6
Ap+Sulf+g	Rho	1	26.81	8.36	0.07	19.74	18.31	0.11	12.66	11.52	1.19	0.00	0.00	0.00	98.77	-
	Cpx	1	49.10	0.73	0.00	7.81	6.51	0.15	13.97	20.86	1.00	0.00	0.20	0.00	100.33	-

Note: Comp. of inclus. = composition of inclusion; H. in Fo = host in Fo.

olivine. Note that rhönite-barren inclusions may contain ilmenite, too. All the silicate melt inclusions coexist with single Cr-spinel and rarely with polycrystalline inclusions (Cr-spinel + rhönite or Cr-spinel + Cr-rich clinopyroxene +Cr-rich ilmenite). Freezing experiments on fluids in bubbles of the silicate melt inclusions showed that fluid is rich in CO_2 (melting point at -57.2 ^oC, homogenization in liquid at -5^oC). Rare rhönite-containing inclusions were occasionally found in olivine-clinopyroxene-spinel cumulate xenoliths in basanitic nephelinite from Mt. Arod. Such inclusions contain also clinopyroxene, sulphide bleb and apatite (Fig. 1h).

HIGH-TEMPERATURE HEATING EXPERIMENTS ON MELT INCLUSIONS

More than 50 primary silicate melt inclusions with rhönite in olivine from alkaline basalts of the six volcanic fields studied were used for homogenization experiments and study the crystallization sequence. Unfortunately, in some cases the complete homogenization (disappearance of the fluid bubble) was not achieved due to reequilibration of the inclusions owing to the existence of a halo around inclusions containing silicate melt ± CO_2 fluid ± sulphide phase (Fig. 1h, 2a,d,h) or even partial leakage during heating. Despite these disadvantages, the melting intervals of daughter phases were established for a large number of silicate melt inclusions (Table 3). All thermometric data support petrographic observations for melt inclusions. Rhönite is one of the earliest crystallized daughter phases with a melting temperature range of 1180-1265^oC. It melted after ilmenite (or Ti-magnetite), apatite (>1100^oC) and clinopyroxene (1130-1240^oC) and before Al-spinel (1255-1320^oC). It should be noted that the same melting intervals for other daughter phases are common of rhönite-barren inclusions. Based on thermometry of the coexisting single CO_2 inclusions and silicate melt inclusions, the trapping pressure may be estimated as high as 3-5 kbar (Table 3).

PHASE CHEMISTRY OF RHÖNITE-BEARING SILICATE MELT INCLUSIONS

Glasses and daughter minerals of rhönite-bearing silicate melt inclusions were analyzed by electron microprobe. The representative analyses are given in Tables 4-5. It should be noted that the majority of the daughter minerals (clinopyroxene, amphibole, magnetite and ilmenite) in vicinity of rhönite in the silicate melt inclusions are enriched in Ti. Moreover, we did not find any essential differences in chemistry of phases between rhönite-bearing and rhönite-barren melt inclusions.

Rhönite

Rhönite has a large variation in major element composition even in inclusions from the same locality. Its compositional variations are remarkable: SiO_2 – 21.4-29.4 wt.%; TiO_2 – 8.1-12.4 wt.%; Cr_2O_3 – up to 3.8 wt.%; Al_2O_3 – 13.2-22.5 wt.%; FeO_{tot} – 12.5-25.0 wt.%; MgO – 10.1-17.3 wt.%; CaO – 9.9-12.7 wt.%; Na_2O –

0.6-2.0 wt.%. Rhönites studied strongly differs from the ideal $\mathbf{Ca_2(Mg,Fe^{2+})_4(Fe^{3+},Al)Ti[Al_3Si_3O_{20}]}$ composition (Fig. 3). We cannot explain such broad deviations. Possibly, it depends on the composition of silicate melt trapped by host olivine and the redox conditions during crystallization. We found no any correlations between compositions of rhönite and other neighboring phases within melt inclusions.

Clinopyroxene and other daughter phases

Clinopyroxenes show strong compositional variations. They are rich in TiO_2 (2.0-6.0 wt.%) and Al_2O_3 (8.0-13.0 wt.%) and poor in SiO_2 (38.0-45.0 wt.%). According to IMA terminology, such compositions belong to the Fe-Al-rich diopside or augite [62]. In some zoned clinopyroxenes the core of crystals contains Cr_2O_3 up to 0.5 wt.%. In general, the core-to-rim evolution of inclusion clinopyroxene is directed towards the increase of Al_2O_3 and TiO_2 and decrease of SiO_2. Such compositional evolution is common for phenocrystal-groundmass clinopyroxenes in the host alkaline basalts [17, 29, 45, Timina et al., 2006, 83].

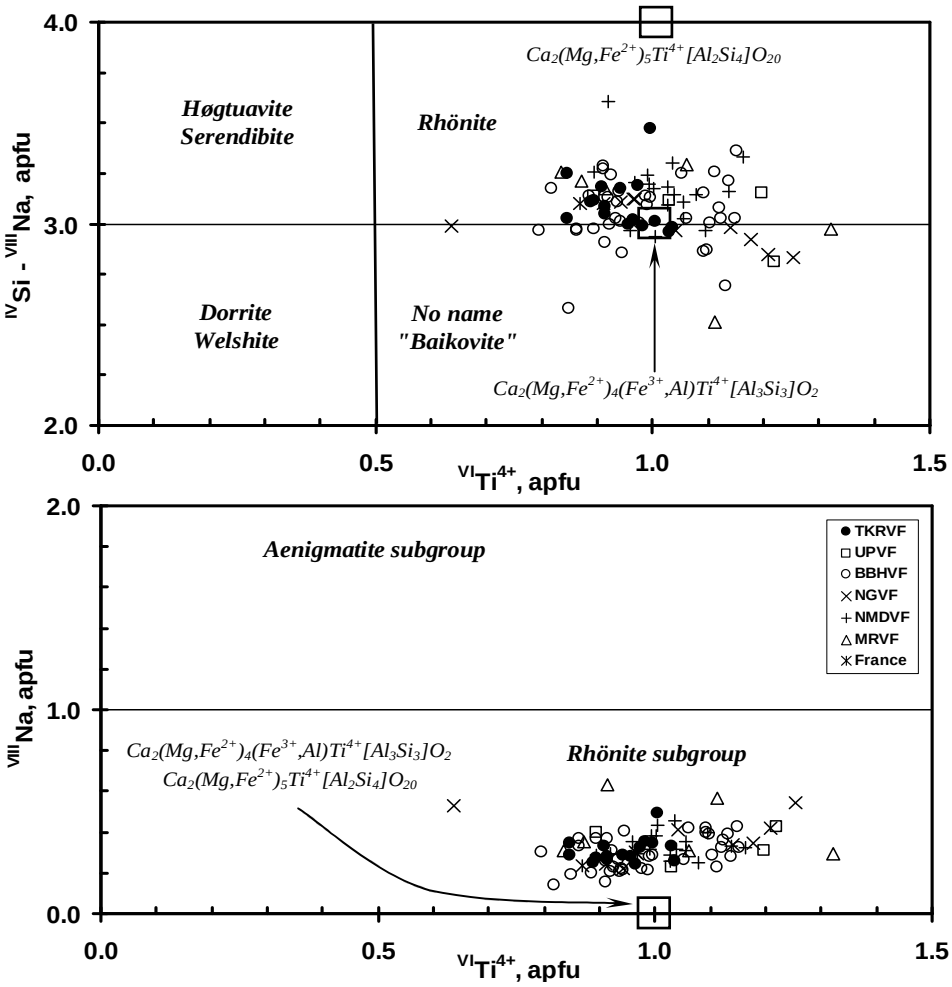

Fig. 3. **Classification diagrams (after Kunzmann [49]) for rhonites from silicate melt inclusions in olivines of alkali basalts.**

Ideal compositions are plotted for comparison. Data from Nagy-Salgó, NGFV [88] and Puy Beaunit, Massif Central, France [39] is included here.

Table 5.

Representative analyses of phases from rhönite-bearing inclusions in olivine from alkali basalts of the BBHVF and NGVF

Comp. of inclus.	Phase	*n*	SiO_2	TiO_2	Cr_2O_3	Al_2O_3	FeO	MnO	MgO	CaO	Na_2O	K_2O	P_2O_5	Cl	Total	H. in Fo
basanite, volcano Badacsony, BBHVF																
Gl+Rho+	Gl	1	62.36	0.11	0.00	27.90	0.86	-	0.08	0.24	2.49	4.62	0.21	-	98.87	74.8
Cpx+Mag+	Rho	2	24.45	9.08	0.29	17.39	22.47	-	12.03	11.65	1.18	0.00	0.00	-	98.53	-
Sulph+g	Cpx	1	46.09	3.79	0.11	8.47	6.95	-	11.79	21.19	1.36	0.00	0.00	-	99.75	-
Gl+Rho+	Gl	1	60.45	0.35	0.00	26.62	1.17	-	0.11	0.25	4.13	6.87	0.02	-	99.97	72.8
Cpx+g	Rho	2	26.30	10.70	0.14	13.23	24.25	-	12.79	9.89	1.60	0.00	0.00	-	98.88	-
basanite, volcano Hegyestű, BBHVF																
Gl+Rho+	Gl	1	56.71	0.00	-	22.44	0.84	0.00	0.00	0.93	3.72	10.92	-	0.00	95.56	84.7
Cpx+Ne+g	Rho	1	25.89	9.23	0.34	19.84	15.11	0.00	15.43	12.66	1.46	0.00	-	-	99.96	-
	Cpx	1	42.65	3.24	-	11.54	7.16	0.00	10.05	23.79	0.80	-	-	-	99.23	-
	Ne	1	41.42	0.00	-	32.51	0.81	0.00	0.00	2.37	14.64	4.59		0.00	96.34	-
Gl+Rho+	Gl Na	1	55.35	1.03	0.00	25.72	1.30	0.01	0.56	0.61	8.31	4.96	0.25	0.12	98.23	84.1
Cpx+g	Gl K	1	51.96	0.70	0.00	24.65	0.74	0.00	0.31	0.42	5.51	14.03	0.26	0.03	98.60	-
	Rho	3	25.22	9.49	0.07	19.22	17.42	0.10	14.58	12.63	0.80	0.01	-	-	99.55	-
	Cpx	2	41.91	3.62	0.01	13.15	6.85	0.09	9.81	23.25	0.64	0.00	0.43	0.00	99.73	-
Gl+Rho+	Gl	2	52.04	1.07	0.00	24.56	2.05	-	0.64	0.91	7.50	9.65	0.28	0.42	99.10	85.0
Cpx+Ap+	Rho	1	24.29	9.45	0.04	18.95	18.71	-	14.33	12.34	0.82	0.00	0.00	0.00	98.93	-
Ilm+Sulph+g	Cpx	2	41.05	4.03	0.00	12.12	8.49	-	10.67	22.32	0.68	0.00	0.20	0.00	99.55	-
basanite, volcano Kabhegy, BBHVF																
Gl+Rho+	Gl K	7	61.59	0.11	0.01	23.31	0.54	0.00	0.07	0.06	6.46	7.18	0.25	0.32	99.91	82.2
Cpx+Amph+	Gl Na	4	61.90	0.18	0.00	25.67	0.50	0.01	0.03	0.34	10.63	0.23	0.31	0.00	99.79	-
Ap+Sulph+	Rho	5	26.53	10.55	0.28	18.76	14.14	0.10	14.61	12.24	1.04	0.00	0.00	0.00	98.25	-
Flsp+g	Cpx	2	43.70	4.14	0.01	11.05	6.14	0.10	11.09	22.57	0.65	0.00	0.41	0.00	99.85	-
	Amph	2	39.26	7.61	0.04	15.82	6.27	0.03	13.30	12.05	2.88	0.85	0.09	0.07	98.23	-
	Flsp	1	62.65	0.12	0.00	23.19	0.43	0.01	0.04	4.15	7.18	0.65	0.00	0.00	98.41	-
Gl+Cr-sp+	Gl K	2	58.85	0.09	0.03	22.26	0.46	0.00	0.02	0.12	4.52	13.34	0.22	0.04	99.94	82.2
Rho+Cpx+	Gl Na	3	61.83	0.22	0.01	25.15	0.37	0.01	0.04	0.26	11.35	0.20	0.18	0.00	99.61	-
Amph+Ap+	Rho	2	26.14	11.10	0.34	18.82	14.37	0.07	14.12	12.32	0.88	0.00	0.00	0.00	98.14	-
Sulph+g	Cpx	3	43.02	4.55	0.02	11.04	6.61	0.07	10.94	22.69	0.69	0.00	0.20	0.00	99.84	-
Gl+Rho+	Gl	1	60.38	0.20	0.02	25.54	0.56	0.00	0.14	0.22	7.20	4.48	0.21	0.27	99.21	81.5
Cpx+Sulph+g	Rho	1	26.22	10.74	0.93	18.20	14.28	0.05	14.85	11.95	1.64	0.00	0.00	0.00	98.87	-
	Cpx	1	43.95	4.07	0.09	11.61	5.69	0.10	11.10	22.36	0.83	0.00	0.20	0.00	100.00	-
basanite, volcano Zalahaláp, BBHVF																
Gl+Rho+Cpx+	Gl	2	62.93	0.61	0.00	23.90	1.04	0.01	0.19	1.32	4.59	3.35	0.99	0.17	99.08	72.2
Ap+Ilm+g	Rho	1	27.45	11.42	0.48	15.30	17.94	0.14	13.21	11.75	1.24	0.00	0.07	0.00	99.00	-
basanite, Eresztvény, NGVF																
Gl+Rho+	Gl	1	55.30	0.14	0.14	25.60	1.67	0.13	0.01	0.11	9.52	6.28	0.04	0.05	98.99	77.1
Cpx+Ap+g	Rho	1	24.90	9.03	0.37	18.10	18.20	0.35	13.80	12.10	0.94	0.00		0.00	97.79	-
basanite, Magyarbánya, NGVF																
Gl+Rho+g	Gl	1	52.60	0.03	0.00	23.20	0.33	0.21	0.04	7.88	12.60	0.96	0.02	0.11	97.98	62.8
	Rho	1	24.30	12.00	0.20	14.00	24.30	0.61	10.10	10.20	2.03	0.00		0.00	97.74	-
basanite, Terbelét, NGVF																
Gl+Rho+	Gl	1	56.70	0.13	0.15	24.90	0.90	0.25	0.17	0.82	9.04	5.89	0.00	0.47	99.42	72.5
Cpx+g	Rho	1	24.10	9.05	0.35	18.40	21.30	0.71	10.70	11.50	0.83	0.00	-	0.00	96.94	-
	Cpx	1	44.30	1.87	0.05	13.00	7.14	0.29	10.30	22.10	0.67	-	-	-	99.72	-
Gl+Rho+	Gl	1	55.60	0.19	0.00	24.90	1.38	0.00	0.34	0.24	9.71	5.67	0.00	0.03	98.06	73.3
Cpx+Sulph+g	Rho	1	24.90	9.38	0.29	18.20	19.80	0.40	11.60	11.30	1.10	0.00	-	0.00	96.97	-
hawaiite, Pécskő, NGVF																
Gl+Al-sp+	Gl	1	62.49	0.78	0.00	26.17	0.54	-	0.14	0.84	2.17	5.19	0.76	0.23	99.31	87.0
Rho+Cpx+	Al-sp	1	0.00	0.70	0.22	64.04	14.83	-	20.06	0.00	0.00	0.00	0.00	0.00	99.86	-
Sulph+g	Rho	1	25.43	11.63	0.12	19.12	14.35	-	15.67	11.64	1.35	0.00	0.04	0.00	99.35	-
	Cpx	1	42.35	6.00	0.03	11.86	4.06	-	12.22	22.13	0.82	0.00	0.04	0.00	99.51	-
Gl+Al-sp+	Gl	2	62.26	0.72	0.00	26.75	0.50	-	0.27	1.22	2.17	3.67	1.47	0.26	99.26	86.0
Rho+Cpx+	Rho	1	25.24	12.42	0.35	19.77	12.50	-	16.44	11.02	1.67	0.00	0.00	0.00	99.41	-
Amph+	Cpx	1	44.13	4.19	0.01	11.41	4.23	-	12.50	21.74	0.69	0.00	0.04	0.00	98.95	-
Sulph+g	Amph	1	38.93	10.21	0.00	13.93	5.78	-	13.44	12.44	2.95	0.68	0.37	0.01	98.74	-

Note: Gl K, Gl Na = coexisting K-rich and Na-rich glasses. Comp. of inclus. = composition of inclusion; H. in Fo = Host in Fo

Daughter Al-spinel is poor in TiO_2 (0.3-0.7 wt.%) and Cr_2O_3 (0.0-1.2 wt.%) belonging to the $FeAl_2O_4$-$MgAl_2O_4$ series. In some inclusions the xenogenic Cr-

spinel is overgrown by Al-spinel. The trapped Cr-spinel has variable composition, is poor in TiO_2 (<5 wt.%) and corresponds to single spinel crystals coexisting with silicate melt inclusions in the host olivine. Daughter magnetite occurring rarely in rhönite-bearing inclusions is rich in TiO_2 (up to 17 wt.%).

Amphibole from inclusions contains up to 10.2 wt.% TiO_2 and belongs to Ti-rich kaersutite. Apatite is rich in fluorine, contents of Cl, SiO_2 and SrO do not exceed 1 wt.%. According to scanning microscopy, sulphide blebs consist mostly of pyrrhotite, which is poor or free in Ni, other phases (pentlandite, chalcopyrite or intermediate solid solution) are minor.

Glass

The compositions of glasses in unheated inclusions are strongly variable in content of SiO_2 (49.5 -65.5 wt.%), Al_2O_3 (20.6-28.2 wt.%), total alkalis (up to 19.5 wt.%), whereas FeO_{tot}, CaO and MgO usually do not exceed 5 wt.%. The Na_2O/K_2O ratio is also highly variable, even for the inclusions from the same locality. In silicate melt inclusions from NGVF and BBHVF (Table 5), coexistence of K- and Na-rich glasses was observed within the single inclusions [44, 46]. Variable composition of glasses may refer to the initial composition of silicate melt trapped by olivine as inclusion. From the other side, it also depends on the total amounts of daughter phases crystallized within the inclusion and their compositions.

DISCUSSION

Occurrence and stability of rhönite in alkali basalts and their xenoliths

The review of the literature on volcanites around the world shows that rhönite occurs mostly as phenocrystal/groundmass and ocelli mineral in silica-undersaturated alumina-rich (miaskitic) volcanic rocks like alkali basalt, alkali lamprophyre, phonolite, tephrite, shoshonite and nephelinite or a phase after Ti-amphibole replacement in deep-seated xenoliths. However, rhönite has never been reported from peralkaline volcanic rocks and related carbonatites. Thus, the presence of rhönite, as an alumina-rich phase, is in accordance with composition of miaskitic rocks.

In alkali basalts rhönite very rarely occurs as phenocryst [42] and is more common as microphenocryst or groundmass mineral. It is more typical of glass-bearing rocks or rocks with quench-textured groundmass [60, 7, 66, 40]. There is a little information about the petrographic relations of rhönite to other minerals in mafic rocks. Lacroix [53], Kyle and Price [52] and Seghedi et al. [73] suggest the following crystallization sequence in the groundmass of alkali basalts: olivine → rhönite → clinopyroxene → Ti-magnetite. However, relationships of olivine-free phenocryst association in more siliceous volcanics (tephrite-phonolite, [42]) indicate reverse sequence: Ti-magnetite → clinopyroxene → rhönite.

Some publications indicate that rhönite is an abundant phase of assemblages, which partially or completely replace amphibole in mega/xenocrysts and mafic-ultramafic xenoliths (Table 1). The genesis of such rhönites may be advocated to

1) solid breakdown of amphibole [50, 31], 2) decompression melting of amphibole [7] or 3) reaction of amphibole with evolved host melt infiltrating into the lithosphere section which the host basalts sampled [74]. In all these cases, the

Table 6.

Chemistry of rhönites after amphibole replacement and from xenoliths in alkali basalts of studied volcanic fields

	1	2	3	4	5	6	7	8	9	10	11
n	*10*	*6*	*8*	*3*	*11*	*13*	*11*	*4*	*13*	*3*	*4*
SiO_2	27.12	25.50	26.01	28.53	23.64	25.97	24.91	28.97	22.48	25.21	24.35
TiO_2	9.18	8.67	8.42	8.47	11.13	10.02	11.30	8.34	13.50	8.87	11.56
Cr_2O_3	0.09	0.03	0.00	0.29	0.00	0.06	0.01	0.06	0.29	0.02	0.20
Al_2O_3	16.20	15.26	16.26	18.93	18.22	15.92	15.95	14.79	17.13	16.51	16.44
FeO_{tot}	18.64	20.37	22.38	9.90	19.44	20.56	20.52	20.29	18.27	25.76	21.72
MnO	0.15			0.07	0.11	0.11	0.14	0.12	0.06	0.15	0.16
MgO	14.73	15.69	12.93	17.77	13.37	13.64	13.39	14.27	13.76	10.48	11.60
CaO	11.09	11.31	11.68	12.07	11.68	11.19	11.34	10.27	11.87	11.24	11.36
Na_2O	1.65	1.86	1.62	1.28	1.05	1.32	1.30	2.02	0.98	1.12	1.15
Sum	98.85	98.68	99.30	97.30	98.64	98.80	98.86	99.11	98.35	99.36	98.54
Fe_2O_3	9.04	16.71	12.50	3.22	7.90	8.38	8.17	9.02	6.55	9.43	6.02
FeO	10.51	5.34	11.13	7.00	12.34	13.02	13.17	12.17	12.38	17.28	16.31
Sum	99.76	100.36	100.56	97.62	99.43	99.64	99.68	100.01	99.00	100.31	99.14
Formula calculated on the basis of 14 cations and 20 oxygens											
Si	3.584	3.362	3.463	3.710	3.173	3.480	3.350	3.828	3.041	3.431	3.324
Al^{IV}	2.416	2.372	2.537	2.290	2.827	2.513	2.527	2.172	2.731	2.569	2.645
Fe^{3+IV}	0.000	0.266	0.000	0.000	0.000	0.007	0.123	0.000	0.228	0.000	0.032
[Z]	6.000	6.000	6.000	6.000	6.000	6.000	6.000	6.000	6.000	6.000	6.000
Al^{VI}	0.107	0.000	0.015	0.612	0.055	0.000	0.000	0.130	0.000	0.079	0.000
Ti^{4+}	0.913	0.859	0.843	0.828	1.124	1.010	1.143	0.828	1.373	0.908	1.187
Cr	0.009	0.003	0.000	0.029	0.001	0.007	0.002	0.007	0.031	0.002	0.022
Fe^{3+VI}	0.898	1.392	1.253	0.315	0.798	0.838	0.703	0.897	0.438	0.966	0.586
Fe^{2+VI}	1.155	0.589	1.239	0.762	1.337	1.409	1.454	1.315	1.376	1.900	1.827
Mn	0.017			0.008	0.012	0.013	0.015	0.013	0.007	0.017	0.018
Mg	2.901	3.085	2.566	3.444	2.674	2.724	2.683	2.810	2.775	2.127	2.360
Ca^{VI}	0.000	0.073	0.084	0.003	0.000	0.000	0.000	0.000	0.000	0.000	0.000
[Y]	6.000	6.000	6.000	6.000	6.000	6.000	6.000	6.000	6.000	6.000	6.000
Ca^{VIII}	1.570	1.524	1.583	1.678	1.680	1.606	1.634	1.453	1.720	1.639	1.661
Na	0.424	0.476	0.417	0.322	0.273	0.344	0.340	0.517	0.256	0.295	0.304
Fe^{2+VIII}	0.006	0.000	0.000	0.000	0.047	0.050	0.027	0.029	0.024	0.066	0.034
[X]	2.000	2.000	2.000	2.000	2.000	2.000	2.000	2.000	2.000	2.000	2.000
Mg#	0.58	0.58	0.51	0.76	0.55	0.54	0.54	0.56	0.57	0.42	0.49
Mg*	0.72	0.82	0.66	0.82	0.67	0.66	0.65	0.68	0.67	0.53	0.56

Note: 1 - xenomorphic grain in clinopyroxene phenocrysts, trachybasalt, Pécskő, NGVF; 2-3 - an product of complete replacement of amphibole xeno/phenocrysts in basalts: 2 - volcano Hegyesd, BBHVF; 3 - volcano Bondoró, BBHVF; 4-8 - an interstitial phase in amphibole-bearing xenoliths: 4 - Ol horblendite, Fülek, NGVF; 5 - Sp clinopyroxenite, pipe Krasnoozerskaya-satellite, NMDVF; 6 - Sp clinopyroxenite, dike Bele, NMDVF; 7 - Ol clinopyroxenite, volcano Uchuchei, UPVF; 8 - Ol clinopyroxenite, UPVF; 9-10 - an interstitial phase in amphibole-free xenoliths: 3 - Sp harzburgite, volcano Ingamakit, UPVF; 10 - clinopyroxenite, pipe Botikha, NMDVF; 11 - Ol-Cpx cumulate xenolith, Mt. Arod, MRVF. Mg# = $Mg/(Mg+Fe_{tot})$; Mg* = $Mg/(Mg+Fe^{2+})$. Formula calculated according to the scheme suggested by Kunzmann [49].

(products after amphibole are represented by the assemblage of olivine ± spinel + rhönite + clinopyroxene ± Ti-magnetite/ilmenite ± plagioclase or foid minerals ± glass (in approximate sequence of crystallization). It is suggested that such phase

association formed at >1000°C during temporary residence of xenoliths in shallow magmatic chamber and cannot be directly related to any metasomatic events occurred in the mantle [74, 31]. Such rhönite-bearing xenocryst and xenoliths are common in studied basalts from the BBHVF, NGVF, NMDVF, MRVF and UPVF

Table 6). In some cases, rhönite occurs in products of complete replacement of amphibole phenocrysts. Moreover, rhönite occurs in "melt pockets" of some xenoliths, which did not contain primary amphibole ([4, 31]; author's data in Table 6). In agreement with Babkine et al. [4], we suggest that such rhönite-bearing assemblages might be formed by local melting of xenolith clinopyroxene with or without participation of host melt or due to penetration of host melt into xenolith.

Kunzmann [48, 49] summarized all known data on rhönite stability. According to this author, rhönite is stable from 850-1000°C at 1 bar to at least 900-1100 °C at 5 kbar; there is no limitation on the oxygen fugacity. The stability of rhönite in alkali basalts experimentally determined by Kunzmann [48] is restricted to pressures below 0.6 kbar, and temperatures from 840-1200°C. Based on experiments [7, 48, 31] indicated that "melt pocket" microphenocrystal association (rhönite + olivine + clinopyroxene + plagioclase) in the Mount Sidley xenoliths formed within a narrow temperature range of 1190-1140°C at pressure <0.5 kbar. Moreover, these authors showed that rhönite replacing kaersutite crystallized under more oxidizing conditions (≈NNO buffer) than rhönite from "melt pockets" (≈QFM buffer).

Our data show that rhönite in olivine-hosted silicate melt inclusions from alkali basalts crystallized within a narrow temperature range (1180-1260°C). However, we could not constrain the stability of these rhönites in terms of formation pressure and oxygen fugacity. Homogenization temperatures for silicate melt inclusions and microthermometry data of coexisting CO_2 inclusions indicate that olivine trapped these inclusions at >1300°C and pressure at least >3-5 kbar. However, it is not known at what pressure rhönite and other daughter phases started to crystallize within the inclusion: at elevated pressure or after decreasing of pressure to less than 0.5-1 kbar. However, by analogy with phenocryst/groundmass rhönite, we suggest that it was at <0.5 kbar. The petrography of studied inclusions indicates the following sequence of crystallization: Al-spinel → rhönite → Ti-Al-clinopyroxene → apatite → amphibole → Ti-magnetite (and/or ilmenite). The small sizes of daughter phases of olivine-hosted silicate melt inclusions do not allow estimating precise oxygen fugacity for rhönite crystallization, although it is possible to evaluate roughly from the crystal chemistry of rhönite (see [31]). However, these estimations give a very wide range (from lower than QFM to NNO), even for inclusion rhönites from particular rock and locality (Fig. 4). Calculations, based on the host olivine-Cr-spinel pair, provides values of oxygen fugacity 1-2.5 log units higher than the QFM buffer for the earliest stage of initial melt crystallization in the Hegyestű and Tergesh basalts [45; Timina et al., 2006].

Our data to some extent contradict the conclusions of Kunzmann [49] about

temperature stability of rhönite. Apparently, some discrepancies may be related to

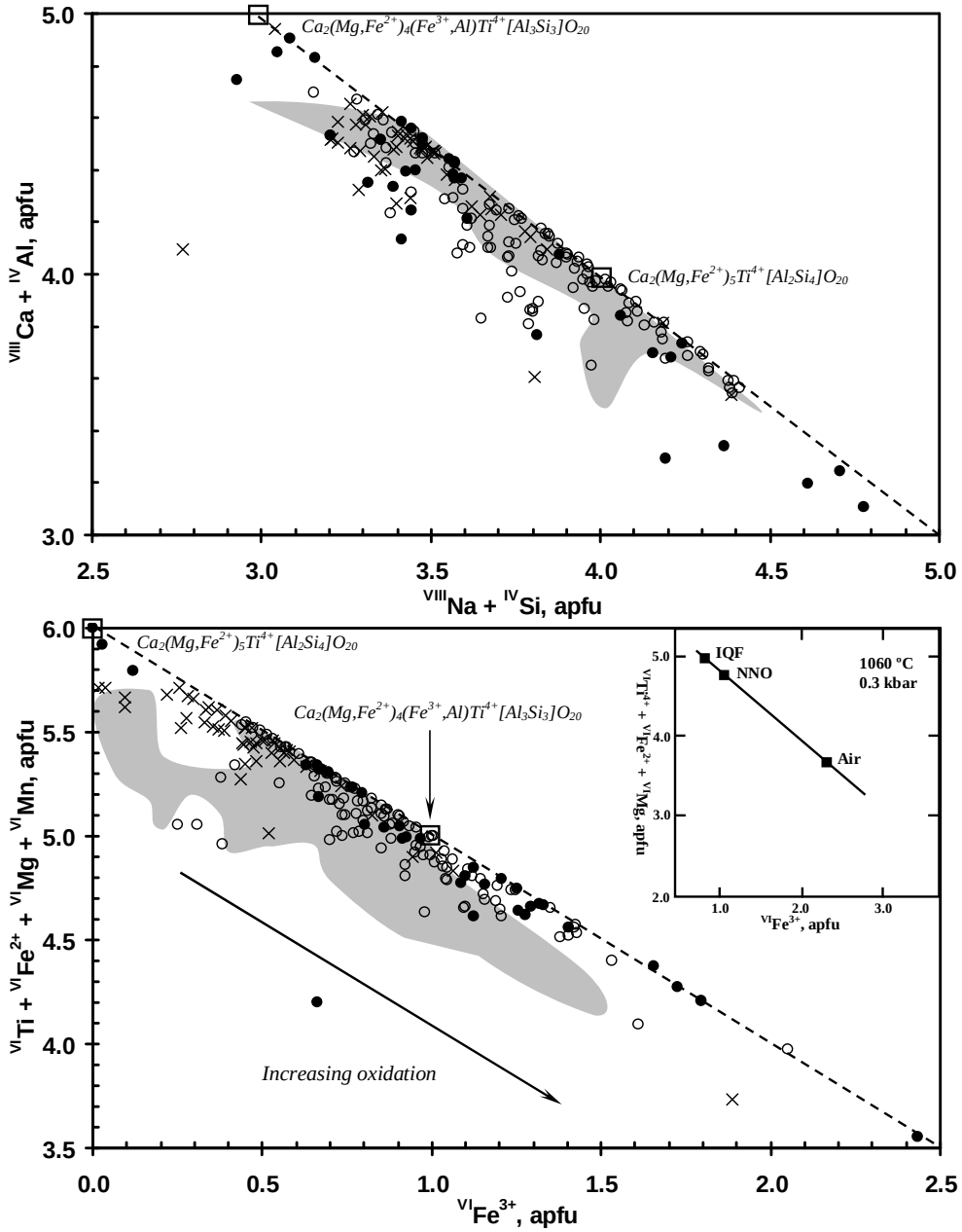

Fig. 4. **Plots of $^{VIII}Na + {}^{IV}Si$ vs. $^{VIII}Ca + {}^{IV}Al$ and $^{VI}Fe^{3+}$ vs. $^{VI}Ti^{4+} + {}^{VI}Fe^{2+} + {}^{VI}Mg + {}^{VI}Mn$ (apfu) for analyses of terrestrial rhönites compared with those in olivine-hosted silicate melt inclusions from alkali basalts (shaded field).**

Solid circles = phenocrystal-groundmass rhönites from alkali basalts [79, 53, 11, 32, 52, 60, 10, 7, 34, 66, 40, 49, 8, 73, 16, 68, 22, 64, 42]; Open circles = rhönites after kaersutite in mafic-ultramafic xenoliths and after xenocrystal/phenocrystal kaersutite from alkali basalts ([52, 60, 33, 74, 31, 1, 88]; author's data from Tab. 6); Cross = rhönite quenched microphenocrysts in "melt pockets" of mafic-ultramafic xenoliths from alkali basalts ([4, 26, 74, 31]; author's data from Tab. 6). Ideal compositions are also plotted for comparison. Inset shows trend of rhönite compositions in nepheline basanite synthesized under IQF, NNO and air conditions at 1060°C/0.3kbar [49].

the chemistry of rhönite because this mineral is highly variable in the contents of Fe^{2+}, Fe^{3+}, and other cations due to isomorphic substitutions. However, there are no

experimental data on the dependence of rhönite chemistry on the temperature. In addition, the chemical and physical conditions of solidification in olivine-hosted melt inclusions and in groundmass of alkaline basalts might be different. Thus, direct study of melt inclusions in rhönite help to establish the immediate PT-conditions for crystallization of this mineral from different environments.

Compositional comparison of olivine-hosted and other rhönites

The new author's data for rhönite from xenoliths of studied volcanic fields are given in Table 6. The general comparison of all worldwide rhönites from alkali basalts and their xenoliths is shown on Fig. 4. Besides olivine-hosted mineral, new rhönite analyses made by the principal author and data available in the literature were conventionally subdivided into the three groups: (1) phenocryst and groundmass rhönite from alkali basalts; (2) rhönite from partial or compete products of amphibole alteration from phenocrysts, xenocrysts and xenoliths; (3) rhönite from amphibole-free ultramafic-mafic xenoliths. It should be noted that some mineral compositions initially labelled as rhönite [35-37, 72] and leucorhönite from burned spoil-heaps [14] are really poor or free in TiO_2. Using 50% rule such species seem to belong to one of theoretical end-members proposed by Kunzmann [49] for the aenigmatite-rhönite family, with general structural formula $\mathbf{Ca_2(Mg,Fe^{2+})_4(Fe^{3+},Al)_2[Al_2Si_4O_{20}]}$. Extraterrestrial rhönites are beyond the scope of this review due to the presence of trivalent titanium in their structure and their origin in extremely reduced conditions [6, 61, 62]. According to Bonaccorsi et al. [8], the majority of terrestrial rhönites are virtually free in Ti^{3+}. In general, very broad variations in composition are common of rhönites from various environments. Olivine-hosted rhönite compositions lie only in very compact region in contrast to those of other rhönites (Fig. 4). The negative correlations of Ca+Al vs. Na+Si and $Ti+Fe^{2+}+Mg+Mn$ vs. Fe^{3+} are pronounced for all rhönites indicating possible isomorphic substitutions with other minerals of the aenigmatite-rhönite family.

Problem of rhönite appearance in olivine-hosted inclusions

The problem why rhönite occurs in some silicate melt inclusions in olivine phenocrysts, whereas other neighbouring inclusions are virtually free in this mineral is arisen by the melt inclusion studies of alkali basalts from different regions. The similar problem is also relevant for alkali basalts with comparable bulk and modal composition. In the case of melt inclusions, it is clear that rhönite-bearing inclusions are generally confined to the core of host olivine whereas rhönite-free inclusions are always situated in the outer zones. In addition, ilmenite or Ti-magnetite is common of rhönite-free inclusions and scarce or absence in rhönite-containing ones. Moreover, there are no essential differences in composition of other daughter phases (e.g., Al-spinel, clinopyroxene) between rhönite-bearing and rhönite-barren inclusions.

It is highly likely that the solution of the problem of rhönite appearance is connected neither with chemical composition of rhönite and other daughter phases nor with distributions of inclusions in host olivine. Possibly, it deals with the

structural peculiarities of rhönite and its paragenesis. The studies of the crystal structure indicate that rhönite is chain silicate [8, 84]. This mineral constantly coexists with clinopyroxene and minerals of the spinel family (Cr-spinel, Al-spinel, Ti-magnetite). Bonaccorsi et al. [8] made the first remarks and interpretations about such close association in different geological environments. Moreover, according to these authors, the rhönite structure represents an alternation of "pyroxene" and "spinel" slabs. In this sense, rhönite is not only a transitional member between Al-spinel and Ti-Al-clinopyroxene in a crystallization sequence, but also an intermediate member of a polysomatic series having spinel and pyroxene as the end-members. This feature of rhönite may indicate that it is a short-lived mineral (or unstable "ephemeral" mineral) and very sensitively reacts on the changes in any parameters during crystallization. In case of melt inclusions or rocks, it maybe the cooling rate and, as a result, clinopyroxene or Ti-magnetite (other spinel) or their coexistence will be more stable paragenesis than rhönite. The association of amphibole + rhönite seems to reflect possible microstructural relations between these minerals.

CONCLUSIONS

1. Rhönite is very rare mineral, which occurs in olivine-hosted inclusions from alkali basalts of different volcanic regions. Usually, rhönite-bearing inclusions are confined to the central parts of host olivine. Such inclusions were trapped at T>1300^{o}C and P>3-5 kbar.
2. The petrography and thermometry of rhönite-bearing inclusions in olivine shows the general sequence: Al-spinel → rhönite → Ti-Al-clinopyroxene → apatite → amphibole, Ti-magnetite (or ilmenite) → glass.
3. Rhönite in olivine-hosted silicate melt inclusions crystallized in a narrow temperature range (1180-1260°C) and at pressure <0.5 kbar. Temperatures for inclusion rhönites are slightly higher than those for phenocrystal/groundmass rhönite from alkali basalts (840-1200^{o}C).
4. The rarity of rhönite both in melt inclusions and other associations in alkali basalts may be explained from its microstructural features. Rhonite is an intermediate member in the polysomatic series spinel-pyroxene. It is suggested that this mineral is not a stable in varying conditions of crystallization. Possibly, the changing in some parameters may lead to preferable crystallisation of clinopyroxene or Ti-magnetite (Al-spinel) or their paragenesis instead of rhönite.

ACKNOWLEDGEMENTS

The first author has benefited greatly from the comments of Yuri Dublyansky who helped to improve the draft version of the manuscript. We thank L.N. Pospelova for help in microprobe analyses of melt inclusions and minerals at the IGM. We are grateful to S.V. Kovyazin and Ye.I. Petrushin for heating experiments with melt inclusions. B.A. Litvinovsky, V.S. Samoylov, T.Ju.

Bazarova and Sz. Harangi are kindly thanked for donating the rock samples from the TKRVF, MRVF and some localities of the BBHVF. We are also grateful to V.G. Mal'kovets for xenolith samples from the Krasnoozerskaya-satellite pipe, NMDVF. This work was supported by SD RAS (integration project 6.15), the Russian Foundation for Basic Research (grants 06-05-65015 to Timina, T.Yu.) and the Hungarian National Scientific Foundation (OTKA) (grants T034922 to Török, K. and T030846 to Szabó, Cs.) and Ministry of Energy Infrastructure, State of Israel (grant ES-16 to Vapnik, Ye.).

REFERENCES

1. **Alletti M., Pompillo M., Rotolo S.G.** Mafic and ultramafic enclaves in Ustica Island lavas: inferences on composition of lower crust and deep magmatic processes // Lithos, 2005, v. 84, p. 151-167.
2. **Ashchepkov I.V., Kepezhinskas V.V., Malkovets V.G., Ovchinnikov Yu.I.** Mantle xenoliths from the Meso-Cenozoic volcanic pipes of Khakassia. UIGGM SD RAS, Novosibirsk, 1995, 39 p.
3. **Ananiev V.V., Okrugin V.M.** Mineralogy of molten inclusions in olivines from high-alumina basalt melts in Kamchatka // Plinius 5, 1991, p. 264-264.
4. **Babkine J., Conquere F., Vilminot J.C., Duong P.K.** Sur un nouveau gaisement de rhönite (Monistrd-d'Allier, Haute Loire) // C. R. Acad. Sci., Paris, 1964, Ser. D 258, p.5479-5481.
5. **Balogh K., Árva-Sós E., Pécskai Z., Ravasz-Baranyai L.** K/Ar dating of Post-Sarmatian alkali basaltic rocks in Hungary // Acta Mineral. Petrogr., 1986, v. 28, p. 75-93.**Beckett J.R., Grossman L., Haggerty S.E.**. Origin of Ti^{3+}-bearing rhönite in Ca-Al-rich inclusions: an experimental study // Meteoritics, 1986, v. 21, p. 332-333.
6. **Boivin P.** Données expérimentales préliminaires sur la stabilité de la rhönite à 1 atmosphère. Application aux gisements naturels // Bull. Minéral., 1980, v. 103, p. 491-502.
7. **Bonnacorsi E., Merlino S., Pasero M.**. Rhönite: structure and microstructural features, crystal chemistry and polysomatic relationships // Eur. J. Mineral., 1990, v. 2, p. 203-218.
8. **Bragin V.Yu., Reutskii V.N., Litasov K.D., Malkovets V.G.** Upper Cretaceous intraplate magmatic events in the North Minusa depression: paleomagnetic and $^{40}Ar/^{39}Ar$ data // Geol. Geofiz., 1999, v. 40, № 4, p. 559-565.
9. **Brooks C.K., Pedersen A.K., Rex D.C.** The petrology and age of alkaline mafic lavas from the Nunatak zone of central East Greenland // Grønlands Geologiske Undersøgelse, Bull., 1979, v. 133, 28 pp.
10. **Cameron K.L., Carman M.F., Butler J.C.**. Rhönite from Big Bend National Park, Texas // Am. Mineral., 1970, v. 55, p. 864-874.
11. **Canil D., Scarfe C.M.** Origin of phlogopite in mantle xenoliths from Kostal Lake, Wells Gray Park, British Columbia // J. Petrol., 1989, v. 30, p. 1159-1179.
12. **Canil D., Scarfe C.M.** Origin of phlogopite in mantle xenoliths from Kostal Lake, Wells Gray Park, British Columbia // J. Petrol., 1989, v. 30, p. 1159-1179.
13. **Chesnokov B.V.** New minerals from burned spoil-heaps of the Chelyabinsk coal basin (tenth report - overview of results for 1982-1995) // Ural. Mineral. Sbornik, 1997, v. 7, p. 5-32 (in Russian, with English Abstr.).
14. **Chesnokov B.V., Vilisov V.A., Bushmakin A.F., Kotlyarov V.A.,** Belogub E.B. New minerals from burned spoil-heaps of the Chelyabinsk coal basin (sixth report) // Ural. Mineral. Sbornik, 1994, v. 3, p. 3-34 (in Russian, with English Abstr.).

15. **Clocchiatti R.** Les fulgurites et roches vitrifiées de l'Etna // E.J.M., 1990, v. 2, p 479-494.
16. **Downes H., Vaselli O., Seghedi I., Ingram G., Rex D., Coradossi N., Pécskay Z., Pinarelli L.** Geochemistry of late Cretaceous – early Tertiary magmatism in Poiana Ruscă (Romania) // Acta Vulcanol., 1995, v. 7, № 2, p. 209-217.
17. **Embey-Isztin A., Downes H., James D.E., Upton B.G.J., Dobosi G., Scharbert H.G., Ingram G.A.** The petrogenesis of Pliocene alkaline volcanic rocks from the Pannonian Basin, Eastern Central Europe // J. Petrol., 1993a, v. 34, p. 317-343.Eyal M., Becker A., Samoylov **V.** Mt. Arod – an Early Cretaceous basanitic volcano with a fossil lava lake // Isr. J. Earth Sci., 1996, v. 45, p. 31-38.
18. **Ficke B.** Petrologische Untersuchungen an Tertiaren basaltischen bis phonolithischen Vulkaniten der Rhön // Tschermars Min. Petrogr. Mitt. Ser., 1961, v. 3, № 7, p. 337-436.
19. **Floss C., Nazarov M.A., Taylor L.A.** Ultrarefractory-depleted rare-earth-element patterns in a rhönite-bearing type B1 calcium-aluminum-rich inclusion from Efremovka // Meteorit. Planet. Sci., 2000, v. 35, p. 53-54.
20. **Fodor R.V., Hanan B.B.** Geochemical evidence for the Trinidade hotspot trace: Columbia seamount ankaramite // Lithos, 2000, v. 51, p. 293-304.
21. **Friedrich L.** The pressure and temperature conditions and timing of glass formation in mantle-derived xenoliths from the Newer Basalts, W. Victoria, Australia. Master's thesis, University of Western Ontario, London, ON, Canada, 2004.
22. **Fuchs L.H.** Occurrence of wollastonite, rhönite, and andradite in the Allende meteorite // Am. Mineral., 1971, v. 56, p. 2053-2068.
23. **Fuchs L.H.** The mineralogy of a rhönite-bearing calcium aluminium rich inclusion in the Allende meteorite // Meteoritics, 1978, v. 13, p. 73-88.
24. **Gamble J.A., Kyle P.R.** The origin of glass and amphibole in spinel-wehrlite xenoliths from Foster Crater, McMurdo volcanic group, Antarctica // J. Petrol., 1987, v. 28, p. 755-779.
25. **Garfunkel Z.** Darfur-Levant array of volcanics – A 140 Ma long record of hot spot beneath the African-Arabian continent and its bearing on Africa's absolute motion // Isr. J. Earth Sci., 1991, v. 40, p. 138-150.
26. **Golovin A.V., Sharygin V.V.** Petrogenetic informativity of fluid and melt inclusions in minerals of deep-seated xenoliths from basanites of the Bele pipe (North-Minusa Depression) // Geol. Geofiz., 2007, v. 48, № 10, p. 1043-1060.
27. **Golovin A.V., Sharygin V.V., Malkovets V.G.** Melt evolution during crystallization of basanites of the Bele pipe, Munusa depression // Geol. Geophis., 2000, v. 41, № 12, p. 1760-1782.
28. **Golovin A.V., Sharygin V.V., Malkovets V.G.** Interstitial associations in deap-seated xenoliths from pipes of the North Minusa depression // Abstracts volume of workshop "Alkaline magmatism of the Earth", Moscow, 2002, p. 34-35 (in Russian).
29. **Grapes R.H., Wysoczanski R.J., Hoskin P.W.O.** Rhönite paragenesis in pyroxenite xenoliths, Mount Sidley volcano, Marie Byrd Land, West Antarctica // Mineral. Mag., 2003, v. 67, p. 639-651.
30. **Grünhagen H., Seck H.A.** Rhönit aus einem melaphonolith von Puy de Saint-Sandoux (Auvergne) // Tschermaks Min. Petr. Mitt., 1972, v. 18, p. 17-38.
31. **Gushchin A.V., Ivanova T.A., Ganzeev A.A.** Tephrite-shoshonite series of South-East Armenia // Geologiay i Razvedka, 1991, № 11, p. 3-14 (in Russian).
32. **Havette A., Clocchiatti R., Nativel P., Montaggioni L.** Une paragenèse inhabituelle à fassaïte, mèlilite et rhönite dans un basalte alcalin contaminé au contact d'un récif coralline (Saint-Lieu, Ile de la Réunion) // Bull. Minéral., 1982, v. 105, p. 364-375.
33. **Heritsch H.** Rhönit-Kristallite in basaltischen Glasern des Steinberges bei Feldbach, Oststeiermark // Mitt. Naturwiss. Ver. Steiermark, 1986, v. 116, p. 43-49
34. **Heritsch H.**. Rontgendaten von Nephelin und Rhönit-Kristalliten aus den basltischen

Glasern des Steinberges bei Feldbach, Oststeiermark // Mitt. Naturwiss. Ver. Steiermark, 1987, v. 117, p. 27-34.
35. **Heritsch H., Ettinger K.** Titanarme Rhönit als Kristallite in basaltischen Glasern des Steinberges bei Feldbach, Steiermark // Mitt. Abt. Miner. Landesmus, Joanneum, 1998, v. 62-63, p. 75-78.
36. **Hurai V., Huraiova M., Konecny P., Thomas R.**. Mineral-melt-fluid composition of carbonate-bearing cumulate xenoliths in Tertiary alkali basalts of southern Slovakia // Mineral. Mag., 2007, v. 71, p. 63-79.
37. **Jannot S., Schiano P., Boivin P.** Melt inclusions in scoria and assosiated mantle xenoliths of Puy Beaunit volcano, Chained ea Puys, Massif Central, France // Contrib. Mineral. Petrol. 2005, 149, 600-612.
38. **Johnston, A.D., Stout, J.H.** Compositional variations of naturally occurring rhoenite // Am. Mineral., 1985, v. 70, p. 1211-1216.
39. **Jones A.P.** Mafic silicates from the nepheline syenites of Motzfeldt centre, South Greenland // Mineral. Mag., 1984, v. 48, p. 1-12.
40. **Kogarko L.N., Hellebrand E., Ryabchikov I.D.** Trace element partitioning between rhonite and silicate melt in Cape Verde volcanics // Geochem. Inter., 2005, v. 43, № 1, p. 1-7.
41. **Kopylova M.G., Rickard R.S., Kleyenstueber A., Taylor W.R., Gurney J.J., Daniels L.R.M.** First occurrence of strontian K-Cr-loparite and Cr-chevkinite in diamonds // Geol. Geophis., 1997, v. 38, № 2, p. 382-397.
42. **Kóthay K., Pető M., Szabó Cs., Török K., Sharygin V.V., Timina T.Ju., Ntaflos T.** A comprehensive silicate melt inclusion study of olivine phenocrysts from Hegyestű (Bakony-Balaton Highland) and Pécskő (Nógrád-Gömör) alkali basalts, Pannonian basin, Hungary // Acta Mineral. Petrogr. Abstr. Ser., Szeged, 2003, v. 2, p. 105-106.
43. **Kóthay K., Szabó Cs., Török K., Sharygin V.V.** A droplet of the magma: Silicate melt inclusions in olivine phenocrysts from alkali basalt of Hegyestű // Földtani Közlöny, 2005, v. 135 № 1, p. 31-55 (in Hungarian with English abstract).
44. **Kóthay K., Sharygin V.V., Török K., Ntaflos Th., Szabó Cs.**. New results in study of silicate melt inclusions in Bakony-Balaton Highland Volcanic Field, Pannonian Basin, Western Hungary // Abstract volume of ECROFI XIX, University of Bern, Switzerland, 2007, 216 p.
45. **Kronz A., Zolgharnian Z., Maier P., Keesmann I.** Rhönit $Ca_4(Fe^{2+},Fe^{3+},Mn,Al,Ti)_{12}(Al,Si)_{12}O_{40}$ in historischen schlacken // Berichte der Deutschen Mineralogischen Gesellschaft, 1992, № 1, p. 165-165.
46. **Kunzmann T.** Rhönit: Mineralchemie, Paragenese und Stabilität in alkalibasaltischen Vulkaniten, Ein Beitrag zur Mineralogenese der Rhönit-Änimagnit-Mischkristallgruppe Dissertation Universität München, 1989, 151 p.
47. **Kunzmann T.** The aenigmatite-rhönite mineral group // Eur. J. Mineral., 1999, № 11, p. 743-756.
48. **Kunzmann T., Spicker G., Huckenholz H.G.** Stabilität von rhönit in natürlichen und synthetischen paragenesen // Fortsch. Mineral., 1986, v. 64, Beihelf 1, 92 p.
49. **Kuzmin D.V., Chupin V.P., Litvinovsky B.A.** The temperatures and compositions of magmas of trachybasalt-comendite association in the Tsagan-Khurtei ridge, West Transbaikalia (by inclusions in minerals) // Geol. Geophis. 1999, v. 40, № 1, p. 60-71.
50. **Kyle P.R., Price R.C.** Occurrences of rhönite in alkalic lavas of the McMurdo Volcanic Group, Antarctica, and Dunedin Volcano, New Zealand // Am. Mineral., 1975, v. 60, p. 722-725.
51. **Lacroix A.** Note sur la rhönite du Puy de Barneire à Saint Sandoux // Bull. Soc. Fr. Mineral. Cristallogr., 1909, v. 32, p. 325-331.
52. **Litasov K., Ohtani E., Simonov V., Taniguchi H.** Melting experiments on the mantle

minerals and basaltic melts: possible relation to the melt-xenolith reactions during magma ascent // Abstr. Vol. 32th IGC, Rio de Janeiro, Brazil, 2000, CD-edition.

53. **Litasov Yu.D.** Alkali basaltic volcanoes Ingamakit and Munduzhyak (Udokan plateau, North Transbaikalia): peculiarities of evolution / In: V.A. Simonov and V.Yu. Kolobov (Editors), Thermobarogeochemistry of Mineral Formation Processes, UIGGM, Novosibirsk, 1992, v. 2, p. 16-29 (in Russian, with English Abstr.).
54. **Litvinovsky B.A., Yarmolyuk V.V., Vorontsov A.A., Zhuravlev D.Z., Posokhov V.F., Sandimirova G.P., Kuzmin D.V.** Late Triassic stage of formation of the Mongolo-Transbaikalian alkaline-granitoid province: data of isotope-geochemical studies // Geol. Geophis., 2001, v. 42, № 3, p. 445-455.
55. **Lofgren G.E., Huss G. R., Wasserburg G.J.** An experimental study of trace-element partitioning between Ti-Al-clinopyroxene and melt: Equilibrium and kinetic effects including sector zoning // Am. Mineral., 2006, v. 91, p. 1596-1606.
56. **Lopez M., Pompilio M., Rotolo S.G.** Petrology of some amphibole-bearing volcanics of the pre-Ellittico period (102-80 Ka), Mt. Etna // Periodico di Mineralogia, 2006, v. 75, № 2-3, p. 151-165.
57. **Lung B., Steinitz G.** K-Ar dating of Mesozoic magmatic rocks in Israel: a review // Isr. J. Earth Sci., 1989, v. 38, p. 89-103.
58. **Magonthier M.C., Velde D.** Mineralogy and petrology of some Tertiary leucite-rhönite basanites from central France // Mineral. Mag., 1976, v. 40, p. 817-826.
59. **Mao H.K., Bell P.M.** Crystal-field effects of trivalent titanium in fassaite from the Pueblo de Allende meteorite // Carnegie Inst. Washington Year Book, 1974, v. 73, p. 488-492.
60. **Mason B., Taylor S.R.** Inclusions in the Allende meteorite // Smiths. Contrib. Earth Sci., 1982, v. 25, p. 1-30.
61. **Morimoto N., Fabriès J., Ferguson A.K., Ginzburg I.V., Ross M., Seifert F.A., Zussman J., Aoki K., Gottardi G.** Nomenclature of pyroxenes // Am. Mineral., 1988, v. 73, p. 1123-1133.
62. NÉDLI ZS., TÓTH T.M. **PETROGRAPHY AND MINERAL CHEMISTRY OF RHÖNITE IN OCELLI OF ALKALI BASALT FROM VILLÁNY MTS., SW HUNGARY // ACTA MINERAL. PETROGR. SZEGED, 2003, V. 44, P 51-56.**
63. **Nono A., Deruelle B., Demaifee D., Kambou R.** Tchabal-Nganha volcano in Adamawa (Cameroon) - Petrology of a continental alkaline lava series // J. Volcanol. Geotherm. Res., 1994, v. 60, p. 147-178.
64. **Olsson H.B.** Rhönite from Skåne (Skania), southern Sweden // Geologiska Föreningens i Stockholm Förhandlingar, 1983, v. 105, p. 281-286.
65. PETRUSHIN YE.I., BAZAROV L.SH., GORDEEVA V.I., SHARYGIN, V.V.**. A HEATING STAGE FOR PETROLOGIC STUDIES OF ALKALINE IGNEOUS ROCKS // INSTRUMENTS AND EXPERIMENTAL TECHNIQUES, 2003, V. 46, № 2, P. 240-243.**
66. **Prestvik T., Torske T., Sundvoll B., Karlsson H.** Petrology of early Tertiary nephelinites off mid-Norway. Additional evidence for an enriched endmember of the ancestral Iceland plume // Lithos, 1999, v. 46, p. 317-330.
67. **Rasskazov S.V., Boven A., Andre L., Liegeois J.P., Ivanov A.V., Punzalan L.** Evolution of magmatism in the northeastern Baikal rift system // Petrology, 1997, v. 5, № 2, p. 101-120.
68. **Rasskazov S.V., Logachev N.A., Brandt I.C., Brandt S.B., Ivanov A.V.** Geochronology and geodynamics in the late Cenozoic: South Siberia – South and East Asia. PH Nauka, Novosibirsk, 2000, 288 p.

69. **Roach I.G.** Mineralogy, textures and P-T relationships of a suite xenoliths from the Monaro volcanic province, New South Wales, Australia // J. Petrol., 2004, v. 45, p. 739-758.
70. **Rondorf A.** Rhönit vom Vulkan Sattel bei Eich/Osteifel // Aufschluss, 1989, v. 40, p. 391-401.
71. **Seghedi I., Vasselli O., Downes H.** Occurrence of rhönite in basanites from Poiana Ruscă Mountains // Roman. J. Mineral., 1995, v. 77, p. 41-41.
72. **Shaw C.S.J., Klügel A.** The pressure and temperature conditions and timing of glass formation in mantle-derived xenoliths from Baarley, West Eifel, Germany: the case for amphibole breakdown, lava infiltration and mineral-melt reaction // Mineral. Petrol., 2002, v. 74, p. 163-187.
73. **Simon S.B., Davis A.M., Grossman L.** Origin of compact type A refractory inclusions from CV3 carbonaceous chondrites // Geochim. Cosmochim. Acta, 1999, v. 63, p. 1233-1248.
74. **Simon S.B., Davis A.M., Grossman L.**. Formation of orange hibonite, as inferred from some Allende inclusions // Meteorit. Planet. Sci., 2001, v. 36, p. 331-350.
75. **Sobolev A.V., Slutsky A.B.** Composition and crystallization conditions of initial melt of the Siberian meimechites in relation to the general problem of the ultrabasic magmas // Sov. Geol. Geophys., 1984, v. 25, p. 93-104.
76. **Sobolev V.S., Kostyuk V.P., Bazarova T.Yu., Bazarov L.Sh.** Melt inclusions in phenocrysts of nepheline basalts // Dokl. AN SSSR, 1967, v. 173, № 2, p. 431-434 (in Russian).
77. **Soellner J.** Über Rhönit, ein neues änigmatitähnliches Mineral und über das Vorkommen und über die Verbreitung desselben in basaltischen Gesteinen // Neues Jahr. Mineral. Mh., 1907, v. 24, p. 475-547.
78. SZABÓ CS., HARANGI SZ., CSONTOS L. **REVIEW OF NEOGENE AND QUATERNARY VOLCANISM OF THE CARPATHIAN-PANNONIAN REGION // TECTONOPHYSICS, 1992, V. 208, P. 243-256.**
79. **Timina T.Ju., Sharygin V.V., Golovin A.V.** Melt evolution during the crystallization of basanites of the Tergesh pipe, northern Minusinsk Depression // Geochem. Inter., 2003, v. 44, № 8, p. 752-770.
80. **Tomita T.** On kaersutite from Dogo, Oki Islands, Japan, and its magmatic alteration and resorption // Shanghai Sci. Inst. J. Sect., 1934, v. 2, № 1, p. 99-136.
81. **Vapnik Ye., Sharygin V.V., Samoilov V., Yudalevich Z., Eyal M.** The petrogenesis of basic and ultrabasic alkaline rocks of western Makhtesh Ramon, Israel: geochemistry, melt and fluid inclusion study // Inter. J. Earth Sci., 2007, v. 96, № 4, p. 639-661.
82. **Walenta K.** Zur kristallographie des Rhönits // Z. Kristallogr., 1969, v. 130, p. 214-230.
83. **Wysoczanski R.J.** Lithospheric xenoliths from the Marie Byrd Land volcanic province, west Antarctica. PhD thesis, Victoria University of Wellington, New Zealand, 1993, 475 p.
84. **Yagi K.** Petrochemical studies on the alkalic rocks of the Morutu District // Sakhalin. Geol. Soc. Amer. Bull., 1953, v. 64, p. 769-810.
85. **Zajacz Z., Kovács I., Falus Gy., Hidas K., Szabó Cs., Ntaflos T.** Cumulate xenoliths in the alkaline basalts of Nógrád-Gömör Volcanic Field (N-Hungary/S-Slovakia): a melt inclusion study // Acta Mineral. Petrogr. Abstr. Ser., Szeged, 2003, v. 2, p. 232-233.
86. **Zajacz Z., Kovács I., Szabó Cs., Halter W., Pettke T.** Evolution of mafic alkaline melts crystallized in the uppermost lithospheric mantle: a melt inclusion study of olivine-clinopyroxenite xenoliths, northern Hungary // J. Petrol., 2007, v. 48, p. 853-883.

UDK 552.321

THE HARDENESSING OF THE ASM DIAGRAM FOR GENETIC ANALYSES OF THE MAGMATIC ROCK SERIES

Anfilogov V.N.

I Min. Ur Br. RAS, Miass

ABSTRACT

The genetic series of the magmatic rocks: basalt-rhyolite, stratifom massif rocks, komatiite and komatiitic basalts, stratiform massifs rocks and alkaline rocks are analyzed by ASM diagram (A – Al_2O_3, S – SiO_2 + TiO_2, M – the sum of the metal oxides mole fraction). It is demonstrated that basalt- rhyolite series of rock form two genetic groups are distinguished of Al_2O_3 content. The andesites are divided on two groups. One group is in the basalt-rhyolite series another is represented by hybrid rocks. The stratiform massifs rocks are represented by two groups also. The first group is combined the Scergaard massif type, where there is no spatial separation of the leucocratic and melanocratic cumulates. The second is combined massifs where these rock compositions are divided. The alkaline rocks form two areas of composition on ASM diagram: the area of basic and ultrabasic compositions and the area of nepheline-fieldspar ones.

INTRODUCTION

There are many different diagrams, which are used for chemical classification of magmatic rocks: QAPF [14], TAS [16] and so on. These diagrams allow to divide the volcanic and intrusive rocks on the different types, but petrology would require a diagram, which allows to describe the magmatic systems evolution. The evolution of the magmatic systems points toward progressive polymerization of melt or toward the framework mineral rock compositions. The polymerization degree is expressible in term of Q:

$$Q = \frac{2(N_{SiO2} + N_{TiO2}) + 3N_{Al2O3}}{2(N_{SiO2} + N_{TiO2}) + 3N_{Ai2O3} + \sum N_{MexOy}}$$

We proposed also the ASM diagram for graphical representation of this parameter for different genetic series of the magmatic rocks [1].

The ASM diagram is build up in form of rectangular triangle with apexes: Al_2O_3, (SiO_2 + TiO_2) and $\sum Me_xO_y$ – the sum of the molecular fraction of Fe_2O_3, FeO, MgO, CaO, Na_2O and K_2O. The content of oxides in the rock is expressed in molecular fraction. In order that Al_2O_3 content variation is more descriptive the (SiO_2 + TiO_2) – Al_2O_3 triangle side must be two times greater than (SiO_2 + TiO_2) - $\sum Me_xO_y$ one. The curves, which is connected the olivine and anorthite composition is represented the cumulose compositions, which are formed as a result of the fractional crystallization of the basalt magma. The strait line, which pass through

(SiO_2 + TiO_2) apex and anorthite point is connected the limiting polymerization compositions of the magmatic melt and magmatic rocks, which are comprised from framework silicates only. The alkaline fieldspar and granite composition are on this line.

THE BASALT-RHIOLRTE SERIESES OF MAGMATIC ROCKS

Two chemical differentiation ways can be realized in magmatic systems: the partial melting and fractional crystallization. The low-fusible fraction of melt is formed by partial melting. It separates from the refractory material and goes up because it has low density. The hard high-melting enriched by olivine composition is accumulated in the melting zone as a result. The melting in the system pyrope - diopside - forsterite allows to illustrate this process [17], figure 2. The partial

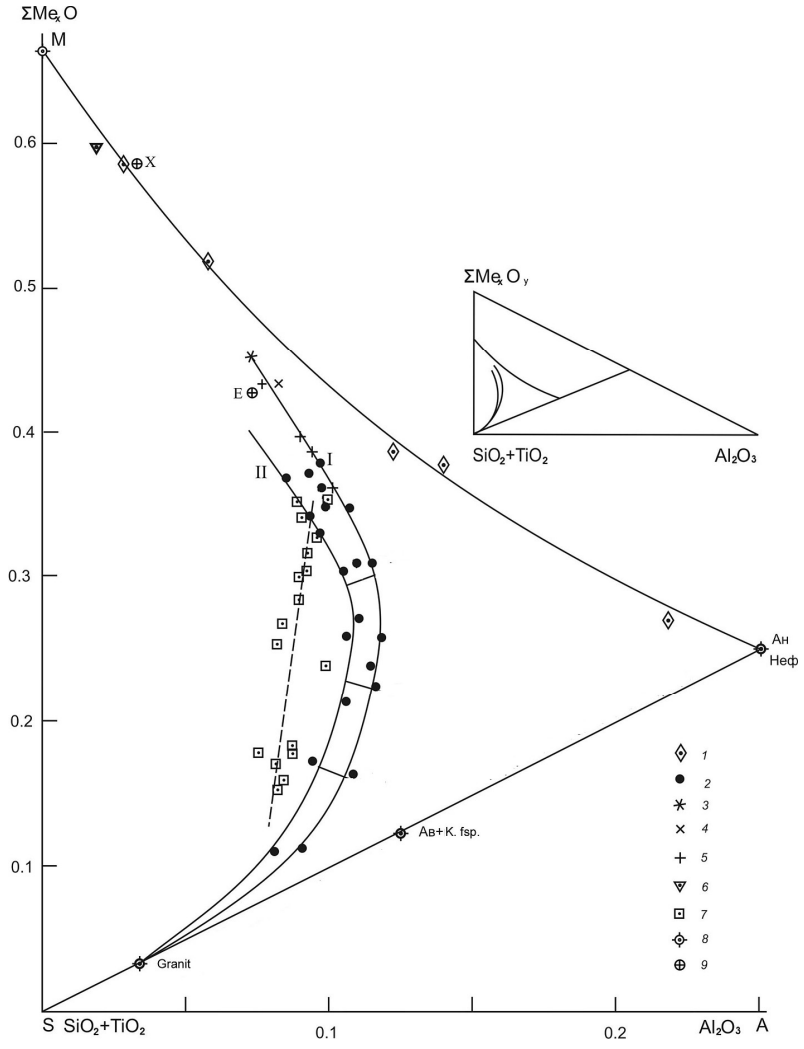

Fig. 1. **The compositions of the basalt-rhyolite series rocks.**

1- cumulative rock of the Ram island massif; 2 – the compositions of the basalt-rhyolite rocks; 3 – the melt composition, which is formed from KLB-1 peridotite at 1475^{o}C and 30kbar; 4 - the melt composition, which is formed from KLB- peridotite at 1425 ^{o}C and 25 kbar; 5 – the melt composition, which are formed as the result of the fractional crystallization of the olivine tholeite; 6 – Ringwood's

pyrolite composition; 7 plateau Parana rockc compositions; 8 – olivine, anortite, nepheline, alkaline fieldspar and granitic compositions; 9 – E and X compositions from figure 2.

melting begins at 1670 ^{o}C in this system. Te eutectic composition, E is smelted at this temperature and refractory composition is transfered to the point R. As soon as the refractory composition has been attained point R the fusion process stopps until the temperature goes up to 1770^{o}C and composition B begins to smelt. The melt composition in the points E, X and R are entered on the ASM diagram together with basaltic, andesitic and rhyolitic ones, figure 1.

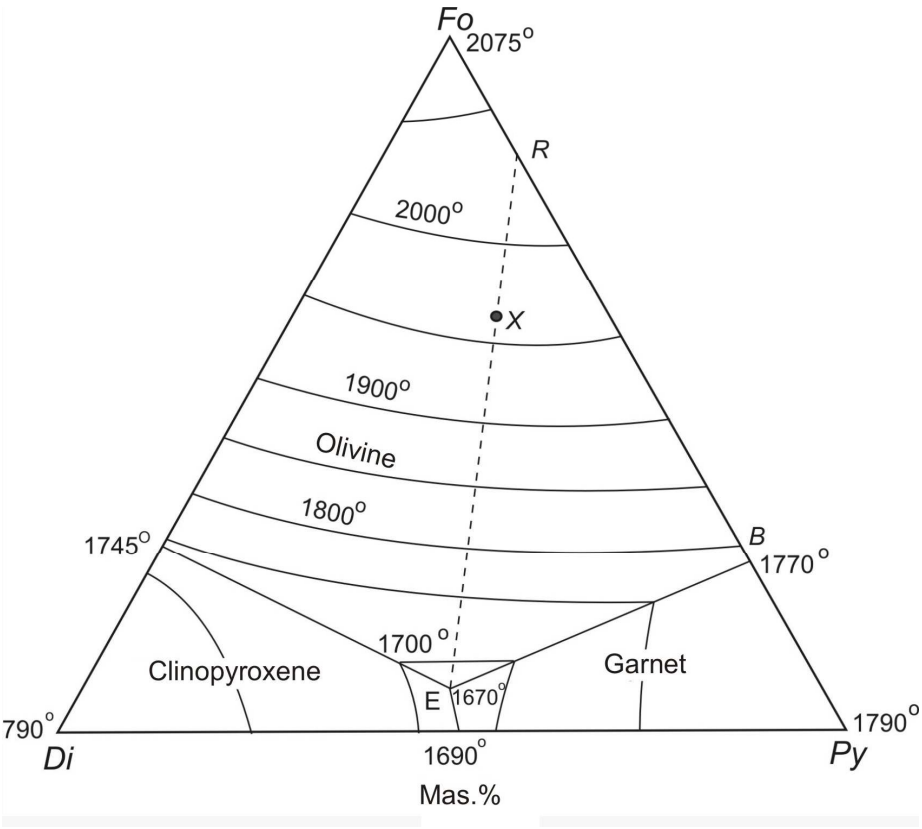

Fig. 2. **The phase relationships in the system anortite-pyrope-olivine at 40kbar.**

The composition of basalt and basic rocks form the narrow variational trend enclosed by two curves. The curve I is begins from the melt composition, which is smelted from the garnet peridotite KLB-1 at 30kbar pressure and 1475^{o}C [12]. The composition E and melt composition, which is smelted at 1425^{o}C are closely spaced to this point. There are the compositions, which are formed by olivine tholeite fraction crystallization [10] on the curve I. By this means the curve I is reflected two processes: the formation and composition of the primary basaltic melt and its changing as the result of fraction crystallization.

The line II compositions differ from line I by the lower Al_2O_3 content and higher SiO_2 one. It seems likely that they have not own primary magma. Using the experimental data Green and Ringwood [10] conceive that line II compositions are formed by the primary melt fractional crystallization in the intermediated

chambers, which are disposed on the level less than 15 km, whereas line I compositions are formed on the deep more than 15 km [10]. The basic rock compositions on the figure 1 are taken from [7].

The lines I and II follow to andesite and dacite compositions and ended at rhyolitic ones, figure 1. There are two andesite-rhyolite series: high- and low-aluminiferous. The Kuril Islands rocks compositions are on the line I and The East Kamchatka ones on the line II, [11, tables 10, 11], figure 1. It is beyond reason to

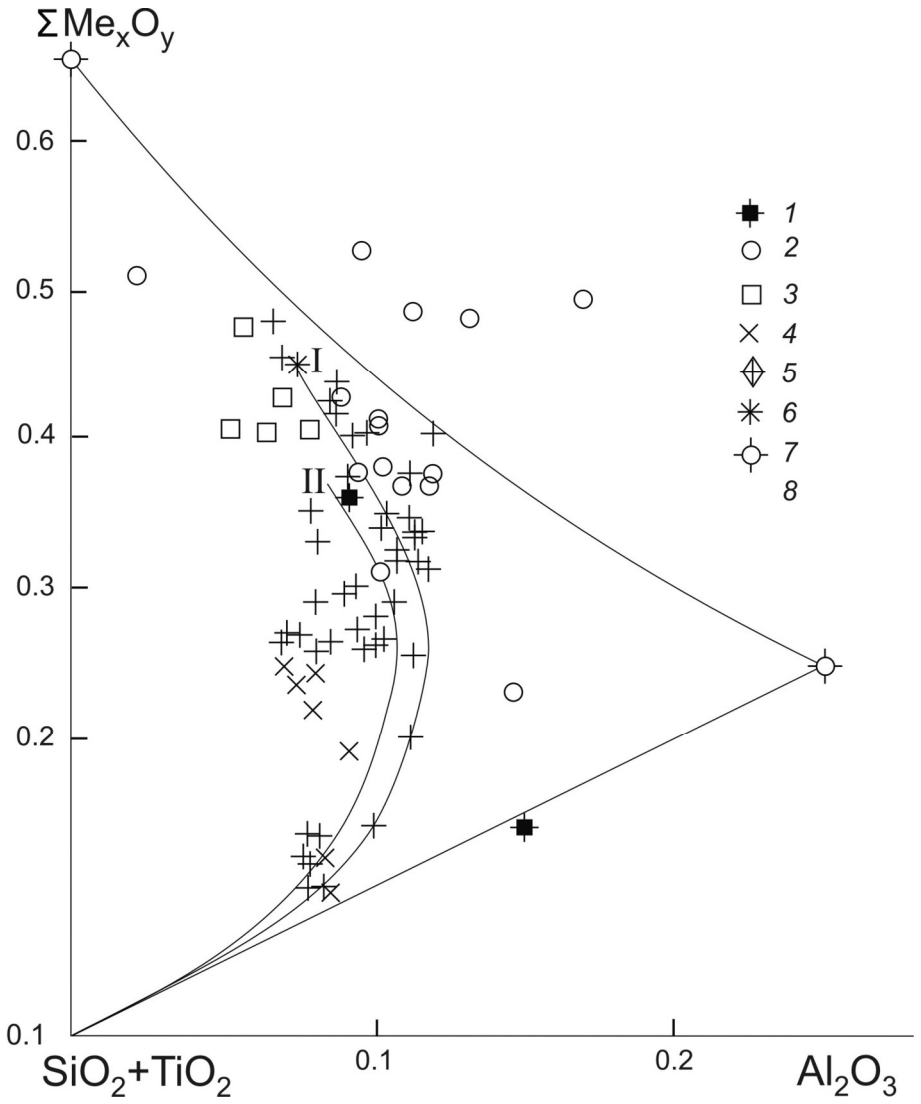

Fig. 3. **The rocks compositions of Scergaard, Alamdjakhski and Norilski layered intrusions.**

1 – the composition of the initial Scergaard intrusive melt; 2 – the composition of the leucocratic cumulates; 3 – the compositions of the melanocratic cumulates; 4, 5 – the ferrodiorite and granophyre compositions; 6 - the melt composition, which is formed from KLB-1 peridotite at 1475^{o}C and 30kbar; 7 – olivine and anortite compositions.

confirm that these rocks were formed by fractional crystallization of the “dry” basaltic magma, which compositions are on the lines I and II. This idea do not receives support among researches now [6]. Nonetheless must be the mechanism,

which gives rise to the uninterrupted series basalt – rhyolite. There are two possible ways for andesite and rhyolite composition formation: by saturation of the basaltic melt with water, or by partial melting of the waterferrous metabasalt. Water suppresses the temperature pyroxene barrier, which is between basaltic and andesitic compositions and waterferrous basaltic melt gains the capacity for evolution to rhyolitic one. The cotectic andesitic melt is formed in the second way. There are basalt-rhyolitic series, which is formed by the basaltic melt contamination of the acid rocks at the same time. Basalt-rhyolitic formation of Parana plateau (Brasil) [4] was formed by this way. It has the bimodal composition distribution and forms own line on the ASM diagram, figure 1.

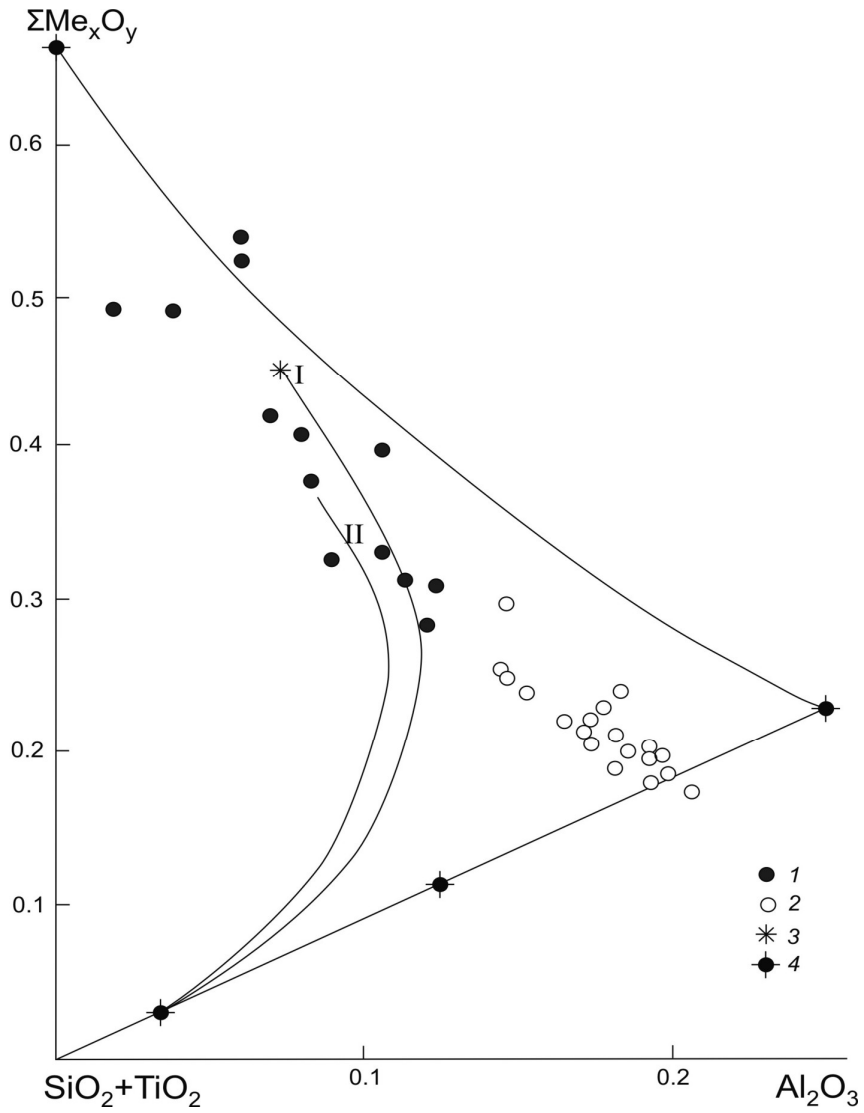

Fig. 4. **The rocks compositions of the Djugdjurski anortosite massif.**

1 – melanocratic rocks; 2 – leucocratic rocks; 3 and 4 – see on the Fig. 1

ASM diagram is shown on the figure 1 is represented the melt compositions, which are flow out on the Earth surface. They form by the mantle substratum and

their compositions depend of fractional crystallization degree, which has been going in the intermediated chamber. The melt, which flowed out on the surface can to contain a quantity of crystals and its composition may be distinct from the primary one.

THE MAGMATIC ROCKS OF THE STATIFORM INTRUSIVES

There are three parameters, which govern the rock composition in stratiform massifs: the melt density, contamination of the country rocks by melt and regular melt updates in the magmatic chamber. The melt density in Skergaard differentiated intrusion and stratiform trappean ones closely related to plagioclase density. There is no spatial separation of the leucocratic and melanocratic cumulates in these intrusions and plagioclase and olivine-pyroxene layers alternate to one another [18]. The compositions of Skergaard, Alamjachski and Norilski

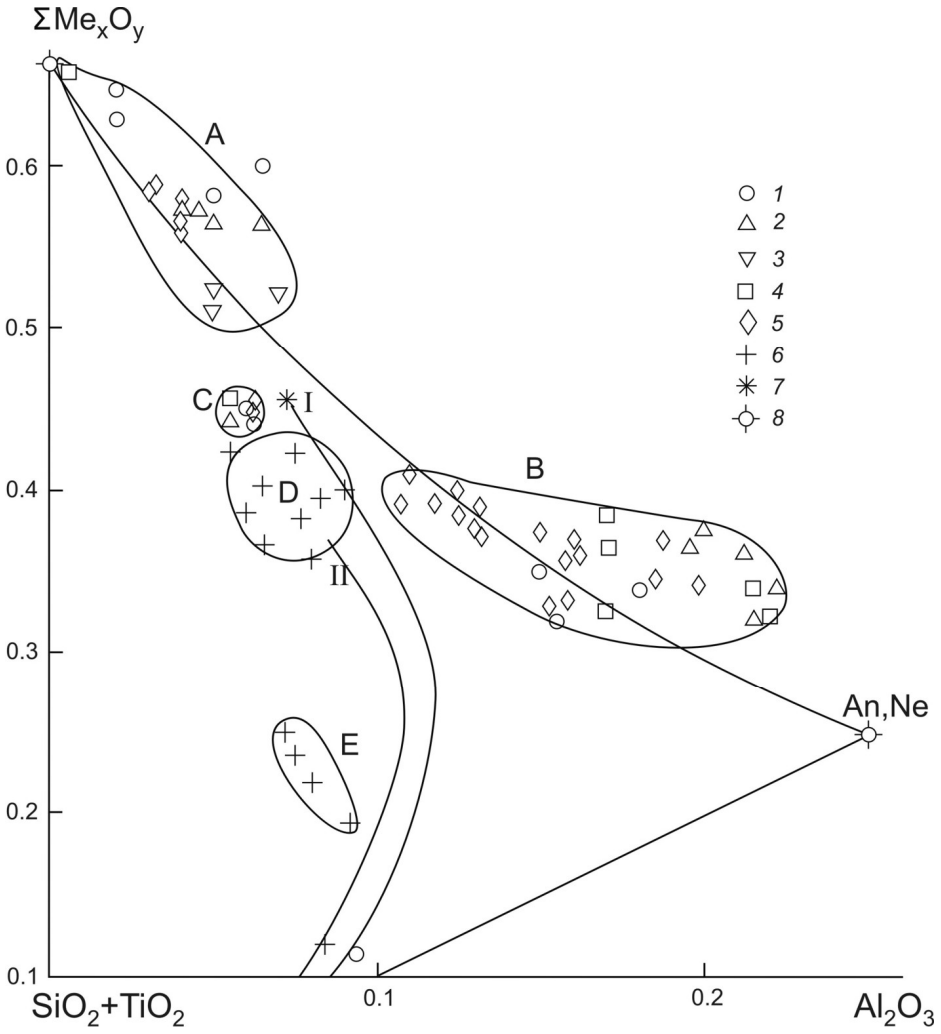

Fig. 5. **The joined ASM diagram for layered massifs.**

A – ultrabasic cumulates; B – leucocratic cumulates; C- pyroxenites; D – basic hybrid rocks; E – acid hybrid rocks. 1 – picrite by Dally; 2 – the layered rocks from the East Goldfield (Australia); 3 – The

layered rocks of island Rum massif; 4 – the rocks of Djanchin intrusion; 5 – the layered rocks of the Stillwater massif; 6 – the layered rocks of Dir lake complex; 7 – Skergaard's ferrogabbro.

intrusions on the ASM diagram are shown on figure 3. The ferrogabbro is the end product of fractional crystallization in Skergaard intrusion. Ferrodiorite and granophyre are forming as a result of the grey gneiss contamination [1, 18]. Their compositions are the same as plateau Parana rocks ones, figure 1. It is agree with $^{87}Sr/^{86}Sr$ in quenched border Skergaard gabbro and in gneiss [18] By this means Skergaad intrusion is the exemplify of magma crystallization in enclosed chamber, which is accompanied by contamination of the country gneiss. This is a reason of the wide scatter of the rocks composition on the ASM diagram, figure 3.

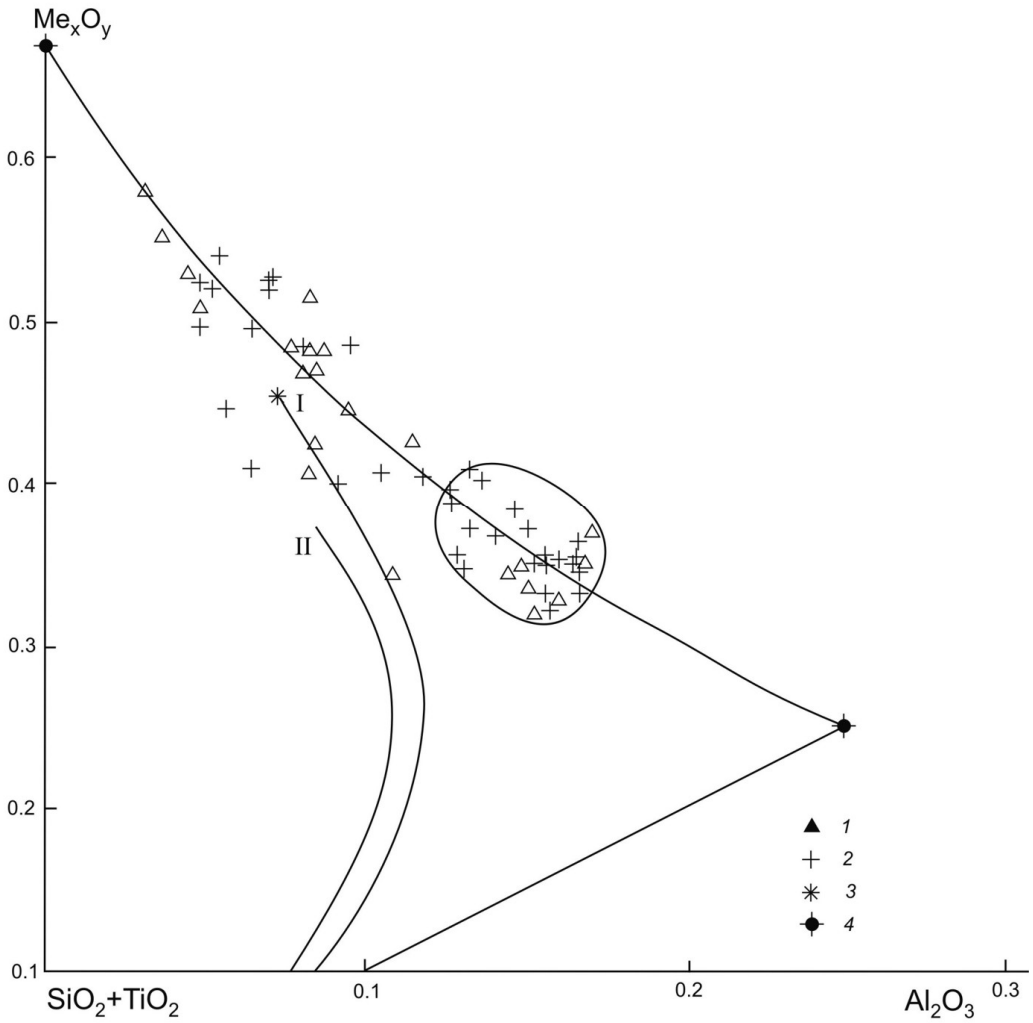

Fig. 6. **The komatiites and komatiitic basalts compositions.**

1 and 2: the mating komatiite and komatiite basalt compositions; 3 and 4 – see Fig. 1.

The rocks compositions of Djugdurski anorthosite massif [15] are shown on the figure 4. The leucocratic and melanocratic compositions of this massif are disposed in two different areas. Origin of the anorthosite is controversial. Once the

lunar anorthosite was investigated it has become evident that it able to form if magma density more than anortite one. It may be accomplished by high TiO_2 content in the melt. The summary ASM diagram for layered intrusions is sown on the figure 5. There are 4 areas of the rocks composition on this diagram. The areas A and B are conformed to leucocratic and melanocratic cumulates. The area C conforms to pyroxenites. The areas D and E are represented by hybrid rocks.

KOMATIITES AND KOMATIITIC BASALTS

ASM diagram for komatiites and komatiitic basalt is shown on the figure 5 [2]. Their compositions form two areas identical with area A and B on the figure 4.

We proposed that komatiite and komatiitic basalts flow out in form of magmatic mush: komatiite as mixture of basaltic melt and crystals of olivine and pyroxene [2, 3] and komatiitic basalt as mixture of basaltic melt and crystals of plagioclase.

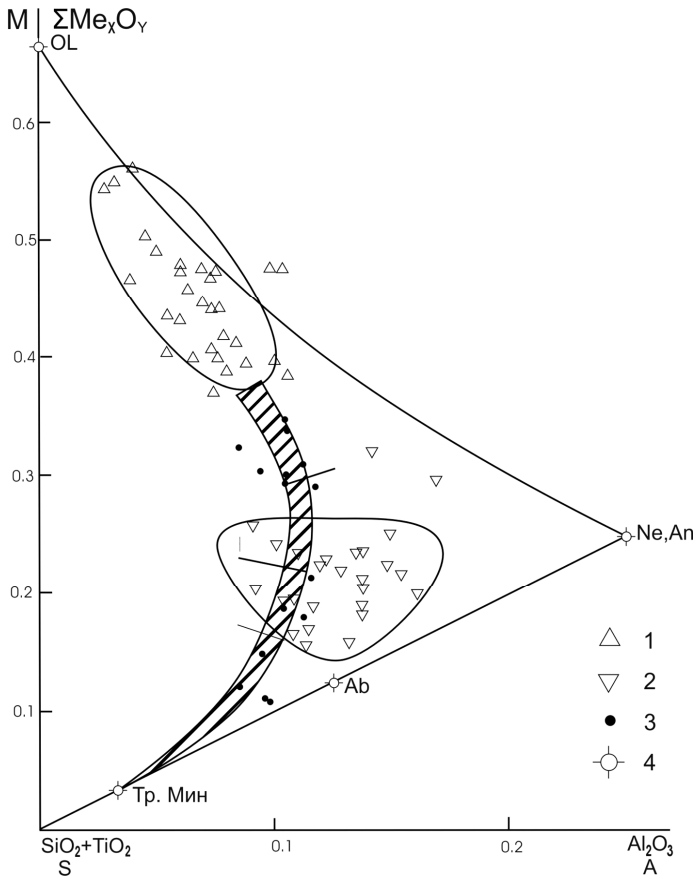

Fig. 7. **The alkaline rocks compositions.**

1 – basic rocks; 2 – leucocratic rocks; 3 – basalt-rhyolite rocks; 5 – see Fig. 1

ALKALINE ROCKS

The compositions of alkaline rocks are shown on the figure 6. They form two areas: A - the area of basic and ultrabasic composition and B - the area of the

nephelin- fieldspar ones. The alkaline basalt, hawaite, basanite, limburgite, ankaramite and another rock compositions are in area A. The Maimecha-Kotuyskaia province is the region where these rocks are represented widely [11]. The typical region of leucocratic alkaline magmatic rocks is Kola peninsula [5, 8]. It is evident that rocks in area I and II are not comagmatic.

Origin of alkaline rocks is contraversal. The rocks, which are formed by the mantle substrate are represented on the figure 1. They never contain nepheline and rhyolite is the resulting product of their evolution. This brings up the question as to transform the quartz-fielspar paragenesisis to nepheline-fielspar one. It can be realized if the basaltic magma interacts with carbonate [20]:

$CaAl_2Si_2O_8 + 2CaCO_3 = Ca_2Al[(SiAl)O_7] + CaSiO_3 + CO_2$

$NaAiSi_3O_8 + 2CaCO_3 = NaAlSiO_4 + CaSiO_3 + 2CO_2$

The gelenite and nepheline components are formed by these reactions and the basaltic magma enriched by CaO. The compositions of the basic alcaline rocks are shifted to ultrabasic ones as a result, figure 7.

CONCLUSIONS

1. The ASM diagram allows to separate the magmatic rocks which are formed by the crystallization of the primary and differentiated melts and leucocratic and melanocratic cumulates.
2. The magmatic rock compositions, which are formed by mantle substrate form on the ASM diagram two variational curves. The compositions of the hybrid rocks form on the ASM diagram own variational curve.
3. The rock compositions of the layered intrusions are formed on the ASM diagram two separated areas.
4. The compositions of komatiites and komatiitic basalts have the same positions on the ASM diagram as layered massifs ones.

REFERENCES

1. **Anfilogov V.N.** Structural-chemical evolution of magmatic systems // Geochimia, 1979, № 10, p. 1439-1445.
2. **Anfilogov V.N.** The origin of komatiites // Uralski mineralogicheski sbornic. Miass, 1997, № 7, p. 155-174.
3. **Anfilogov V.N.** The magmatic mush as rock-forming systems // Geology and metallogeny of the ultrabasic- basic and granitic intrusive associations of the folded regions. Ekaterinburg, 2004,p. 10-14.
4. **Belleni G., Comin-Chiarmonti P., Marques L.S et al.** Petrogenesis aspects of acid and basaltic lavas from The Parana Plateau (Brasil): Geological, mineralogical and petrochemical relationships // J. Petrol., v. 27, part 4, p. 915-944.
5. **Bussen I.V., Sakharov A.S.** Petrology of the Lavozerski alkaline massif. Nauka, Leningrad, 1972, 296 p.
6. **Crawford A.J., Fallon T.J., Eggins S.** The origin if island arc high-alumina basalts // Contrib. Mineral. Petrol., 1987, v. 97, p. 417-430.

7. **Dmitriev L.V., Sharaskin A.Ya., Garanin A.V.** The main characteristics of the ocean bottom magmatism // The problems of petrology. Nauka, Moscow, 1976, p. 173-189.
8. **Galakhov A.V.** Petrology of the Khibinski alkaline massif. Nauka, Leningrad, 1975, 256 p.
9. **Green D.H.** Experimental melting studies on a upper mantle composition at high pressure under water saturated and water-undersaturated conditions // Earth Planet Sci. Lett., 1973, v. 19, № 1, p. 37-53.
10. **Green D.H., Ringwud A.E.** The genesis of basaltic magmas // Contrib. Mineral. Petrol., 1967,v. 15, № 2, p. 103-190.
11. Gulinski intrusion of ultra basic and alkaline rocks. Eliseev H.A., Sheinman Y.M. (Eds) Moscow, 1961, 274 p.
12. **Hirose K., Kushiro I.** Partial melting of dry peridotites at high pressure: Determination of compositions of melts segregated from peridotitee using aggregates of diamond // Earth Planet Sci Lett., 1993, v. 114, p. 477-489.
13. **Kuznetcov Y.A.** The main types of the magmatic formations. Nedra, Moscow, 1964, 387 p.
14. **Le Bas M.J., Le Maitre R.W., Streckeisen A., Zanettin B.** Cemical classification of volcanic rocks based on the total alkali-silica diagram // J. Petrol., 1988, v. 27, p.745-750.
15. **Lennikov A.M.** The petrology of the Djugdjurski anortozite massiff. Nauka, Moscow, 1968, 158 p.
16. **Streckeisen A.** To each plutonic rocks its proper name // Earth science reviews // International Magazine for geo-scientists, 1976, v. 12, p. 1-33.
17. **Yoder H.S.** Generation of basaltic magma. National Academy of Scienses. Washington, D.C., 1976, 237 p.
18. **Wager L., Brown G.** Layered igneous rjcks. Oliver& Boyd. Edinburg and London, 1968, 551 p.